NUREG/CR-2791
SAND82-7067

Methodology for Evaluation of Insulation-Debris Effects

Containment Emergency Sump Performance
Unresolved Safety Issue A-43

Prepared by J. Wysocki, R. Kolbe

Burns and Roe, Inc.

Sandia National Laboratories

Prepared for
U.S. Nuclear Regulatory Commission

Availability of Reference Materials Cited in NRC Publications

Most documents cited in NRC publications will be available from one of the following sources:

1. The NRC Public Document Room, 1717 H Street, N.W.
   Washington, DC 20555
2. The NRC/GPO Sales Program, U.S. Nuclear Regulatory Commission,
   Washington, DC 20555
3. The National Technical Information Service, Springfield, VA 22161

Although the listing that follows represents the majority of documents cited in NRC publications, it is not intended to be exhaustive.

Referenced documents available for inspection and copying for a fee from the NRC Public Document Room include NRC correspondence and internal NRC memoranda; NRC Office of Inspection and Enforcement bulletins, circulars, information notices, inspection and investigation notices; Licensee Event Reports; vendor reports and correspondence; Commission papers; and applicant and licensee documents and correspondence.

The following documents in the NUREG series are available for purchase from the NRC/GPO Sales Program: formal NRC staff and contractor reports, NRC-sponsored conference proceedings, and NRC booklets and brochures. Also available are Regulatory Guides, NRC regulations in the *Code of Federal Regulations,* and *Nuclear Regulatory Commission Issuances.*

Documents available from the National Technical Information Service include NUREG series reports and technical reports prepared by other federal agencies and reports prepared by the Atomic Energy Commission, forerunner agency to the Nuclear Regulatory Commission.

Documents available from public and special technical libraries include all open literature items, such as books, journal and periodical articles, and transactions. *Federal Register* notices, federal and state legislation, and congressional reports can usually be obtained from these libraries.

Documents such as theses, dissertations, foreign reports and translations, and non-NRC conference proceedings are available for purchase from the organization sponsoring the publication cited.

Single copies of NRC draft reports are available free upon written request to the Division of Technical Information and Document Control, U.S. Nuclear Regulatory Commission, Washington, DC 20555.

Copies of industry codes and standards used in a substantive manner in the NRC regulatory process are maintained at the NRC Library, 7920 Norfolk Avenue, Bethesda, Maryland, and are available there for reference use by the public. Codes and standards are usually copyrighted and may be purchased from the originating organization or, if they are American National Standards, from the American National Standards Institute, 1430 Broadway, New York, NY 10018.

GPO Printed copy price: $8.00

DISCLAIMER

NUREG/CR--2791

DE83 001108

NUREG/CR-2791
SAND82-7067

Methodology for Evaluation of Insulation-Debris Effects

Containment Emergency Sump Performance Unresolved Safety Issue A-43

Manuscript Completed: August 1982
Date Published: September 1982

Prepared by
J. Wysocki, R. Kolbe

Burns and Roe, Inc.
185 Crossways Park Drive
Woodbury, NY 11797

Under Subcontract to
Sandia National Laboratories
Albuquerque, NM 87185

Prepared for
Division of Safety Technology
Office of Nuclear Reactor Regulation
U.S. Nuclear Regulatory Commission
Washington, D.C. 20555
NRC FIN A1296

LEGAL NOTICE

This Report was prepared by Burns and Roe, Inc., as part of work sponsored by the Sandia National Laboratories (Albuquerque). Conclusions or recommendations contained in this report may be predicated upon information published or officially sanctioned by, or received from, utility companies, without independent verification by Burns and Roe, Inc., Neither Sandia National Laboratories, Burns and Roe, Inc. nor any person acting on behalf of either: (a) makes any warranty or representation, express or implied, with respect to the accuracy, completeness, or suitability for any use or purpose of the information contained in this report, or that the use of any information, apparatus, method, or process disclosed in this report may not infringe privately owned rights, nor (b) assumes any responsibility for the use of information, apparatus, method, or process disclosed in this report.

The debris effects calculations for five specific plants in Appendices A through E are included to illustrate the methodology developed and the dependence on plant design parameters. These calculations shall not be submitted by plant owners to fulfill regulatory requirements.

ABSTRACT

The postulated failure of high energy piping within a light water reactor containment has raised safety questions related to the generation of insulation debris, the migration of such debris to the containment emergency sump screens and the potential for severe screen blockages. High, or total, screen blockages could result in impairment of the long term RHR recirculation systems. Debris considerations are an integral part of the unresolved Safety Issue A-43, Containment Emergency Sump Performance.

This report develops calculational methods and debris transport models which can be used for estimating the quantities of debris that might be generated by a LOCA, the transport of such debris, methods for estimating screen blockages and attendant pressure losses. Of necessity, conservative assumptions are employed and the calculations are shown to be plant specific since the types and quantities of insulation, equipment location and break locations determine debris generation, transport and potential for sump blockage. Plant layout and sump location, which determine migration paths, are also important. Calculational procedures for estimating break jet impingement effects and blocked screen pressure losses are included.

Appendices A through E contain illustrative calculations for five operating plants which were analyzed using this debris evaluation methodology. These calculations clearly illustrate the dependency on plant containment layout, sump location and design, and types and quantities of insulation employed.

TABLE OF CONTENTS

LIST OF FIGURES

LIST OF TABLES

ACKNOWLEDGEMENTS

The author wishes to acknowledge the contributions of several individuals in the production of this report, especially the efforts of Ronald Kolbe for preparing Appendices C through E, Lawrence Reinert for preparing the figures in Appendices A through E, Catherine Meara for editing the final manuscript, and Maureen Condon and Norma Santanello for a superlative typing effort on the final manuscript.

SUMMARY

The methodology described in this report provides a procedure for estimating the insulation debris generation and transport associated with postulated piping failures within primary containment. In addition to quantifying the extent of insulation debris generation and transport, the method provides guidance in assessing the consequences of recirculation sump screen blockage.

The method addresses debris generation by pipe whip, pipe impact and jet impingement mechanisms. Pipe whip and pipe impact generate insulation debris due to the motion of unrestrained piping segments and also due to the impact of such piping segments with structures, components or other piping systems. Jet impingement generates debris by subjecting the insulation to a high velocity, high differential pressure field which effectively strips the insulation from the target. This mechanism is responsible for generating the vast majority of insulation debris.

The transport model of insulation debris is developed in two stages: initial or short term, and final or long term transport. The short term transport phase lasts during the blowdown event. Pipe whip, pipe impact and jet impingement are the mechanisms by which insulation debris is transported from its point of attachment on piping systems or components to other regions of containment.

The long term transport phase begins at the termination of blowdown. Dislodged insulation is subjected to a circulating water flow due to the operation of the containment recirculation pumps. Fluid velocity, debris density, debris size and effects of containment water on insulation debris integrity are analyzed to determine if long term transport occurs and, if so, by what mechanism.

The sump effects model analyzes the pressure drop across the screens caused by partial blockage of the screen inlet area due to debris accumulation. The increased pressure drop is considered acceptable if adequate recirculation pump net positive suction head (NPSH) margin still exists at rated pump flows.

Tables 1 through 4 identify the five plants selected for analysis. These tables give information relating to reactor manufacturer, architect-engineer, quantities and types of insulation used, qualitative description of potential adverse effects on recirculation sump performance due to debris accumulations, and employing the methodology developed herein, quantities of debris which are calculated to be transported to the sump.

The placement, type and quantity of insulation presented in Appendices A through E is based on utility supplied drawings which were issued for information purposes. Burns and Roe did not attemp to verify that the supplied drawings reflect as-built conditions. Consequently, the calculations presented in Appendices A through E are not meant as final calculations for the purposes of satisfying regulatory requirements.

Plants were selected based on relative quantities of insulation types employed (Table 2) to provide a spectrum of insulation type/quantity ratios for analysis. NUREG/CR-2403 and Supplement 1 were used in this selection process.

Tables 3 and 4 illustrate the key findings of this analysis: criticality of sump placement and dependence on plant specific information.

Sumps should be placed in areas which do not receive direct jet impingement but do receive water from more than one area of containment.

Plant specific information regarding type of insulation is vital. Reflective metallic and totally encapsulated insulations give the least potential for unacceptable screen blockage while fibrous insulation of any type in relatively small quantities can lead to severe screen blockage.

Finally, generalizations regarding acceptable blockage based on percentage of free screen area are inappropriate. Rather, calculations of debris screen blockage, as outlined in this report, should be undertaken to determine the impact on net positive suction head (NPSH).

Table 1

Reactor Plants Selected for Detailed Investigation of
Insulation Debris Generation Potential

Plant and Location	Reactor	Rating	Startup Date	Utility	Architect-Engineer
Salem Unit 1, Salem, NJ	W-PWR	1090 MWe	1977	Public Service Electric & Gas Co.	Public Service Electric & Gas Co.
Arkansas Unit 2, Russellville, AR	CE-PWR	858 MWe	1980	Arkansas Power & Light Co.	Bechtel
Maine Yankee, Wiscassett, ME	CE-PWR	790 MWe	1972	Maine Yankee Atomic Power Co.	Stone and Webster
Sequoyah Unit 2, Daisy, TN	W-PWR	1148 MWe	1982	Tennessee Valley Authority	Tennessee Valley Authority
Prairie Island Unit 1 Redwing, MN	W-PWR	520 MWe	1973	Northern States Power Company	Fluor Power Services

W - Westinghouse
CE - Combustion Engineering
PWR - Pressurized Water Reactor

Table 2

Types and Areas of Insulation Used Within the
Primary Coolant System Shield Wall

Plant	Types of Insulation and Areas (ft^2)					
	Reflective Metallic	Totally Encapsulated	Mineral Fiber/Wool Blanket	Calcium Silicate Block	Unibestos Block	Fiberglass
Salem Unit 1	6700	0	13200*	-	-	-
Arkansas Unit 2	6300	7400	-	-	-	200
Maine Yankee	2900	-	6700	3500	2000	100
Sequoyah Unit 2	18500	-	-	-	-	-
Prairie Island Unit 1	19180	-	-	-	-	510

*Both totally and semi-encapsulated cerablanket are used; however inside containment only totally encapsulated is employed.

Note: See NUREG/CR-2403 and Supplement No. 1.

Table 3

Summary Table

Plant and Research Manufacturer	Type of Insulation Utilized	Location of Emergency Sump	Assessment of Migration Potential of Debris Generated as a Result of a Pipe Break
Salem Unit 1 (W)	Reactor vessel, primary coolant piping, pressurizer, reactor coolant pumps and bottom part of steam generator use reflective metallic insulation. Upper part of steam generator uses semiencapsulated cerablanket insulation. Main steam, feedwater, residual heat removal, safety injection, and chemical and volume control system piping use totally encapsulated cerablanket. Service water and component cooling water piping use antisweat insulation.	Outside the reactor coolant system shield wall below basement floor. Water drains into emergency sump through trenches in the floor.	Postulated breaks resulted in large quantities of debris. Calculations indicate total screen blockage to occur. Calculations showed that large quantities of debris would be generated by postulated breaks. They further showed the potential for total screen blockage. However, this plant design has large debris intercept areas, in addition to the local sump screen. This, when coupled with the low recirculation velocities within containment, results in a low blocked screen ΔP which does not result in insufficient NPSH.
Arkansas Unit 2	Reactor coolant piping, reactor vessel, bottom head of steam generator, and pressurizer use reflective metallic insulation. Feedwater pressurizer safety relief valve and balance of steam generator blowdown piping use totally encapsulated calcium silicate or expanded perlite block with stainless steel jacketing. Chilled water piping uses fiberglass with stainless steel jacketing.	Outside the reactor coolant systems shield wall below basement floor.	Total calculated debris is large but is incapable of either migrating to the sump (reflective metallic) or being drawn into the screens (calcium silicate). Extensive blockage of the inboard screens occurs but out-board screens are more than adequate to pass the required flow without introducing unacceptable head losses. Refer to Appendix B.

Table 3

Summary Table (Cont'd.)

Plant and Reactor Manufacturer	Type of Insulation Utilized	Location of Emergency Sump	Final Assessment of Migration Potential of Debris Generated as a Result of a Pipe Break
Maine Yankee 1	Reactor vessel uses reflective metallic insulation. Pressurizer, reactor coolant pumps, and steam generators use calcium silicate molded block jacketed insultation for non-removable sections and mineral fiber/wool for removable sections. Primary coolant piping uses removable mineral fiber/wool blankets. Main steam, feedwater, residual heat removal, and chemical and volume control system piping use calcium silicate or unibestos molded block insulation. Component cooling lines use fiberglass jacketed antisweat insulation.	Outside the reactor coolant system shield wall below basement floor.	Plant calculations show that for some of the postulated breaks total screen blockage can occur due to the transport of unencapsulated fibrous insulation. Since the sump screen area is small (108 ft^2), the calculated pressure drop (6.3 psi) is excessive. Further investigation is necessary to confirm the fibrous bed pressure drop correlation employed. Refer to Appendix C.
Sequoyah Unit 2 (W)	All piping and equipment within the shielded crane wall area uses reflective metallic insulation.	Inside the crane shield wall below containment floor.	While a large percentage of the sump intake area is estimated to be blocked (approximately 74%), the remaining screen area is capable of passing the required recirculation flow without excessive head loss. Thus pump NPSH requirements are not impaired. Refer to Appendix D.

Table 3

Summary Table (Cont'd.)

Plant and Reactor Manufacturer	Type of Insulation Utilized	Location of Emergency Sump	Final Assessment of Migration Potential of Debris Generated as a Result of a Pipe Break
Prairie Island Unit 1 (W)	Mirror insulation is used on reactor vessel, steam generator, reactor coolant pump, pressurizer, excess let down heat exchanger, regenerative heat exchanger, surge line, high pressure safety injection loop, primary coolant piping, steam generator blowdown lines, pressurizer spray piping, chemical and volume control piping, accumulator, low pressure safety injection, feedwater, main steam, auxiliary feedwater, residual heat removal, steam generator supports. Fiberglass insulation is used on main steam and feedwater hangers and restraints.	Outside reactor coolant shield wall, below basement floor.	The estimated quantity of insulation debris generated is large but is unable to migrate to the sump (reflective metallic). The quantity of fibrous insulation generated is not sufficient to block a sump screen area large enough to cause excessive pressure drop. Refer to Appendix E.

Table 4

Summary of Findings

Plant	Break	Debris* Generated	Debris* At Sump	Total* Sump Screen Area	Blocked* Sump Screen Area	Percent Blockage	Note
Salem Unit 1	Hot Leg	2692	1197	1078 **	1078 **	100	1
	Cold Leg	4737	2290	↓	1078 **	100	1
	Main Steam	-	0	↓	0	0	2
	Feedwater	-	0	↓	0	0	2
Arkansas Unit 2	Main Steam	7161	6517	287	95	33	3
	Feedwater 1	278	0	287	189	66	4
	Feedwater 2	97	-	-	-	-	5
Maine Yankee	Main Steam	3314	-	108	-	-	6
	Hot Leg 1	1071	-	↓	-	-	6
	Hot Leg 2	1642	-	↓	-	-	6
	Crossover 1	1642	-	↓	-	-	6
	Crossover 2	1596	394	↓	108	100	7
	Cold Leg	431	-	↓	-	-	6
	Emerg. Feed.	215	-	↓	-	-	6
Sequoyah Unit 2	Feedwater	248	15	41	15	37	8
	Hot Leg	2840	27	↓	27	66	9
	Coolant Pump	1009	15	↓	15	37	8
	Hot Leg	2840	27	↓	27	66	9
	S.G. No. 4	528	20	↓	20	49	9
	S.G. No. 1	3257	15	↓	15	37	8
	Loop Closure	5632	15	↓	15	37	8
Prairie Island Unit 1	Main Steam	4316	39	60	39	65	8
	Feedwater	1299	0	↓	0	0	10
	Hot Leg	4131	39	↓	39	65	8
	Cold Leg	1221	0	↓	0	0	10
	Crossover	5009	39	↓	39	65	8

*Units of ft^2

**Total debris intercept area available in this plant to accept LOCA-generated debris. The sump screen area at the sump is 68 ft^2.

Table 4

Summary of Findings (Cont'd.)

Notes:

1) As insulation is fibrous, uniform deposition is assumed (i.e., 100% of sump screens are blocked). Pressure drop is insufficient to adversely affect NPSH.

2) No debris reaches sump region due to gratings as shown in Figure A-24.

3) Entire inboard screen blocked; outboard screen has sufficient unblocked area.

4) Entire outboard screen blocked; inboard screen has sufficient unblocked area.

5) Scoping analysis - Feedwater 1 was more severe.

6) These cases are parts of a scoping analysis. Cold leg failure was most limiting.

7) Screen blockage is calculated to be total. Calculated pressure drop across fibrous debris bed is sufficient to offset any available NPSH margin, subject to assumption of total sump screen blockage with no credit for debris capture in transport.

8) Blockage acceptable from pressure drop standpoint.

9) Blockage as percentage of screen area is high, but pressure drop is acceptable.

10) Insulation does not reach sump.

METHODOLOGY FOR

EVALUATION OF INSULTATION DEBRIS

1.0 INTRODUCTION

The destruction of insulation from pipes and process vessels within containment resulting from the postulated pipe break has not been systematically studied. It is the purpose of this document to present methods to estimate the sources, generation, transport mechanisms, and effects of such insulation debris within containment on containment emergency sump performance. The methods as developed represent multistep procedures and are presented in outline form as Attachment 1.

A minimal degree of knowledge concerning pipe break analysis, blowdown calculations, safety system operation and the general nature of pressurized water reactor (PWR) operation is assumed in this document. For readers unfamiliar with any of these subjects, the reference material identified in Attachment 5 may prove helpful.

2.0 DETERMINATION OF INITIATING EVENTS

The initiating event for the insulation debris study is the postulated pipe rupture described in Ref. 1. This reference provides guidance for selecting the number, orientations and locations of the postulated ruptures within containment. Pipe breaks outside containment are not considered in this analysis as they do not generate insulation debris which could reach the emergency core cooling system (ECCS) pump suctions.

For plants which have already filed Final Safety Analysis Reports (FSAR's), the design basis break locations inside containment, hereafter referred to as postulated rupture locations (PRL), are tabulated. The PRL's may be found in FSAR Section 3.6.2 for plants filing under the revised format. For plant FSAR's filed prior to the revised format effective date, the information may be located in FSAR Chapter 15 - Accident Analysis, Chapter 3 - Design of Structures, Components, Equipment and Systems, Chapter 6 - Engineered Safety Features, or an Appendix.

By reviewing the FSAR, the number of design basis pipe break locations, their orientations, and sizes can be determined. As Ref. 1 provides the guidance for selection of design basis break locations, no further break locations need be postulated for this analysis.

Having identified those breaks postulated within containment, including all longitudinal failures, circumferential failures and postulated through-wall leakage cracks for both restrained and unrestrained pipes, a screening process is undertaken to reduce to a minimum the number of breaks requiring detailed analysis. This screening process considers such items as break size, orientation and location, which can be used to eliminate certain breaks from consideration. For example:

- o Breaks with concrete floors interposed between the break location and the sump need not be considered if no path exists by which generated debris can migrate to the sump.

- o Breaks for which the expanding fluid jet does not impinge on insulated targets need not be considered. The quantity of debris generated by pipe whip/pipe impact is minor and will not produce sump blockage effects as severe as postulated ruptures which target large insulated areas with the escaping fluid jet. (Refer to Appendices A through E. The debris summary tables indicate the quantities of debris generated by each mechanism.)

- o Small diameter breaks in the same location and with orientations similar to large diameter breaks can be assumed to provide less severe degrees of sump blockage. Small diameter pipes will produce lower energy jets whose expansion at any axial distance produces smaller jet diameters with corresponding reductions in the quantities of debris generated.

- o Breaks which do not result in ECCS actuation need not be considered since the recirculation mode will not be activated.

- o Generally, longitudinal breaks need not be considered since circumferential pipe failures produce greater impingement forces over greater areas. Analysis of longitudinal failures is required only in those cases where postulated circumferential pipe failures do not target large areas of containment accommodating insulated targets.

The PRL's selected for analysis should be obtained in the following manner:

a. From the FSAR, identify all PRL's within containment for both restrained and unrestrained piping. In addition, determine the orientation (circumferential or longitudinal) of each break.

b. From the breaks identified above, select those which are:

   (1) Large diameter (i.e., hot legs, cold legs, crossover, etc.)

   (2) Oriented toward locations of large, insulated targets (i.e., steam generators, pressurizer, reactor coolant pumps, primary system piping, insulated tanks, etc.)

c. By inspection, select four or five major or limiting high energy pipe breaks for further analysis. Without performing a detailed analysis at this point, determination of the angle of divergence (using the Attachment 2 procedure) may be useful in selecting the break location which targets the greatest number of large, insulated targets. Superposition of the divergence angle on the piping system at each break location is a means of rapidly determining those breaks most likely to impact the greatest number of large insulated targets. The overriding concern is to select those breaks that can result in a maximum quantity of insulation debris.

d. Depending on containment design, equipment layout and recirculation sump placement, the postulated ruptures may be limited to the steam generator cavity or annulus region or may be required in both regions. Select ruptures so as to maximize the transport of debris to the sump during either short term or long term transport.

At this point in the analysis, the number, orientation and location of the postulated ruptures for the debris study should have been established.

3.0 INSULATION DEBRIS GENERATION

Following the evaluation of design basis break locations and selection of major breaks (Section 2.0), the amount of insulation debris generated by postulated failure at each location must be estimated. Three mechanisms (pipe whip, pipe impact and jet impingement) are postulated for insulation debris generation.

3.1 Pipe Whip

The discharge of high pressure and temperature fluid following a circumferential complete pipe rupture causes large, unbalanced forces to develop on unrestrained pipe segments. Where piping restraints are provided, such that pipe motion is limited, no insulation debris would be generated due to pipe whip.

For conservatism in this analysis, all insulation on the ruptured segment(s) between the break location and the plastic hinge is assumed to constitute debris. (See Section 4.1 for transport of pipe whip generated debris.) A plastic hinge is assumed to form in conformance with the guidance provided in Ref. 1. The development of a plastic rather than elastic hinge permits greater pipe motion and consequently results in increased number of insulation targets. If desired, a detailed finite element piping stress analysis can be performed to determine the actual hinge type formed, thereby providing a means to estimate the amount of conservatism in this assumption.

The free end segment(s) move(s) through an arc defined by the piping segment geometry, the direction of the reaction force and the location of the plastic hinge. Impact of the free end segment(s) on other piping or equipment gives rise to the second mechanism of debris generation, namely, pipe impact.

3.2 Pipe Impact

The pipe impact will generate additional insulation debris. For this analysis, it is assumed that five fabrication lengths of insulation are dislodged: two lengths upstream and two lengths downstream of the impact point, and one length at the point of impact. The assumption of five fabrication lengths (a total of 10 to 15 linear feet) of insulation is used to estimate the debris generated by pipe impact, given the lack of actual data or related information. As such, it is only an assumption, the accuracy of which would have to be verified by analysis of the transient pipe impact event. In addition, following the guidance of Ref. 1, the impacted pipe may then rupture and thus become another source of insulation debris generation. If this is the case, the additional pipe(s) are analyzed in exactly the same manner as the initiating event.

3.3 Jet Impingement

During the motion of the ruptured segment(s), a fluid jet exits at the break plane and expands into the containment volume. This jet may possess sufficient energy to further dislodge pipe and equipment insulation.

While the duration of actual pipe motion is short, all targets which intercept the jet must be analyzed for debris generation due to impingement by the high energy fluid jet.

In the case of restrained pipes, the direction of the fluid jet is known and varies in accordance with the FSAR analysis submitted. The principal effects and magnitudes of the jet forces, such as the stagnation pressure which varies with distance and the methods for dealing with "shadowing", are presented in more detail as Attachments 2 and 3.

All targets subjected to stagnation forces in excess of 0.5 psig are assumed to contribute to insulation debris generation. A value, in this methodology 0.5 psig, is required to set a limit on axial displacement from the break plane beyond which further insulation debris generation is not considered. In Ref. 2, 0.5 psig is identified as the lower limit causing damage to fragile structural elements such as glass windows. Outdoor installations are routinely subjected to high winds, rain, sleet and related natural phenomena without damage to insulation. Thus the 0.5 psig value was selected for conservatism. Stagnation pressures greatly exceed the 0.5 psig cutoff in all the cases appearing in Appendices A through E, and consequently all insulation intercepted by the jet is assumed to constitute debris.

Although all targeted insulation components subjected to stagnation pressures in excess of 0.5 psig are assumed to contribute to debris generation, this is an unlikely event yielding greater quantities of debris than would actually occur. However, without detailed information regarding the failure mechanisms which govern the release of insulation from pipes, vessels and related components, the above assumption is expected to yield conservative quantities of debris.

The degree of conservatism of this assumption is difficult to determine because many unknowns are involved, including but not limited to:

a. The types of insulation and methods of attachment vary from plant to plant. The ability of these prefabricated panels and their attachments to withstand jet loads is untested.

b. Initial orientation of the insulation with respect to the impinging jet must be determined with special attention to the location of seams in the insulation relative to the jet.

c. The orientation, expansion and two-phase structure of the fluid jet are not readily amenable to current analysis techniques.

d. The transient nature and spatial distribution of the jet load applied on the insulation are uncertain.

For these reasons, a more detailed analytical determination of insulation debris generation via jet impingement was not warranted at this time. If an analytic model incorporating all of the above concerns were developed, the resulting quantities of generated debris would still require probabilistic assessment to account for the random nature of debris distribution. Such an assessment was not considered feasible and is beyond the scope of this document.

For jets emanating from the exit plane of whipping pipes, the jet expands as defined above but is not fixed in space. The jet is assumed to sweep along the arc traced by the motion of the free end segment(s). This is reasonable owing to the rapid development of the jet following the postulated rupture.

Jet impingement is by far the most significant of the insulation debris generation mechanisms. The travel distance, coupled with the jet divergence, results in targeting a large number of structures away from a single PRL. Thus containment layout is very important.

At this point, the quantities of insulation generated by each mechanism for each PRL would have been identified. Appendices A through E present examples evaluating expanding jets and targeted materials.

4.0 DEBRIS TRANSPORT

The mechanisms which result in transport of insulation debris within containment have been divided into two categories:

Short term transport refers to debris motion caused by the initiating event. Pipe whip, pipe impact and jet impingement mechanisms give rise to short term transport. Short term transport terminates at the end of the blowdown transient.

Long term transport begins at termination of short term transport and continues as long as the ECCS recirculation mode is active.

The ECCS recirculation mode is not activated immediately following termination of the blowdown event. For 15-30 minutes the refueling water storage tank (RWST) inventory is injected into the reactor pressure vessel (RPV) without dependence on the containment emergency sump for recirculation of water. The transport models do not treat the ECCS injection phase as a separate event for the following reasons:

a) Floating, neutrally buoyant and certain types of hygroscopic insulation are assumed to transport to the sump during recirculation system operation. (Refer to Sections 4.4.2 and 4.6.2.) The ECCS injection phase flow velocities deal only with submerged debris.

b) While local velocities in the immediate vicinity of the break are high, velocity drops sharply with increased distance from the break location due to the expanding area available for flow. For typical ECCS flow rates of 8000 gpm and post-LOCA containment water levels (before ECCS injection, i.e., inventories of primary system, passive safety injection tanks and steam generator) of 6 inches, velocities 10 feet from the break location are approximately 0.6 ft/sec. Table 5 indicates the effect of this velocity on densities and sizes of debris. The table indicates that only small debris particles (less than 3 in. dia.) will move. These particles can roll to the screens but due to the presence of curbing will not block the screens.

c. As the table indicates, large sump area blockages will not occur as large sunken debris cannot be transported to the screen.

4.1 Short Term Transport - Pipe Whip

Pipe whip is considered part of the initiating event for unrestrained pipes. As identified previously, the pipe insulation from the break location to the point of rotation (plastic

Table 5

Particle Motion at $\bar{V}$ = 0.6 ft/sec

Particle	R or L in.	W in.	H in.	V_{M_3} ft^3	F_A lbf	F_N lbf	F_M lbf	Motion
Sphere	1/4	-	-	3.8×10^{-5}	5.6×10^{-4}	-	-	Yes
Sphere	1/2	-	-	3.0×10^{-4}	2.26×10^{-3}	-	-	Yes
Sphere	1	-	-	2.4×10^{-3}	9.07×10^{-3}	8.74×10^{-3}	5.24×10^{-3}	Yes
Sphere	1.5	-	-	8.18×10^{-2}	2.04×10^{-2}	3.97×10^{-2}	2.38×10^{-2}	No
Sphere	2.0	-	-	1.9×10^{-2}	3.6×10^{-2}	1.06×10^{-1}	6.37×10^{-2}	No
Block	1.0	1	1	5.7×10^{-4}	2.9×10^{-3}	1.347×10^{-3}	8.08×10^{-4}	Yes
Block	12	3	12	.25	.104	1.73	1.039	No
Block	12	3	6	.125	.104	.814	.488	No
Block	12	3	3	.0625	.104	.354	.212	No
Block	24	3	12	.5	.209	3.46	2.079	No
Block	24	3	6	.25	.209	1.628	.976	No
Block	24	3	3	.125	.209	.709	.425	No

Notes: Equations 14, 17, 18 and 19 with

ρ_w = 62 lbm/ft^3
C_D = 1.2 -
ρ_m = 12 lbm/ft^3
ρ_T = 130 lbm/ft^3
A_p = πR^2 or L x W ft^2
$\bar{V}$ = 0.6 ft/sec
μ_f = 0.45 -
F_L = F_A lbf

Where

V_M = volume of insulation (including voids)
F_N = normal force
F_A = force available to cause motion
F_M = force required to cause motion
If $F_M > F_A$ no motion occurs

hinge) is assumed to form debris. This is reasonable as no forces are transmitted beyond the plastic hinge. The affected insulation quantity is, therefore, the insulation attached to the moving pipe segment(s). This debris is assumed to be transported in a direction tangent to the arc of rotation at the point where rotation stops due to impact with other pipes, containment structures or process equipment. For cases where impact does not occur, the insulation is assumed to be distributed uniformly along the arc of rotation but ejected in a direction normal instead of tangent to the arc.

In either case, the velocity of the ejected debris is assumed sufficient to cause the debris to move in a straight line. For the pipe whip mechanism, the force which accelerates the debris is applied only while the debris is in contact with the moving pipe segment. Consequently, the insulation debris will move in a straight line after separation with the pipe segment.

Section 4.1 describes how to determine:

a. Quantity of insulation debris formed by pipe whip

b. Direction of debris after separation from pipe

c. Point of impact on containment walls, structures or equipment.

Illustrative examples are provided in Appendices A through E.

Finally, all insulation generated by pipe whip is assumed to drop vertically after impact with structures and equipment, as external forces are no longer acting on the insulation debris. The debris is essentially acting as a projectile and will terminate its motion upon contact with the containment structure or equipment. For debris ejected normal to the arc of rotation of the whipping pipe, the insulation will be entrained in the fluid jet and is therefore discussed in Section 4.3.

4.2 Short Term Transport - Pipe Impact

Unrestrained moving pipes can impact other piping or equipment and, in so doing, dislodge insulation which adds to the total debris within containment. This is called the pipe impact debris generation mechanism. The extent of debris generation is assumed to be two fabrication lengths on either side of the point of impact plus one length at the point of impact.

For block insulation, banded to large diameter pipe or process vessels, the failure of five banded segments is assumed, one at the point of impact and two on either side.

The direction of pipe impact generated debris is assumed tangent to the arc of rotation of the impacting pipe segment at the point of impact. The velocity vector of the impacting pipe is in this direction, and it is assumed that the resulting debris would travel in essentially the direction of the applied force.

Velocities of the debris are assumed sufficient to cause motion in a straight line until impact occurs with walls, equipment or other structures. The debris is then assumed to drop vertically until reaching a floor, grate or other support. No external force acts on the debris after pipe impact, and the debris will be stopped by impact with structures or equipment within containment. In the absence of external forces, the debris would fall under the action of gravity. For debris generated by pipe impact which is entrained by the fluid jet exiting a pipe segment, refer to Section 4.3.

4.3 Short Term Transport - Jet Impingement

It is virtually impossible to determine with a sufficient degree of accuracy the stagnation pressure required to dislodge insulation from pipes, vessels, etc., without applicable data. However, a cut-off value of 0.5 psig is conservatively assumed. Insulation experiencing stagnation pressures greater than or equal to this value is assumed to add to the debris formed by other mechanisms.

Attachment 2 is a stepwise procedure for determining thrust, jet expansion angle and stagnation pressure function, given piping system pressure and enthalpy. The procedure of Attachment 2 is based partly on Refs. 3 and 4, with modifications to suit this methodology, and is shown in Figure 1.

The stagnation pressure function is included to compute the pressure within the jet cone as a function of axial distance from the break exit plane. The divergence angle is computed to determine the rate at which the jet expands.

Knowing the diameter of the postulated piping failure, and the divergence angle and stagnation pressure function as computed in Attachment 2, the distance to the 0.5 psig stagnation plane can be determined. This distance, also illustrated in Figure 1, determines the zone of influence of the jet exiting the postulated rupture.

Given the jet angle and stagnation pressure equation as developed in Attachment 2, the distance from the break exit plane to the 0.5 psig stagnation region can be determined. This, along with plan, elevation and isometric drawings of the containment, permits determination of the targeted components and consequently the amount of insulation debris generated.

Figure 1

Jet Divergence Angles

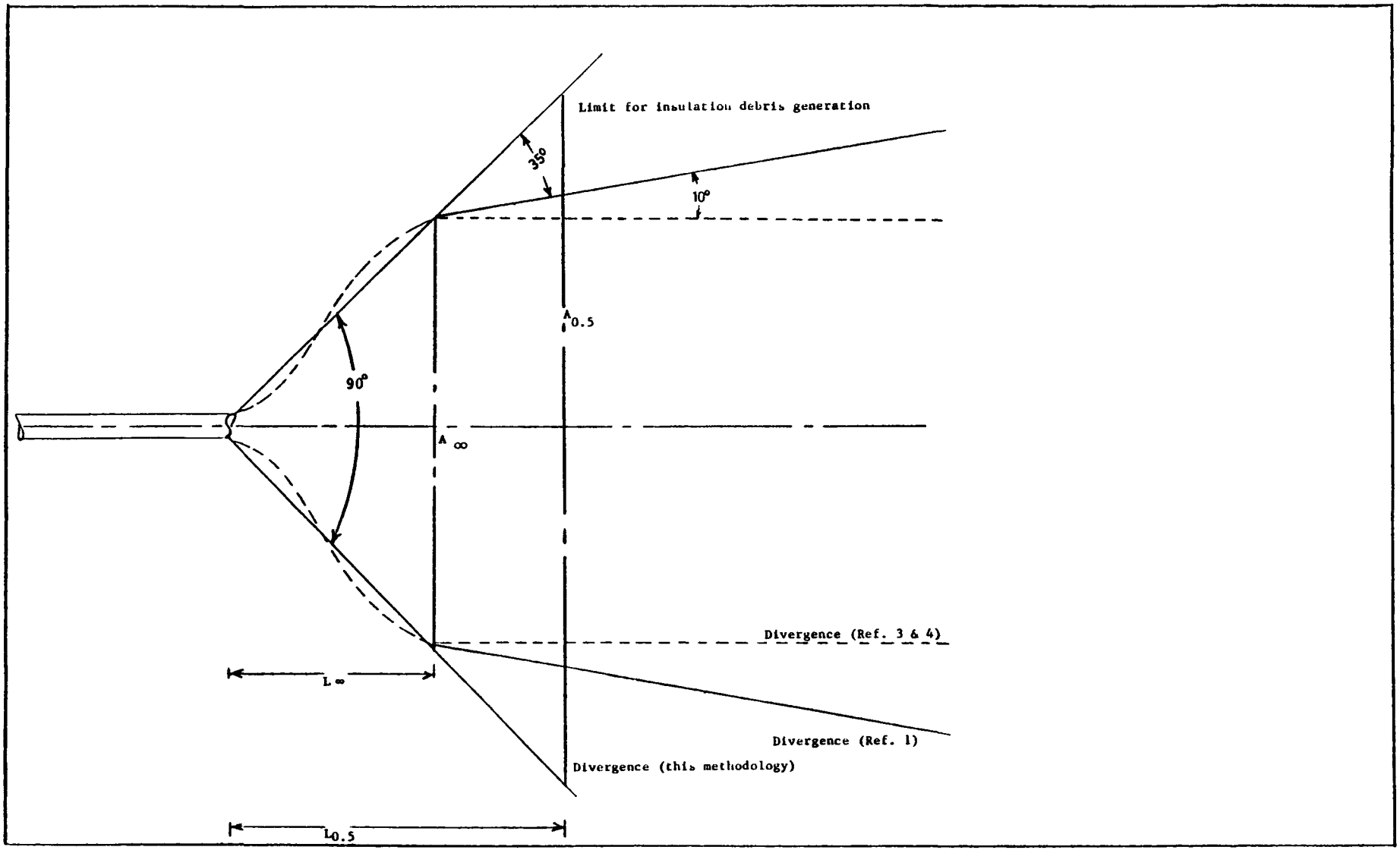

For obscured or "shadowed" jets, the procedure in Attachment 3 is used to define thrust, jet expansion angle and stagnation pressure function. Using either Attachment 2 or 3 and the 0.5 psig stagnation pressure, the quantity of insulation debris can be determined.

The insulation debris is initially assumed to be uniformly distributed within the jet cross section at all axial distances from the break plane. Actually, some debris would be accelerated in tangential and radial directions. However, the magnitude of these accelerations is based on factors not readily quantifiable, including orientation of the debris surfaces with respect to the applied jet force, nature of the jet phases (for two-phase jets), shape of the debris and local perturbations of the jet velocity due to flow around structures, components and equipment within containment.

Of even greater significance is the lack of knowledge of how insulation is released from intercepted surfaces. The orientations of debris particles can be greatly influenced by the failure mechanisms associated with jet impingement.

These uncertainties make the precise analytic determination of actual debris trajectories impossible. Therefore, it is assumed that insulation debris initially distributes itself randomly within the jet. If the long term transport calculations indicate that the debris ejected through doorways, hatches, vents, etc., has a substantial impact on sump performance, the assumption of uniform distribution must be reexamined. It is recommended that the procedure of Attachment 6 be followed to estimate the degree of non-uniformity in the debris distribution within the jet and the short term transport by jet impingement calculation be revised. If the long term transport and sump evaluations still find acceptable NPSH margins, the analysis can be considered acceptable.

The jet impingement induced debris does not stop at walls. The jet stagnates at the wall with a pressure determined by the stagnation pressure equation. As this represents a non-equilibrium condition, the flow moves parallel to the surface on which the axial motion of the jet stagnated. Again, insulation debris is initially assumed uniformly distributed within the jet.

Insulation debris can pass through doorways, hatches, etc. if the jet encounters such openings. As the insulation is initially assumed to be uniformly distributed throughout the jet cross section, the portion exiting the ventway is equal to the total debris amount multiplied by the extended vent-to-jet area ratio. Figure 2 illustrates the impingement of a jet on a structure having openings and defines the concept of an extended vent. The percentage of the insulation flowing through the

Figure 2

Jet Flow through Openings

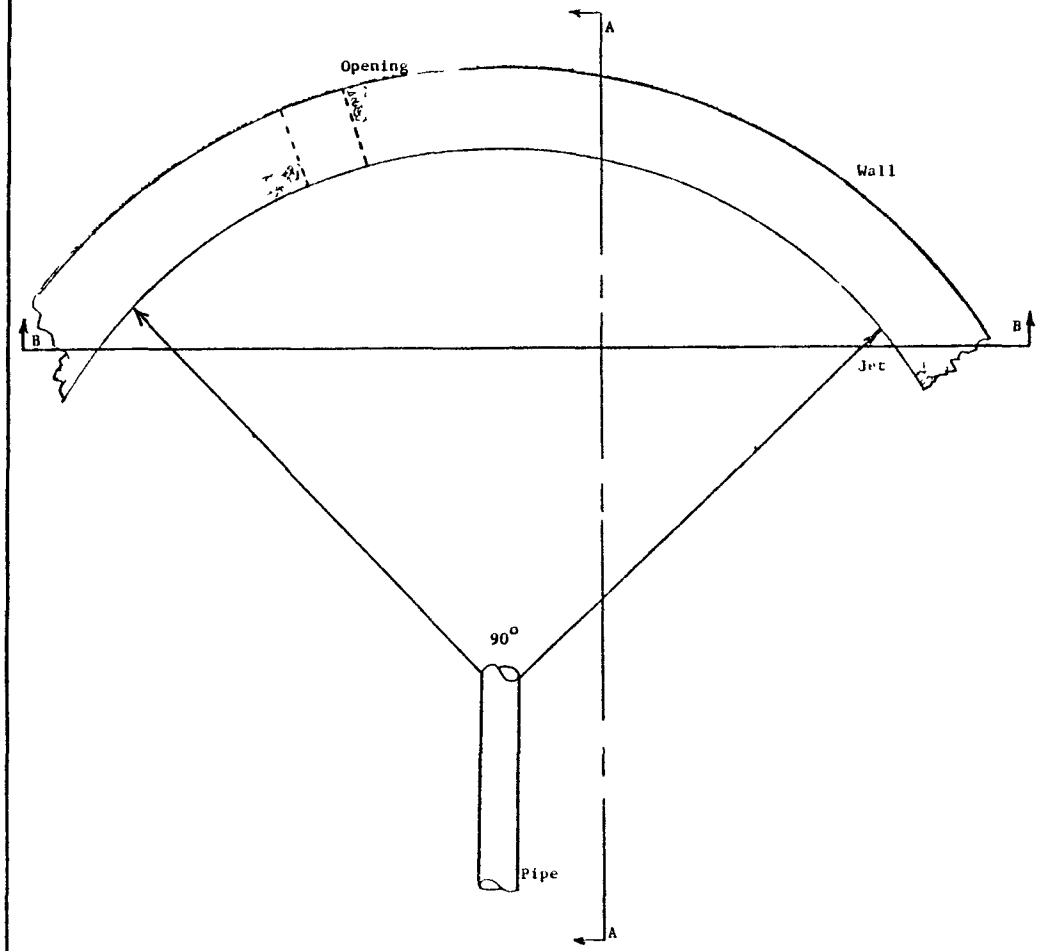

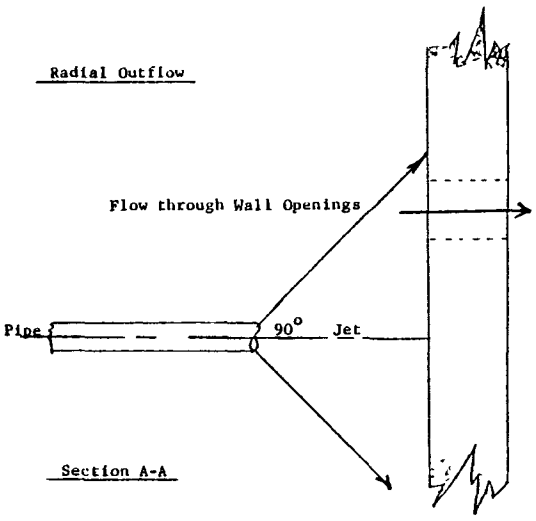

Radial Outflow of Stagnated Jet

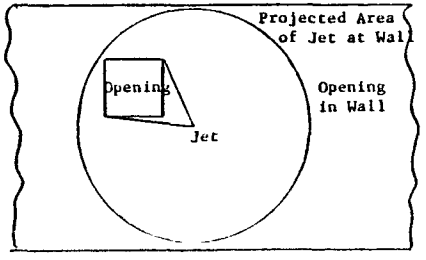

Section B-B

The extended vent includes the area of the triangle formed by connecting the outermost vent corners with the jet centerline. The debris within this triangle plus that within the vent area is assumed to exit the vent. The total debris is then: Debris ejected = Total debris x[Vent area + extended area vent]/jet area.

opening is given as the ratio of the extended opening area to the jet cross sectional area at the plane of impact (see Figure 2, Section B-B).

No stagnation of the radial outflow is assumed to distort the pressure field at the plane of stagnation. This is reasonable owing to the large ventways in the crane wall which would allow the radially flowing fluid a path to escape.

Even if vent paths for the radial outflow do not exist, no increase is expected in debris carryover through the openings. The direction of motion is radially outward from the center of the jet. A change of direction without externally applied forces would be required for additional debris to pass through the opening (see Figure 3 and Section A-A). The debris particle following trajectory T1 will, when striking the wall, be subjected to a force tending to move it away from the opening while the debris particle following trajectory T2 will pass through the opening.

For doorways, etc., within the radial flow zone of a stagnated jet, the insulation debris exiting the ventway is equal to the total debris amount multiplied by the ratio of the angle subtended by the vent to 360°. Again the debris velocity is assumed sufficient to cause straight line motion. Figure 4 illustrates this situation. The jet stagnates on the wall and radial outflow results. The arc subtending the door opening divided by 360° represents the fraction of the debris which exists the area. (Openings not in the immediate vicinity of the stagnated jet may pass additional debris. The specific plant layout will determine the possibility of multiple paths for jet ejected debris.)

4.4 Long Term Transport - Recirculation Phase

4.4.1 Background

The postulated rupture of primary system piping in a PWR results in rapid depressurization of the RPV with consequent loss of core cooling ability. The safety injection phase of PWR operation provides for the immediate post-LOCA cooling requirements of the core while the residual heat removal (RHR) system accomplishes long term core cooling. It is with the RHR portion of post-LOCA ECCS operation that the long term transport model concerns itself.

Following the ECCS safety injection phase when the contents of the RWST are injected into the RPV, system valving is aligned to provide for a recirculating flow of water to the core.

FIGURE 3

STAGNATION WITH CONSTRICTED RADIAL OUTFLOW

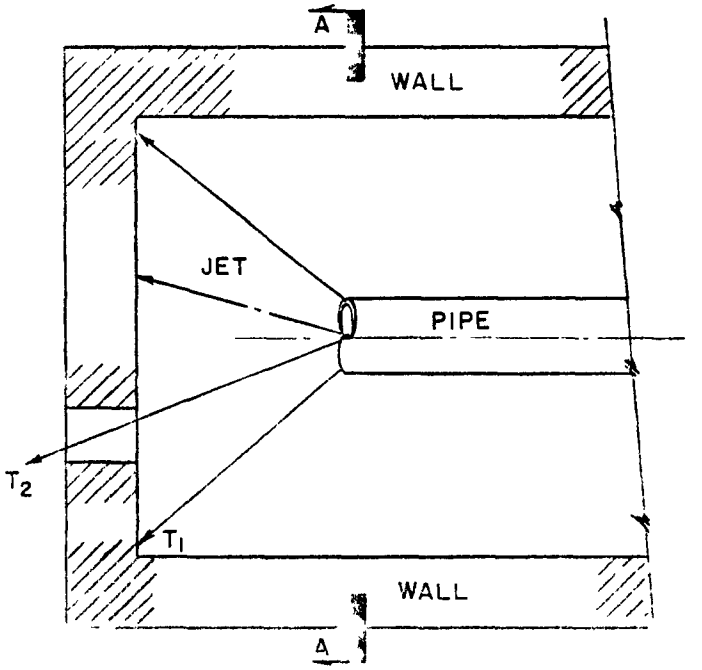

PLAN

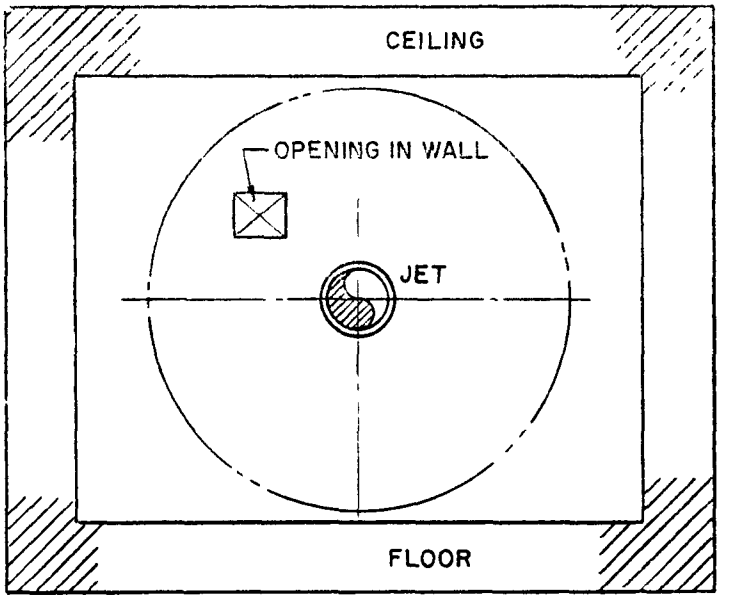

SECTION A-A

NOTES:

T_1 - TRAJECTORY OF DEBRIS PARTICLES HITTING WALL.

T_2 - TRAJECTORY OF DEBRIS PARTICLES PASSING THROUGH OPENING.

Figure 4

Radial Outflow through Doors

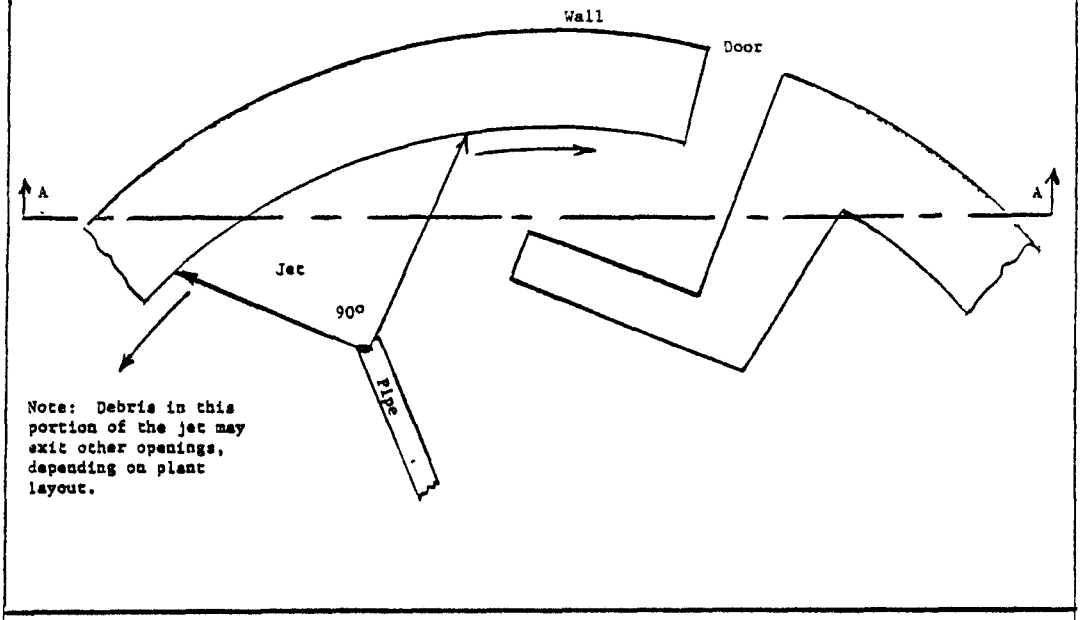

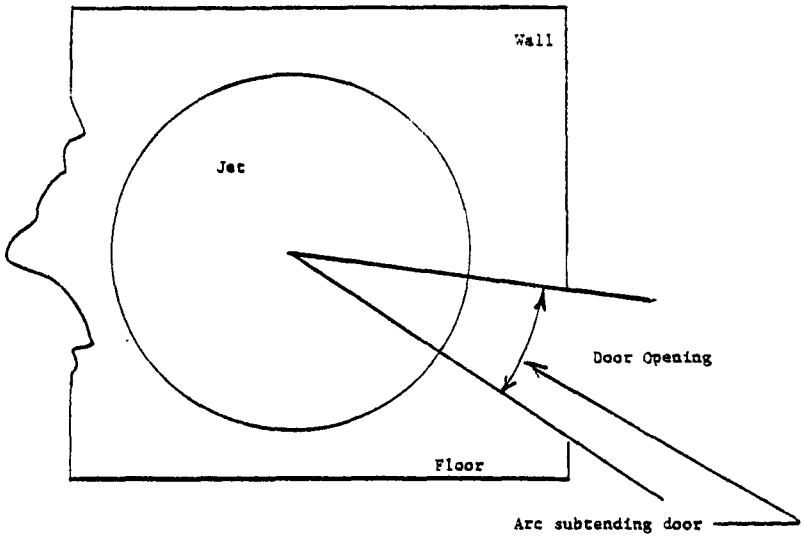

Section A-A

Fraction ejected is $\frac{\text{arc subtending door}}{360}$

Following the ECCS safety injection phase when the contents of the RWST are injected into the RPV, system valving is aligned to provide for a recirculating flow of water to the core.

The RHR pumps take suction from a sump inside containment, pass the flow through a heat exchanger to reduce the water temperature and inject the cooled flow into the RPV. This cooled water, after absorbing heat from the core, cascades through the primary system break onto the containment floor. From here the water is returned to the sump, and the cycle is repeated. The flow from the break to the sump is capable of entraining insulation debris and blocking the sump screens.

Since the recirculation sump is generally not isolated by barriers from the LOCA, the object of the long term transport analysis is to establish migration patterns for insulation debris within containment. The flow pattern within containment is complex due to the presence of equipment supports, shield walls, openings in compartments, floor slopes and related hydraulic resistances. The method of Section 4.4.1.1 may be used to estimate recirculation flow velocities within various regions of containment; it includes the following simplifying assumptions: water cascading from the break location eventually migrates back to the recirculation sump, no stagnant areas within containment exist, and transport velocity is sufficient to deliver floating debris to the sump screens. These assumptions are considered to produce an upper bounding limit on the quantity of floating debris reaching the sump screens.

The transport mechanism for sinking debris is complex because of the presence of hydraulic resistances. Accordingly, the following assumptions apply to sinking debris: the force required to transport sinking debris (see Section 4.5) is given as the product of the coefficient of friction between the debris and the floor and the normal force exerted by the debris on the floor surface. Buoyancy and lift effects are included in the determination of the normal force.

4.4.1.1 Containment Flow - Recirculation Mode

During the recirculation phase of ECCS operation, water from the containment sump is withdrawn by the RHR pumps, cooled in the RHR heat exchanger and returned to the containment via the safety injection system and the containment sprays.

Assuming that all return flow is via the safety injection system maximizes the local velocities within the crane wall where most insulation debris is generated, which, in turn, increases the liklihood of debris transport. This assumption is conservative with respect to debris transport to the sump.

Flow within containment is assumed to be represented by a number of parallel open channel flows. Accordingly, pressure drop from the break region to the sump is constant for each flow path, and the summation of mass flows through the various paths equals the break flow rate which, in turn, equals the pump flow rate. Figure 5 illustrates the above assumptions. Flows are assumed to exit all ventways in the crane wall. The magnitude of the flow rate through each vent is dependent upon the hydraulic resistance presented by the path. This section defines the hydraulic resistance and provides a means of estimating each pathway's flow rate. For incompressible flows:

$$\Delta P = \rho \frac{K}{2g_c} V^2 \qquad [1]$$

$$\bar{V} = \frac{m}{\rho A} \qquad [2]$$

$$\Delta P = \frac{K}{2g_c \rho} \frac{m^2}{A^2} \qquad [3]$$

where

P - pressure drop - lbf/ft^2

ΔK - hydraulic resistance coefficient - -

g_c - Newton's constant - $lbm\text{-}ft/lbf\text{-}sec^2$

Figure 5

Flow within Containment

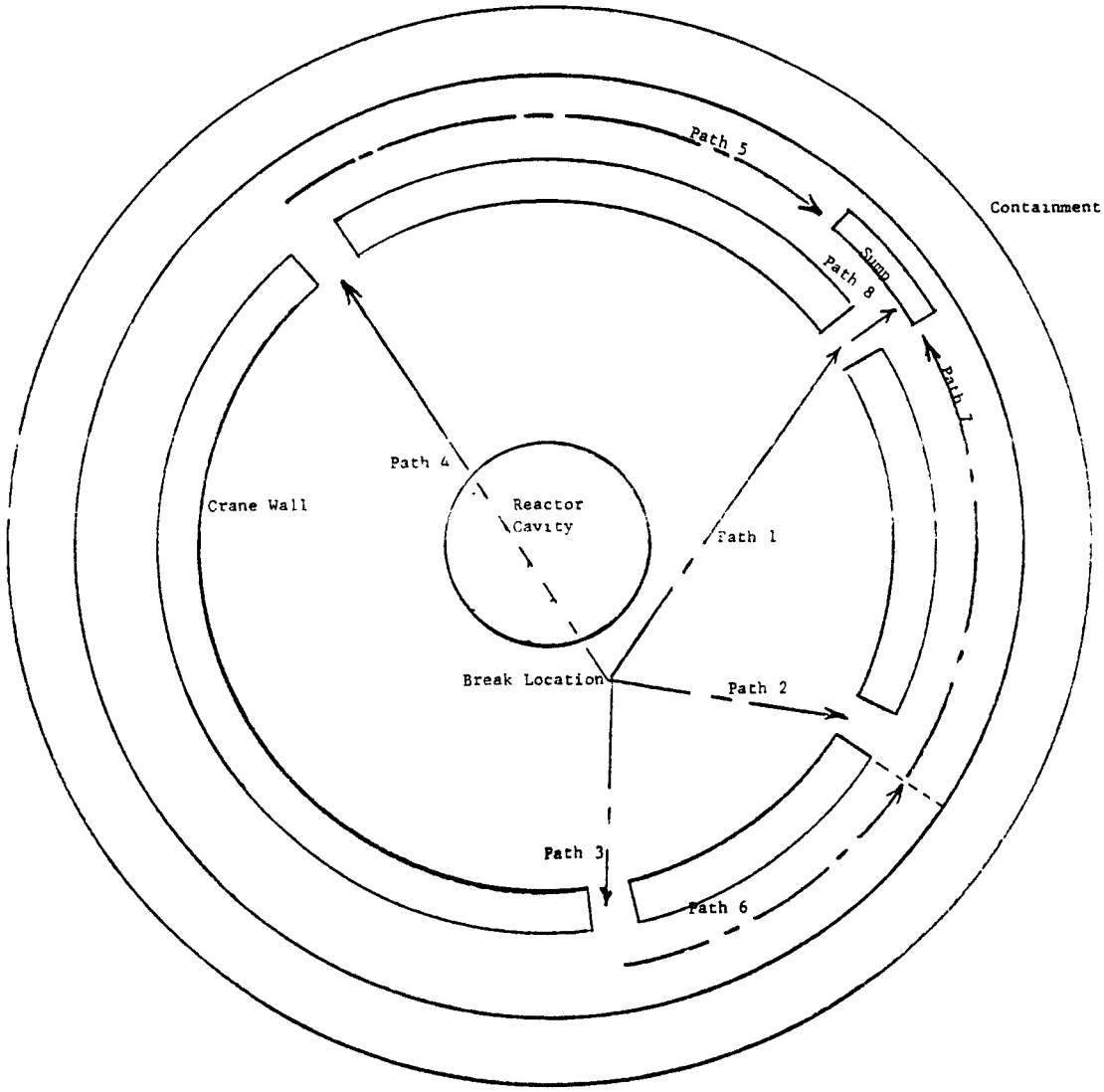

ρ	- density of fluid	- lbm/ft^3
A	- flow area	- ft^2
$\dot{m}$	- mass flow rate	- lbm/sec
$\bar{V}$	- velocity of flow	- ft/sec

A resistance network for the flows in Figure 5 can be constructed as follows where resistances R1 through R8 correspond to flow paths 1 through 8 in Figure 5.

Network 1

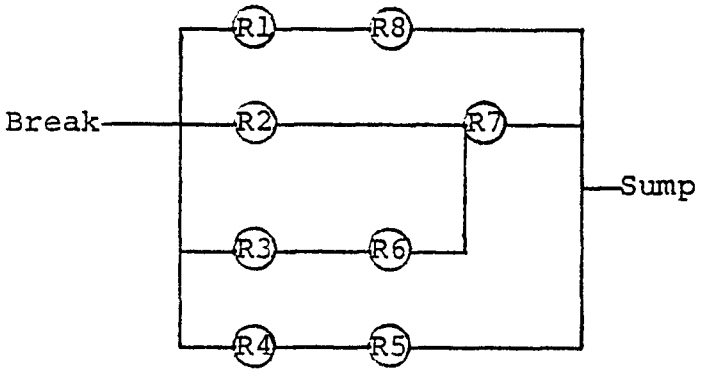

The flow, $\dot{m}$ is known and is equal to ECCS flow rate. Defining C as $\frac{1}{2g_c\rho}$, Equation 3 can be rewritten as:

$$\Delta P_i = C\frac{K_i}{A_i^2}\dot{m}_i^2 \qquad [4]$$

where

ΔP_i	- pressure drop path i	- lbf/ft^2
C	- defined above	- -
K_i	- hydraulic resistance coeff. of path i	- -
A_i	- area of path i	- ft^2
$\dot{m}_i$	- mass flow rate through path i	- lbm/sec

The hydraulic resistance, K_i is determined as follows:

$$K_i = \frac{fL}{D_H} \qquad [5]$$

where

f	- friction factor (velocity function - Ref. 3)	- -
L	- path length	- ft
D_H	- hydraulic diameter	- ft

and the hydraulic diameter, D_H, is given as:

$$D_H = 4 \times \frac{\text{Area of stream}}{\text{Wetted perimeter}}$$

Setting $C\frac{K_i}{A_i^2}$ equal to R_i, the branch resistance, a network can be reduced to a single equivalent resistance by application of Equations 6 and 7 to each branch.

Determination of Equivalent R

The following rules apply:

Resistances in series add.

Resistances in parallel follow the reciprocal law.

Given

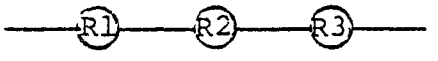

$$R_{equivalent} = R1 + R2 + R3 \qquad [6]$$

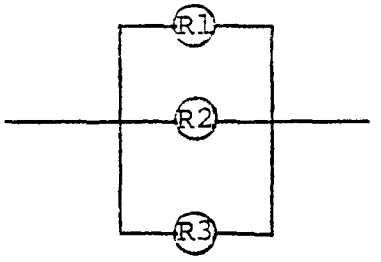

$$R_{equivalent} = \left[\frac{1}{\sqrt{\frac{1}{R1}} + \sqrt{\frac{1}{R2}} + \sqrt{\frac{1}{R3}}}\right]^2 \qquad [7]$$

The series resistances in the network are reduced as follows:

Combine R1 + R8 = RA

Combine R3 + R6 = RB

Combine R4 + R5 = RC

The network is now:

Network 2

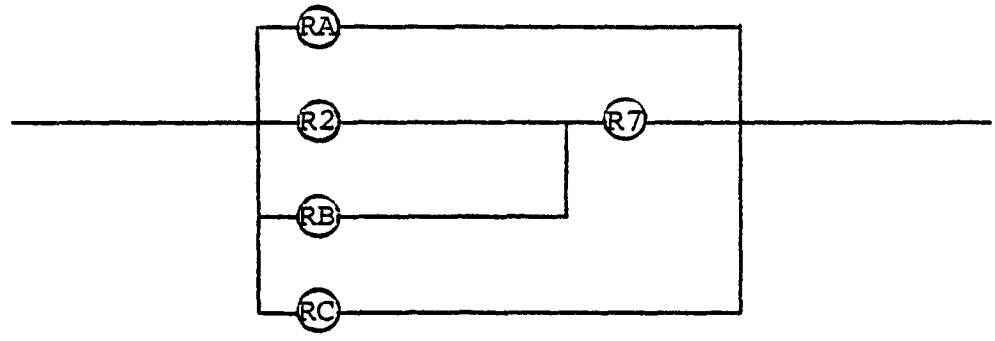

Combining parallel resistances R2 and RB

$$RD = \left[\frac{1}{\sqrt{\frac{1}{R2}} + \sqrt{\frac{1}{RB}}}\right]^2 \qquad [8]$$

The network is now:

Network 3

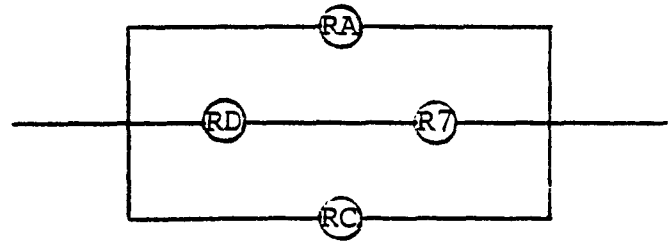

Combining RD and R7, RE = RD + R7. [9]

Giving the network

Network 4

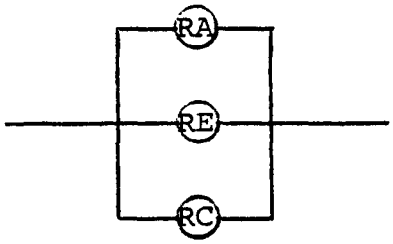

which is reduced to $R_{equivalent}$ as:

$$\left[\frac{1}{\sqrt{\frac{1}{RA}}+\sqrt{\frac{1}{RE}}+\sqrt{\frac{1}{RC}}}\right]^2 = R_{equivalent} \qquad [10]$$

Referring to Equation 4,

$$\Delta P_{total} = R_{equivalent}\, \dot{m}^2_{ECCS} \qquad [11]$$

This gives ΔP overall.

Referring to Network 1, ΔP_{total} across resistances R1 and R8 can be used to determine flow through this branch as follows:

$$\Delta P_{total} = (R1 + R8)\dot{m}_i^2 \qquad [12]$$

or

$$\dot{m}_i = \sqrt{\frac{\Delta P_{total}}{(R1 + R8)}} \qquad [13]$$

By similar applications of the hydraulic equations, all mass flows can be determined, and path velocities are determined from Equation 2.

Notes:

ΔP_{total} - is the overall network pressure drop from which the individual branch flows can be determined.

K_i - varies depending on the geometry of the flow paths (submerged rectangular openings, open channel flow, etc). Ref. 5 provides methods of determining K_i for various geometries.

This method takes no account of recirculated flows within various compartments, flow around obstructions, etc. For an analysis of this nature such refinements are considered unwarranted.

4.4.2 Debris Class

The insulation debris is divided into the following classes:

Sinking	Floating
Reflective Metallic	Nonhygroscopic
Metallic Jacketing	Hygroscopic
	Fibrous

Generally, sinking debris is transported to the sump if fluid drag caused by local containment velocities is sufficient to overcome frictional forces when buoyancy and lift forces are considered. Floating nonhygroscopic debris is assumed to transport to the sump, and floating hygroscopic insulation is assumed to transport as described in Section 4.6.2. Fibrous debris is assumed to transport as described in Section 4.7.

4.4.2.1 Reflective Metallic

Reflective metallic insulation, while having a bulk density less than that of water, will sink as it is not sealed against water infiltration.

4.4.2.2 Metallic Jacketing

Several types of insulation are protected from mechanical abuse with metal (stainless steel or aluminum) jackets. These jacketing materials will sink.

4.4.2.3 Nonhygroscopic

Unjacketed nonhygroscopic insulation will remain afloat indefinitely if the insulation density is less than that of water. Jacketed or totally encapsulated nonhygroscopic insulation will float if the density of the composite is less than that of water.

Neither will be taken into the pump if the water level in containment is such that the intake screens are completely submerged. For sump screens which are not completely submerged, refer to Section 4.6.1.

4.4.2.4 Hygroscopic

Whether unjacketed hygroscopic insulation floats depends upon its equilibrium moisture absorption and resulting density. Equilibrium densities greater than that of water produce sunken debris while densities less than water produce floating debris. Should equilibrium density approach that of water, the debris is assumed neutrally buoyant. Unjacketed or totally encapsulated hygroscopic insulation will float if the equilibrium density of the composite is less than that of water.

4.4.2.5 Fibrous Insulation

With encapsulated or jacketed fibrous insulation, the buoyancy of the water-saturated, metal jacketed, fiber filled composite structure will determine if the material floats. Unencapsulated fibrous insulation will form floating floc, slowly settling individual fibers and flocs which sink immediately (Ref. 6). (Refer to Section 4.7.)

Section 5.2.1 discusses pressure drop from beds of incompressible solids. Section 5.3 discusses pressure drop due to accumulation of fiber floc, and Section 5.4 discusses pressure drop arising from accumulations of individual fibers which form compressible mats. These methods are applicable regardless of the debris particle density.

4.5 Transport - Sinking Debris

The determination of whether sinking debris is transported to the recirculation sump is a two-step process. The first step involves the determination of the force required to cause motion and the second involves determination of the force available to cause motion.

4.5.1 Force Required to Cause Motion

$$F_M = \mu_f F_N \qquad [14]$$

where F_M - force required to cause motion

μ_f - coefficient of static friction

F_N - normal force (exerted by the debris as modified by lift and buoyancy effects)

4.5.2 Normal Force

For an arbitrarily shaped particle of density ρ_m and volume $\forall_M$ the normal force is determined as follows:

4.5.2.1 Nonhygroscopic Materials, No Voids

$$F_N = (\rho_m - \rho_w)\ \forall_m \frac{g}{g_c} - F_L \qquad [15]$$

where F_N - normal force - lbf

ρ_m - density of material - lbm/ft^3

ρ_w - density of water - lbm/ft^3

$\forall_m$ - volume of material - ft^3

g - local acceleration of gravity - ft/sec^2

g_c - Newton's constant - $ft\text{-}lbm/lbf\text{-}sec^2$

F_L - lift force - lbf

4.5.2.2 Nonhygroscopic Materials, Voids Present (i.e., Reflective Metallic Insulation)

$$F_N = \sum_i (\rho_{mi} - \rho_w)\ \forall_{mi} \frac{g}{g_c} - F_L \qquad [16]$$

where F_N - normal force - lbf

ρ_{mi} - density of material for layer i - lbm/ft^3

ρ_w - density of water - lbm/ft^3

$\forall_{mi}$ - volume of material in layer i - ft^3

g - local acceleration of gravity - ft/sec^2

g_c - Newton's constant - $ft\text{-}lbm/lbf\text{-}sec^2$

F_L - lift force - lbf

Where the insulation is composed of several layers of differing materials, the above equation is used to compute the normal force, i.e., reflective metallic using stainless steel outer and inner walls and aluminum internal sheets. Where the insulation is composed of a single material, Equation 16 reduces to Equation 15. Note that the volume of the voids (air filled spaces) is ignored in Equation 16. The volume term applies only to the materials comprising the insulation.

4.5.2.3 Hygroscopic Materials

Volume fraction of material, $V_F = \frac{\rho_m}{\rho_T}$ [17]

where ρ_m - density of material - lbm/ft^3

ρ_T - theoretical density of material - lbm/ft^3

V_F - volume fraction of material in insulation - -

Equation 17 is used to determine the volume of material present in the insulation. The following equation determines the normal force for hygroscopic materials:

$$F_N = (\rho_T - \rho_w)\ V_F\ V_m - F_L$$

where ρ_T - theoretical density of material - lbm/ft^3

ρ_w - density of water - lbm/ft^3

V_F - void fraction - -

V_m - volume of material - ft^3

F_N - normal force - lbf

F_L - lift force - lbf

Depending on the materials involved and the construction of the insulation, one or more of the equations above must be used to obtain the normal force. In Sections 4.5.2.1 through 4.5.2.3, the normal force is modified by a lift force, F_L.

The final information required to use Equation 14 is the coefficient of friction between the surfaces.

4.5.2.4 Coefficient of Friction

The coefficient of friction between the debris and containment floor is a function of the material involved and the relative velocity between the surfaces. The following data is extracted from Ref. 7.

Coefficients of Friction for Use with Equation 14

Containment Floor	Debris 2	Static Coefficient of Friction	Dynamic Coefficient of Fricition
Concrete	Metal Insulation	0.45	0.3
Concrete	Fibrous Insulation	0.3	0.21
Concrete	Solid Insulation	0.6	0.42

4.5.3 Force Balances - Sunken Debris

4.5.3.1 Force Available to Cause Motion

The available force to cause motion is given by

$$F_A = \frac{C_D A_p \rho_w \bar{V}^2}{2 g_c} \qquad [19]$$

where F_A - force available to cause motion - lbf

C_D - drag coefficient - -

A_p - area of particle normal to flow - ft^2

ρ_w - density of water - lbm/ft^3

$\bar{V}$ - velocity of flow - ft/sec

g_c - Newton's constant - $lbm\text{-}ft/lbf\text{-}sec^2$

The drag coefficient is tabulated in Ref. 8 for various geometries and flow velocities and is not included here. The area normal to flow is the projected area of the particle in the direction of flow. (The two-dimensional surface an observer would see if looking at the object from the upstream side in the direction of flow.) Velocity of flow is the velocity of the recirculating flow within containment at the location of the debris as determined by Section 4.4.1.1 for the containment in general and Section 4.5.4 for the regions near the sump.

4.5.3.2 Motion of Sunken Debris

Three possible actions can occur with sunken debris: debris tumbles, debris slides, debris remains stationary. Following blowdown, the orientation of debris in containment with respect

to containment flows is unknown. Accordingly, for each of these potential motions, the following assumptions were made:

4.5.3.2.1 Debris Tumbles

Debris is assumed to have maximum suface area oriented normal to the flow. In this instance only, F_L is assumed to be zero. Equations 14 and 19 are solved, with a static μ_f used. The possibilities are as follows:

F_A exceeds F_M - motion occurs - proceed to Section 4.5.3.2.2.

F_A does not exceed F_M - motion does not occur - transport of this debris is not possible.

4.5.3.2.2 Debris Slides

Debris which moves under the 4.5.3.2.1 calculation procedure will eventually orient itself such that the maximum surface area is oriented parallel to the containment floor. As the debris is in motion, a static friction coefficient is inappropriate, and the dynamic friction factor values must be used in Equation 14. Solving Equations 14 and 19 with lift set equal to available force, two conditions exist:

F_A exceeds F_M - motion continues to occur - debris is transported to the screens.

F_A does not exceed F_M - debris which began tumbling will rest on containment floor.

4.5.3.2.3 Debris Remains Stationary

Where small quantities of debris are generated and scattered over wide areas of containment, the assumption of maximum surface area exposed normal to flow is unrealistically conservative. Rather, the orientation placing the center of gravity of the debris closest to the floor and exposing the greatest surface area of the debris particle to containment recirculation flow which is consistent with this location of center of gravity is assumed.

Again Equations 14 and 19 are solved using the static value of μ_m and assuming lift equal to available force in Equation 14. Two conditions exist:

F_A exceeds F_M - debris in motion - refer to Section 4.5.3.2.2.

F_A does not exceed F_M - debris remains in place and does not transport to the sump.

Examples of the calculations for sunken debris transport are included in Appendices A through E.

4.5.4 Velocity in the Near Sump Region

Section 4.4.1.1 provides a method for determining the mass flow rate through the various paths between the break location and the sump. As velocity is defined by Equation 20, the values of $\dot{m}$, ρ, and A must be determined.

$$\bar{V}_S = \frac{\dot{m}}{\rho A}$$

where

$\dot{m}$	- mass flow rate (for each path as determined by Section 4.4.1.1)	- lbm/sec
ρ	- fluid density	- lbm/ft^3
A	- flow area	- ft^2
$\bar{V}_S$	- velocity of flow across a specific area (at a rate of $\dot{m}$ passing through a path area A)	- ft/sec

In the containment area in general, the use of each individual open area is acceptable for determining velocity. In the region near the sump, the velocity must be based on the proximity of flow path area reductions with respect to the sump screens. Refer to Figure 6. The circulating flow in the annulus ($\dot{m}_1$) and the steam generator cavity flow ($\dot{m}_2$) combine in the annulus to produce total flow ($\dot{m}_3$). Assuming, no other flows, the velocity in the annulus upstream of pad 1 is:

$$\bar{V}_S = \frac{\dot{m}}{\rho A}$$

where

$\dot{m}$ - 1105 lbm/sec (8000 gpm ECCS rate)

ρ - 62 lbm/ft^3

A - path area upstream of pad 1 (10 ft wide by 3 ft deep)

or

$$\bar{V}_S = \frac{1105}{62 \times 30} = 0.59 \text{ ft/sec.}$$

Figure 6

Typical Annulus/Sump Region

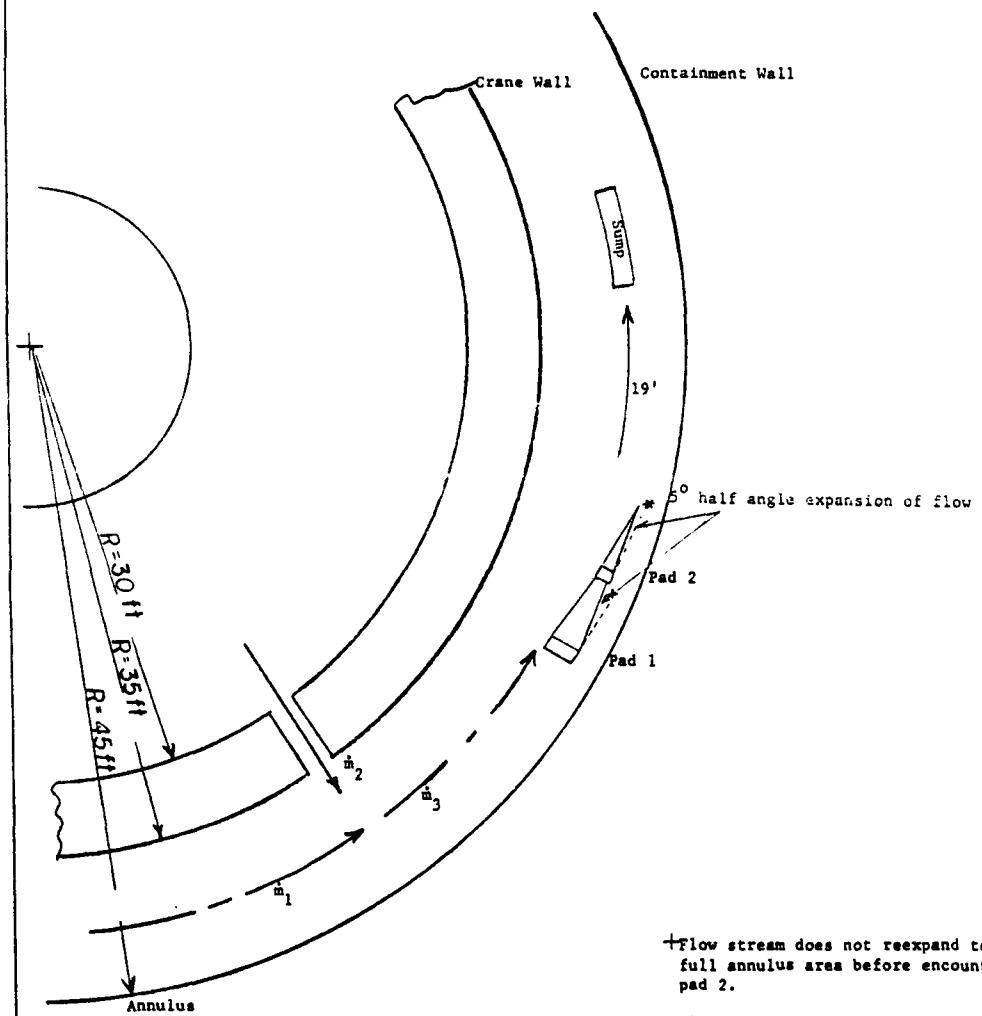

+Flow stream does not reexpand to full annulus area before encountering pad 2.

*Flow stream does reexpand to full annulus area before encountering sump.

Notes:
1) Containment water level is assumed to be 3 ft
2) Annulus 10 ft wide
3) Pad 1: 2 ft wide 2 ft from containment wall
4) Pad 2: 1 ft wide 2 ft from containment wall
5) Pad 1-Pad 2 separation 5 ft

In passing around pad 1, the flow area is reduced from 30 ft^2 to 24 ft^2 (8 ft wide and 3 ft deep). Consequently, velocity increases by 30/24 to 0.74 ft/sec. Once beyond pad 1, the flow expands to refill the entire annulus passage, but not immediately beyond the downstream edge of the pad. Rather, the flow expands with a 5° half angle of divergence as indicated on Figure 6 until the annulus path is refilled. The expansion as a function of downstream distance from an obstruction is given as:

$$E_x = L \tan (5^\circ) \text{ or } E_x = 0.0875\ L \qquad [21]$$

where

L - length downstream from obstruction - ft

5 - half angle of divergence - degrees

E_x - flow expansion downstream of obstruction (use $2E_x$ for obstructions which channel flow to center of annulus and consequently allow both sides of flow to expand) - ft

In the example given, the flow area reduction was caused by a 2 ft wide equipment pad. Consequently, the flows exiting downstream of the pad must expand 2 ft or 1 ft per path, before rejoining. Since each path expands at the rate of 0.0875 L, the downstream distance at which the paths merge, is:

$$1.0 = 0.0875\ L$$

$$L = 11.4 \text{ ft}$$

Figure 6 shows pad 2 in the flow stream 5 ft downstream of pad 1, which is before the flows have recombined. Substituting this 5 ft value into Equation 21 yields a per-stream expansion of 0.44 ft. The flow area at the upstream face of pad 2 is then:

$$[8 + 2(0.44)] \times 3 = 26.6 \text{ ft}^2$$

where

8 ft - annulus opening with pad 2 width subtracted

2(0.44)ft - two flows expanding for 5 ft

3 ft - water depth

and velocity at the upstream face of pad 2 is 0.67 ft/sec (from Equation 20 with A = 26.6 ft^2). The flows around pad 2 and any other restrictions are handled in similar fashion.

As the flow approaches the sump, the velocity is determined as developed above. For obstacles sufficiently close to the

sump screens, the flow will not expand fully, and local velocities will be higher than those based on unblocked annulus areas.

4.6 Transport - Floating Debris Non-Fibrous

If the following conditions are met, no significant downward velocity exists to cause floating debris entrainment, and no consideration of screen blockage is necessary.

a. Sump screens are completely submerged.

b. Insulation is nonhygroscopic.

c. Vortex formation does not occur.

For situations where the above conditions are not met, the analysis of potential entrainment will vary as described in the following paragraphs.

4.6.1 Sump Screens not Completely Submerged

This condition is illustrated in Figure 7. The water level in containment is insufficient to completely cover the sump screens, and consequently all floating debris reaching the sump region impinges on the screens. The following section presents a simple method of determining if floating debris that impinges on non-submerged screens is drawn further down (see Figure 8).

4.6.1.1 Floating Debris - Sump Screen not Submerged

Floating debris is assumed to migrate to the sump. Whether substantial sump blockage occurs is determined by evaluating the local velocity available to overcome the debris buoyant force and cause the debris particles to be submerged and brought to the screen face.

4.6.1.2 Criterion for Submergence of Floating Debris at Non-Submerged Screens

The criterion for determining if upstream debris particles will add to the debris cover depicted in Figure 7 or will be submerged and swept to the screen face under the debris cover as depicted in Figure 8 is defined below.

4.6.1.2.1. Velocity Require for Submergence

The velocity at which a debris particle of thickness t will be submerged is given by Ref. 9 as

Figure 7

Non-Submerged Screens

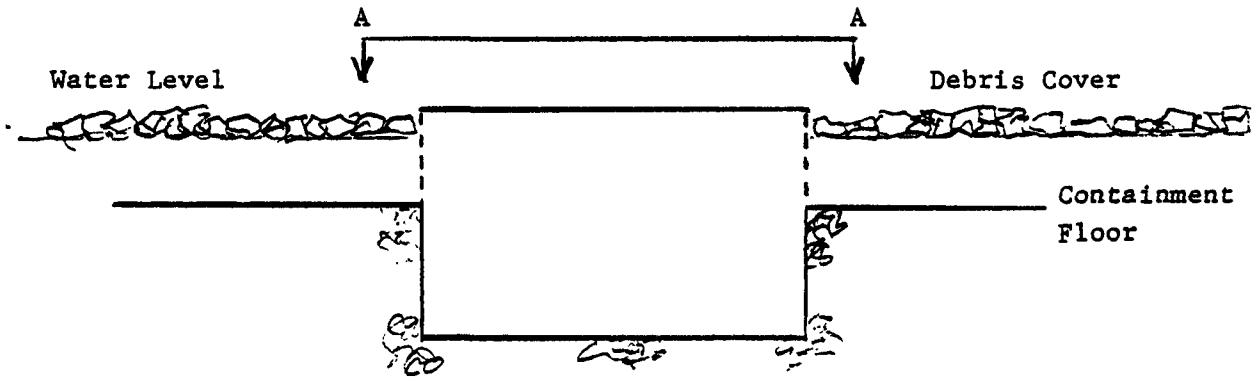

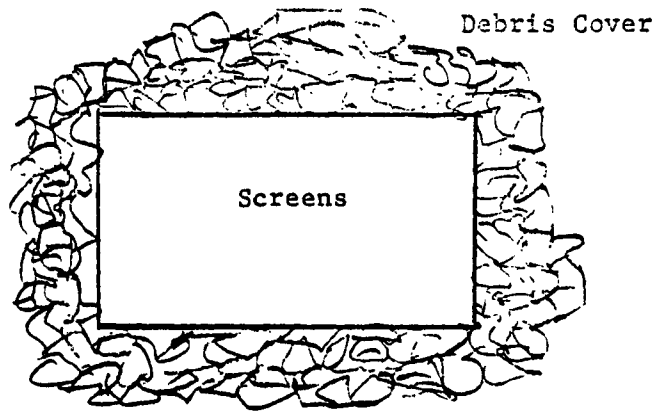

Section A-A

Figure 8

Entrainment of Floating Debris at Non-Submerged Screens

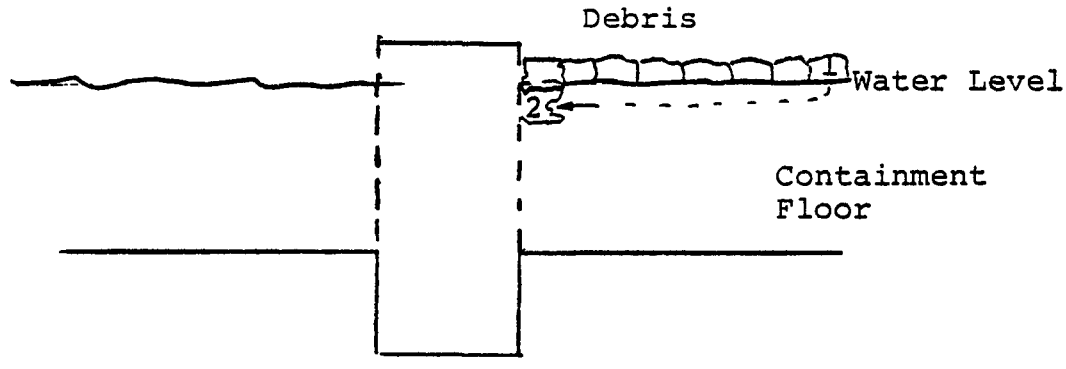

1) Initial debris position.
2) Debris after submergence.

$$\bar{V}_c = \frac{[gt(1 - \rho'/\rho)]^{1/2} [2(1 - t/h')]}{[5 - 3(1 - t/h')^2]^{1/2}} \quad [22]$$

where

$\bar{V}_c$ - velocity at which submergence occurs - ft/sec
g - local acceleration of gravity - ft/sec^2
t - debris thickness - ft
ρ - debris density - lbm/ft^3
ρ - fluid density - lbm/ft^3
h' - depth of approach flow - ft

4.6.1.2.2 Approach Velocity

Approach velocity is based on full containment water depth and localized containment area with the effects of upstream flow restriction evaluated as in Section 4.5.4.

4.6.1.2.3 Submergence Evaluation

If the local velocity as determined by Section 4.5.4 exceeds the critical velocity developed as Equation 22, the debris is assumed to transport under the debris cover and come to rest on the screens. The effect of this blockage must then be evaluated based on the procedures developed in Section 5.0. Table 6 provides critical submergence velocities as determined by Equation 22 for a number of particle sizes and water depths.

Table 6

Typical Debris Sizes and Critical Submergence Velocities
(based on Equation 22)

Thickness (in.)	Water Depth (ft)	Velocity at which Submergence occurs* (ft/sec)
1/8	2	0.72
1/4	2	1.0
1/2	2	1.4
1	2	1.9
2	2	2.4
3	2	2.7
1/8	4	0.73
1/4	4	1.02
1/2	4	1.43
1	4	1.9
2	4	2.6
3	4	3.1
1/8	6	0.729
1/4	6	1.03
1/2	6	1.44
1	6	2.0
2	6	2.74
3	6	3.25

*Assuming $\rho' = 12$
$\rho = 60$

4.6.2 Insulation is Hygroscopic

For hygroscopic insulation, a determination must be made regarding maximum water absorption and resulting density. Four conditions exist:

a. Very slow absorption - density less than water at maximum absorption

b. Very fast absorption - density less than water at maximum absorption

c. Very slow absorption - density greater than water at maximum absorption

d. Very fast absorption - density greater than water at maximum absorption

In this context, very fast absorption implies attaining equilibrium water content in 5 or 10 minutes. All other speeds are considered very slow.

Conditions a and b are considered to apply to indefinitely floating debris. Condition d is considered to apply to sinking debris. Condition c is considered to produce debris which floats long enough to reach the containment sump where it sinks. Accordingly, the condition c hygroscopic insulation must be analyzed as both floating and sinking debris, the more limiting result should be used in assessing sump effects.

4.6.3 Vortex Formation is Present

The effects of vortex formation on debris entrainment are beyond the scope of this document.

4.7 Transport - Fibrous Insulation (near neutral buoyancy)

Little information exists in the literature describing the behavior of fibrous (fiberglass, mineral wool, rock wool, etc.) insulation subjected to the conditions existing in containment post-LOCA. The method presented here for the transport of fibrous insulation is therefore conservative for the following reasons.

All free fibrous insulation generated by the pipe rupture is assumed to float and eventually migrate to the sump. While it is recognized that this assumption probably overestimates the quantity of insulation transported to the sump, no definitive data exists which would justify a reduction in the amount of insulation that is assumed to form and be transported.

It becomes necessary to characterize the condition of the fibrous insulation debris when it has migrated to the sump. Of particular interest is whether individual fibers are suspended in the flow due to failure of the insulation covering. Individual fibers are of particular concern as they have been shown in Ref. 6 to produce mats of fiber at the sump screen. With sufficient material present, the screens become rapidly plugged and cause pressure drops sufficient to exceed NPSH margins. The analysis of sump screen pressure drop due to fiber blinding (matting) is performed in two steps.

4.7.1 100% of Insulation Migrates

Under this assumption, the maximum screen head loss will be determined. All fibrous insulation dislodged by pipe whip, impact or jet impingement is assumed to be individual fibers which reach the sump screens. If the pressure drop resulting from this assumption is acceptable, it is not necessary to proceed with the Section 4.7.2 calculations. The pressure drop is then evaluated as indicated in Section 5.4.

4.7.2 Less Than 100% Migration

Ref. 6 indicates that four types of debris are formed as a consequence of LOCA jet interaction with fibrous insulation:

Type 1 - Large floating fragments 2 to 8 in. diameter
(20-30%) 0.4 to 2 in. thick

Type 2 - Fluffy fragments which immediately sink
(40-50%)

Type 3 - Fine suspended fibers
(20-30%)

Type 4 - A sand like material

Types 1 through 3 account for most of the insulation debris formed. (The figures in parenthesis represent the relative percentages.)

Ref. 6 states further that type 1 insulation will sink in the presence of hot (60°C) water sprays in 2 to 5 days. As the containment spray system is in operation following a LOCA, the necessary conditions which cause type 1 insulation to sink exist. As a delay of 2 to 5 days occurs before generated debris sinks, it is reasonable to assume that all type 1 insulation sinks in the vicinity of the sump screens. Consequently, fibrous insulation is analyzed as follows:

- o Assume 30% of the total debris sinks near the screens. Assess the entrainment possibilities as discussed in Section 4.5.

- o Assume 40% of the total debris sinks immediately. Assess the potential transport of sinking debris using velocities as determined in Section 4.4.1.1.

- o Assume 30% of the total debris forms fine suspended fibers in the containment water. Assess the transport and blockage potential according to Section 5.4.

This analysis assumes that 100% of all fibrous insulation is broken up, freeing the individual fibers. It is unlikely that all fibrous insulations will be opened and shredded, but in the absence of data to the contrary the assumption is used to ensure conservatism.

5.0 SUMP EFFECTS

The important sump effect and the major safety issue relates to additional head loss across the screens caused by debris which has migrated to the sump. Depending on the available and required NPSH, the additional head loss may create a condition of insufficient margin. The purpose of this section is to identify the additional head loss attributable to insulation debris accumulation on the sump screens. A determination must then be made, based on plant specific pump requirements, regarding the effect of this increased screen pressure drop.

5.1 Head Loss for Unblocked Screens

The expression for head loss across a resistance placed in the flow path is:

$$h = \frac{K\bar{V}^2}{2g_c} \qquad [23]$$

where h - head loss - ft of fluid

K - hydraulic resistance coefficient - -

$\bar{V}$ - velocity of flow - ft/sec

g_c - Newton's constant - lbm-ft/lbf-sec^2

The resistance coefficient is a function of screen opening area and screen Reynolds number. The expression for K (Ref. 5) then becomes:

$$K = \left(\frac{n}{c^2}\right)\left(\frac{1-\alpha^2}{\alpha^2}\right) \qquad [24]$$

where n - number of screens in series - unitless

c - screen discharge coefficient - unitless

α - fractional free projected screen area - unitless

Combining Equations 23 and 24 yields

$$h = \left(\frac{n}{c^2}\right)\left(\frac{1-\alpha^2}{\alpha 2}\right)\left(\frac{\bar{V}^2}{2g_c}\right) \qquad [25]$$

Ref. 5 gives a plot of screen discharge coefficients vs. Reynolds numbers in the range 0.1 to 10^5.

Equation 25 is used to determine the pressure loss across unblocked screens.

5.2 Head Loss Due to Debris Accumulation

5.2.1 Large, Discrete Debris

This category includes all insulation except free, suspended fibers:

5.2.1.1 Totally Impermeable Debris

Items such as metallic jacketing which are impervious to flow act as blind faces on the screens, effectively reducing the available screen area. These materials are treated as described in Section 5.1, making proper allowances for reduced screen area and attendant increased velocity.

5.2.1.2 Porous Beds of Solids

When individual particles of solids accumulate at the screen due to entrainment by the flowing fluid, a bed of material will develop, the thickness of which is dependent upon the quantity of debris generated and deposited within the near sump region (see Section 4.5.4).

This method assumes that all debris within the near sump region is sized so that it does not pass the screens. A pressure drop across the resulting bed thickness is then evaluated. The bed thickness is dependent upon bed shape which, in turn, is dependent upon sump screen configuration.

Using the mass flow rates determined in Section 4.4.1.1 and the local velocities determined in Section 4.5.4, the transport potential for sunken debris can be established. Sections 4.5.1 through 4.5.3 determine the forces required and the forces available to cause motion. For those sunken debris particles which move and are transported to the sump screens, Ref. 5 gives the following as the pressure drop across stationary beds of solids:

$$\Delta P = \frac{2 f_m G^2 \ell (1-\varepsilon)^{3-N}}{D_p g_c \rho \phi^{3-N} \varepsilon^3} \qquad [26]$$

where ΔP - pressure drop - lbf/ft^2

f_m - modified friction factor - (see Ref. 5)

G - mass flux - lbm/ft^2-sec

ℓ - bed depth - ft

ε - bed void fraction - -

N - exponent - (see Ref. 5)

D_p - particle diameter - ft

g_c - Newton's constant - lbm/-ft/lbf-sec^2

ρ - fluid density - lbm/ft^3

ϕ - shape factor - (see Ref. 5)

5.3 Beds of Type 1 Fibers

According to Section 4.7.2, approximately 30% of the fibrous insulation forms type 1 fibrous debris, all of which is assumed to migrate to the sump screens and then sink. This section evaluates the pressure loss due to this phenomenon.

The debris is assumed to cover the screen uniformly. This is reasonable owing to the random nature of the occurrence of sinking and to the fact that as sections of screen become blocked, the velocity of flow near the remaining unblocked section will increase, causing debris to migrate toward the high velocity regions.

Ref. 10 gives the following as a means of determining pressure drop through beds of fibers:

$$\frac{d(\Delta P)}{d\ell} = \left[\frac{3.5\ \mu\ q\ S_v^2}{A_b}\right] (1-\varepsilon)^{1.5}\ [1 + 57(1-\varepsilon)^3] \qquad [27]$$

where $\frac{d(\Delta P)}{d\ell}$ = pressure gradient in bed - $dynes/cm^2/cm$

ℓ - bed depth - cm

μ - fluid viscosity - poise

q - fluid flow rate - cm^3/sec

S_v - fiber specific surface - cm^2/cm^3

ε - bed void fraction/total - -

A_B - bed area normal to flow - cm^2

Equation 27 can be integrated for type 1 fiber flocs, as ε is assumed constant and equal to the fabricated porosity. Therefore, all terms in Equation 27 are known with the exception of ε the bed void fraction which is defined in Ref. 10 as:

$$\varepsilon = 1 - \nu C' \qquad [28]$$

where ε - bed void fraction - ratio of void volume/bed volume

ν - hydrodynamic fiber specific volume - cm^3/g

C' - bed density - g/cm^3

Values of ν and Sv as given by Ref. 10 follow:

Material	ν (cm^3/g)	S_v (cm^2/cm^3)	
Nylon	0.904	2050	[typical for polymeric fibers]
Dacron	0.725	2340	[typical for polymeric fibers]
Glass	0.384	2420	[typical for inorganic fibers]

This information is sufficient to evaluate screen pressure drop due to accumulation of fiber flocs. (Refer to Attachment 4 where a sample calculation is provided.)

The pressure drop obtained from Equation 27 is in $dynes/cm^2$. The conversion to pounds per square inch is as follows (Ref. 11):

$$\Delta P \left(\frac{dynes}{cm^2}\right) \times 1.45037 \times 10^{-5} = \Delta P \left(\frac{lbf}{in^2}\right)$$

5.4 Individual Fiber Accumulations

This section describes the method used to evaluate pressure drop arising from accumulation of individual fibers on sump screens.

According to Section 4.7.2, approximately 30% of fibrous insulation debris is composed of individual fibers. These fibers are suspended in the flow and, owing to their very low settling velocities, are assumed to migrate to the sump. It is further assumed that these fibers uniformly block the sump screens.

The equation developed in 5.3 will be used to determine the pressure drop associated with individual fiber accumulations, with the following modifications.

Bed Porosity

In Section 5.3 the porosity of the fiber flocs is assumed equal to the porosity of the original, uncompressed insulation. This is reasonable as the fibers have their original orientations and will resist compressive forces caused by fluid interactions. In the case of individual fibers, the mat created by trapping these

fibers on the sump screens has few if any fibers oriented parallel to the direction of flow (Ref. 10). Accordingly, the resulting mat porosity will be lower than the porosity of the original insulation.

Equation 27 can be integrated stepwise if incremental segments of bed depth are sufficiently small to permit assuming ε to be constant for that depth increment. The procedure follows:

Constant terms in Equation 27:

μ - fluid viscosity - temperature dependent with known temperature variation

q - fluid flow rate - constant or known function of time

S_v - fiber specific surface (see Section 5.3)

A_b - bed area normal to flow

These terms are combined into a single term ψ equal to

$$\psi = \frac{3.5\ \mu\ q\ S_v^2}{A_b} \qquad [29]$$

giving

$$\frac{d(\Delta P)}{d\ell} = \psi\ (1-\varepsilon)^{1.5}\ [1+57(1-\varepsilon)^3] \qquad [30]$$

where all terms except ψ are defined in Section 5.3.

Ref. 10 gives for bed void fraction ε as a function of pressure,

$$\varepsilon = 1 - \nu C' \qquad [31]$$

where ε - bed void fraction - -

ν - hydrodynamic fiber specific volume - cm^3/g

v

C - bed density - g/cm^3

and Ref. 10 also gives for C',

$$C' = Mp_s^N \qquad [32]$$

where C' - bed density - g/cm^3

M,N - constants (empirical) - -

P_s - mechanical compaction pressure - $dynes/cm^2$

The mechanical compression pressure P_s at any point in the mat is equal to the sum of all upstream frictional drag plus the frictional drop past the fibers at that point. Accordingly, Equation 32 can be integrated starting at the upstream face where $P_s = 0$.

Using small increments of ℓ, P_s in Equation 32 is equal to the summation of all ΔP up to that position in the mat, and C' can be determined. Bed void fraction ε is computed using Equation 31 yielding pressure drop over increment ℓ via Equation 30. The summation of all these ΔP's is the overall pressure drop. This type of stepwise procedure is easily programmed for computer solution so that sensitivity analyses on the size ℓ can be easily performed.

5.5 Evaluation of Pressure Drop Due to Accumulated Debris

Two terms are involved in the evaluation of increased head loss due to debris accumulation. The first term involves increased head loss through the screens due to increased flow velocity through reduced screen area. The second term involves the head loss due to the accumulated debris iteself.

5.5.1 Head Loss Due to Increased Screen Flow Rate

Section 5.1 evaluated the head loss across unblocked screens. Using the available flow area and required ECCS flow rate, the flow velocity across the screen can be determined. The screen area is equal to the area unblocked by impermeable debris. Consequently, reflective metallic insulation panels, metallic jacketing, etc., present on the sump screens completely block the available flow area while cal-sil debris, rock wool or mineral wool fibers do not.

The design screen head loss is subtracted from this head loss due to blockage to determine the increase in head loss due to loss of flow area.

5.5.2 Accumulated Debris

The methods developed in Sections 5.2, 5.3 and 5.4 are used to determine head loss through accumulated debris. These losses (alone or in combination depending on the types of insulation present in containment) are added to the loss determined in Section 5.5.1 to obtain the overall head loss increase attributable to debris accumulation.

5.6 Blocked Sump Screen Evaluation

The losses determined in Section 5.5 are compared to the NPSH margin of the pump. If the head loss of Section 5.5 exceeds the design margin, the pump NPSH requirements at rated flow will not be met with the possibility of cavitation occurring in the pumps or suction piping.

For head losses as determined in Section 5.5 which do not exceed NPSH design margins, engineering judgement is required to determine if remaining NPSH margin is adequate under the most severe operating conditions that the pumps will experience. Additional hydraulic criteria must be satisfied to establish the acceptability of sump operation. That is, this methodology addresses only the debris issue as it relates to sump performance at increased head loss. Independent evaluations of hydraulic performance of the sump are also required to determine overall sump design acceptability.

6.0 JET IMPINGEMENT ASSUMPTIONS

The methods for dealing with the quantity of debris formed and transported by jet impingement are presented in Sections 3.3 and 4.3. This section discusses the assumptions implicit in these methods.

6.1 Jet Expansion Angle

The jet expansion angle as computed in Attachment 2 is a function of vessel stagnation pressure and fluid enthalpy. As little variation in stagnation pressure exists in the primary piping of a PWR (in comparison with the fluid static pressure) the variation in jet angle due to pressure differences in the primary loop is negligible. In similar fashion, the variation in fluid enthalpy in the primary circuit is also small, resulting in a small contribution to jet expansion angle changes.

Attachment 2 provides the blowdown mass rate, exit pressure and jet reaction thrust for saturated blowdown. The subcooling present in a PWR is not directly addressed by the Attachment 2 methodology. Consequently, the blowdown is evaluated as a saturated liquid blowdown using the enthalpy of the fluid at the break location to determine the thermodynamic state point. The rationale is as follows:

a. Extremely rapid depressurization from initial pressure to saturation due to the high sonic velocity in liquid.

b. Development of two phase conditions during continued blowdown.

c. Two phase jet at pipe break exit plane.

These occurrences lead to the conclusion that most of the blowdown occurs as a flashing liquid, implying saturation conditions at prevailing fluid enthalphy.

6.2 Interaction With Targets

Hot legs, cold legs and crossover piping are of major interest due to their connection to the reactor pressure vessel, a reservoir of high temperature and high pressure fluid. Attachment 2 illustrates a 90 degree divergence angle as applied to jets emanating from these piping systems. This yields 2 ft of diametrical growth in jet cross section for each foot of axial separation between break and target. Consequently, at relatively short distances (5 to 6 ft) large targets (10 to 15 ft diameter) are completed intercepted by the jet. (Refer to Figure 9.)

At greater distances, this effect is even more pronounced as jet expansion is assumed to occur at the initial rate. Therefore, it is reasonable to assume that significant jet deflection does not occur due to the presence of large targets.

Figure 9
Jet Target Interaction

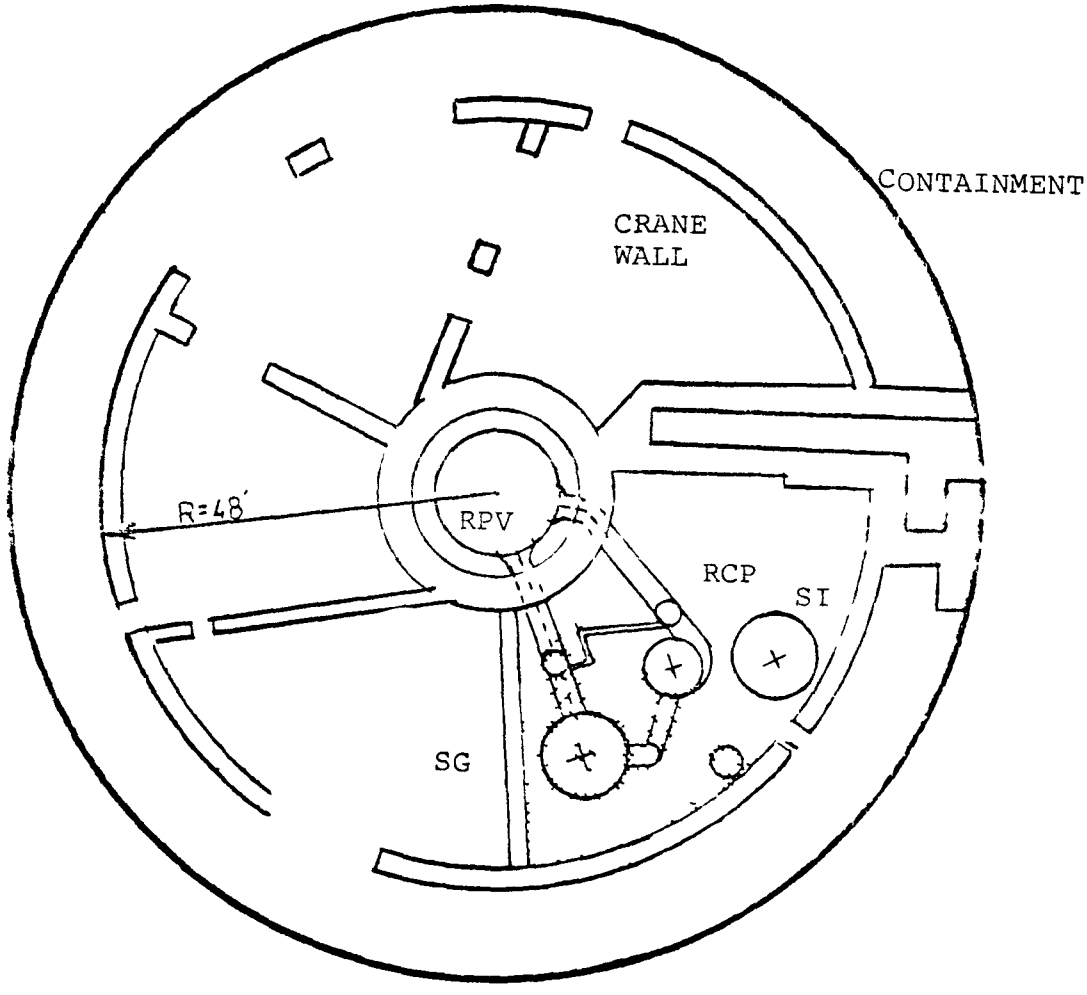

LEGEND:

RCP - REACTER COOLANT PUMP
RPV - REACTER PRESSURE VESSEL
SG - STEAM GENERATOR
SI - SAFETY INJECTION TANK

7.0 EQUATION REFERENCES

Equation Number	Use	Reference
1	Darcy's equation	12
2	Continuity equation	12
3	Substitution of Equation 2 into Equation 1	
4	Restatement of Equation 3	
5	Definition of K_i	5
6	Equivalent resistance formula	Derived from Equation 1
7	Equivalent resistance formula	Derived from Equation 1
8,9,10	Applications of Equations 6 and 7	
11	Restatement of Equation 4	
12	Restatement of Equation 4 with branch resistances	
13	Rearrangement of Equation 12	
14	Frictional force	13
15,16,17, 18	Normal force with buoyancy and lift	14
19	Drag force	14
20	Conversion of mass flow to velocity	12
21	Expansion of jet with 5° half angle	
22	Submergence velocity	15
23	Darcy's equation	12
24	Screen discharge resistance	5
25	Substitution of Equation 24 into Equation 23	

Equation Number	Use	Reference
26	Pressure drop through porous solid beds	5
27,28,30, 31,32	Pressure drop through compressible beds	10
29	Substitution of terms in Equation 27	

8.0 NOMENCLATURE

Variable	Meaning	Units
A	Flow area	ft^2
A_b	Bed area normal to flow	ft^2
A_{Di}	Total area of debris in segment i	ft^2
A_E	Exit area	ft^2
A_i	Area of path i	ft^2
A_p	Area of particle normal to flow	ft^2
$A_{0.5}$	Area of jet at jet pressure = 0.5 psig	ft^2
A_∞	Area of jet at full expansion	ft^2
c	Screen discharge coefficient	-
C	Substitution variable	$1/2\ g_c\rho$
C	Bed density	g/cm^3
C_D	Drag coefficient	-
D_E	Diameter of exit	ft
D_H	Hydraulic diameter	ft
D_p	Particle diameter	ft
$\Delta P/\ell$	Pressure gradient in bed	$dynes/cm^2/cm$
D_∞	Diameter of jet at full expansion	ft
E_x	Flow expansion downstream of obstruction	ft
f	Friction factor	-
f_m	Modified friction factor	-
F_A	Force available to cause motion	lbf
F_B	Buoyant force	lbf
F_L	Lift force	lbf

Variable	Meaning	Units
F_M	Force required to cause motion	lbf
F_N	Normal force	lbf
g	Local acceleration of gravity	ft/sec^2
g_c	Newton's Constant	$lbm\text{-}ft/lbf\text{-}sec^2$
G	Mass flux	$lbm/ft^2\text{-}sec$
G_E	Exit mass flux	$lbm/ft^2\text{-}sec$
G_M	Maximum mass flux	$lbm/ft^2\text{-}sec$
h	Head loss	ft
h'	Depth of approach flow	ft
H	Height	in
h_f	Liquid enthalpy	Btu/lbm
h_{fg}	Vaporization enthalpy	Btu/lbm
h_g	Vapor enthalpy	Btu/lbm
h_o	Stagnation enthalpy	Btu/lbm
K	Hydraulic resistance coefficient	-
K'	Slip ratio	-
K_i	Hydraulic resistance coefficient of path i	-
ℓ	Bed depth	ft or cm
L	Length	in or ft
$L_{0.5}$	Distance at which jet area equals $A_{0.5}$	ft
L_∞	Distance to full jet expansion	ft
$\dot{m}$	Mass flow rate	lbm/sec
$\dot{m}_i$	Mass flow rate through path i	lbm/sec
M	Constant	-

Variable	Meaning	Units
n	Number of screens in series	-
N	Exponent	-
P	Pressure	psia
ΔP	Pressure drop	lbf/ft^2
ΔP_i	Pressure drop path i	lbf/ft^2
P_{Di}	Percentage of debris in 10° segment i	%
P_E	Exit pressure	lbf/ft^2
P_o	Stagnation pressure	psia
P_s	Mechanical compaction pressure	$dynes/cm^2$
P_∞	Receiver pressure	lbf/ft^2
q	Fluid flow rate	cm^3/sec
Q	Flow rate	gpm
r	Particle radius	ft
R	Radius	ft
R_e	Inside radius	ft
R_i	Flow path resistance	$lbf/lbm^2\text{-}in^2$
R_o	Outside radius	ft
s_f	Liquid Entropy	Btu/lbm °R
s_{fg}	Vaporization entropy	Btu/lbm °R
s_g	Vapor entropy	Btu/lbm °R
s_o	Stagnation entropy	Btu/lbm °R
S_v	Fiber specific surface	cm^2/cm^3
γ	Debris thickness	ft
T	Jet thrust	lbf

Variable	Meaning	Units
$\forall_F$	Volume fraction of material in insulation	-
V_m	Volume of material	ft^3
$\bar{V}$	Velocity of flow	ft/sec
$\bar{V}_c$	Velocity at which submergence occurs	ft/sec
$\bar{V}_s$	Velocity of flow across a specific area	ft/sec
v_f	Liquid specific volume	ft^3/lbm
v_{fg}	Vaporization specific volume	ft^3/lbm
v_g	Vapor specific volume	ft^3/lbm
v_{ME}	Momentum specific volume	ft^3/lbm
v_∞	Receiver specific volume	ft^3/lbm
W	Width	in
X	Quality	-
Y_∞	Radial expansion due to angle β through distance L_∞	ft
α	Fractional free projected screen area	-
ε	Bed void fraction	-
π	Pi	-
$\emptyset$	Shape factor	-
ρ	Fluid density	lbm/ft^3
ρ'	Debris density	lbm/ft^3
ρ_I	Density of insulation ($\rho_I < \rho_w$)	lbm/ft^3
ρ_m	Density of material	lbm/ft^3
ρ_w	Density of water	lbm/ft^3

Variable	Meaning	Units
ρ_T	Theoretical density of material	lbm/ft^3
μ	Fluid viscosity	poise
μ_f	Coefficient of friction	--
ν	Hydrodynamic fiber specific volume	cm^3/g
ψ	Substitution variable	$\frac{3.5\ \mu\ q\ S_v^2}{A_b}$

9.0 REFERENCES

1) NUREG-0800
Standard Review Plan for the Review of Safety Analysis Reports for Nuclear Power Plants
LWR Edition
U.S. Nuclear Regulatory Commission
SRP No. 3.6.2, July 1981

2) Fundamentals of Fire and Explosion Hazards
G. Grelecki
Hazards Research Group
Denville, NJ
AICHC Today Series
pg. A-28 through A-57

3) "Maximum Flow Rate of a Single Component, Two Phase Mixture"
F.J. Moody
Transactions of the ASME
February 1965, page 134 and following

4) Prediction of Blowdown Thrust and Jet Force
F.J. Moody
ASME Publication 69-HT-31
May 1969

5) Chemical Engineers Handbook
Robert H. Perry, Consultant
Cecil H. Chilton Senior Advisor
McGraw-Hill Book Company

6) Loviisa Emergency Cooling System. Model Tests
(Translated from the Finnish-Preliminary Review Copy, provided by SNL, Albuquerque) Report Number 93K168FN

7) Kent's Mechanical Engineers' Handbook
12th Edition
Wiley
Colin Carmichael

8) "Tables of Hydrodynamic Mass Factors for Translational Motion"
K.T. Patton, 1965
ASME Paper 65-WA/UNT-2

9) Froude Criteria for Ice Block Stability
Journal of Glaciology, Vol. 13, No. 68
1974, pg. 307 and following

10) "Internal Pressure Distribution in Compressible Mats Under Fluid Stress"
W.L. Ingmanson
B.D. Andrews
R.C. Johnson
Technical Association of the Pump and Paper Industry
Volume 42, No. 10, October 1959

11) Handbook of Chemistry and Physics
CRC Press
53rd Edition
Page F-256 and following

12) Flow of Fluids through Valves, Fittings, and Pipe
Crane Technical Paper 410

13) Engineering Mechanics, Vector Edition, Vol. 1,
Higdon and Stiles, Prentice-Hall, Inc.
1962

14) Unit Operations of Chemical Engineering, 2nd Edition,
McCabe & Smith, McGraw-Hill Book Co.

15) Criterion for Ice Block Stability, Journal of Glaciology,
Vol. 13, No. 68, 1974

16) Model Study of the Sequoyah RHR Sump
Report No. WM28-1-45-102; Oct. 1978
Tennessee Valley Authority
Division of Water Management
Water Systems Development Branch

ATTACHMENT 1

METHODOLOGY FLOW DIAGRAM

ATTACHMENT 1

METHODOLOGY FLOW DIAGRAM (Sheet 1 of 4)

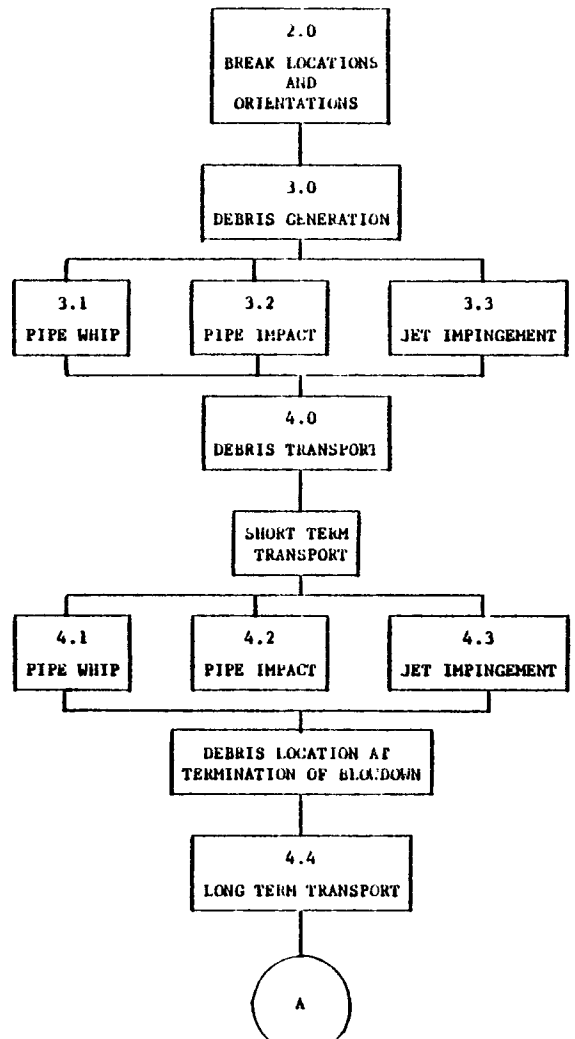

METHODOLOGY FLOW DIAGRAM (Sheet 2 of 4)

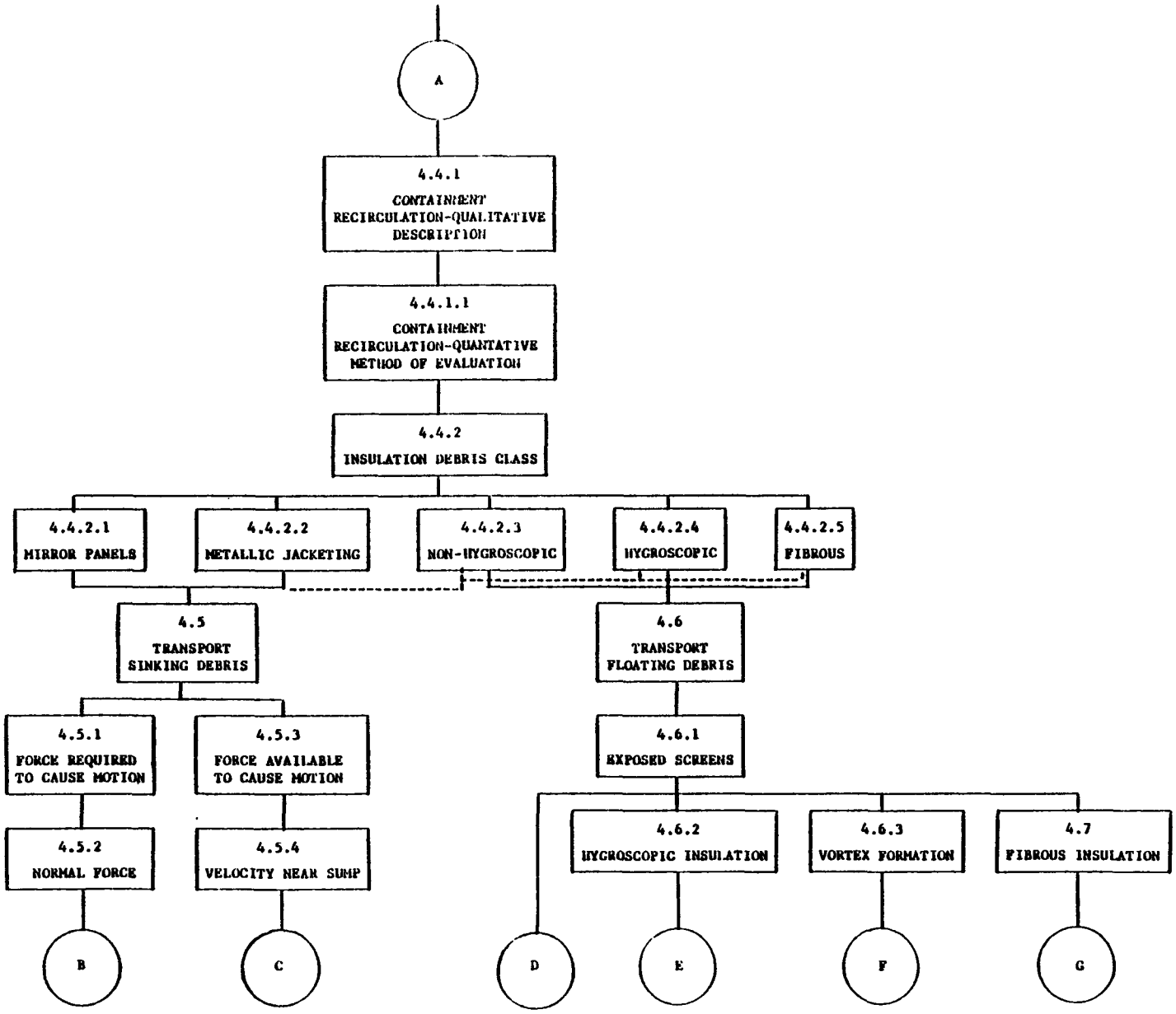

METHODOLOGY FLOW DIAGRAM (Sheet 3 of 4)

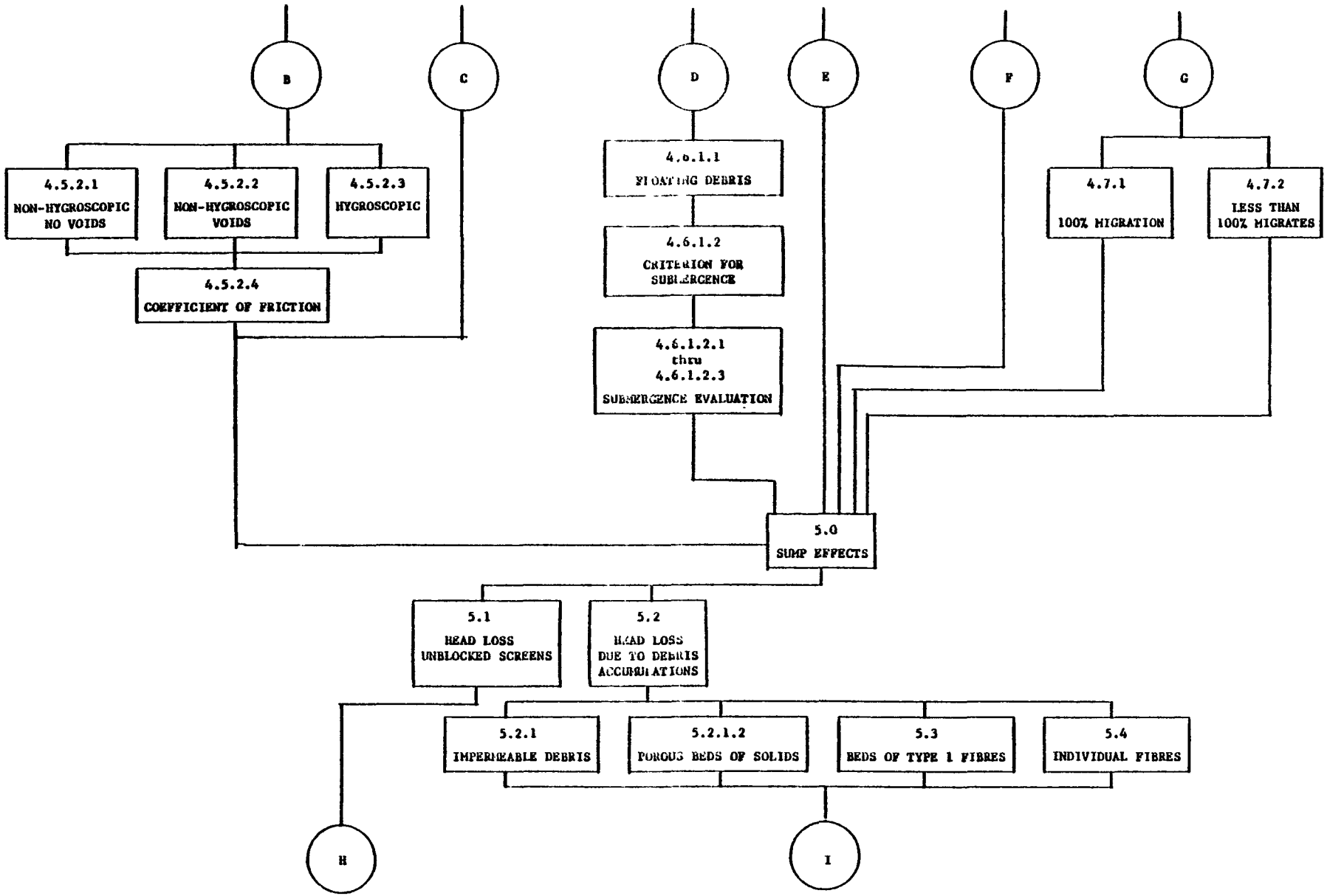

METHODOLOGY FLOW DIAGRAM (Sheet 4 of 4)

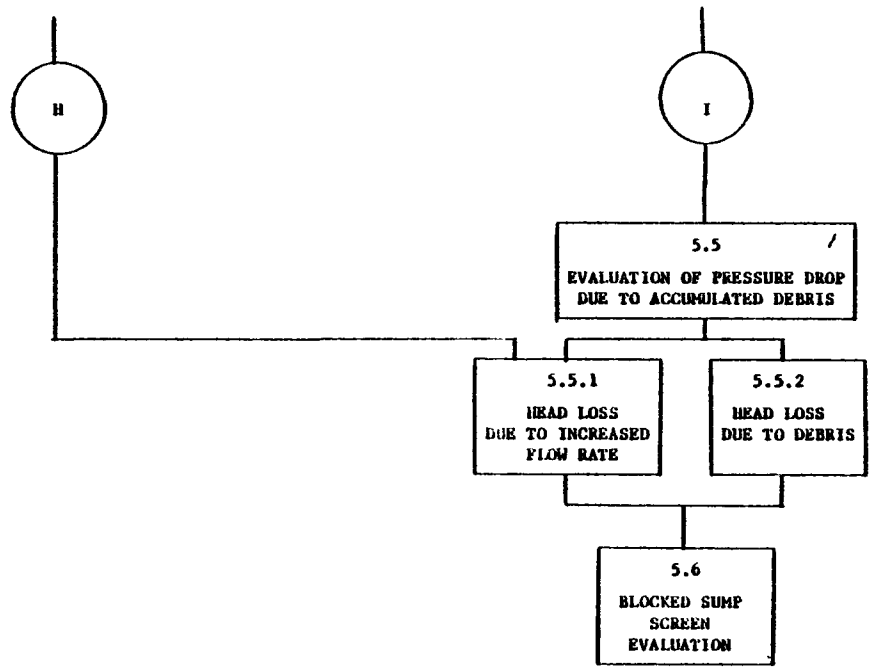

ATTACHMENT 2

JET CALCULATIONS

Attachment 2

Jet Calculations

1.0 DETERMINATION OF MAXIMUM BLOWDOWN FLOW RATE AND EXIT PLANE PRESSURE (Ref. 3)

$$G_M = \sqrt{\frac{2g_c J \left[h_o - h_f - \frac{h_{fg}}{s_{fg}} (s_o - s_f)\right]}{\left[K' \frac{(s_g - s_o) v_f}{s_{fg}} + \frac{(s_o - s_f) v_g}{s_{fg}}\right]^2 \left[\frac{s_o - s_f}{s_{fg}} + \frac{s_g - s_o}{K^2 s_{fg}}\right]}} \qquad [A-1]$$

where G_M - maximum mass flux - lbm/sec-ft^2
J - mechanical equivalent of heat - 778 ft-lbf/Btu
g_c - Newton's constant - lbm-ft/lbf-sec^2
h_o - stagnation enthalpy - Btu/lbm
h_f - liquid enthalpy - Btu/lbm
h_{fg} - vaporization enthalpy - Btu/lbm
s_{fg} - vaporization enthalpy - Btu/lbm °R
s_o - stagnation entropy - Btu/lbm °R
s_f - liquid entropy - Btu/lbm °R
s_g - vapor entropy - Btu/lbm °R
v_f - liquid specific volume - ft^3/lbm
v_g - vapor specific volume - ft^3/lbm

$$K' = \left(\frac{v_g}{v_f}\right)^{1/3} \qquad [A-2]$$

where K' - slip ratio of liquid and vapor phases

With saturation line properties h_f, h_g, h_{fg}, s_f, s_g, s_{fg}, v_f, v_g, and K' solely functions of pressure, Equation [A-1] will yield a maximum if:

$$\left(\frac{\partial G}{\partial P}\right)_{K'} = 0 \text{ and } \left(\frac{\partial G}{\partial K'}\right)_{P} = 0 \qquad [A-3]$$

where G - mass flux - lbm/ft^2-sec
P - pressure - psia

Substituting Equation A-2 into Equation A-1 and solving subject to Equation A-3, the maximum mass flux, G_M, and the exit plane pressure P_E, at any h_o and s_o are determined.

2.0 PREDICTION OF BLOWDOWN THRUST AND JET FORCE (Ref. 4)

The blowdown jet load is composed of a static term and a momentum term as follows:

$$\frac{T}{A_E} = (P_E - P_\infty) + \frac{G_M^2 \, v_{ME}}{2g_c} \qquad [A-4]$$

where T	- jet thrust	- lbf
A_E	- pipe exit area	- ft^2
P_E	- pipe exit pressure	- lbf/ft^2
P_∞	- receiver pressure	- lbf/ft^2
G_M	- maximum mass flux (Equation A-1)	- $lbm/sec\text{-}ft^2$
v_{ME}	- momentum specific volume	- ft^3/lbm
g_c	- Newton's Constant	- $lbm\text{-}ft/lbf\text{-}sec^2$

and

$$v_{ME} = [X \, v_g + (1-X) \, K' \, v_f] \left[X + \frac{1-X}{K'}\right] \qquad [A-5]$$

where v_g	- vapor specific volume	- ft^3/lbm
X	- quality	- -
v_f	- liquid specific volume	- ft^3/lbm
K'	- slip ratio	- -

Note: All properties in Equation A-5 are evaluated at P_E.

Equations A-4 and A-5, with G_M from equation A-1, yield the blowdown jet thrust per square foot of break area for known h_o and s_o.

3.0 JET EXPANSION

As the jet exits the pipe, internal pressure and jet/receiver air interaction, tend to expand the jet. Ref. [3] gives for expansion of the jet:

$$\frac{A_\infty}{A_E} = \frac{G_E^2}{g_c} \frac{v_{M\infty}}{(T/A_E)} \qquad [A-6]$$

where A_∞ - area of jet at full expansion - ft^2

A_E - exit area - ft^2

G_E - exit mass flux - $lbm/sec\text{-}ft^2$

$v_{M\infty}$ - momentum specific volume evaluated at receiver pressure - ft^3/lbm

(T/A_E) - jet thrust per unit pipe area - lbf/ft^2

The distance required to expand the jet from A_E to A_∞ is given (Ref. 3) as:

$$L_\infty = \frac{D_E}{2} \left(\sqrt{\frac{A_\infty}{A_E}} - 1\right) \qquad [A-7]$$

4.0 JET EXPANSION ANGLE

Figure A2-1

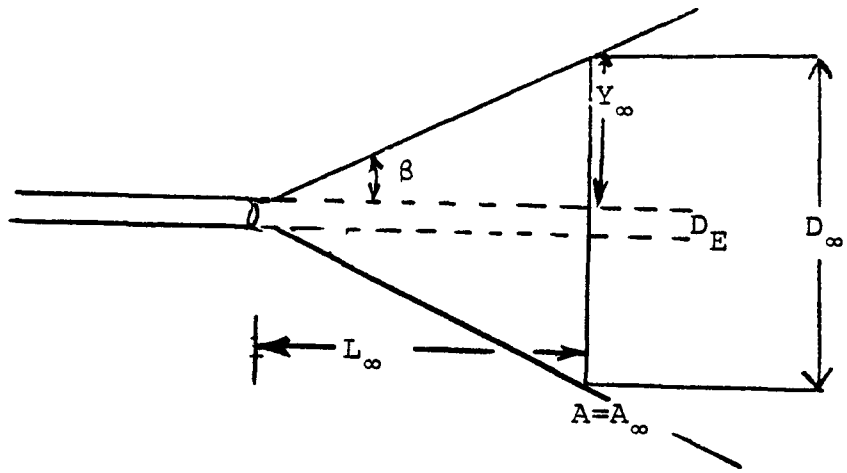

In Figure A2-1, conical flow is assumed, and all thermodynamic quantities and velocity are assumed constant along rays.

For a circular jet:

$$A_\infty = \frac{\pi D_\infty^2}{4}$$

and knowing A_∞/A_E (Equation A-6)

then

$$Y_\infty = \frac{D_\infty - D_E}{2}$$

and

$$\text{Tan } \beta = \frac{Y_\infty}{L_\infty}$$

yielding

$\beta = 45$. The jet expansion angle equals $2\beta = 90°$.

5.0 CALCULATION PROCEDURE

The equations of the previous four sections have been combined into a single procedure which follows:

5.1 Given P_o and h_o, find G_M and P_E from Figures A2-2 and A2-3

FIGURE A2-2

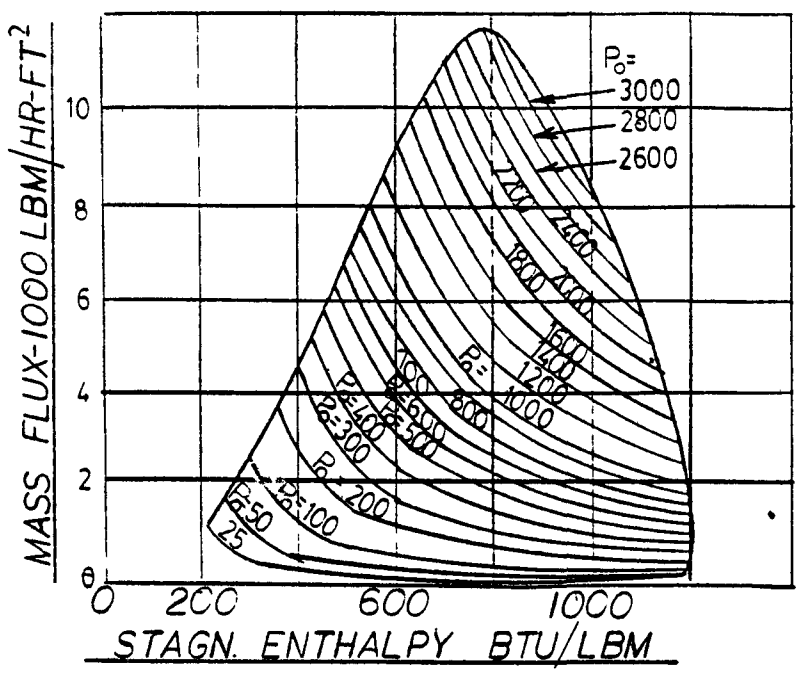

FIGURE A2-3

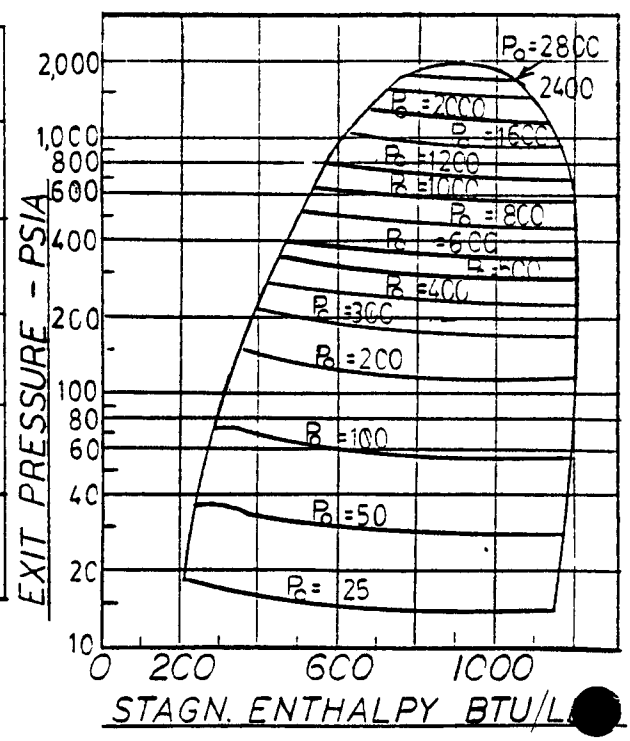

P_o = _____psia; h_o = _____Btu/lbm; G_M = _____lbm/sec-ft^2;

P_E = _____psia

5.2 At P_E -

h_f = _____Btu/lbm; h_{fg} = _____Btu/lbm; h_g = _____Btu/lbm;

v_f = _____ft^3/lbm; v_{fg} = _____ft^3/lbm; v_g = _____ft^3/lbm

$$X_E = \frac{h_o - h_f}{h_{fg}} = \_\_\_\_\_ \quad K'_E = \left(\frac{v_g}{v_f}\right)^{0.333} = \_\_\_\_\_$$

Find v_{ME} as $[X_E v_g + (1-X_E)\, v_f K']_E \left[X_E + \frac{1-X_E}{K'}\right]_E$ = _____

Find $T/A_E = 144\ (P_E - 14.7) + \frac{G_M^2\, v_{ME}}{g_c}$ = _____

$$v_{M\infty} = [X\, v_g + (1-X) v_f K']_\infty \left[X + \frac{1-X}{K'}\right]_\infty$$

Where ∞ denotes receiver conditions (i.e., 14.7 psia)

Then $v_g = 26.7989$, $v_f = .0167$ } saturation conditions at 14.7 psia

$K' = 11.707$

$$X_\infty = \frac{h_o - h_f}{h_{fg}} = \_\_\_\_\_$$

$v_{M\infty}$ = _____

$$\frac{A_\infty}{A_E} = \frac{G_M^2\, v_{M\infty}}{g_c\ (T/A_E)} = \_\_\_\_\_$$

$$L_\infty = \frac{D_E}{2}\left[\sqrt{\frac{A_\infty}{A_E}} - 1\right] = \_\_\_\_\_$$

5.3 Distance to 0.5 psig Stagnation Plane

Knowing T/A_E and A_E, the jet area at 0.5 psi stagnation pressure is:

$A_{0.5} = T/72$

and $\beta = 45°$

then $L_{0.5} = \sqrt{\frac{T/72}{\pi}} - \frac{DE}{2}$ = _____

ATTACHMENT 3

CALCULATION PROCEDURE FOR "SHADOWED" BREAKS

Attachment 3

Calculation Procedure for "Shadowed" Breaks

Circumferential ruptures of restrained pipes may not result in full displacement as shown in figure A3-1. The resulting jet is characterized as follows:

a. For the unshadowed segment (crescent shaped opening), use procedure of Attachment 2.

b. For the slot segment, use the procedure outlined herein.

The fluid jet exiting the slot segment has its axis oriented normal to the pipe centerline. The half-angle of divergence is assumed to be 10° and the thrust developed by the jet is:

$$T = 144\ M\ P_o\ A_E \quad \text{(Ref. 4)}$$

where T = jet thrust - lbf

M = multiplier - 1.26, steam

- 2, subcooled water

P_o = stagnation pressure - psia

A_E = exit area - ft^2

Figure A3-1

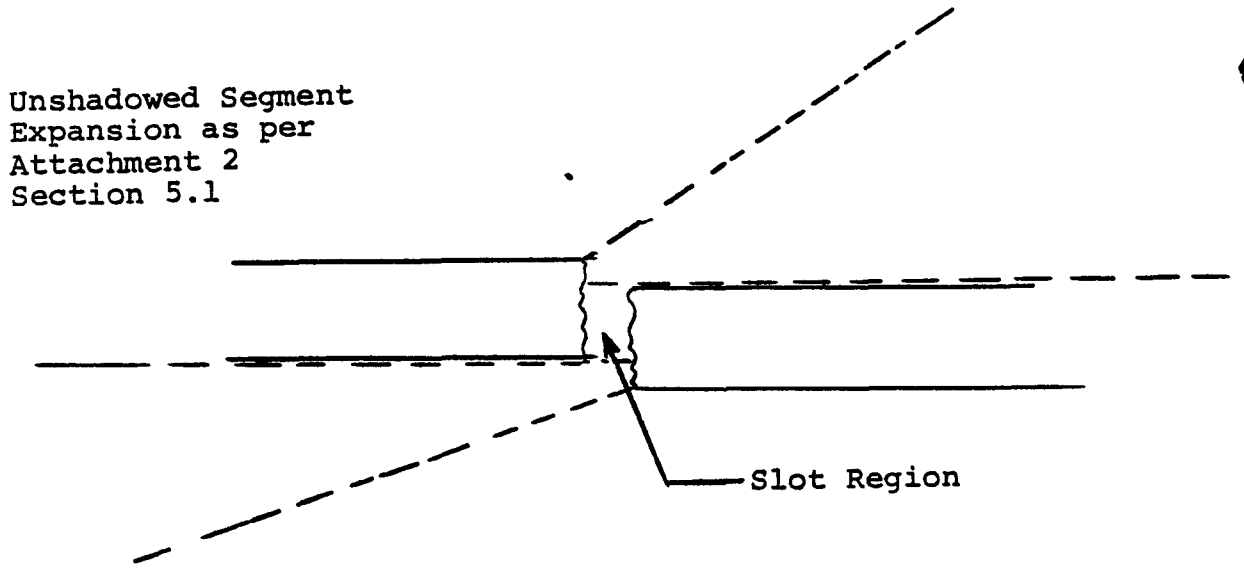
Unshadowed Segment
Expansion as per
Attachment 2
Section 5.1
Slot Region

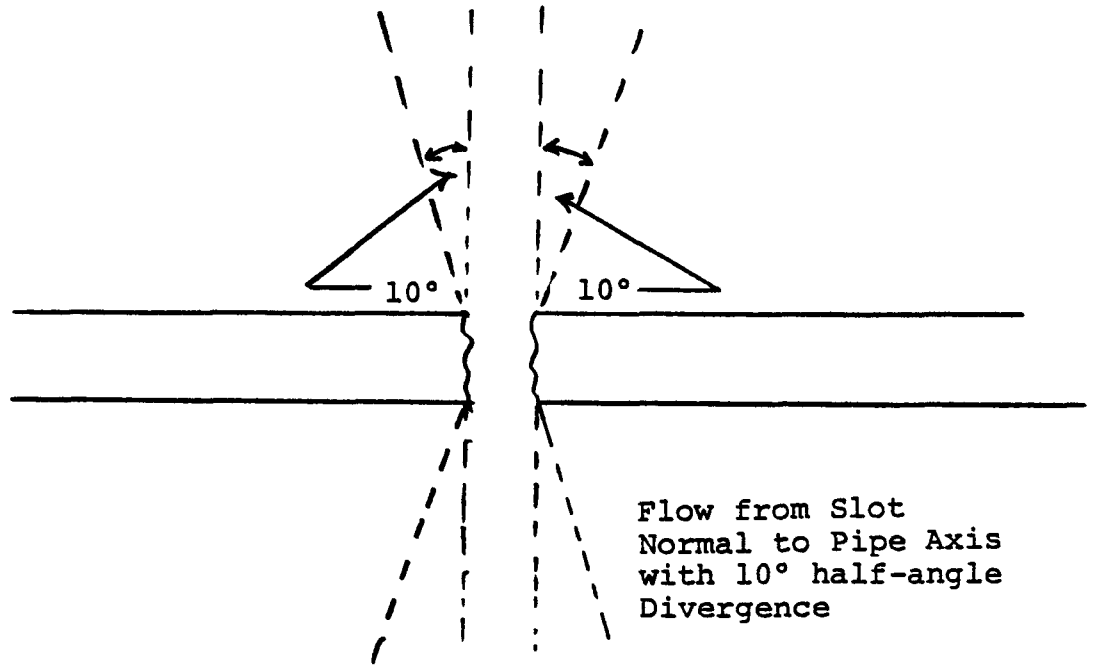
10°
10°
Flow from Slot
Normal to Pipe Axis
with 10° half-angle
Divergence

ATTACHMENT 4

SAMPLE PRESSURE DROP CALCULATION - FLOW THROUGH FIBROUS DEBRIS

Attachment 4

Sample Pressure Drop Calculation - Flow

Through Fibrous Debris

From Section 3.3 and 4.3 assume 750 ft^2 of 3 in. fiberglass insulation has been removed as a result of a postulated piping failure. Section 4.7.2 indicates:

a. 30% floats for a period of time

b. 40% sinks immediately

c. 30% forms suspended individual fibers.

Accordingly, 30% of 750 ft^2, or 225 ft^2, of 3 in. insulation forms suspended individual fibers.

Referring to Section 5.3, the following quantities must be determined:

ℓ	- bed depth	- cm
μ	- fluid viscosity	- poise
q	- fluid flow rate	- cm^3/sec
S_v	- fiber specific surface	- cm^2/cm^3
A_b	- bed area normal to flow	- cm^2
ε	- bed void fraction	- -

These values for glass fiber from Section 5.3 are:

$\varepsilon = 1 - \nu C'$

$\nu = 0.384\ cm^3/g$

$S_v = 2420\ cm^2/cm^3$

The value for C' is assumed equal to 0.0721 g/cm^3.

Assume ECCS flow equal to 3500 gpm ($3.208 \times 10^5\ cm^3/sec$).

Assuming a screen area of 150 ft^2 ($1.394 \times 10^5\ cm^2$), the bed depth is:

$$\frac{225\ ft^2 \times \frac{3}{12}\ \frac{in.}{in./ft}}{150\ ft^2} = 0.38\ ft\ (11.4\ cm)$$

Then $\ell = 11.4$ cm

$A_b = 1.394 \times 10^5\ cm^2$

$q = 2.208 \times 10^5\ cm^3/sec$

$\mu = 0.0068$ poise

$S_v = 2420\ cm^2/cm^3$

$\varepsilon = 1 - \nu C' = 0.972$

Then

$$\Delta P = \left[\frac{3.5(0.0068)(2.208\times10^5)(2420)^2}{1.394 \times 10^5}\right](1-.972)^{1.5}[1+57(1-.972)^3]11.41$$

Equation [27]

$\Delta P = 11900\ dynes/cm^2$

or

$= 0.17$ psi

NOTE: The values used in this example are typical and are not meant to apply to any particular insulation, sump, or ECCS flow rate.

ATTACHMENT 5

SELECTED REFERENCE MATERIALS

Attachment 5

Selected Reference Materials

United States Nuclear Regulatory Commission Regulatory Guides

Guide Number	Title
1.1	Net Positive Suction Head for Emergency Core Cooling and Containment Heat Removal System Pumps
1.46	Protection Against Pipe Whip Inside Containment
1.70	Standard Format and Content of Safety Analysis Reports for Nuclear Power Plants
1.82	Sumps for Emergency Core Cooling and Containment Spray Systems

NUREG-0800
Standard Review Plan for the Review of Safety Analysis Reports for Nuclear Power Plants

Section Number	Title
3.6.2	Determination of Rupture Locations and Dynamic Effects Associated with the Postulated Rupture of Piping
6.2.1.3	Mass and Energy Release Analysis for Postulated Loss-of-Coolant Accidents

Final Safety Analysis Report (NUREG-0800 Format)

Chapter Number	Title
3	Design of Structures, Components, Equipment and Systems
4	Reactor
5	Reactor Coolant System and Connected Systems
6	Engineered Safety Features
7	Instrumentation and Controls
15	Accident Analysis

ATTACHMENT 6

NON-UNIFORM DEBRIS DISTRIBUTION IN JETS

Attachment 6

Non-Uniform Debris Distribution in Jets

For cases where the degree of sump screen blockage is significant, the assumption of uniform debris distribution is not nesessarily conservative. The following is a method of quantifying the degree of non-uniformity.

Refer to Figure A6-1 which shows a typical primary system failure with a 90° expansion angle. The outermost jet lines representing the 90° divergence angle bound nine interior jet boundaries located 10° apart. The non-uniform distribution is computed as follows:

a. Compute area of insulated target sections within each 10° section of the jet

b. Assume no mixing of adjacent 10° sections.

Debris distribution as a percentage is then

$$P_{Di} = \frac{100 \times A_{Di}}{\Sigma A_{Di}}$$

where P_{Di} - percentage of debris in 10° segment i

A_{Di} - area of debris in segment i

ΣA_{Di} - total area of debris in jet (determined in Section 3.3)

The jet of Figure A6-1 when stagnated might have the distribution in Figure A6-2. The arc subtended the door is unchanged from the uniform case, but the debris quantity is now:

Debris ejected =

$$\Sigma\left(\frac{\text{Debris in segment i x area of segment i in subtended angle}}{\text{Area of segment i}}\right)$$

That is, the summation of the total debris in each segment when multiplied by the ratio of each segment's area in the subtended angle to that segment's total area gives the total debris ejected. This value for ejected debris is used in the transport models if it represents a larger quantity of insulation.

Figure A6-1
Non-Uniform Debris Distribution

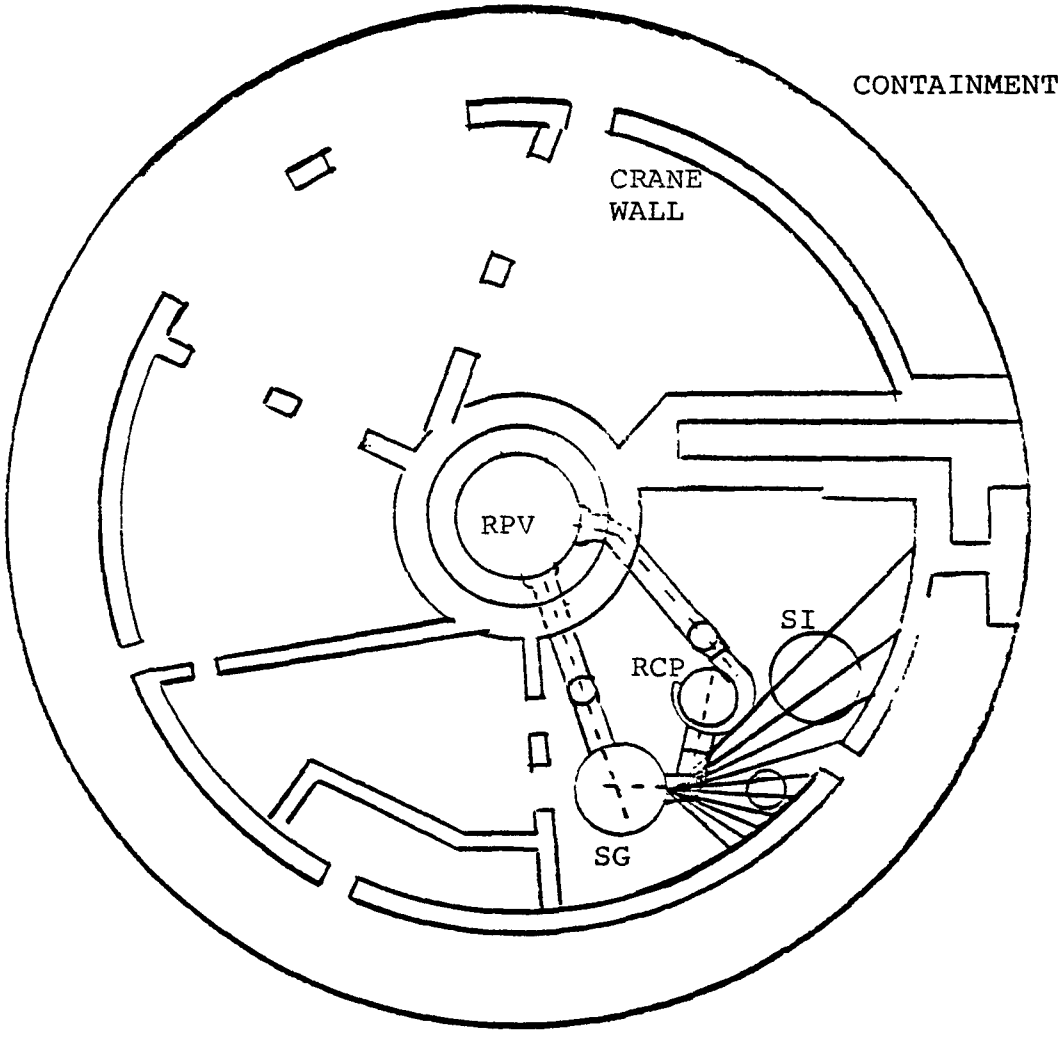

LEGEND:

RCP-REACTOR COOLANT PUMP

RPV-REACTOR PRESSURE VESSEL
SG-STEAM GENERATOR
SI-SAFETY INJECTION TANK

Figure A6-2

Sample Debris Distribution

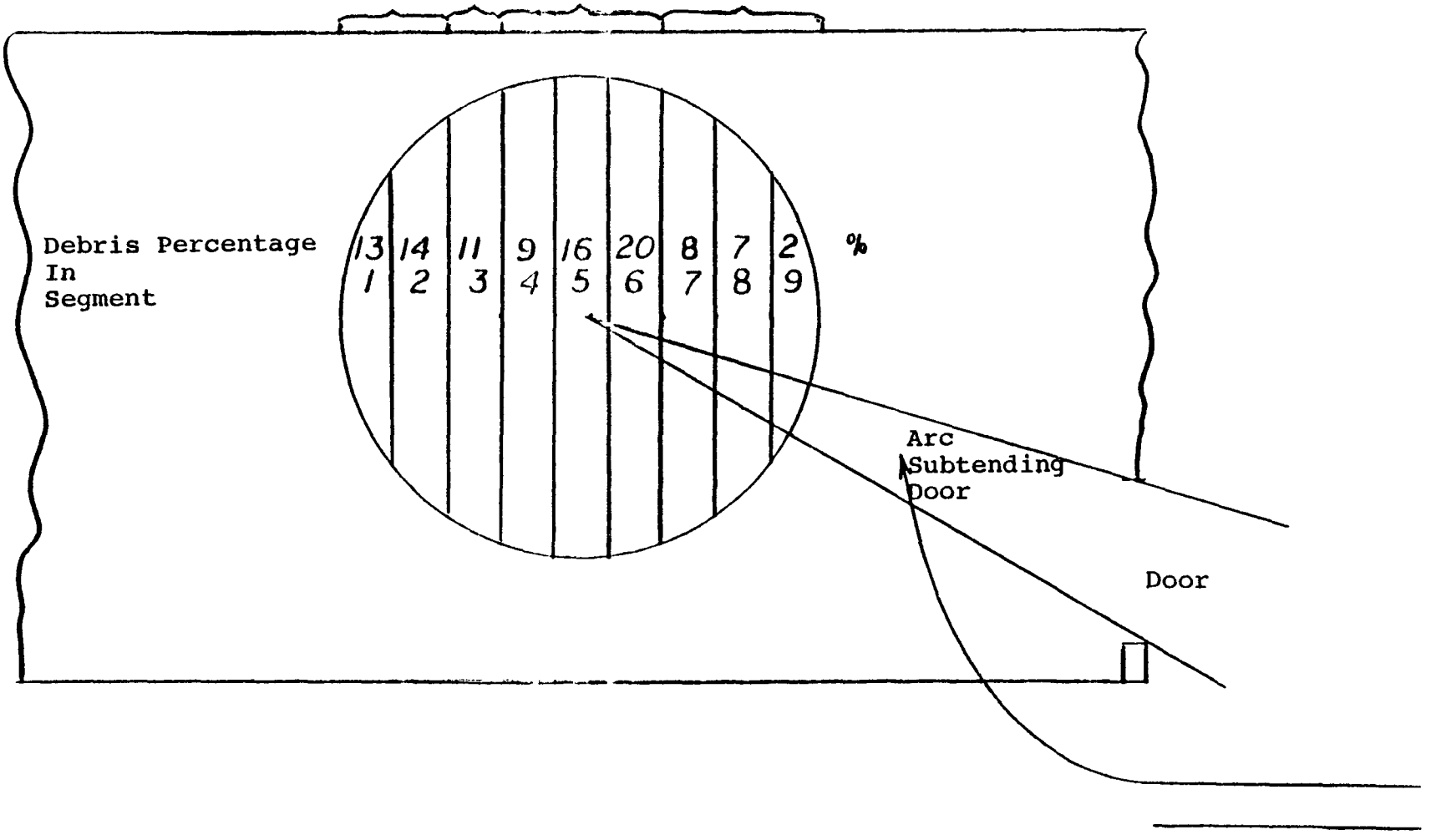

Note

In Appendices A through E, each break is analyzed according to the methods set forth in the basic report in a paragraph with the corresponding number. Therefore, such paragraph numbers are used many times in each appendix. In the appendices, references to paragraphs and equations relate to numbers in the basic report.

APPENDIX A

SALEM UNIT 1

Appendix A

Salem Unit 1

1.0 BACKGROUND

The Salem Unit 1 plant was selected for analysis because it uses several types of insulation. The insulation inside containment is reflective metallic, totally encapsulated, and mineral fiber/wool blanket.

2.0 DETERMINATION OF INITIATING EVENTS

The Salem Unit 1 FSAR discusses breaks inside containment in Section 14.3. However, design basis break locations are not supplied. The location of initiating events is therefore selected in accordance with guidance provided in SRP 3.6.2. Four systems are evaluated: main steam, feedwater, hot leg, and cold leg. Figures A-1 and A-2 illustrate the design basis break locations. These locations were chosen for the following reasons:

Break 1: Hot Leg Failure

System piping is large diameter, high pressure, high temperature and connected to a fluid reservoir. These are the conditions required to produce a sustained blowdown jet. The break is chosen such that a large insulated target is affected, in this case, the steam generator. The jet is oriented in such a manner that debris may be ejected through the shield wall opening (refer to Figure A-3).

Break 2: Cold Leg Failure

The cold leg was chosen for reasons similar to those for the hot leg. The cold leg, as chosen, has a more direct path toward the shield wall opening.

Figure A-1

REACTOR CONTAINMENT ARRANGEMENT

SALEM UNIT NO. 1

ELEVATION VIEW

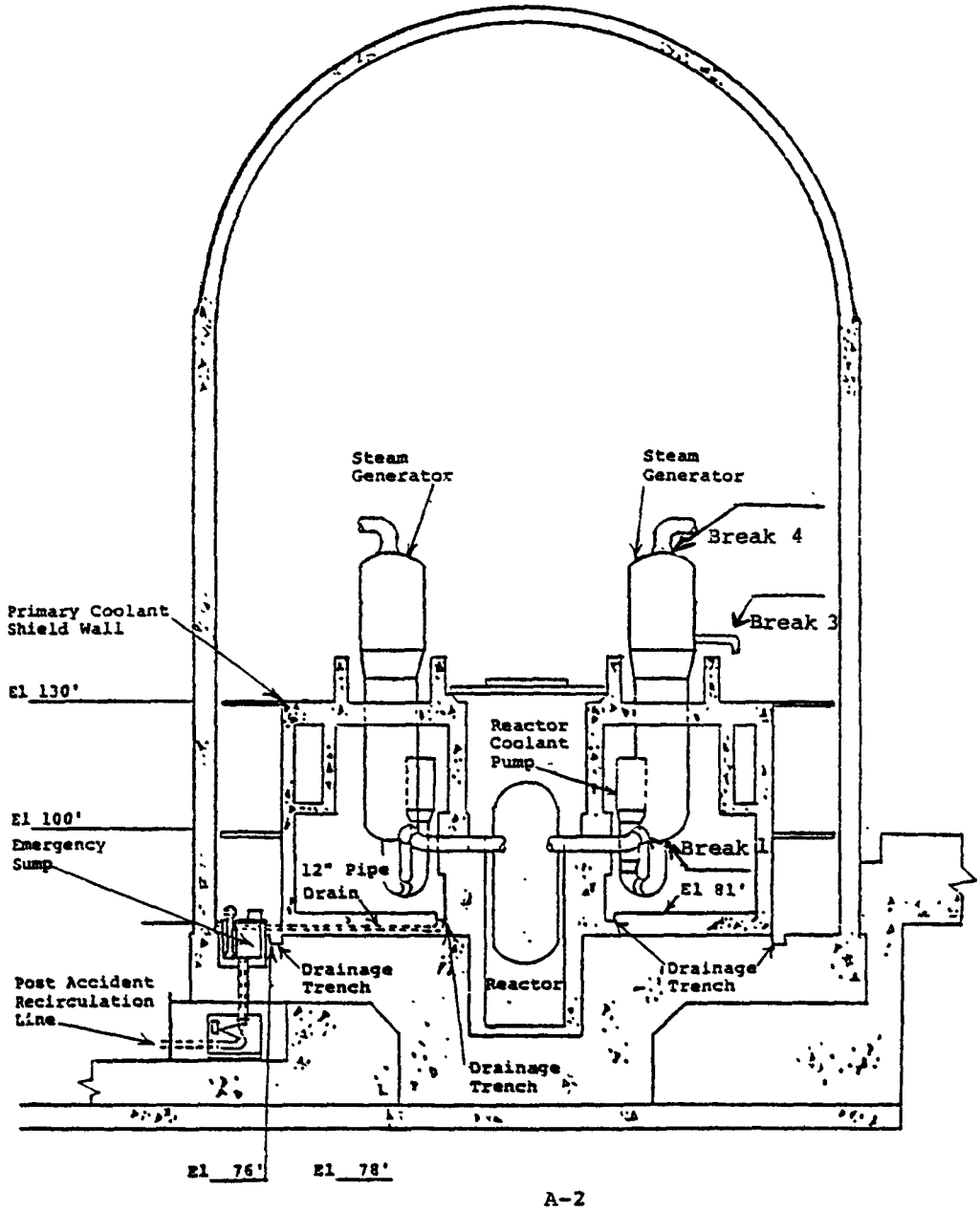

FIGURE A-2

REACTOR CONTAINMENT ARRANGEMENT

SALEM UNIT NO. 1

PLAN VIEW

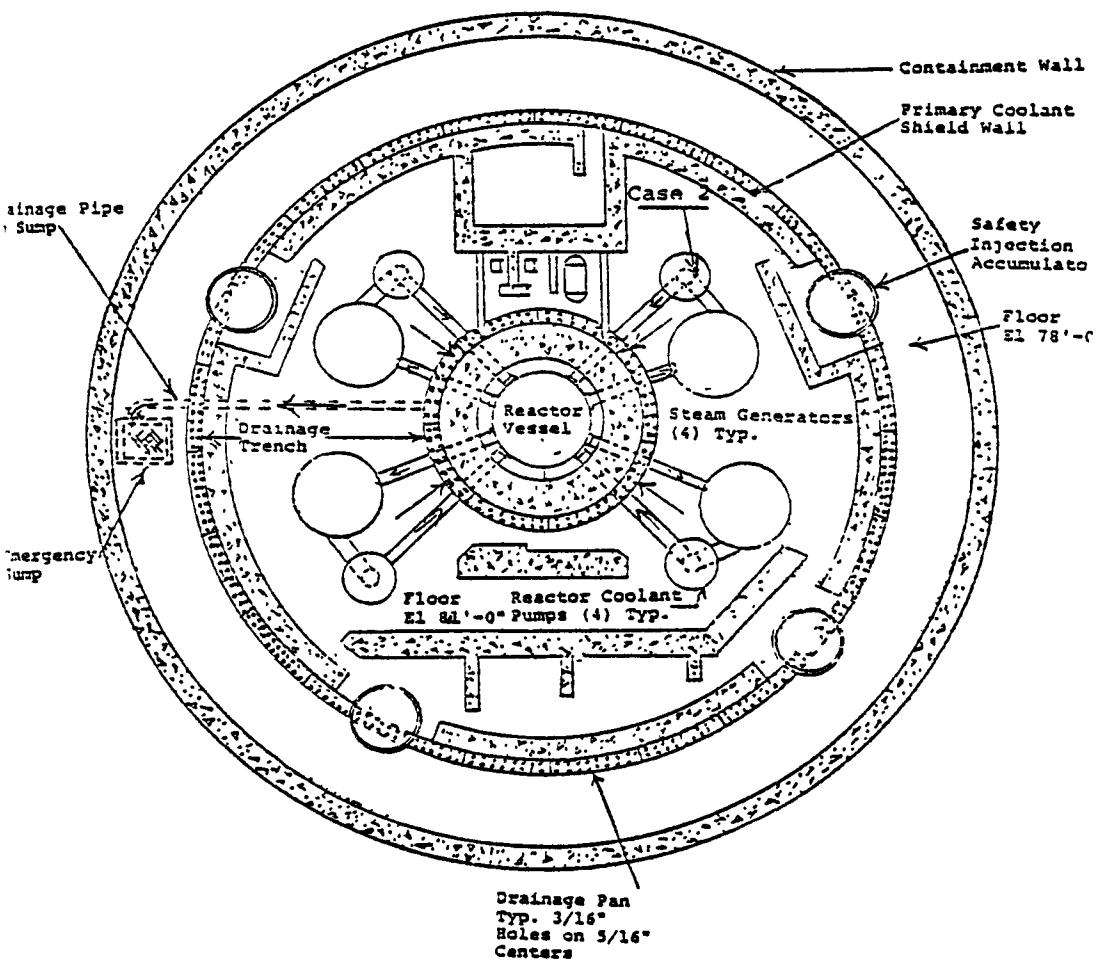

FIGURE A-3
CONTAINMENT ELEVATIONS 78'-0" & 100'-0"

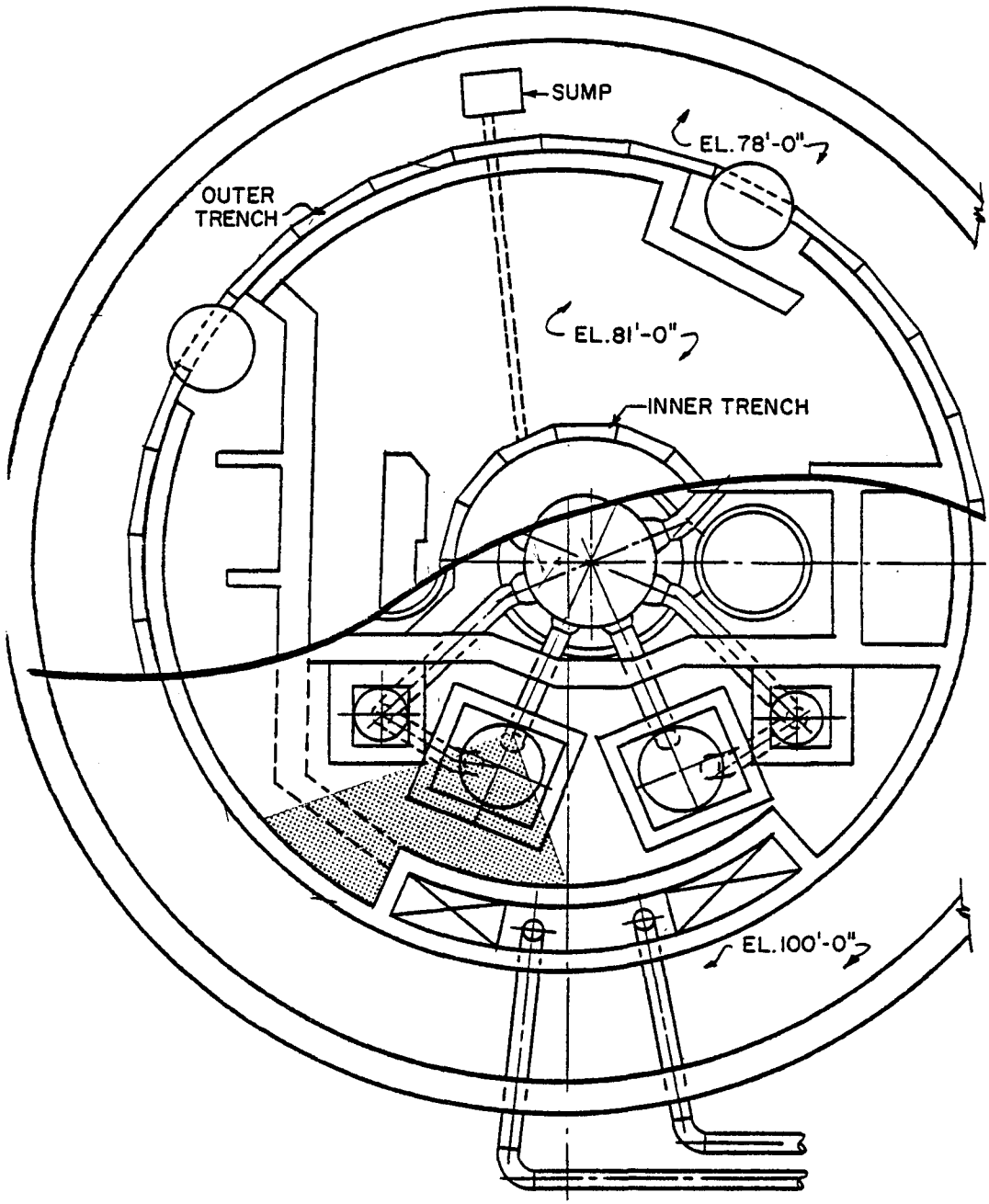

Break 3: Feedwater Line Failure

Break 3 represents one of the two limiting cases for pipe failures above elevation 130 feet (the other being break 4). Main steam and feedwater lines represent limiting cases as they are the largest diameter lines connected to a reservoir of high temperature and pressure fluid. The jet orientation is such that the upper region of the steam generator is completely intercepted by the jet.

Break 4: Main Steam Line Failure

The main steam break location is chosen such that the resulting jet fully encompasses the steam generator and directs debris toward the containment floor.

3.0 DEBRIS GENERATION

The following sections describe the quantity of insulation debris generated by each of three mechanisms for each break.

Break 1: Hot Leg Failure

3.1 Pipe Whip

As shown on Figures A-4 and A-5, the hot leg will rotate rigidly downward, with rotation taking place about the reactor cavity penetration. This pipe segment is 8 feet long with a diameter of 34 inches. It is covered with 3.5 inches of reflective metallic insulation which is assumed to produce 78 ft^2 of debris. As the break location is assumed at the steam generator nozzle, there is only one piping segment.

3.2 Pipe Impact

The lack of any piping in the trajectory of the ruptured hot leg indicates that no insulation debris is generated by this mechanism for this pipe failure.

FIGURE A-4
BREAK I: HOT LEG FAILURE

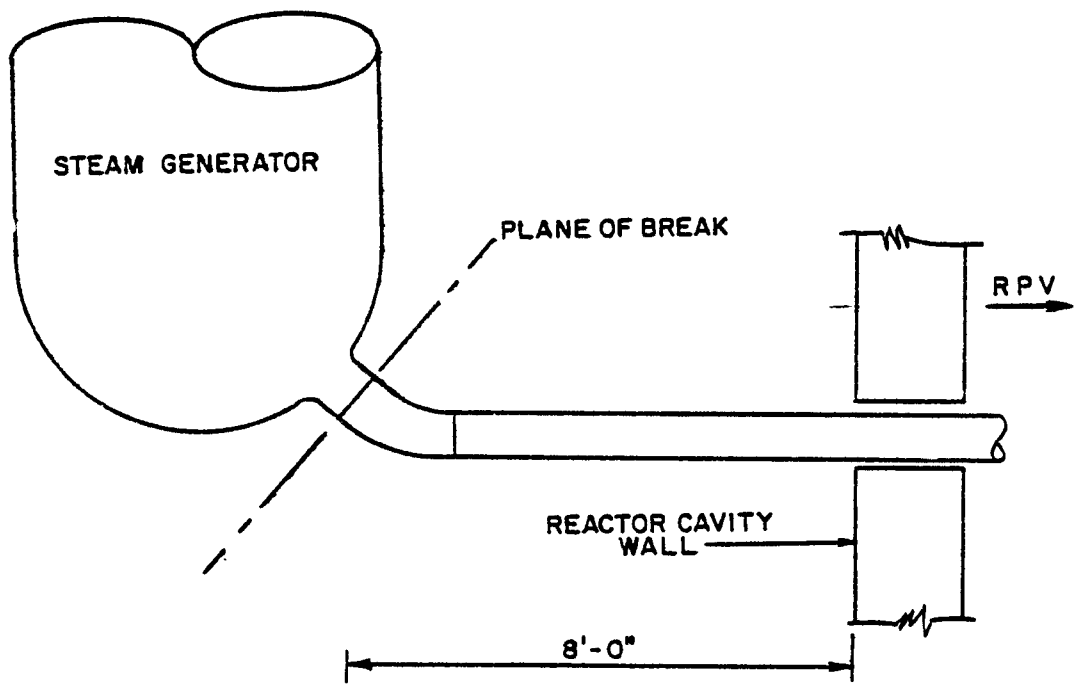

FIGURE A-5
BREAK 1: HOT LEG FAILURE

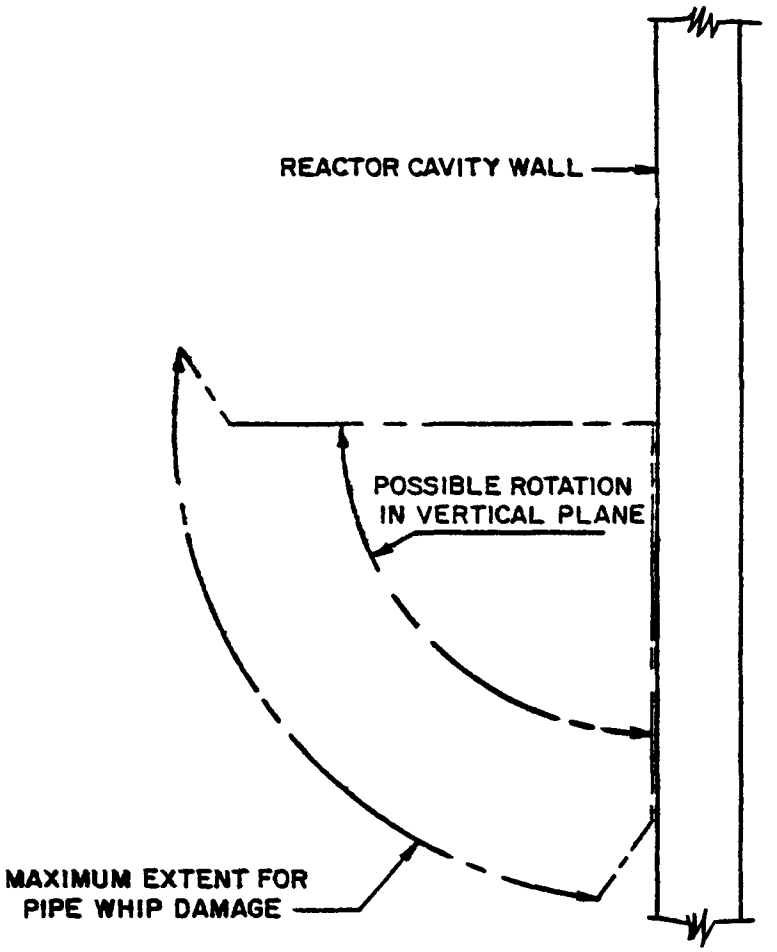

3.3 Jet Impingement

Figures A-6 through A-11 illustrate the path of the hot leg jet. The procedure of Attachment 2 is used to determine the thrust load, distance to full jet expansion and jet divergence angle.

Attachment 2 provides for known stagnation pressure, stagnation enthalpy and break areas:

$T/A_E = 294,350 \text{ lbf/ft}^2$

$L_\infty = 8.2 \text{ ft}$

$2\beta = 90°$

This indicates that the jet expands with equal axial and radial velocities.

The distance to the 0.5 psig stagnation plane (also from Attachment 2) is 76 feet. As containment radius is approximately 70 feet, all targets intercepted by the jet are affected.

Measuring the length and diameter of all piping within the expanded jet produces the summary of insulation debris shown on Table A-1.

4.0 DEBRIS TRANSPORT

4.1 Short Term Transport - Pipe Whip

Failure of the hot leg imparts a downward rotation to the hot leg pipe, with motion terminating when the pipe impacts the outer surface of the reactor cavity. The insulation is assumed to move tangent to the arc of rotation of the pipe at the point of impact, striking the reactor cavity wall and falling to the floor of the steam generator cavity.

4.2 Short Term Transport - Pipe Impact

As no pipe impacts occur, no transport by this mechanism exists.

FIGURE A-6

BREAK I: HOT LEG FAILURE JET PATH, ELEV. 81'-0"

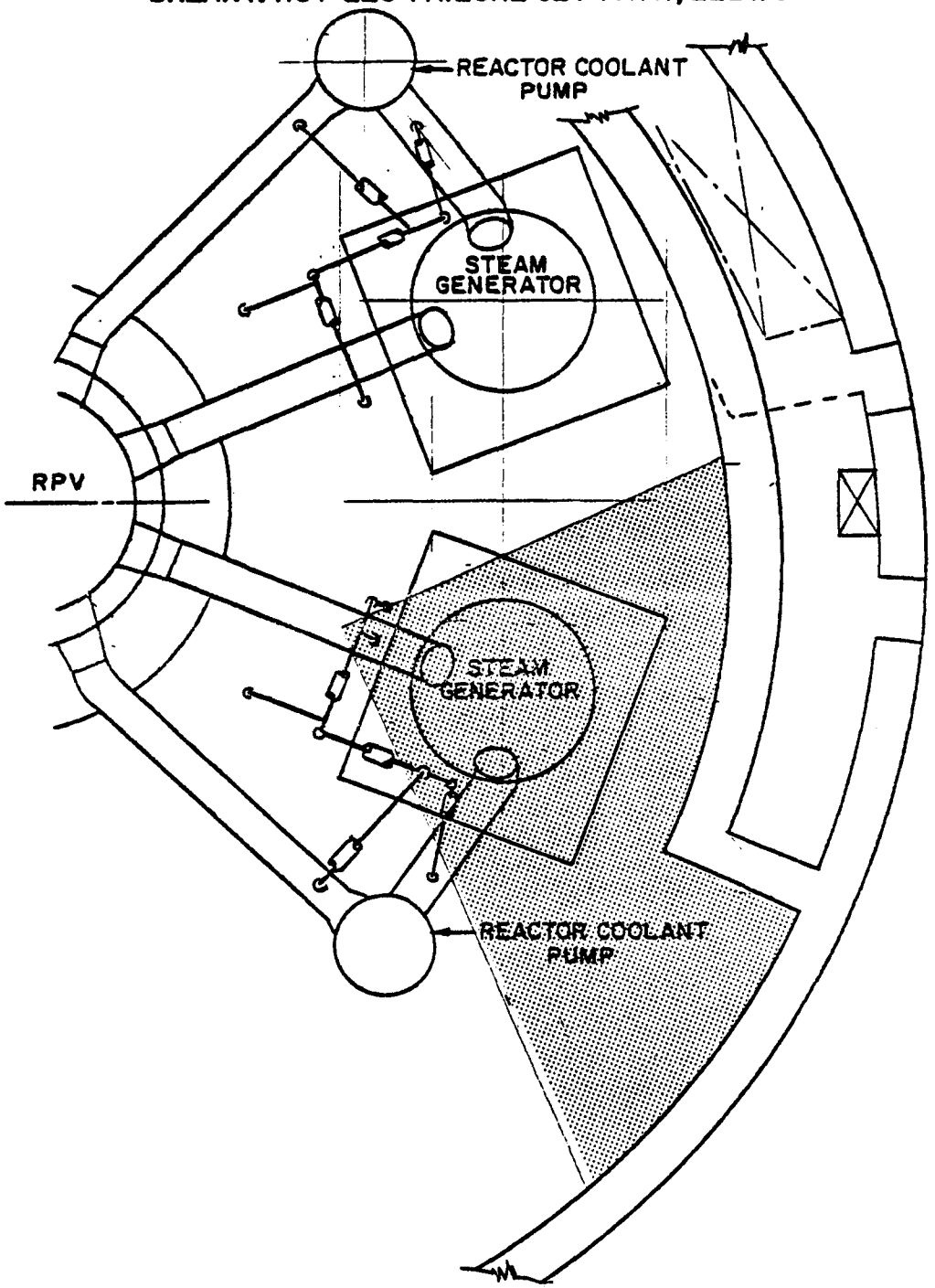

FIGURE A-7
BREAK I: HOT LEG FAILURE JET PATH, ELEV. 100'-0"

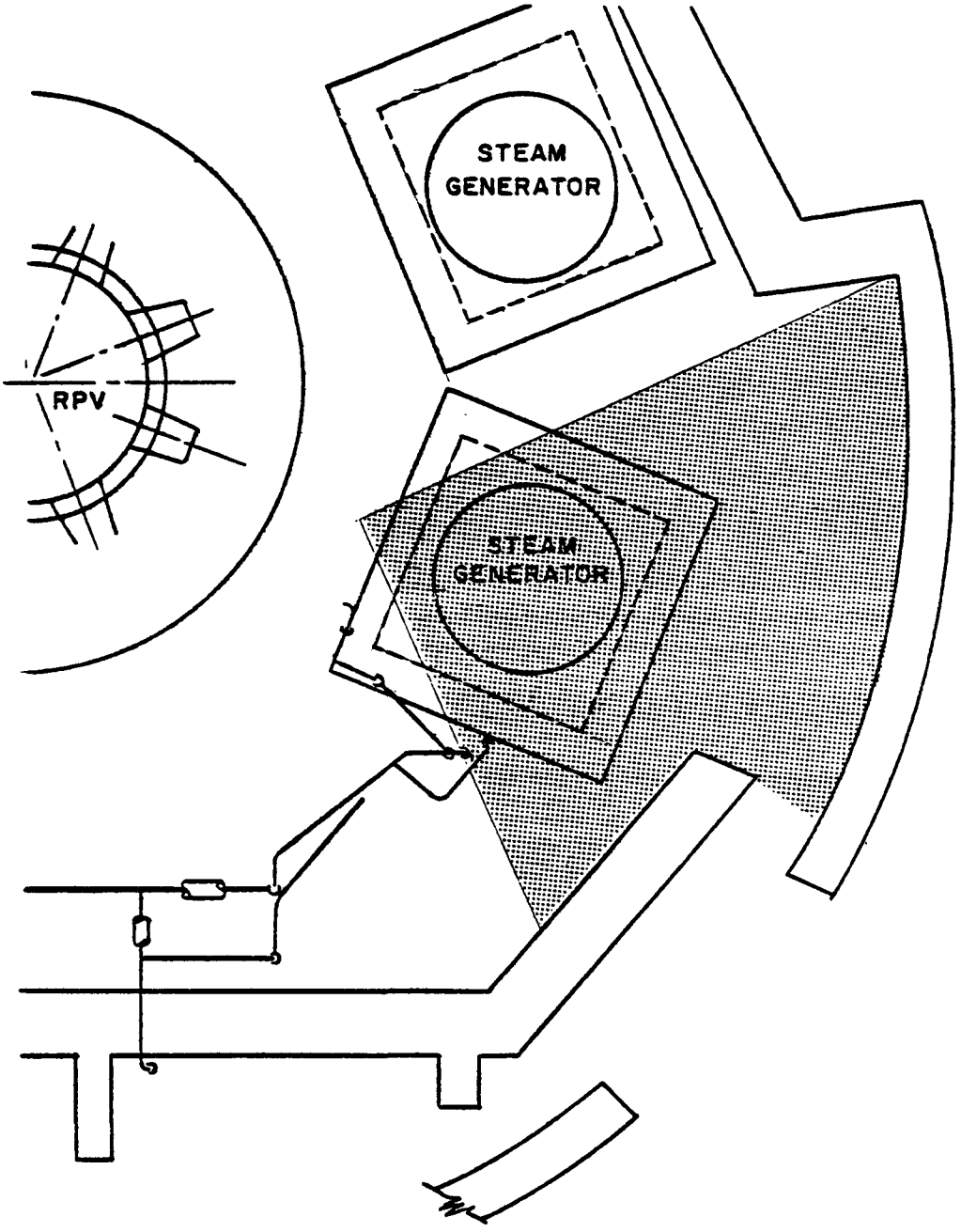

FIGURE A-8
BREAK I: HOT LEG FAILURE JET PATH, ELEV. 100'-0"

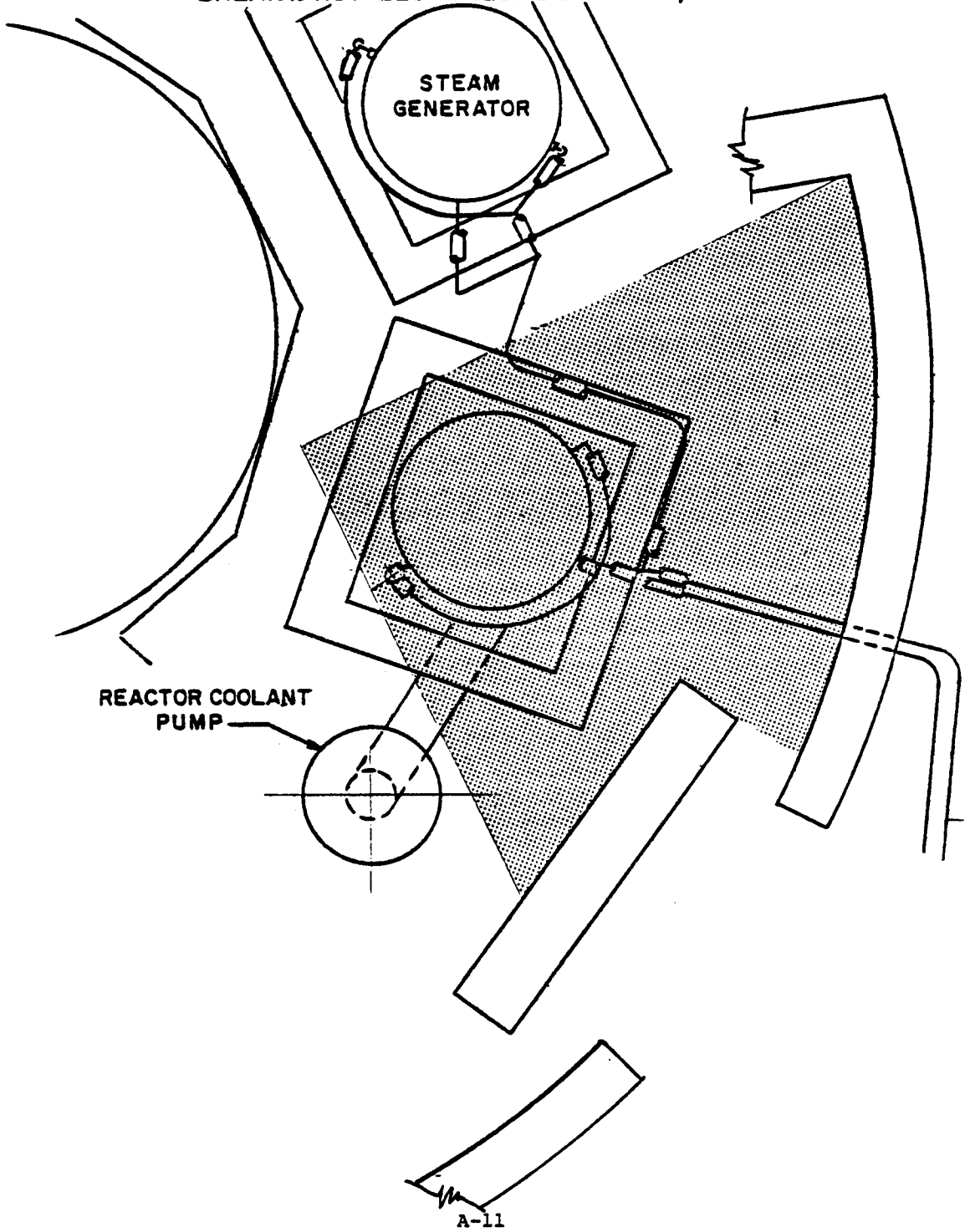

FIGURE A-9

BREAK I: HOT LEG FAILURE JET PATH, ELEV. 81'-0"

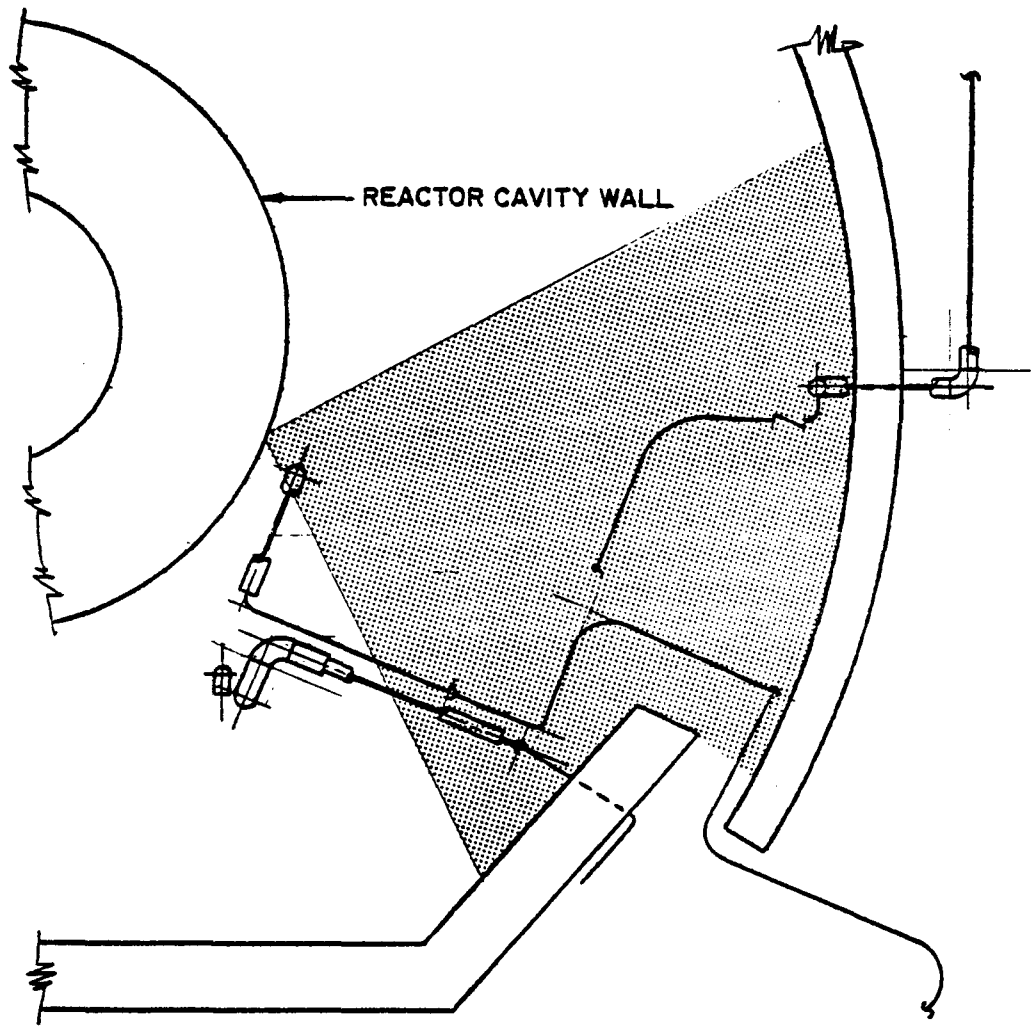

FIGURE A-10
BREAK 1: HOT LEG FAILURE JET PATH, ELEV. 100'-0"

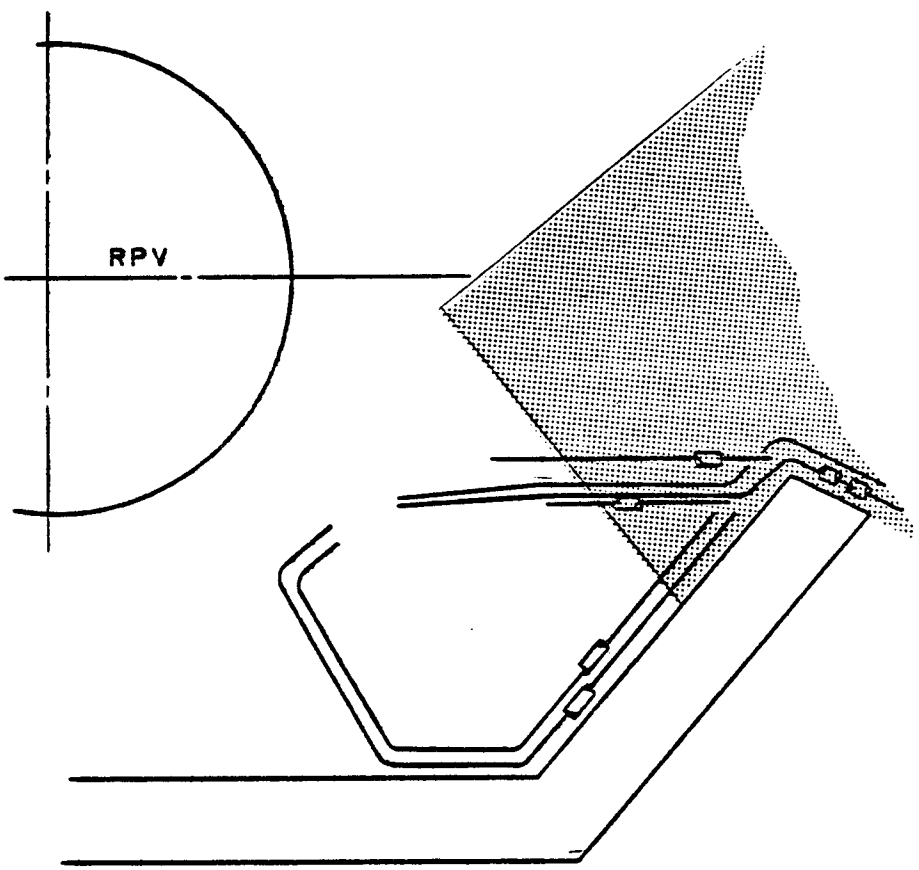

FIGURE A-11
BREAK I: HOT LEG FAILURE JET PATH, ELEV. 81'-0"

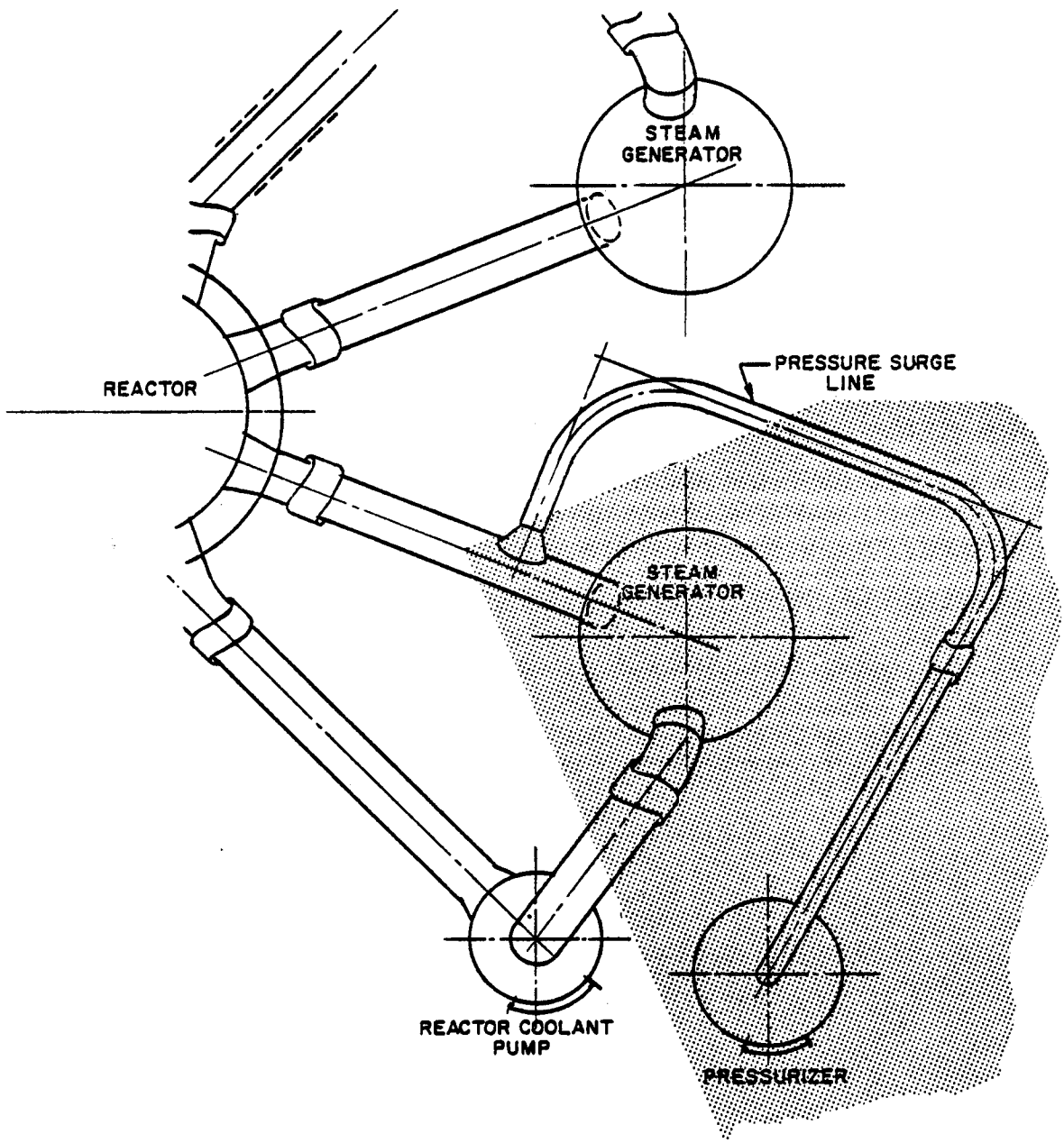

Table A-1

Debris Summary, Break 1: Hot Leg Failure

Line or Item	Length within Jet Cone (ft)	Diam. (in.)	Area of Insulation (ft^2)	Thickness (in.)	Type of Insulation
Steam Generator (Cylindrical)	28	144	1100	3.5	SE
Steam Generator (Bottom Head)	-	144	225	3.5	RM
Hot Leg	8	34	78	3.5	RM
Crossover	18	36	186	3.5	RM
Cold Leg	10	3	17	1.5	RM
SG Blowdown A	30	2	27	1.5	SE
SG Blowdown B	60	3	70	1.5	SE
RHR A	15	6	35	3	E
RHR B	17	10	51	1.5	E
Cooling Line A	15	2	12	1	AS
Cooling Line B	15	4	20	1	AS
Cooling Line C	15	6	27	1	AS
Pressurizer Surge	65	14	297	3.5	RM
Pressurizer	21	96	547	3.5	RM

Total Debris Generated (ft^2):

(RM)	Reflective Metallic	1350
(E)	Encapsulated	86
(SE)	Semi-Encapsulated	1197
(AS)	Anti-Sweat	59
	TOTAL	2692

SG - steam generator
RHR - residual heat removal

4.3 Short Term Transport - Jet Impingement

Figure A-12 illustrates the path of the hot leg jet. Part of the jet is intercepted by the near shield wall; the remainder stagnates on the outer wall (B). As insulation debris is initially assumed uniformly distributed within the jet, the quantity of debris reaching the outer wall is given as:

$$I_B = I_T \times \left[\frac{A_{A'} - A_A}{A_{A'}} \right] \qquad [A\text{-}1]$$

where I_B - debris reaching outer wall - ft^2
I_T - debris in jet field - ft^2
A_A - area of jet striking near shield wall - ft^2
$A_{A'}$ - area of jet at wall if no obstructions were present - ft^2

The following diagram illustrates the method:

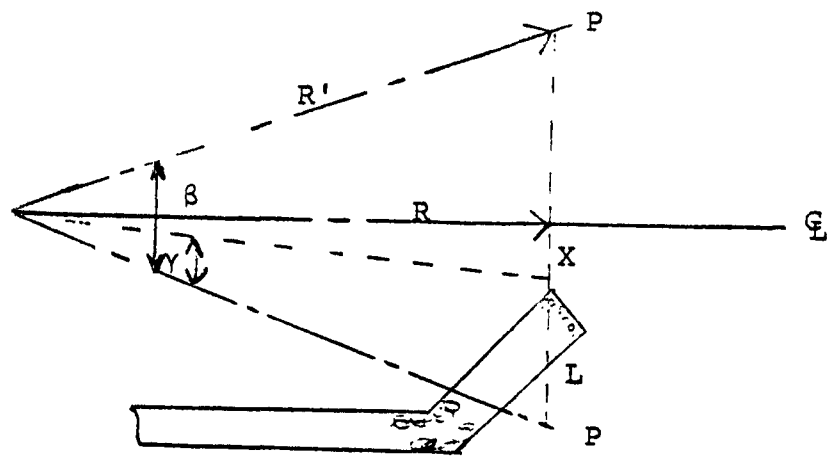

Line PP cuts the jet centerline at radial position R. Angle β is the jet divergence computed by the Attachment 2 method, and angle γ represents the portion of the jet intercepted by the near shield wall. The jet diameter at R is given by:

FIGURE A-12
HOT LEG JET PATH

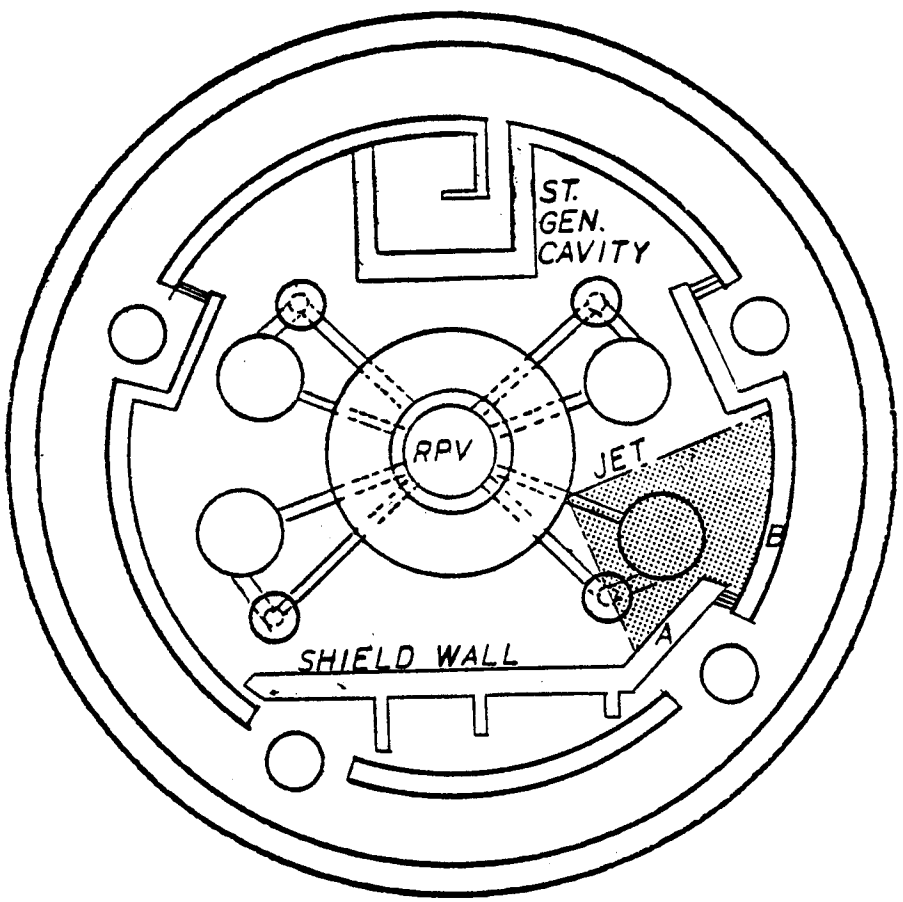

$$D_R = D_E + 2(R)\ \tan(\beta) \qquad [A-2]$$

and the jet area by

$$A_R = \frac{\pi\ D_R^2}{4} \qquad [A-3]$$

For the segment striking the near shield wall:

$$\text{Tan}\ \beta = \frac{X+L}{R} \qquad [A-4]$$

$$\text{Tan}\ (\beta - \gamma) = \frac{X}{R} \qquad [A-5]$$

$$L = R\ \tan\ (\beta) - R\ [\tan\ (\beta - \gamma)] \qquad [A-6]$$

$$L = 27\ [\tan\ (45) - \tan\ (45\text{-}20)]$$

$$L = 14.4$$

Therefore, the jet at plane PP, which has a circular cross section, has a segment with height equal to 14.4 feet which strikes the near shield wall. The following illustration describes this.

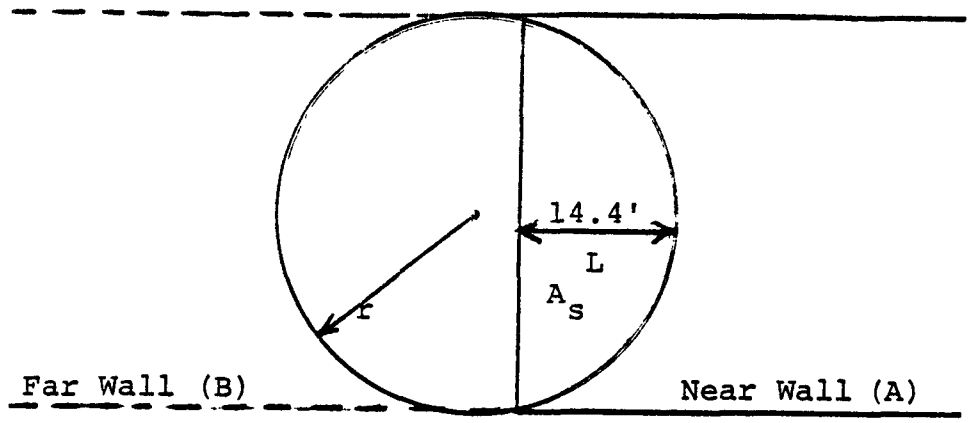

The segment area is given as:

$$A_s = r^2\ \cos^{-1}\ [\frac{r-L}{r}] - (r-L)\ \sqrt{2rL-L^2} \qquad [A-7]$$

where r - jet radius at radial position R (equal to $D_R/2$) - ft

L - segment height of stagnated jet - ft

A_s - area of the jet segment stagnated on near wall - ft^2

$$A_s = 27^2 \cos^{-1}\left[\left(\frac{27-14.4}{27}\right)\right] - (27-14.4)\sqrt{2(27)(14.4)-14.4^2}$$

$$= 490.28$$

From Equation A-3, $A_R = 2500$

Therefore 490/2500, or 19.6% of the debris in the jet stagnates on the near shield wall. The remaining 80.4% of the debris is transported by the jet to the far wall. In summary:

Debris in jet field (I_T)	- 2692 ft^2
Debris stopped at wall A	- 527 ft^2
Debris transported to wall B (I_B)	- 2164 ft^2

Figure A-12 also shows a door leading to the annulus region. The amount of debris ejected through the door, assuming a uniform debris distribution, is given by Equation A-8 through A-10. Refer to the following sketch.

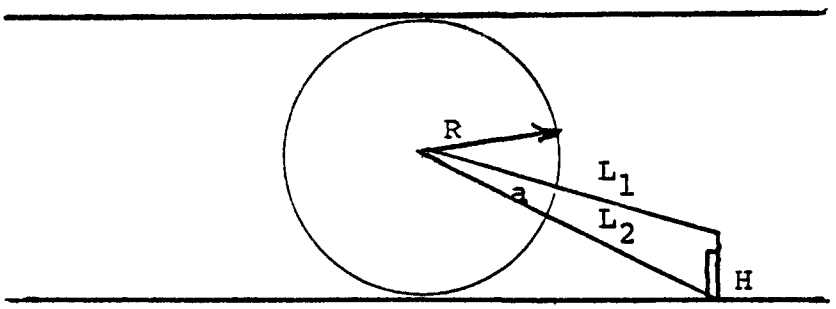

where a - angle which subtends door - degrees
R - jet radius at outer wall - ft
L_1 - distance from jet ℄ to door top - ft
L_2 - distance from jet ℄ to door bottom - ft
H - height of door - ft

For triangle L_1, L_2, H:

$$H^2 = L_1^2 + L_2^2 - 2 L_1 L_2 \cos a \qquad [A-8]$$

$$\text{Cos } a = \frac{L_1^2 + L_2^2 - H^2}{2\,L_1\,L_2} \qquad \text{[A-9]}$$

From plant drawings:

$H - 8.6$

$L_1 - 21.9$

$L_2 - 21.9$

$$\text{Cos } a = \frac{21.9^2 + 21.9^2 - 8.6^2}{2(21.9)(21.9)}$$

$$\text{Cos } a = 0.922$$

$$a = 22.8$$

The quantity of debris reaching the outer wall which is then ejected through the door is given as:

$$I_E = I_B \frac{a}{360} \qquad \text{[A-10]}$$

where I_E - debris ejected - ft^2

I_B - debris reaching outer wall - ft^2

a - angle which subtends door - degrees

Therefore:

$$I_E = 2164 \times \frac{22.8}{360}$$

$$I_E = 135 \text{ ft}^2$$

Table A-2

Short Term Transport Summary, Break 1: Hot Leg Failure (ft^2)

Phenomena	Generated	Contained within Shield Wall	Ejected To Annulus
Pipe Whip	78	78	0
Pipe Impact	0	0	0
Jet Impingement	2692	2557	138

4.4 Long Term Transport - Recirculation Phase

After the blowdown phase is complete, the ECCS pumps are activated to reflood the core. The pumps initially take suction from the refueling water storage tank (RWST), switching to the containment recirculation sump upon receipt of a low water level signal in the RWST.

The object of the long term transport analysis is to determine the motion of the debris generated by the initiating event. The short term transport analysis provides the starting locations of all debris items, and the long term analysis follows these items as they are transported within containment. Depending upon the types of insulation present within containment, the long term transport problem is approached in different ways.

There are four openings in the crane wall leading to the containment annulus area (Figure A-2). Due to recirculation sump intake placement (i.e., one trench inside the crane wall, one trench outside the crane wall, and a screened sump outside the crane wall) the calculations presented in Section 4.4.1.1 are modified as follows.

4.4.1.1 Containment Flow - Recirculation Mode

Maximum velocity occurs across the minimum flow areas at the doors leading to the annulus. If this velocity is insufficient to transport the sunken debris, transport from inside the crane wall to the annulus is not a consideration for sunken debris.

ECCS pump flow rate - 9000 gpm (from FSAR)

Door area - Water depth 4 ft. (from FSAR)

- Width 2 at 4 ft. (from plant drawings)
  1 at 3.5 ft. (from plant drawings)
  1 at 3 ft. (from plant drawings)

Total area - 58 ft^2

$$\text{Velocity} = 9000 \frac{gal}{min} \times \frac{1\ min}{60\ sec} \times \frac{1\ ft^3}{7.48\ gal} \times \frac{1}{58\ ft^2} = 0.35 \frac{ft}{sec}$$

Reflective metallic (RM) insulation 3.5 in. thick weighs approximately 4.4 lbm/ft^2 or 15 lbm/ft^3 (bulk density). As steel weighs approximately 490 lbm/ft^3, the mirror insulation is approximately 97% voids, or 1 ft^3 of RM insulation contains 0.03 ft^3 of metal:

$$V_{metal} = 2 \times 4 \times \frac{3.5}{12} \times 0.03 = 0.07\ ft^3$$

Applying Equation 16 to panel:

$$F_N = (490-62)0.07\ g/g_c - F_A$$

$$F_N = 30 - F_A\ lbf$$

using $\mu_f = 0.45$ (Section 4.5.2.4)

$$F_A = \frac{C_D\ A_p\ \rho_w\ \bar{V}^2}{2g_c}$$

As C_D is a function of Reynolds number, the Reynolds number N_{RE} is determined as follows:

$$N_{RE} = \frac{D_p\ \bar{V}\ \rho}{\mu}$$

where D_p - particle diameter = $2\sqrt{\frac{A_p}{\pi}}$

A_p - panel area assuming 4 ft. x 3.5 in. side is normal to flow

$\bar{V}$ - velocity of flow

ρ - fluid density

μ - fluid viscosity

$$N_{RE} = \frac{2\sqrt{\frac{1.166}{\pi}}\ (0.35)(62)}{6.72 \times 10^{-4}}$$

$$= 40{,}000$$

Therefore, flow is turbulent and $C_D = 1.2$.

Therefore: $F_A = \frac{1.2(\frac{3.5}{12} \times 4)(62)(0.35)^2}{2(32.2)}$

$F_A = 0.165$ lbf

then $F_N = 30 - 0.165$

and from Equation 14 $F_M = \mu_f F_N = 0.45(29.83) = 13.4$ lbf

As indicated in Section 4.5.3, sunken debris will remain where it is at the termination of blowdown.

Encapsulated cerablanket is treated in the same fashion as reflective metallic insulation. As the enclosing structure has a bulk density of approximately 15 lbf/ft^3, the encapsulated cerablanket material would initially float with approximately 25% of its volume submerged, leading to water infiltration and consequent sinking.

Semi-encapsulated cerablanket is fibrous insulation with an external metallic lagging. Consequently, the lagging is treated as sinking debris (Section 4.5) and the cerablanket as fibrous insulation (Section 4.7).

Table A-1 indicates that 1197 ft^2 of semi-encapsulated cerablanket insulation debris is generated by the hot leg failure. Following the procedures developed in Section 4.7, 100% of this material is assumed to be transported to the sump and consequently cause blockage. If the additional head loss generated by this debris accumulation is not in excess of the pump NPSH margin, this level of blockage is acceptable.

From plant drawings,

Sump screens area - 142 ft^2

Inner trench area - 239 ft^2

Outer trench area - 697 ft^2

Total trench area - 1078 ft^2

Total trench area is used as sump intake area since the paths to the sump are independent. Assuming uniform deposition of the fibrous debris, the debris accumulation is

$$\frac{\left[\frac{3.5}{12} \times 1100 + \frac{1.5}{12} \times 97\right]}{1078} = 3.7 \text{ in.}$$

Equation 27 gives:

$$\frac{\Delta P}{L} = \frac{3.5\ \mu_q\ S_v^2}{A_b} (1-\varepsilon)^{1.5} \left[(1+57(1-\varepsilon)^3\right]$$

Using the data in Section 5.3:

$\mu \doteq 0.0068$ (water 120°F)

$q = 9000$ gpm (5.677×10^5 cm^3/sec)

$S_v = 2420$ cm^2/cm^3

$A_b = 1078$ ft^2 gross area (55% blockage due to presence of 1/8 x 1/8 in. screen) gives 485 ft^2 or 4.5×10^5 cm^2

$\varepsilon = 1 - \nu C' = 1 - 0.384\ (0.0961) = 0.963$

$C' = 6$ lbm/ft^3 (0.0961 g/cm^3)

$\nu = 0.384$ cm^3/g

$\ell = 3.7$ in. (9.4 cm)

and

$$\frac{\Delta P}{\ell} = \frac{3.5(0.0068)(5.677 \times 10^5)(2420)^2}{4.5 \times 10^5} (1-0.963)^{1.5}\left[1+57(1-0.963)^3\right]$$

$$= (1.761 \times 10^5)(0.00712)(1.003)$$

$$= 1257 \text{ dynes/cm}^2\text{/cm}$$

$\Delta P = .17$ psi

An increased pressure loss of .17 psi can be accommodated regardless of the available pump NPSH margin. Sound engineering practice demands that NPSH margins exceed this order of magnitude by a substantial amount.

5.0 SUMP EFFECTS

The lack on any substantial pressure drop due to accumulated debris eliminates the need to perform detailed sump pressure drop calculations.

Regarding the assumption of uniform debris distribution with the jet, Section 4.4.1 assumes all debris which can migrate reaches the sump intakes. Since the sump has intakes both within and without the crane wall, any redistribution from that assumed would result in decreased pressure drop in one region and increased pressure drop in the other.

For this plant, the actual short term transport debris distribution in the jet is immaterial as the long term transport assumption of uniform screen blockage leads to maximum pressure drop.

Conclusion

The hot leg failure dislodges reflective metallic and encapsulated cerablanket insulations, neither of which can be transported along the containment floor. Semi-encapsulated cerablanket is also dislodged. Assuming that all dislodged semi-encapsulated cerablanket floats, migrates to the sump trenches and sinks, an acceptable increase in pressure drop results. Accordingly, debris accumulations due to the hot leg failure have no effect on the recirculation sump performance.

3.0 DEBRIS GENERATION

Break 2: Cold Leg Failure

3.1 Pipe Whip

Figures A-13 and A-14 illustrate the location of the rupture point and hinge location. The pipe is 36 in. OD and the segment length is 11.9 ft. The 3.5 in. reflective metallic insulation from the break location to the hinge is ejected and generates 123 ft^2 of debris. As the rupture occurs at the steam generator nozzle, there is only one pipe segment.

FIGURE A-13
BREAK 2: COLD LEG FAILURE, PLAN VIEW

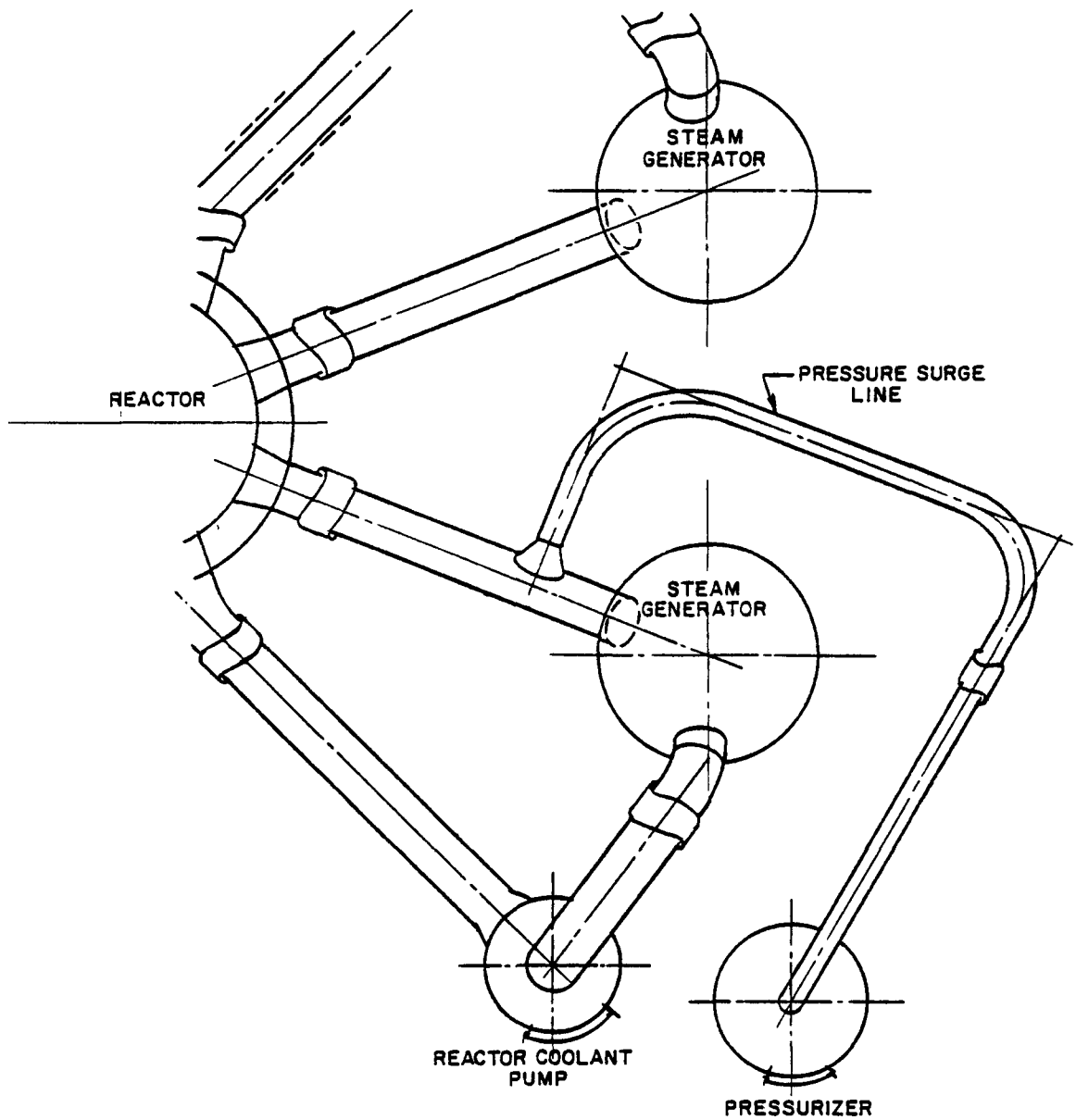

FIGURE A-14
BREAK 2: COLD LEG FAILURE ELEVATION VIEW.

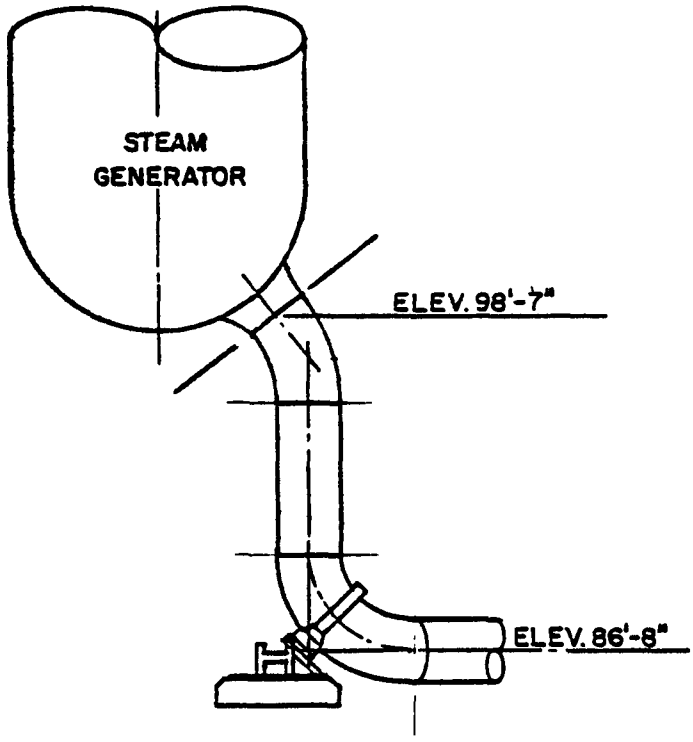

3.2 Pipe Impact

The segment is restrained as illustrated on Figure A-14. Consequently, no impact of the free segment occurs. No debris is generated by this mechanism.

3.3 Jet Impingement

Table A-3 summarizes the debris generated by the cold leg jet. Figures A-15 through A-20 show the cold leg jet path.

4.0 DEBRIS TRANSPORT

4.1 Short Term Transport - Pipe Whip

Failure of the cold leg causes a downward motion of the piping segment, with the free end moving toward the reactor coolant pump. The insulation will move tangent to the arc of rotation at the point where the whipping pipe is stopped by the restraint.

4.2 Short Term Transport - Pipe Impact

No impact occurs.

4.3 Short Term Transport - Jet Impingement

The cold leg failure requires consideration of both jets - the jet exiting the crossover pipe, or east jet, and the blowdown flow from the steam generator or, west jet. The data from Table A-3 can be further classified as east or west traveling as shown in Table A-4.

Figure A-21 illustrates the paths of the east and west traveling jets. As can be seen, the west jet traps the generated debris in a blind corner. To be ejected from the steam generator cavity, the debris would have to change direction twice; once upon contact with the west wall to turn the debris southeast and again near the southwest crane wall opening where the southeast traveling debris would have to move southwest to be ejected. These changes in direction are not expected to occur. The west jet debris is therefore not assumed to be ejected to the annulus.

Table A-3

Debris Summary, Break 2: Cold Leg Failure

Line	Length (ft)	Diam.	Area (ft^2)	Thickness (in.)	Type of Insulation
Crossover	11.9	3.027'	123	3.5	RM
Reactor Coolant Pump	25	7'	570	3.0	RM
Pressurizer	21	8'	547	3.5	RM
Pressurizer Surgeline	35	14"	160	3.5	RM
Steam Generator 23	28	12'	1100	3.5	SE
Steam Generator 23	*	12'	225	3.5	RM
Steam Generator 21	28	12'	1100	3.5	SE
Steam Generator 21	*	12'	225	3.5	RM
Hot Leg 21	9.3	34"	91	3.5	RM
Cold Leg 21	5	3.027'	52	3.5	RM
Hot Leg 23	14	34"	137	3.5	RM
Safety Injection	15	14"	60	1.5	E
RCP Coolant	62	2"	48	1.0	AS
RCP Coolant	62	3"	64	1.0	AS
RCP Coolant	62	4"	81	1.0	AS
SG Blowdown	60	2"	55	1.5	SE
SG Blowdown	30	3"	35	1.5	SE
Coolant Line	54	3"	64	1.5	E

Total debris generated (ft^2):

(RM)	Reflective Metallic	2130
(E)	Encapsulated	124
(SE)	Semi-Encapsulated	2290
(AS)	Anti-Sweat	193
	TOTAL	4737

SG - steam generator
RCP - reactor coolant pump

FIGURE A-15

BREAK 2: COLD LEG FAILURE JET PATH, ELEV. 81'-0"

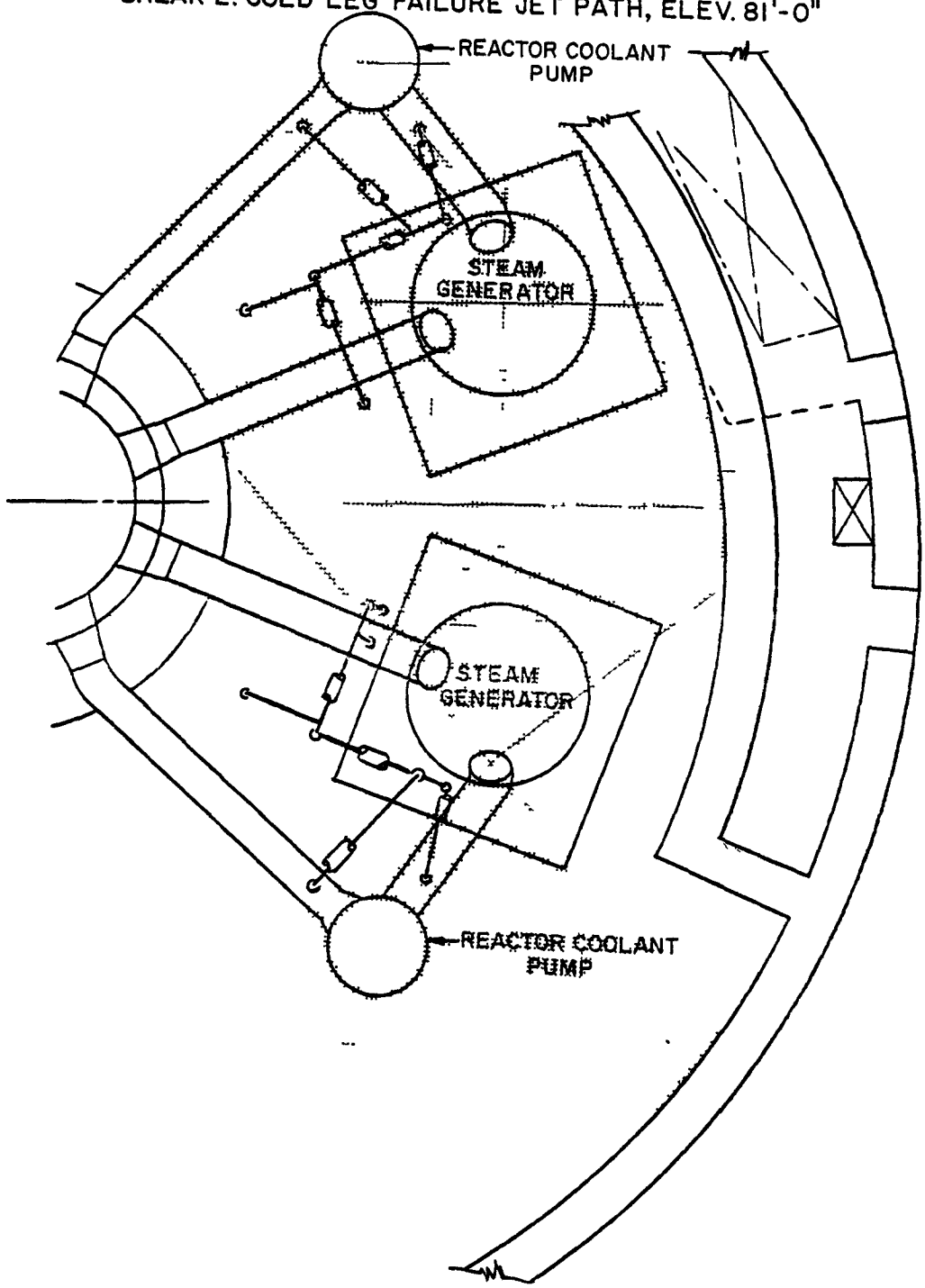

FIGURE A-16

BREAK 2: COLD LEG FAILURE JET PATH, ELEV. 81'-0"

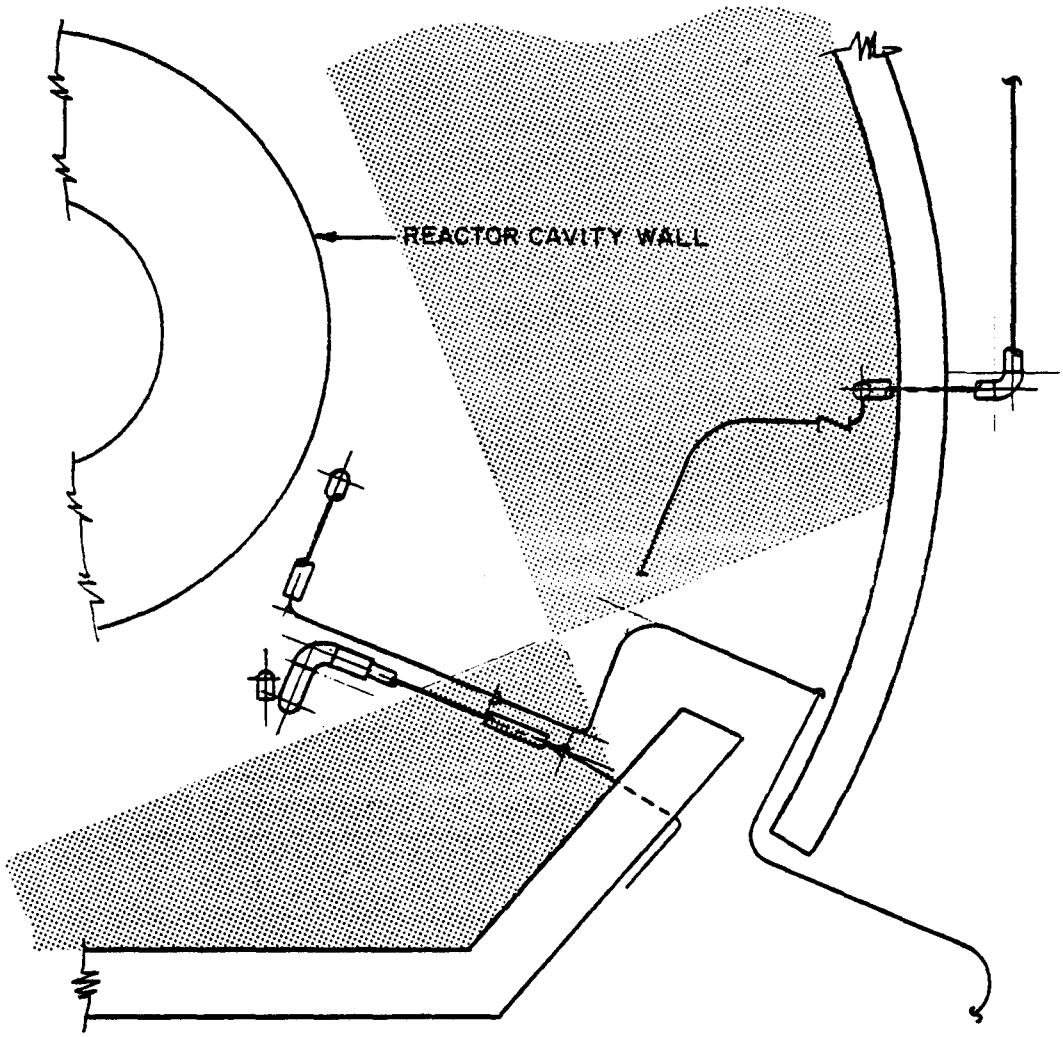

FIGURE A-17
BREAK 2: COLD LEG FAILURE JET PATH, ELEV. 100'-0"

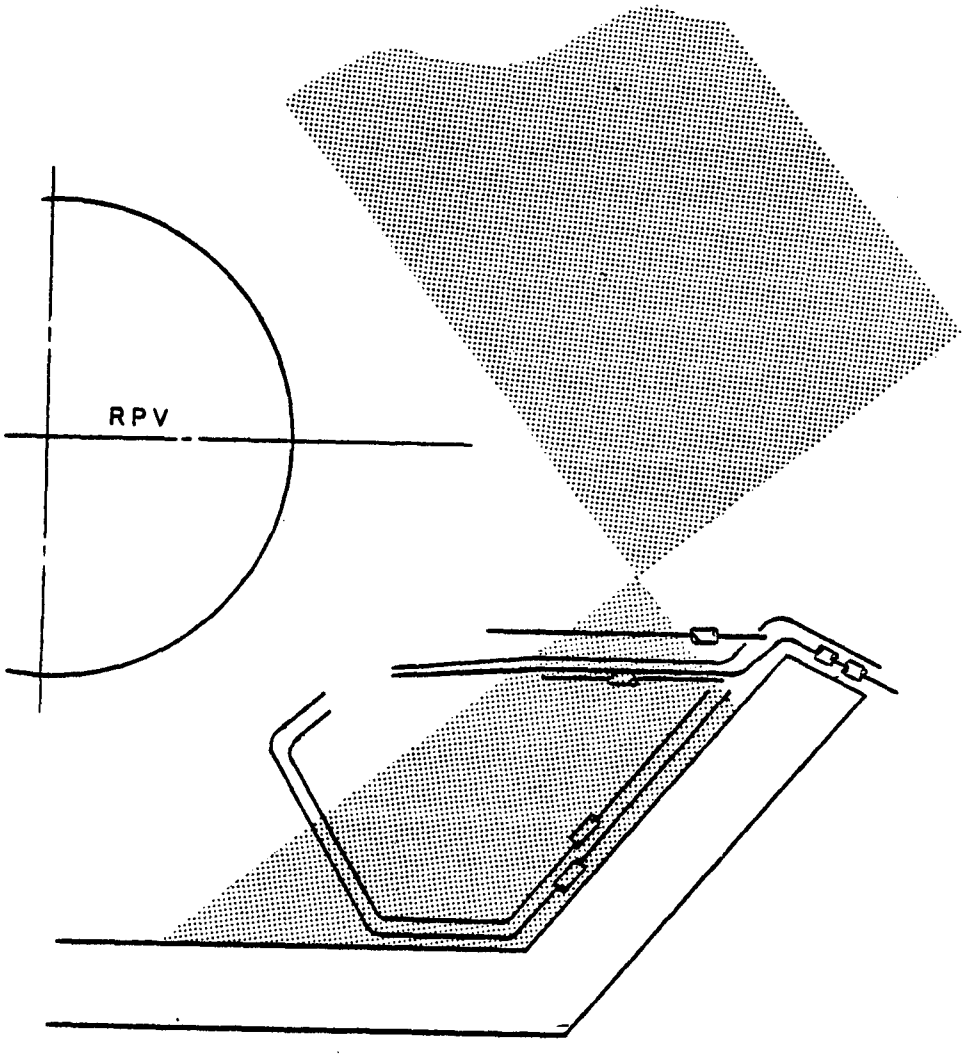

FIGURE A-18
BREAK 2: COLD LEG FAILURE JET PATH, ELEV. 100'-0"

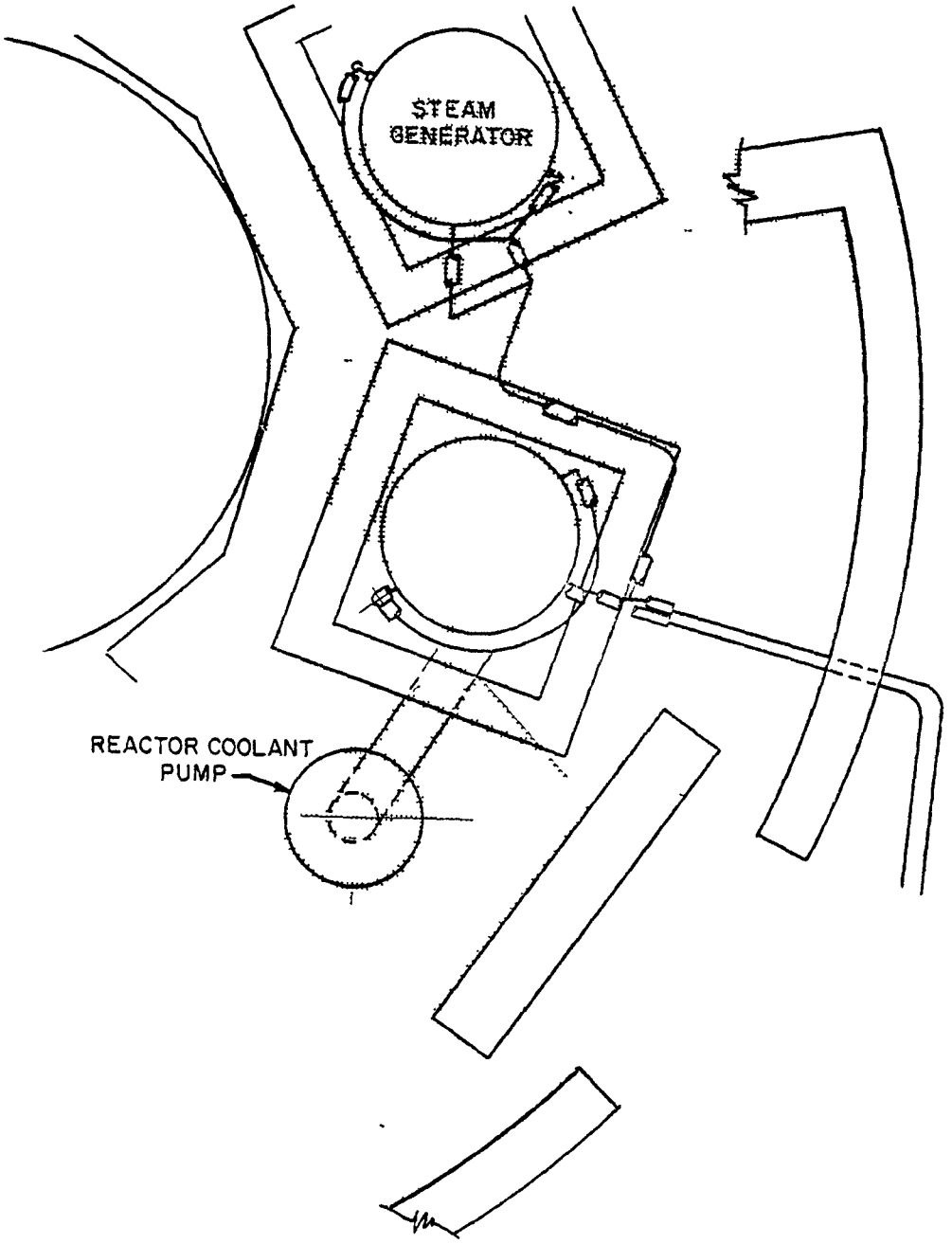

FIGURE A-19
BREAK 2: COLD LEG FAILURE JET PATH, ELEV. 81'-0"

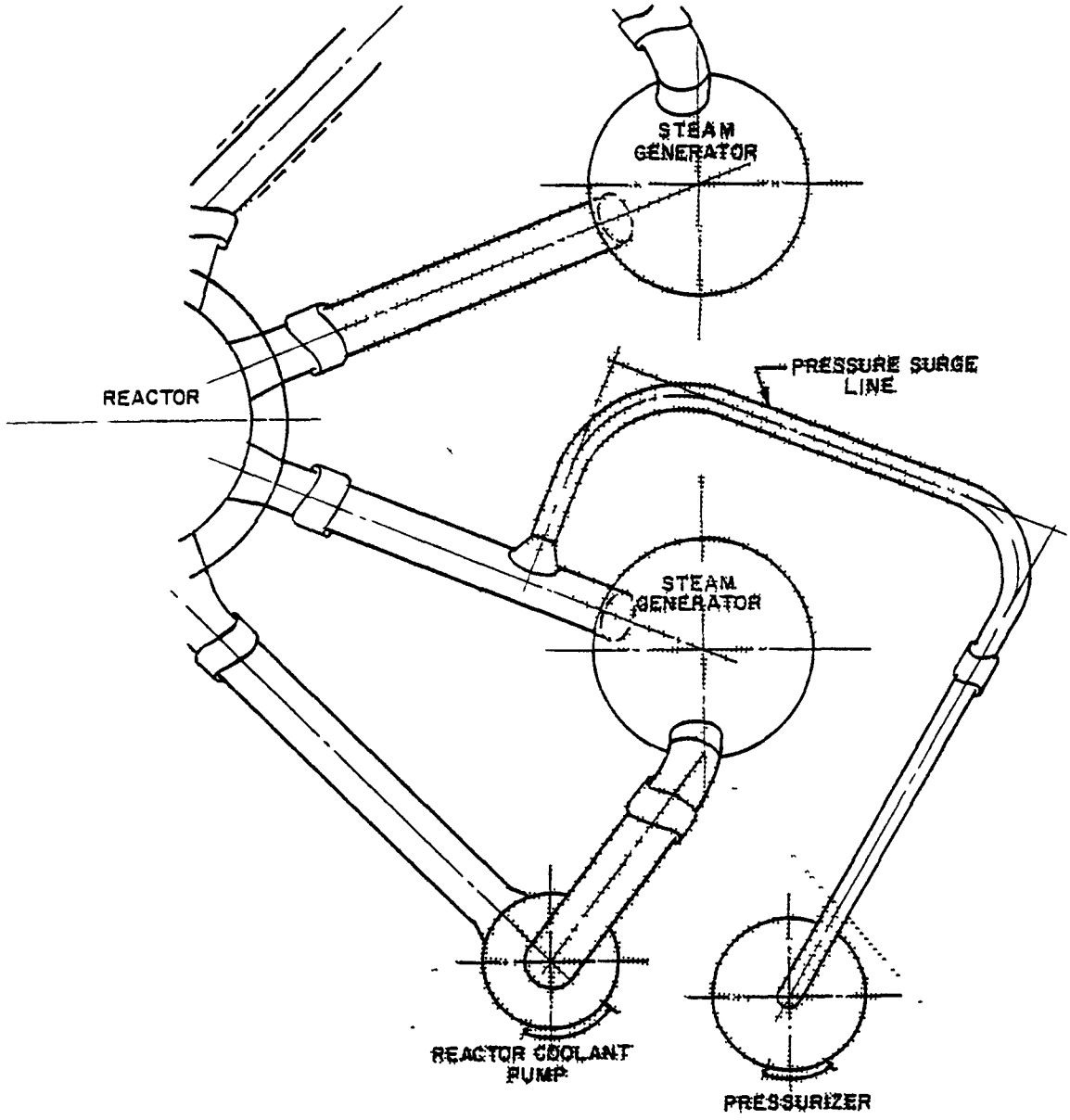

FIGURE A-20
BREAK 2: COLD LEG FAILURE JET PATH, ELEV. 100'-0"

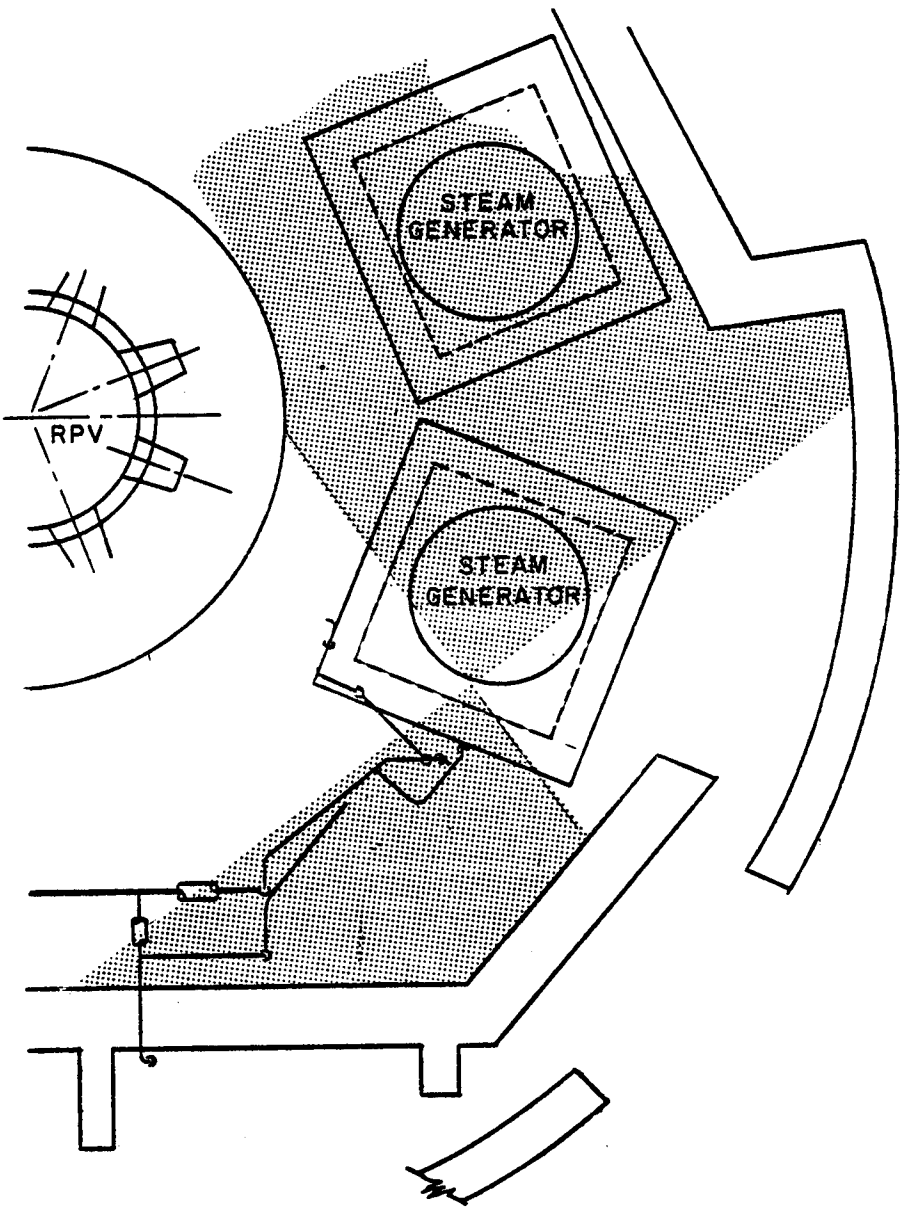

Table A-4

Debris Distribution Summary, Break 2: Cold Leg Failure

Insulation Type	Thickness (in.)	Amount Contained In East Jet (ft^2)	Amount Contained In West Jet (ft^2)
Reflective Metallic	3.5	562	890
	3.0	0	678
Encapsulated	3.5	0	0
	1.5	64	60
Semi-Encapsulated	1.5	2290	0
Anti-Sweat	1.0	0	193
		2916	1821

FIGURE A-21

BREAK 2: COLD LEG FAILURE EAST-WEST JET, ELEV. 80'-0"

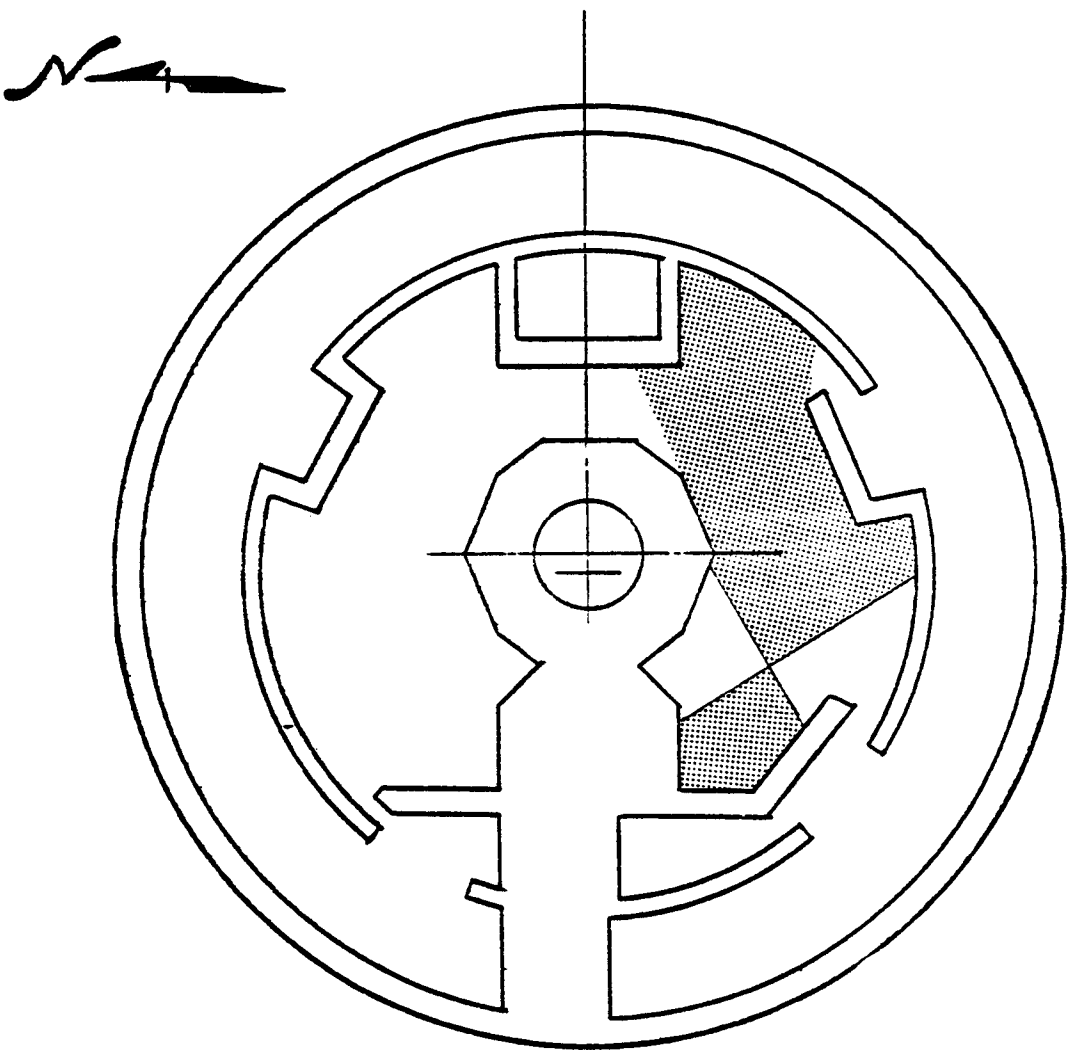

The east jet, due to its divergence, strikes the crane wall, as well as the two shielding walls illustrated. The east jet expands at a 45 degree half-angle (divergence computed using the Attachment 2 procedure) while the jet subtends a 50 degree segment of the crane wall on which stagnated debris could be ejected to the annulus. The remaining 40 degree section of the blowdown jet stagnates debris in blind pockets or transports debris away from the crane wall openings.

Consequently, the fraction ejected equals:

$$\text{Total debris} \times \frac{\text{Area of jet stagnated}}{\text{Area of jet}}$$

A circular jet with central angle β, has a radius R at any axial distance L, equal to $R = L \tan(\beta/2)$.

Consequently,

$$\text{Debris stagnated} = \underset{\text{(from Table A-4)}}{\text{total debris}} \times \frac{[\text{Tan}(\frac{50}{2})]^2}{[\text{Tan}(45)]^2}$$

$$= 2916 \times 0.22$$

$$\text{Debris stagnated} = 641 \text{ ft}^2$$

Consequently 641 ft^2 of insulation which is stagnated on the east wall is available for transport to the annulus.

Referring to the hot leg analysis, the crane wall opening is 8 ft. 6 in. high, and referring to Figure A-21 the jet centerline is 13 ft. from the opening in the crane wall. Proceeding as in the case of the hot leg:

$$\text{Cos } a = \frac{13^2 + 13^2 - 8.5^2}{2(13)^2}$$

$$a = 38^\circ$$

and 10.5% of the debris, or 67 ft^2, is ejected to the annulus.

Table A-5 summarizes the debris produced by the cold leg failure for each debris generation mechanism.

Table A-5

Short-Term Transport Summary, Break 2: Cold Leg Failure (ft^2)

Jet	Pipe Whip	Jet Impingement	Trapped by Crane Wall	Ejected to Annulus
East	0	2916	2849	67
West	123	1821*	1821*	0
Total	123	4737	4670	67

*Includes debris generated by pipe whip.

4.4 Long Term Transport - Recirculation Phase

Refer to the hot leg analysis for a discussion of long term transport.

4.4.1.1. Containment Flow - Recirculation Mode

As indicated in the hot leg analysis, containment velocities are insufficient to transport sunken debris of the type formed inside containment.

4.4.2.5 Fibrous Insulation

Table A-3 indicates that 2290 ft^2 of semi-encapsulated fibrous insulation debris is formed. Assuming that this debris uniformly blocks both trenches and the screens, a bed 7.2 in. deep will result. As pressure drop varies linearly with bed thickness, the pressure drop computed for the hot leg can be used.

$$\frac{\Delta P}{\ell} = 1257 \text{ dynes/cm}^2/\text{cm}$$

$$\ell = 7.2 \text{ in. or } 18.2 \text{ cm}$$

$$\Delta P = 1257\ (18.2)$$

$$= 22877 \text{ dynes/cm}^2 \text{ or } .33 \text{ psi}$$

This increased head loss should not effect recirculation pump NPSH margin adversely.

5.0 SUMP EFFECTS

An investigation of sump effects is not warranted owing to the small pressure drop imposed by the accumulated debris. Again, as in the hot leg case, the actual distribution of debris in the jet is not material. The sunken debris cannot be transported by the highest containment velocities so its position is not of concern and the fibrous debris is assumed to migrate to the sump regardless of initial position. As the sump pressure loss increase is acceptable, these assumptions need not be verified. In this specific case, debris distribution assumptions need not be verified as the initial distribution assumptions have no effect on the quantity of debris reaching the sump screens.

Breaks 3 and 4: Main Steam and Feedwater Line Failures

Figures A-22 through A-24 illustrate the routing of the main steam and feedwater lines from the steam generators to the containment penetrations. Concrete floors or grating interposed between these lines and the containment sump region will serve to confine any debris generated in the region above them and prevent debris migration to the sump.

Referring to Figure A-1, the 130 ft. elevation is a concrete slab capable of confining both debris and the jet flow while the 100 ft. elevation is a steel grate capable of restraining debris but incapable of intercepting the blowdown fluid flow. However, the location of the main steam and feedwater lines in the annulus with respect to door openings, the quantity of insulation available outside the crane wall below elevation 100 ft., and the fact that two trench systems and a screened sump are used are all sufficient to conclude that blockage of the sump screen to an extent which would effect pump NPSH requirement is not possible.

FIGURE A-22

BREAK 3&4: MAIN STEAM AND FEEDWATER FAILURES

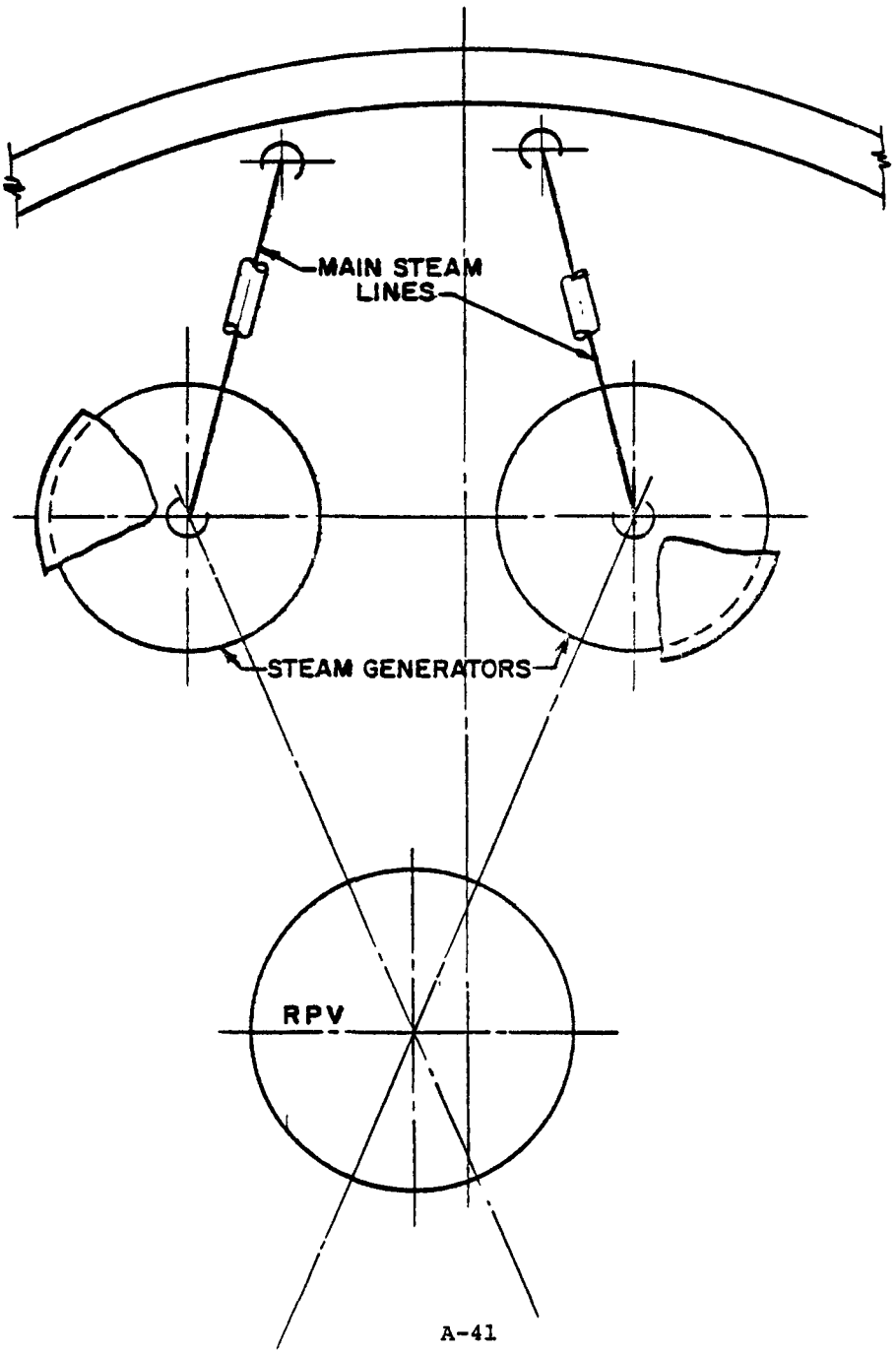

FIGURE A-23
BREAK 3&4: MAIN STEAM AND FEEDWATER FAILURES

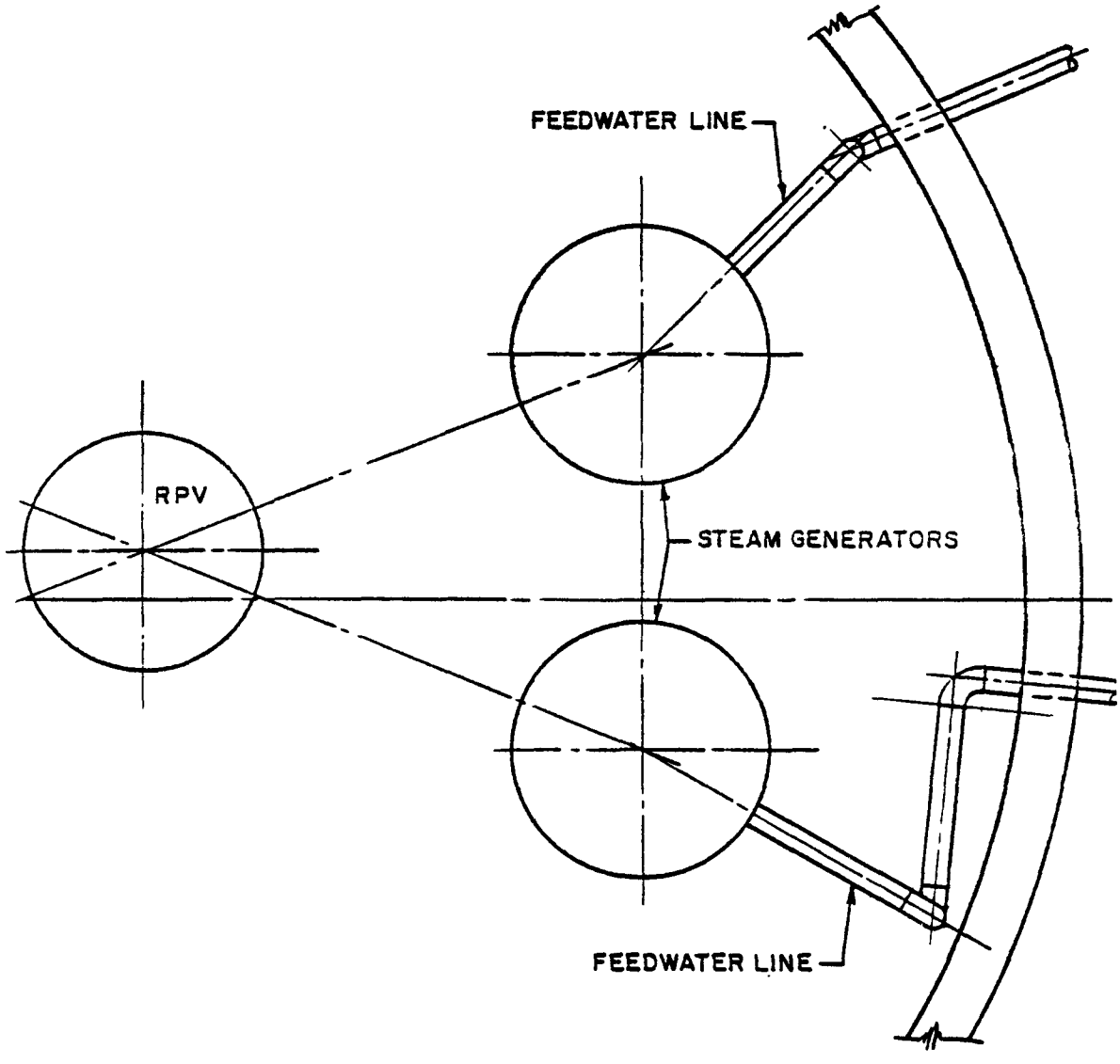

Figure A-24

Break 3 and 4: Main Steam and Feedwater Line Failures

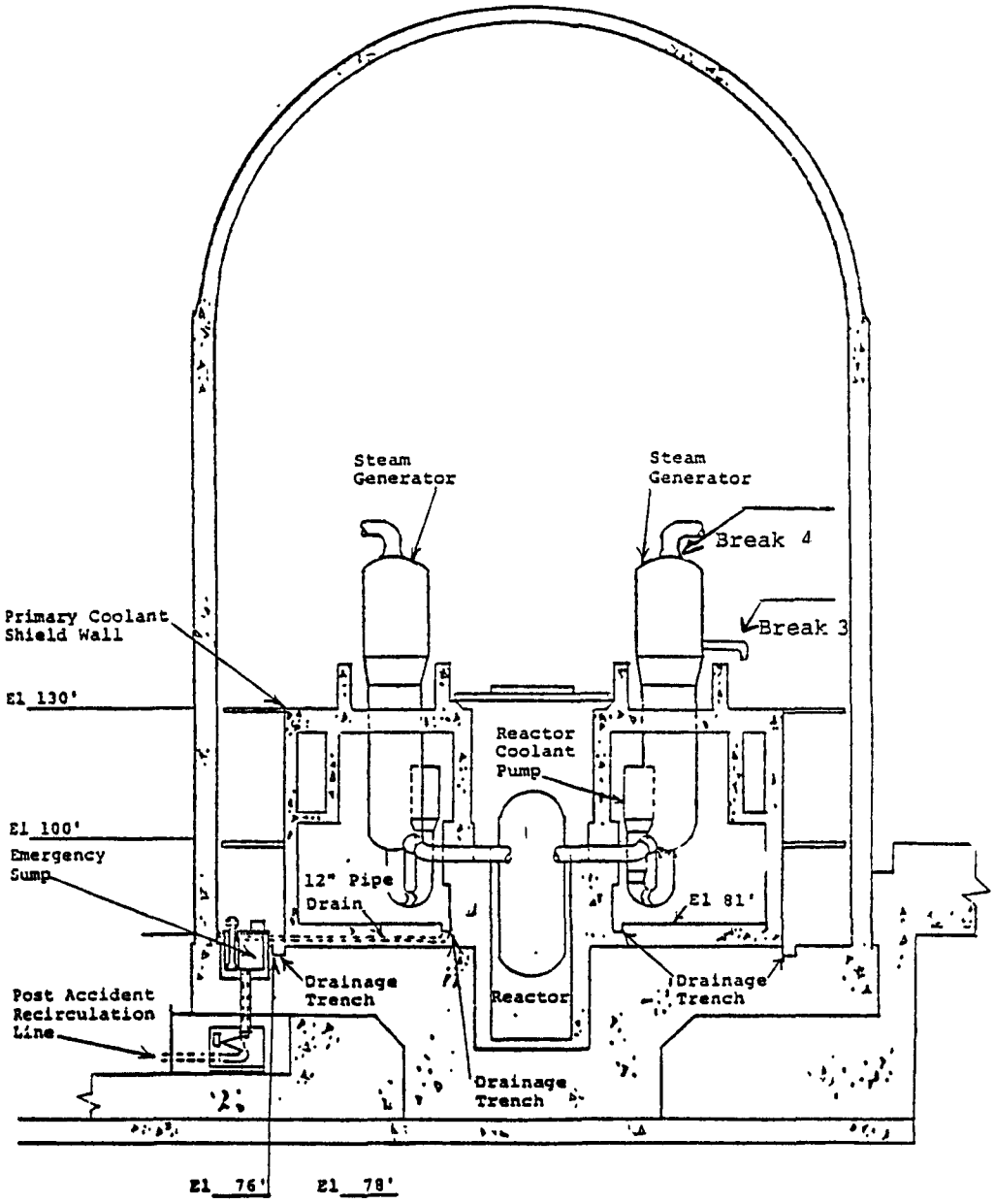

APPENDIX B

ARKANSAS NUCLEAR ONE - UNIT 2
(ANO2)

Appendix B

Arkansas Nuclear One - Unit 2 (ANO2)

1.0 BACKGROUND

ANO2 was selected for analysis because of the placement of the recirculation sump. The plant uses reflective metallic and totally encapsulated calcium silicate insulation within containment.

2.0 DETERMINATION OF INITIATING EVENTS

The ANO2 FSAR in Section 3.6 and Appendix 3A lists over 100 postulated rupture locations for high energy pipes within containment. A scoping analysis was performed to limit the detailed review of debris generation, transport and sump interaction to those breaks which are considered limiting. This scoping analysis was performed twice: once to obtain the limiting break within the steam generator cavity and once to identify the limiting break in the containment annulus.

Scoping Analysis

The considerations involved in defining the limiting breaks were:

Break must be at one of the locations presented in the FSAR

Break must target large, insulated structures, pipes, etc. (Refer to Figure B-1 through B-5 for floors, gratings, etc. whcih limit debris transport.)

As a result of this analysis, the following systems were selected: hot leg, cold leg, crossover pipe (connects reactor coolant pumps with steam generator), feedwater, and main steam.

Figure B-1

Containment Plan View Elev. 336

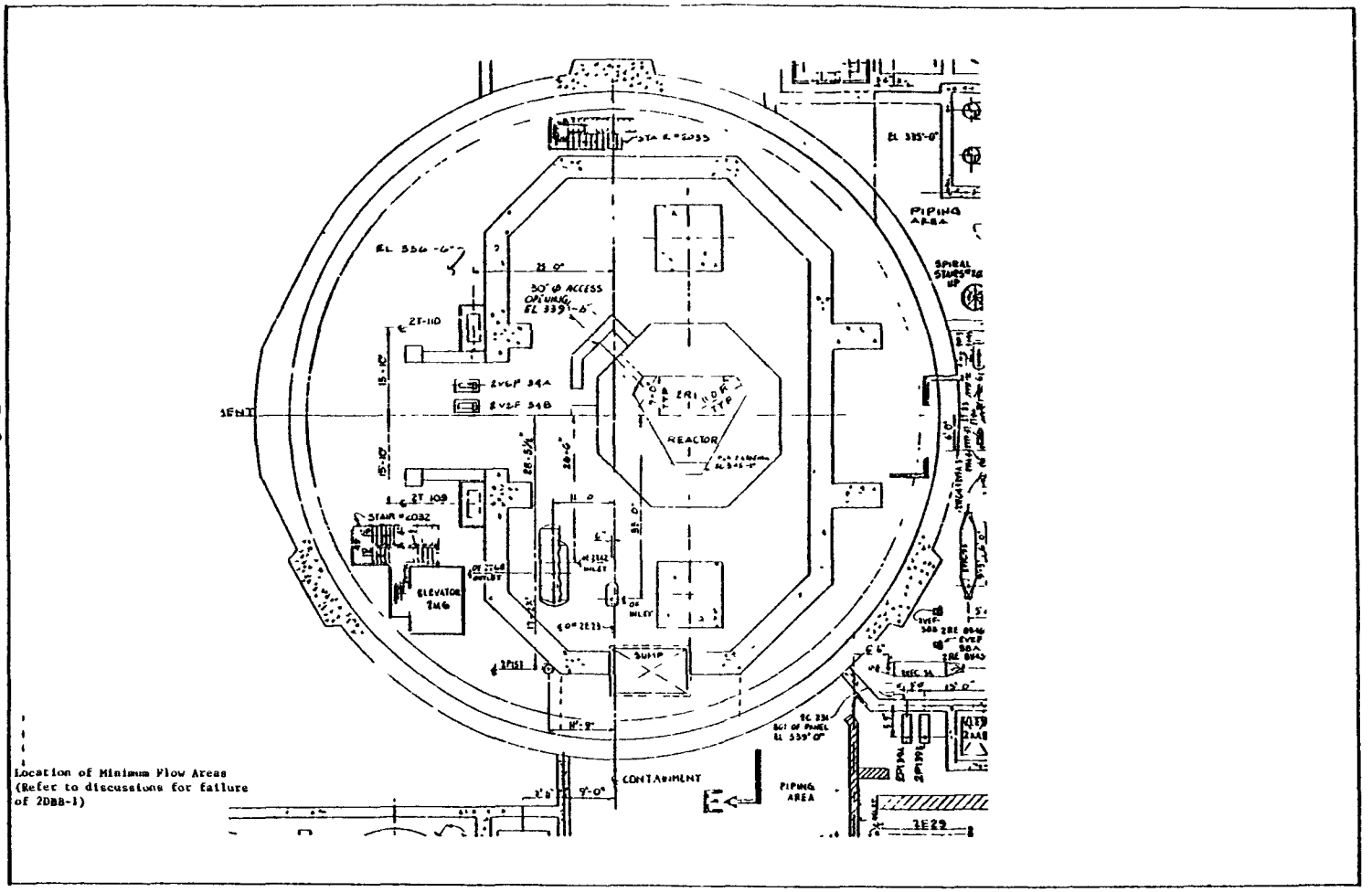

Figure B-2

Containment Plan View Elev. 357

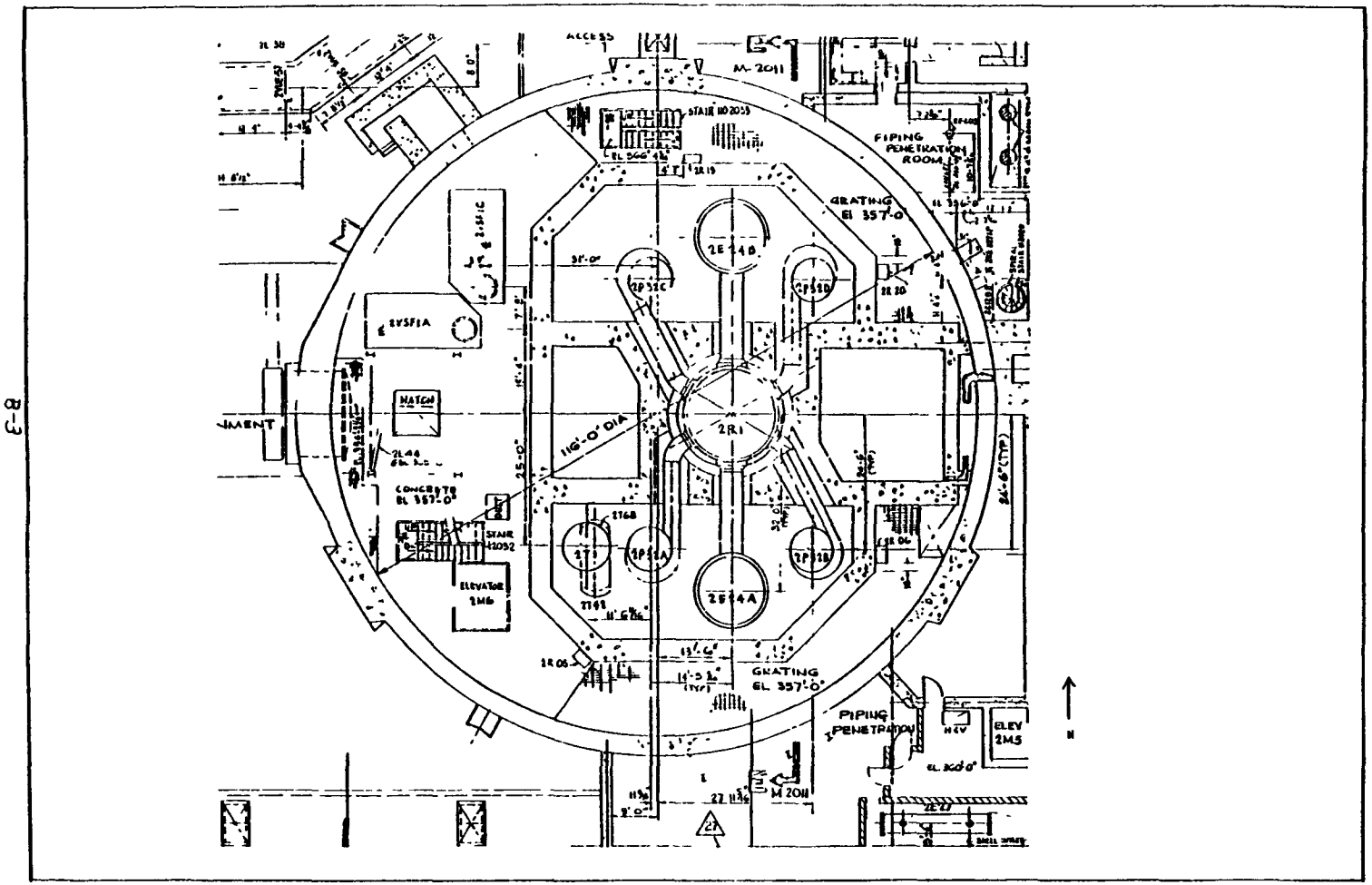

Figure B-3

Containment Plan View Elev. 386

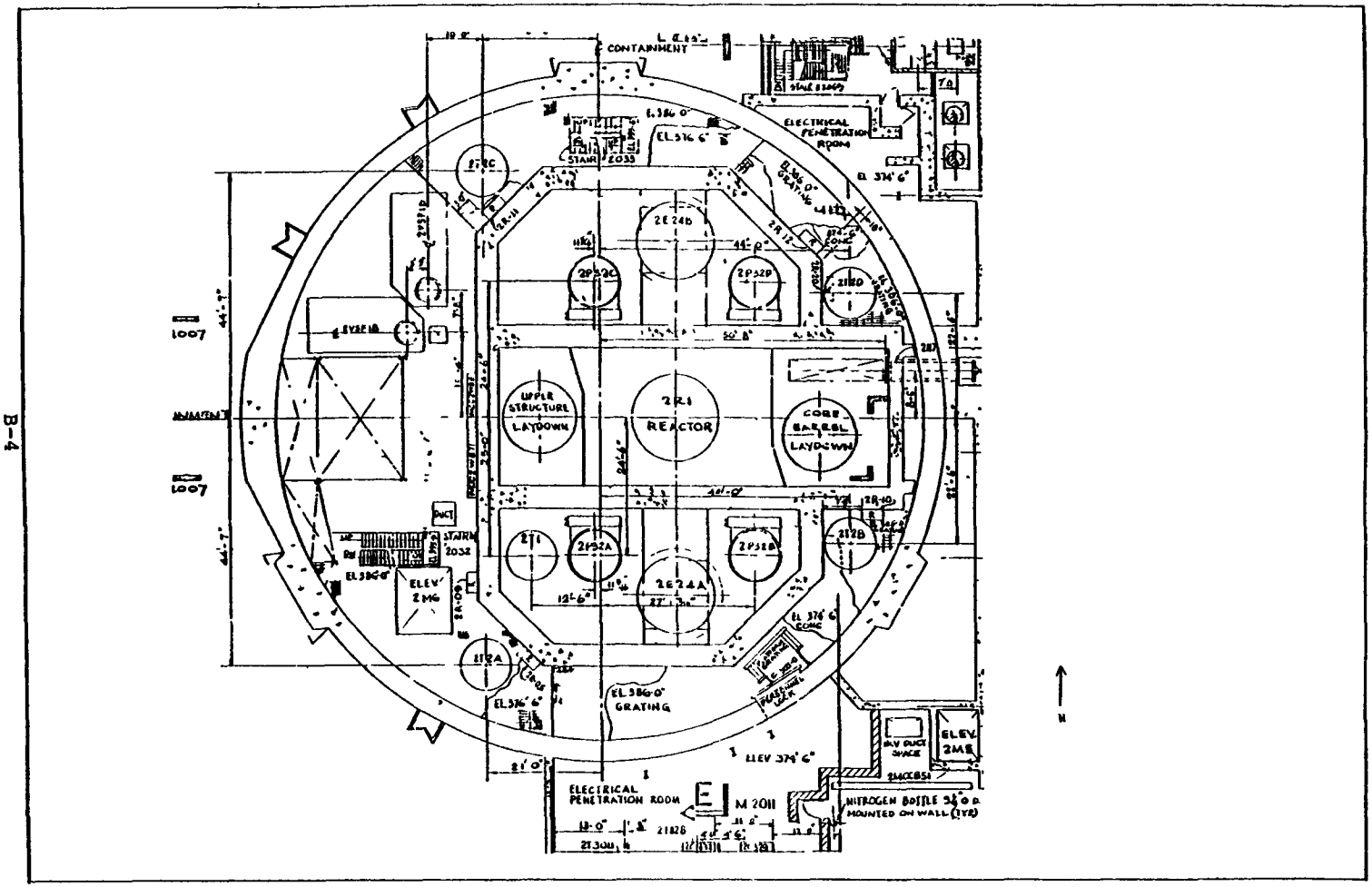

Figure B-4

Containment Plan View Elev. 405

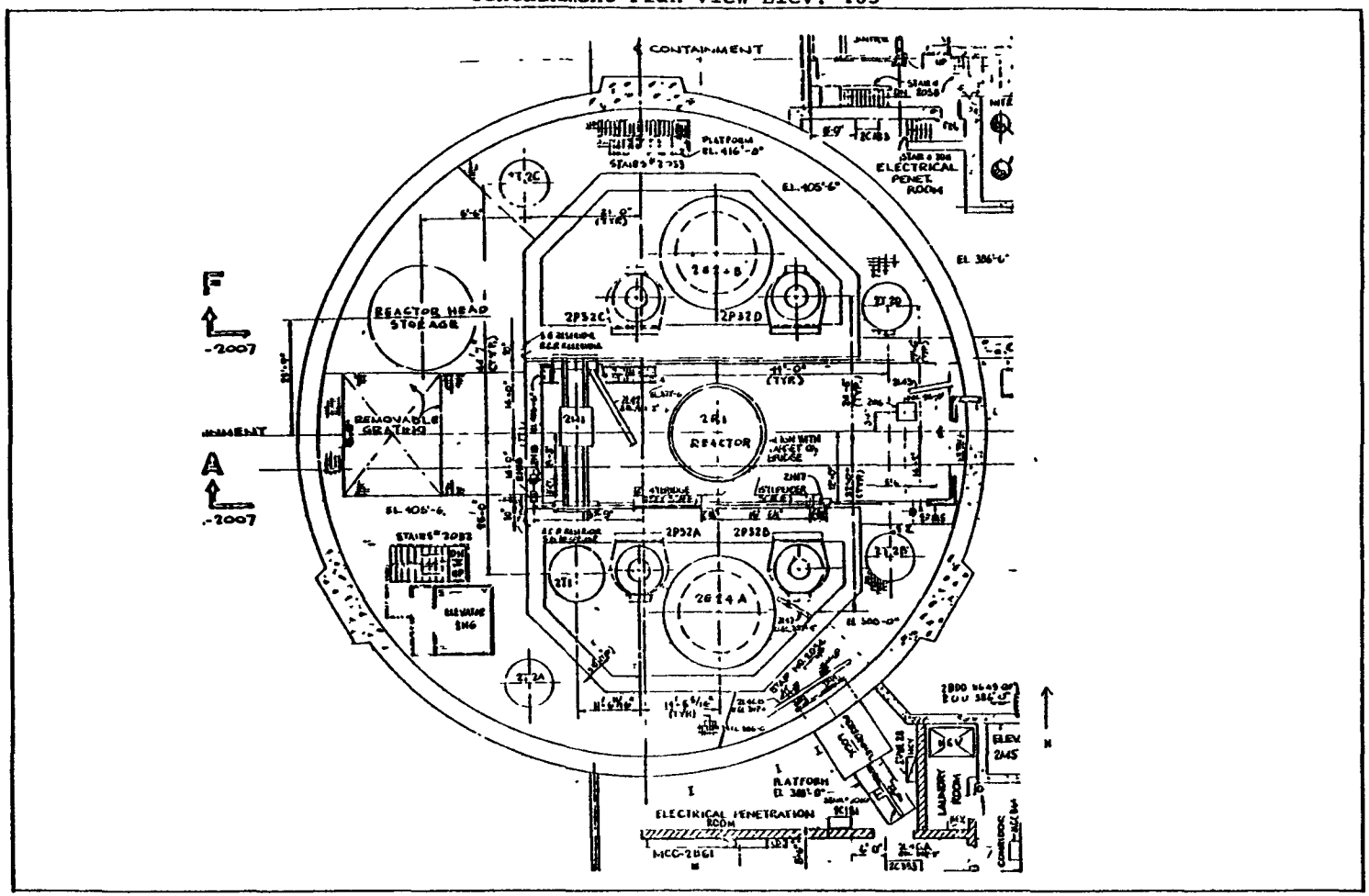

Figure B-5

Containment Plan View Elev. 426

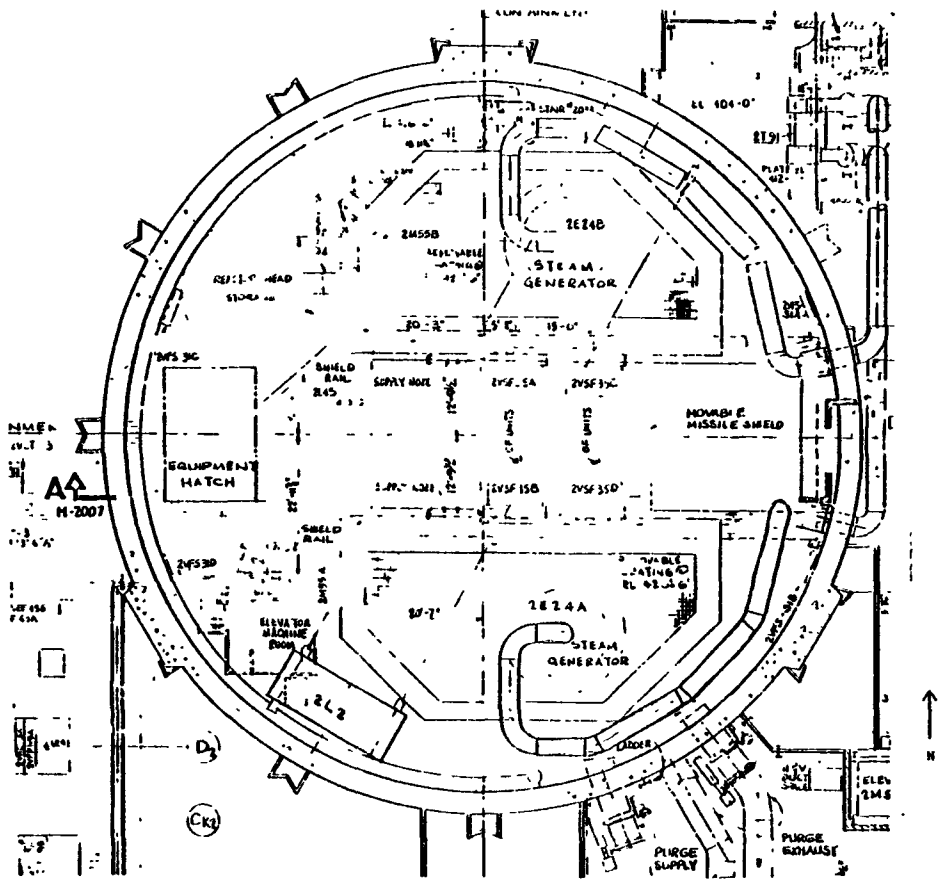

Further analysis revealed that a postulated failure of 2EBB-1 (main steam) at the steam generator nozzle has the capability of targeting all insulation within the steam generator cavity below elevation 395 ft. (approximately). Consequently, this is the limiting failure within the steam generator cavity.

The limiting failure within the annulus region cannot be determined visually. The analysis for the annulus region considers a number of breaks from which the limiting failure is obtained.

Break 1: Main Steam Line

3.0 INSULATION DEBRIS GENERATION

3.1 Pipe Whip

As the main steam line is restrained, no pipe whip occurs, and debris generation by this mechanism is not considered.

3.2 Pipe Impact

Without pipe whip, a pipe impact is not possible. Therefore, this debris generation mechanism is not considered.

3.3 Jet Impingement

Based upon full load pressure and fluid enthalpy in the main steam line, the blowdown jet thrust, pressure field and divergence angle are determined from the procedure presented in Attachment 2. This information enables a plot of the jet diameter as a function of distance from the exit plane to be generated.

Figures B-6 through B-10 illustrate the path of the main steam jet as well as the hot leg, cold leg and crossover pipe jets. Table B-1 summarizes the insulation debris generated by the main steam failure, which targets the largest number of insulated components in the steam generator cavity.

Figure B-6

Mainsteam, Hot Leg, Cold Leg and Crossover Failures Elev. 357

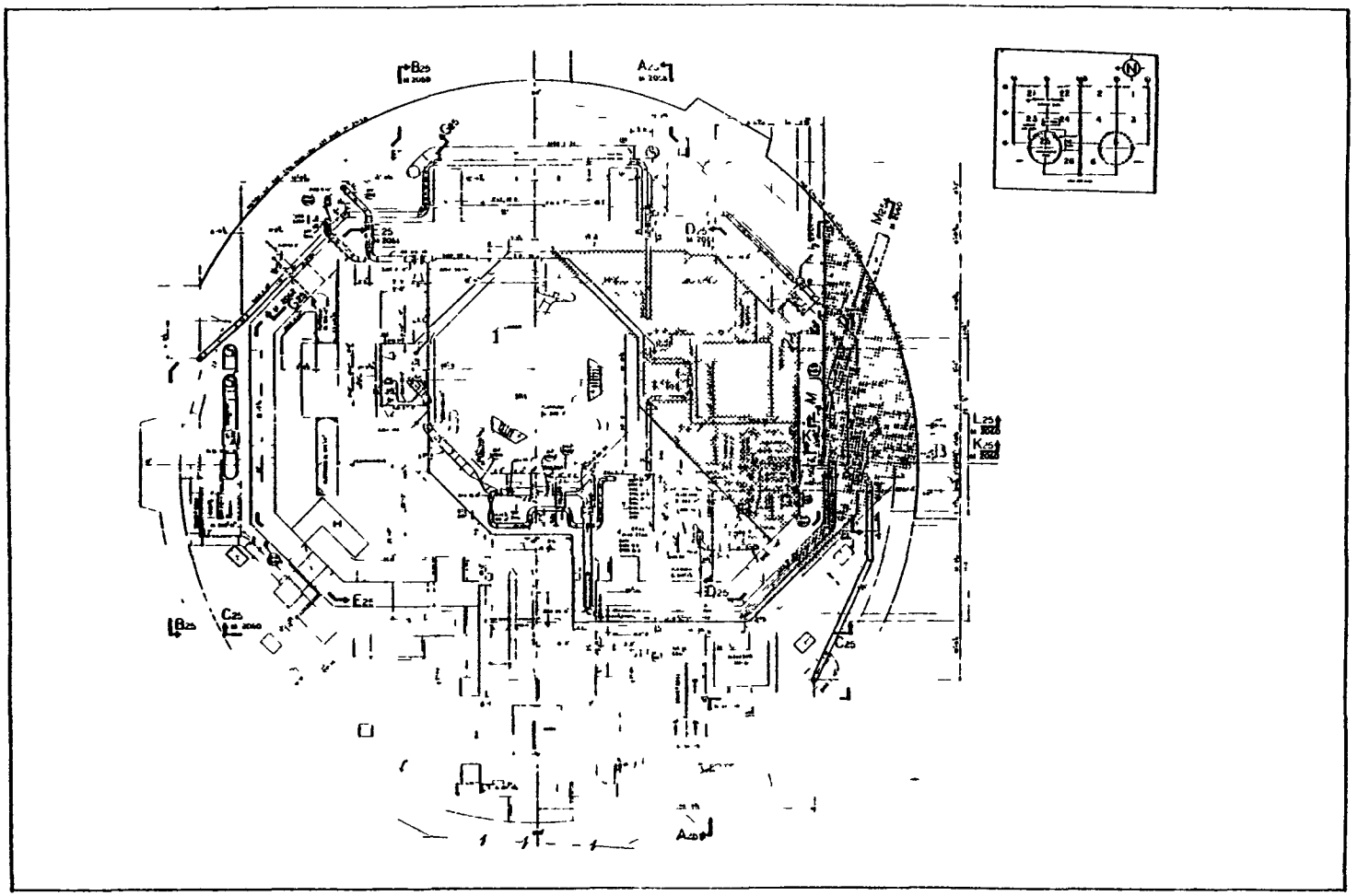

Figure B-7

Mainsteam, Hot Leg, Cold Leg and Crossover Failures Elev. 376

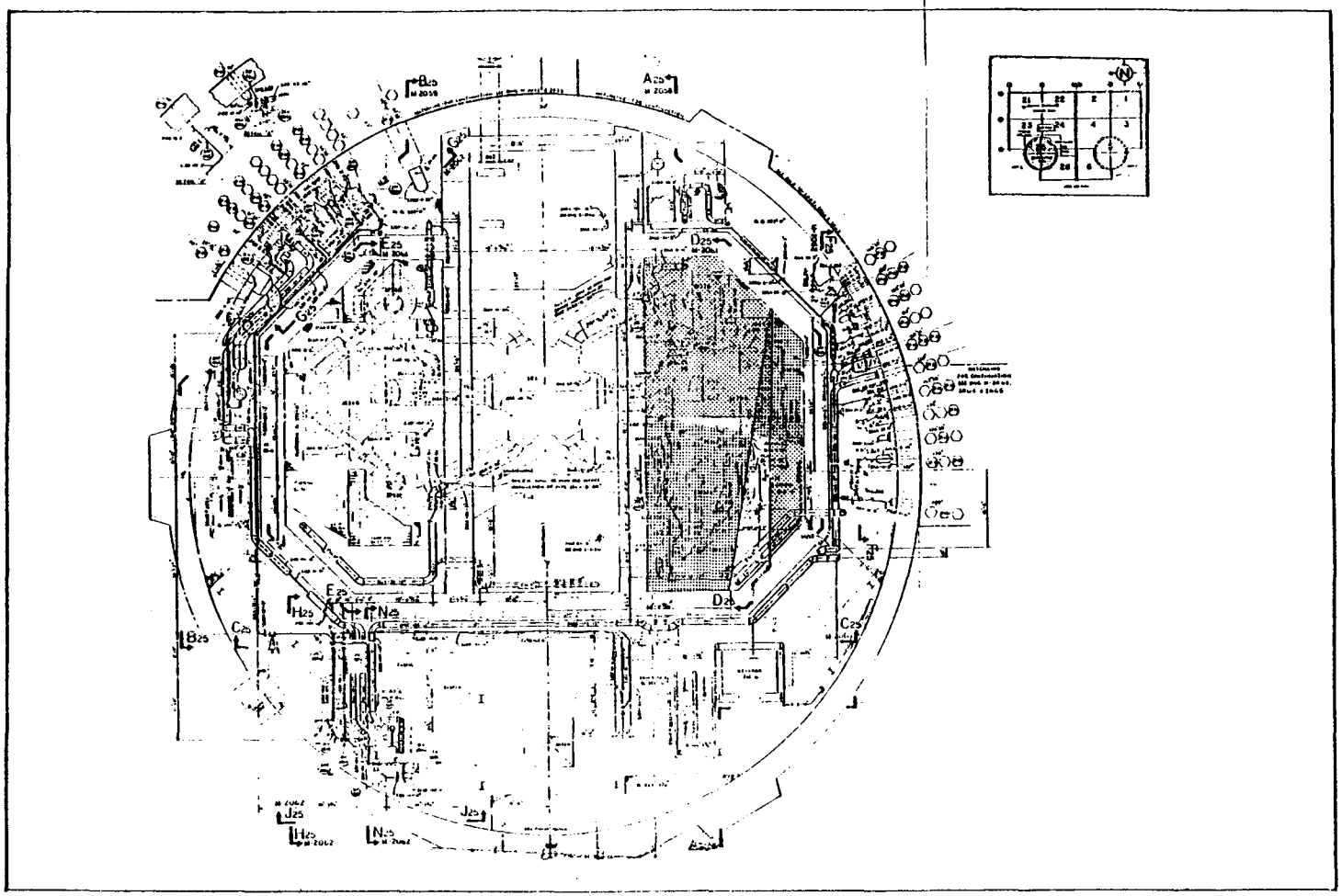

Figure B-8

Mainsteam, Hot Leg, Cold Leg and Crossover Failures Elev. 386

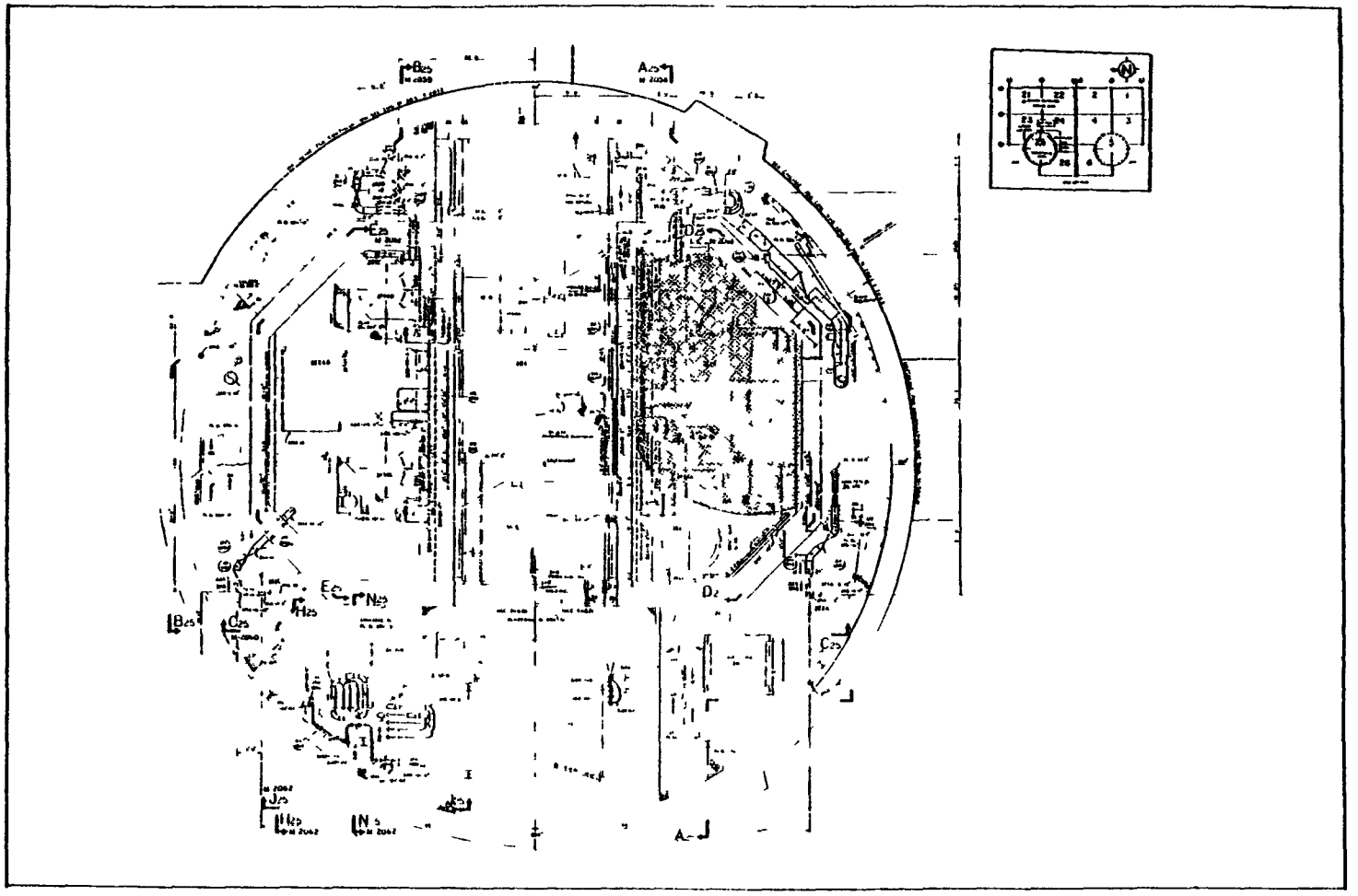

Figure B-9

Mainsteam, Hot Leg, Cold Leg and Crossover Failures Elev. 405

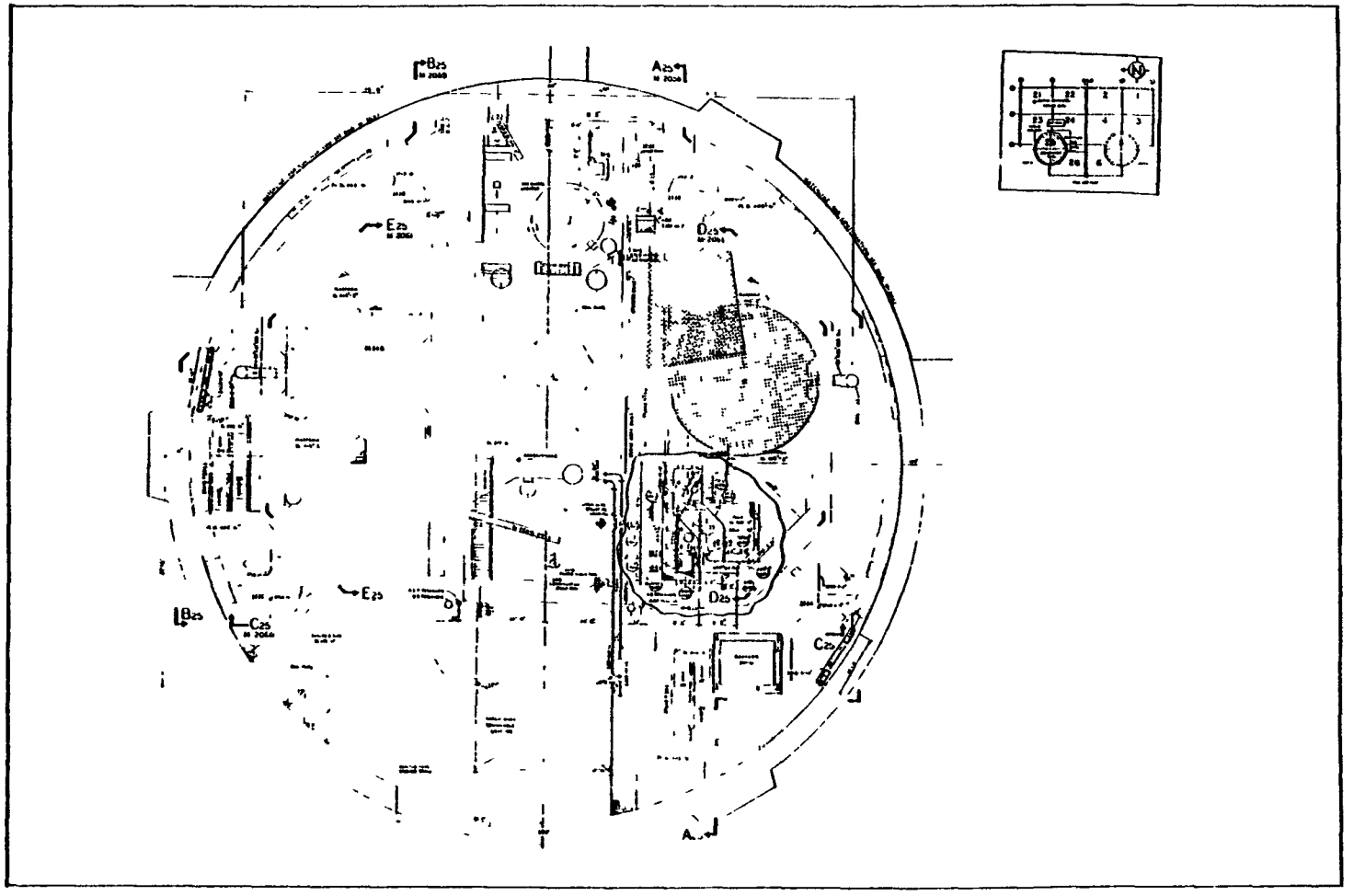

Figure B-10

Mainsteam, Hot Leg, Cold Leg and Crossover Failures Elevation View

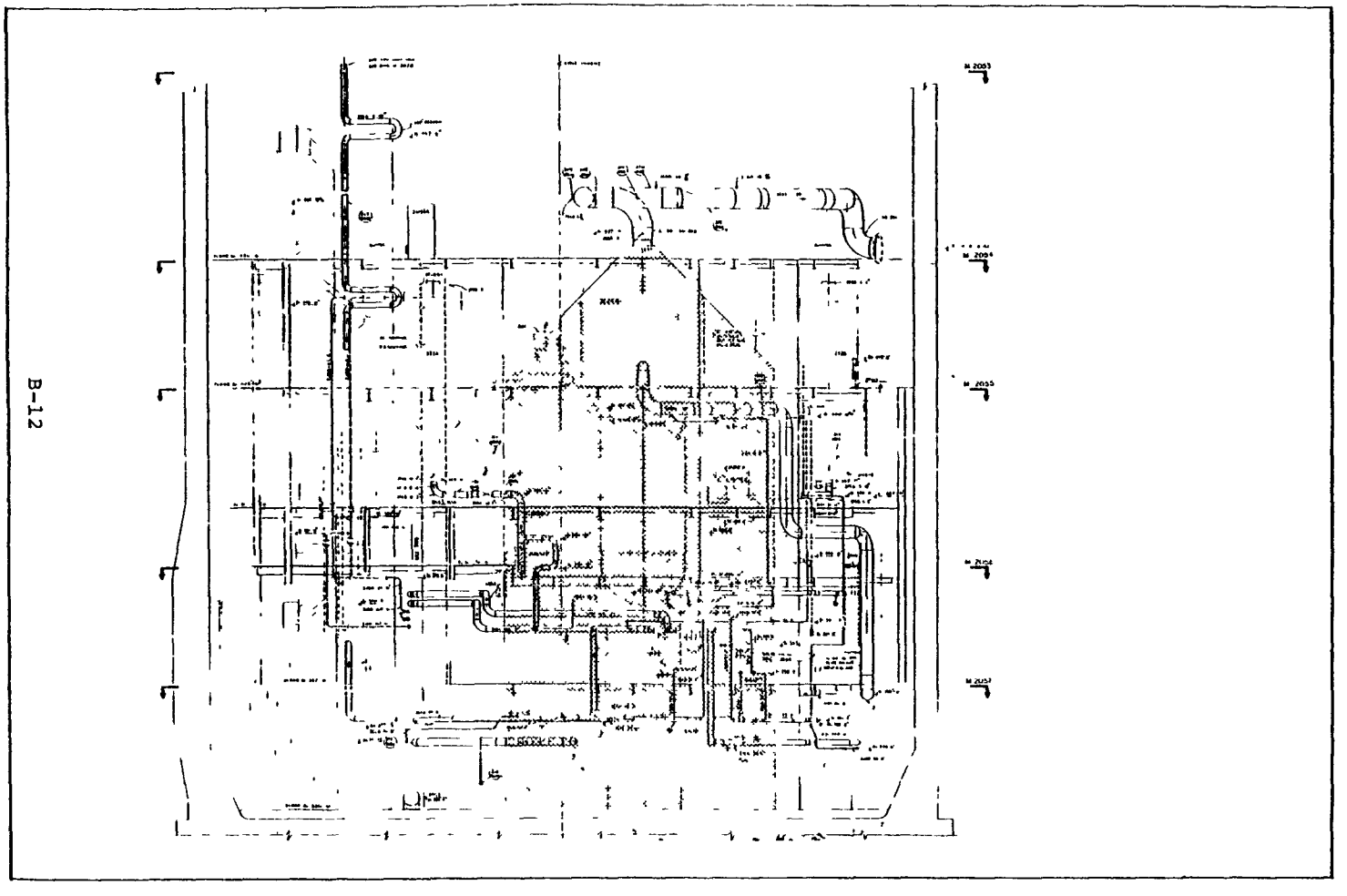

Table B-1

Debris Summary, Break 1: Main Steam Line

Component Targeted	Diam. (ft)	Length (ft)	Insul. Thick. (in.)	Type	Area (ft^2)
2HCC -86	0.66	-	-	-	-
2FCC -1	0.83	13.5	3	E	458
2CCB -1	0.66	16.5	3	E	47
2T42	5	15	3	E	247
2GCB -5	1.166	37.5	3	E	166
2NCC -87	0.66	-	-	E	-
2CCA -1	3.5	10	3.5	RM	119
2CCA -6	2.5	8	3.5	RM	70
2CCA -5	2.5	30	3.5	RM	263
2CCA -4	2.5	6	3.5	RM	52
2CCA -3	2.5	32	3.5	RM	280
2CCA -22	1	50	3.5	RM	202
2BCA -1	1	43	3.5	RM	174
2P32A	10	2.5	3.5	RM	80
2P32B	10	2.5	3.5	RM	80
2E24A-1	13.75	*	3.5	RM	300
2E24A-2	13.75	30.8	3	E	1354
2E24A-3	20	30.8	3	E	1959
2CCA -21	1	34	3	RM	133
2T1	8.875	30.75	3	RM	880
2EBB -1	3.17	27	4	E	297

*Spherical bottom

Total debris generated (ft^2):			
	(RM)	reflective metallic	2633
	(E)	encapsulated	4528
		total	7161

4.0 DEBRIS TRANSPORT

4.1 Short Term Transport - Pipe Whip

As no whipping occurs, this mechanism is not considered.

4.2 Short Term Transport - Pipe Impact

As no pipe whip occurs, pipe impact is not possible. Therefore this mechanism is not considered.

4.3 Short Term Transport - Jet Impingement

All insulation within the jet cone is removed from the affected target and transported in the direction of jet travel, to the steam generator cavity floor. This assumes no retention of insulation debris within the steam generator cavity by the partial grating floors shown on Figures B-7 through B-10.

As the steam generator cavity has openings to the containment annulus region, the transport of debris through these openings must be considered. The perimeter of the steam generator cavity at the floor 9.5 elevation (336 ft) is 176 ft 7 in. while the free vent perimeter is 15 ft 9.5 in. The ejected fraction of the debris is therefore (assuming uniform debris distribution):

$$F_j = \frac{15'9.5"}{176'7"} = 9\%$$

Total debris generated by the main steam line failure (Table B-2) is 7161 ft^2, and ejected debris is 0.09 x 7161, or 644 ft^2.

Table B-2

Short Term Transport Summary, Break 1: Main Steam Line Failure

Debris Generated (ft^2)	Debris Remaining Within SG Cavity (ft^2)	Debris Ejected (ft^2)	Type
2633	2397	236	Reflective Metallic
4528	4120	408	Encapsulated
7161	6517	644	Total

SG - steam generator

4.4 Long Term Transport - Recirculation Phase

Three types of debris must be investigated: reflective metallic, encapsulated calcium silicate which is intact, and encapsulated calcium silicate whose encapsulating structure has been breached, releasing particles of calcium silicate.

4.4.1.1 Containment Flow - Recirculation Mode

Although a main steam line failure does not result in ECCS activation (primary system is intact), the assumption is made that recirculation flow is established for the purpose of assessing potential sump blockage.

The ANO2 FSAR gives for the ECCS pump complement:

High Pressure Core Injection	- 3 pumps at	825 gpm
Containment Spray	- 2 pumps at	2000 gpm
Total Flow		6475 gpm

Figure B-1 shows that all flow within containment flows either to the south (ECCS sump within the steam generator cavity) or west and the south to the ECCS sump in the containment annulus. Due to the large quantity of debris generated within the steam generator cavity and the fact that the sump screens act as a pathway for steam escape during blowdown, the sump screens within the steam generator cavity (hereafter referred to as the inboard screens) are assumed to be completely blocked.

For the purposes of long term transport, all flow is therefore assumed to exit through the west wall opening. As all debris within the steam generator cavity must pass through this opening to reach the annulus, the velocity through this opening will determine if debris within the shield wall can reach the containment annulus.

The water depth in containment is calculated from the primary system water inventory (ANO2 FSAR):

Safety Injection Tanks	- 4 at	1,480 ft^3
Steam Generators	- 2 at	1,598 ft^3
Refueling Water Storage Tank	- 1 at	53,500 ft^3
Sodium Hydroxide Tank	- 1 at	1,600 ft^3
Total Water into Containment*	-	64,016 ft^3

*No credit taken for primary loop inventory except steam generators

Figure B-2 indicates a containment diameter of 116 ft, giving a plan area of 10,568 ft^2. Not including displacement effects of steam generator wall, equipment foundations, etc., the post LOCA water level is:

$$\frac{\text{Water volume}}{\text{Plan area}} = \frac{64,016}{10,568} = 6.1 \text{ ft of water in containment.}$$

Figure B-6 shows the west opening to be 21 ft across, giving a flow area of 21 ft wide by 6.1 ft deep, or 127.5 ft^2.

Given total ECCS flow of 6475 gpm, or 14.5 ft^3/sec, the flow velocity through this opening is:

$$14.5 \text{ ft}^3/\text{sec} \times \frac{1}{127.5 \text{ ft}^2} = 0.11 \text{ ft}^3/\text{sec}$$

Appendix A, Section 4.4.1.1 indicates this velocity is insufficient to move reflective metallic or intact totally encapsulated calcium silicate insulation.

Calcium silicate which is no longer encapsulated may move as follows:

From Equation 14

$$F_M = \mu_f F_N$$

where F_M - force required to cause motion

μ_f - the friction coefficient

F_N - normal force existed by the debris as modified lift and buoyancy affects

and from Equation 19

$$F_A = \frac{C_D A_p \rho_w \bar{V}^2}{2g_c}$$

where F_A - force available to cause motion

C_D - drag coefficient

A_p - area normal to velocity of flow

ρ_w - fluid density

$\bar{V}$ - flow velocity at debris location

g_c - Newton's conversion constant

For motion to occur $F_A \geq F_M$. Assuming particles are roughly spherical and calcium silicate in contact with concrete,

then

$V = 4/3\ \pi\ R^3$

$A_p = \pi\ R^2$

ρ_I = 13 lbm/ft^3 bulk; 160 lbm/ft^3 theoretical

μ_f = 0.6 (Section 4.5.2.4)

Table B-3 presents the results of a motion analysis for various sized particles. As can be seen, only small particles are capable of transport. Particles smaller than 1/4 in. diameter will move in a flow of 0.11 ft/sec when the effects of buoyancy, lift and drag are included in the evaluation. These particles will reach the sump screens but arrive near the screen-floor interface and accordingly will not produce screen blockage to any appreciable degree.

For example, assuming that all 408 ft^2 of ejected encapsulated calcium silicate were ruptured and formed 1/4 in. particles, a total of 408 ft^2 x 3 in./12 in/ft = 102 ft^3 of debris would be formed. Further, assuming a 45° inclined angle of repose, the 102 ft^3 of debris would reach the first 2 ft of the screen, leaving the upper 4 ft unblocked. This would result in a 50% increase in screen pressure drop over the unblocked case.

5.0 SUMP EFFECTS

As total screen blockage does not occur, the sump effects are limited to increased screen pressure drop due to increased screen flow (inboard screen and first two feet of outboard screen are assumed blocked). ANO2 uses two screens in series a No. 14 (3/16 in. opening) and a No. 4 (3.5/64 in. opening).

Equation 25 is used to determine the increased head loss. Initial screen head loss:

Table B-3

Motion Analysis for Various Sized Particles

Particle Radius in.	Particle Area $in.^2$	Particle Volume $in.^3$	N_{RE}	C_D	F_A	F_N	F_M	Motion
1/16	0.012	0.00102	53	3	2.97×10^{-6}	1.73×10^{-6}	1.04×10^{-6}	Yes
1/8	0.049	0.0082	105	2	7.9×10^{-6}	2.97×10^{-5}	1.78×10^{-5}	No
1/4	0.196	0.065	211	1.5	2.38×10^{-5}	2.77×10^{-4}	1.66×10^{-4}	No
1/2	0.785	0.523	423	1.2	7.6×10^{-5}	2.33×10^{-3}	1.40×10^{-3}	No

N_{RE} - Reynolds number

C_D - drag coefficient

F_A - force available to cause motion

F_N - normal force exerted by debris as modified by lift and buoyancy affects

F_M - force reqiured to cause motion

Note: If $F_A \geq F_M$, motion occurs.

$$h = \left(\frac{n}{c^2}\right)\left(\frac{1-\alpha^2}{\alpha^2}\right)\left(\frac{\bar{V}^2}{2g_c}\right)$$

Initial screen area - 250 ft^2 (98 ft^2 inboard, 152 ft^2 outboard)
Flow - 6275 gpm or 14.5 ft^3/sec
Velocity - 14.5/250 or 0.06 ft/sec

Screen data and head loss calculations are summarized in Tables B-4 through B-6.

Table B-4

Screen Data

Screen	Opening (in.)	Fraction Open %
No. 14	3/16	50.5
No. 4	3.5/64	32.0

Table B-5

Head Loss - Unblocked Screens

Screen	N_{RE}	c	α	$\bar{V}$ (ft/sec)	h (ft of fluid)
No. 14	62.5	0.7	0.32	0.06	1×10^{-3}
No. 4	211	1.0	0.505	0.06	1.63×10^{-4}

With the blockage described above, the velocity increases to 0.148 ft/sec. The increased head loss is as follows:

Table B-6

Head Loss - Inboard Screen and Portion of Outboard Screen Blocked

Screen	N_{RE}	c	α	$\bar{V}$ (ft/sec)	h (ft of fluid)
No. 4	99	0.8	0.32	0.148	4.7×10^{-3}
No. 14	334	1.05	0.505	0.148	9.0×10^{-4}

Original head loss - 1.163×10^{-3}
Blocked head loss - 5.6×10^{-3}
Increase in head loss - 4.43×10^{-3}

This is an insignificant increase in head loss.

Total blockage of the inboard screen with 33% blockage of the outboard screen will not adversely affect ECCS sump performance. In both cases blocked screens were assumed to pass zero flow. In actuality a reduced flow rate through these debris accumulations would exist, further lowering the total pressure drop. The main steam failure will not affect the ECCS sump performance.

Limiting Break Outside the Steam Generator Cavity

2.0 DETERMINATION OF INITIATING EVENTS

A number of breaks were chosen outside the steam generator compartment to assess the debris generation potential of pipe failures in the annulus region. Table B-7 summarizes the break locations. The break numbers are from the FSAR.

Table B-7

Postulated Breaks - Containment Annulus Region

Line	Break Number	Consequence
2DBB-1 (Feedwater)	5	Break at SG inlet. Jet outside of SG compartment is prevented from reaching sump by floor at el. 376'6". Not considered.
	90	Vertical run to SG. Break is above grating at el. 374'6".
	125	At containment penetration. Quantity of insulation affected need not be determined as jet targets a smaller area than break 90. (See Figures B-15, B-16).
2DBB-2	5	Same as 2DBB-1 break 5.
(Feedwater)	55	Debris which can travel to sump is below el. 357'6". Amount is insignificant.
	90	Debris below el. 357'6" can reach sump.
	115	Break above el. 357'6". Debris will be trapped by floor.
	120	See 115 above.

Figures B-11 through B-19 illustrate the paths of the postulated jets. Break 90 on either line 2DBB-1 or -2 will be limiting as it generates the greatest amount of debris which can reach the sump.

3.0 DEBRIS GENERATION - BREAK 90 LINES 2DBB-1 AND -2

3.1 Pipe Whip

Feedwater lines within containment are restrained. Pipe whip is therefore not considered.

3.2 Pipe Impact

In the absence of pipe whip, pipe impact is not possible.

3.3 Jet Impingement

The jets exiting break 90 for lines 2DBB-1 and -2 strike a number of targets. Tables B-8 and B-9 summarize the debris generation for each break.

Table B-8

Debris Summary, Break 90: Line 2DBB-1

Component	Diameter (in.)	Length (ft)	Area (ft^2)	Type
2DBB-1	24	22.5	139	Encapsulated
2CCA-21	5	2	3	Encapsulated
2CCA-23	8	20	42	Encapsulated
2HCB-4	10	33	86	Encapsulated
2HCC-8	8	4	8	Encapsulated
Total			278	

Table B-9

Debris Summary Break 90: Line 2DBB-2

Component	Diameter (in.)	Length (ft)	Area (ft^2)	Type
2DBB-2	24	9	57	Encapsulated
2HCB-4	10	8	21	Encapsulated
2CCA-23	8	3	6	Encapsulated
2HBB-9	10	2	5	Encapsulated
2JBD-99	10	1.5	4	Encapsulated
2DBB-8	4	3	3	Encapsulated
Total			96	

Figure B-11

Feedwater Failure Elevation View

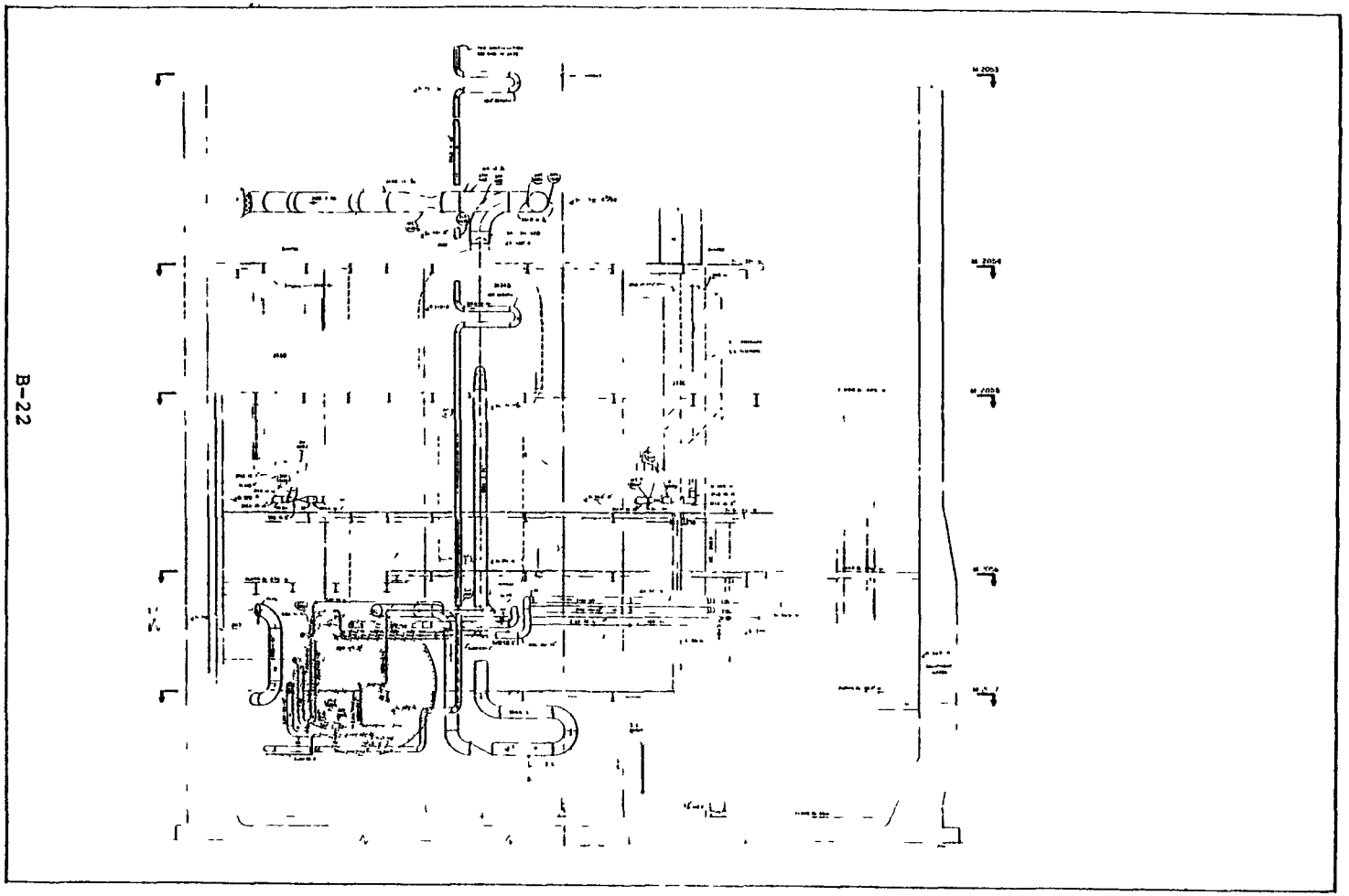

Figure B-12

Feedwater Failure Elevation View

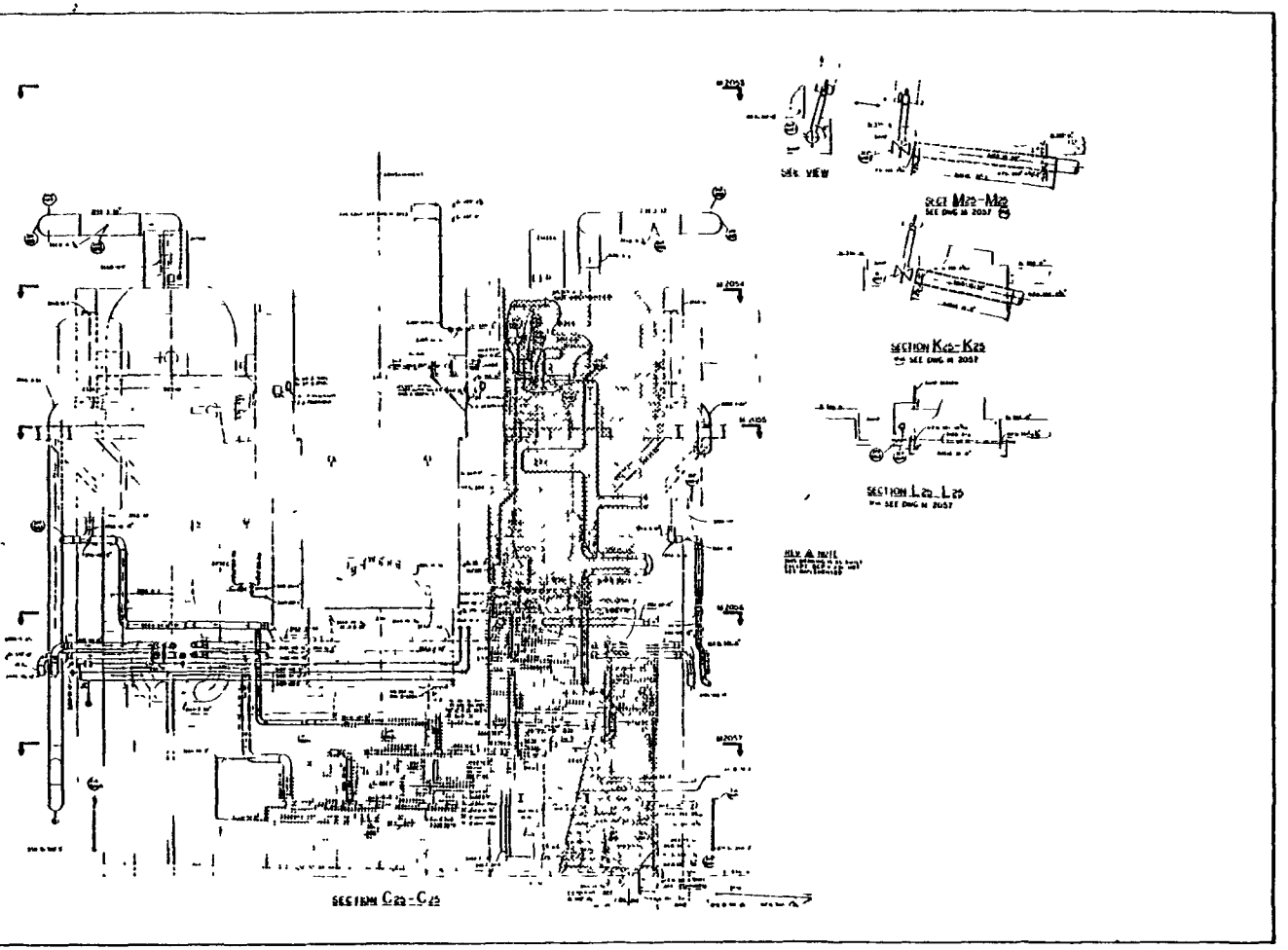

Figure B-13

Feedwater Failure Elev. 405

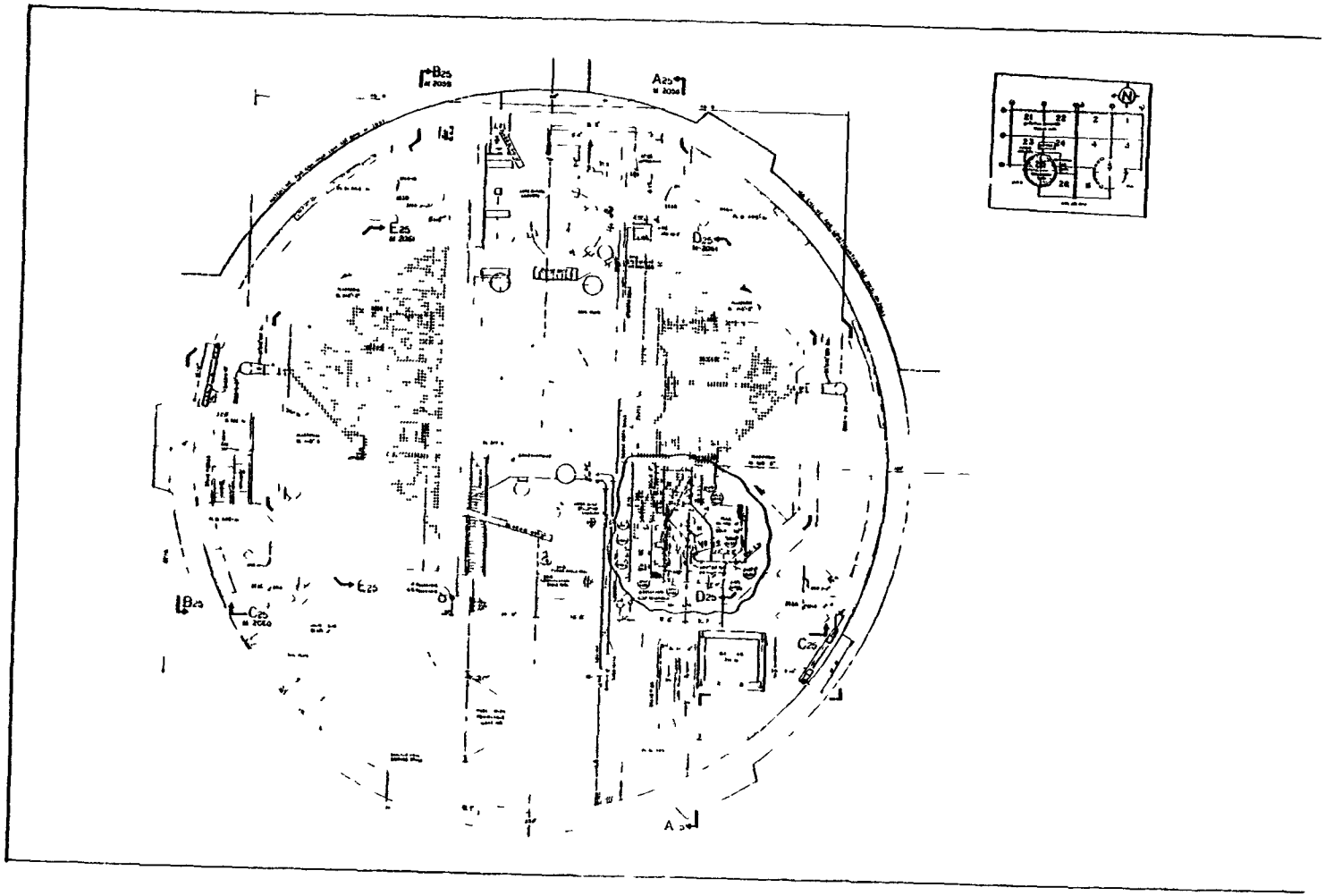

Figure B-14

Feedwater Failure Elev. 386

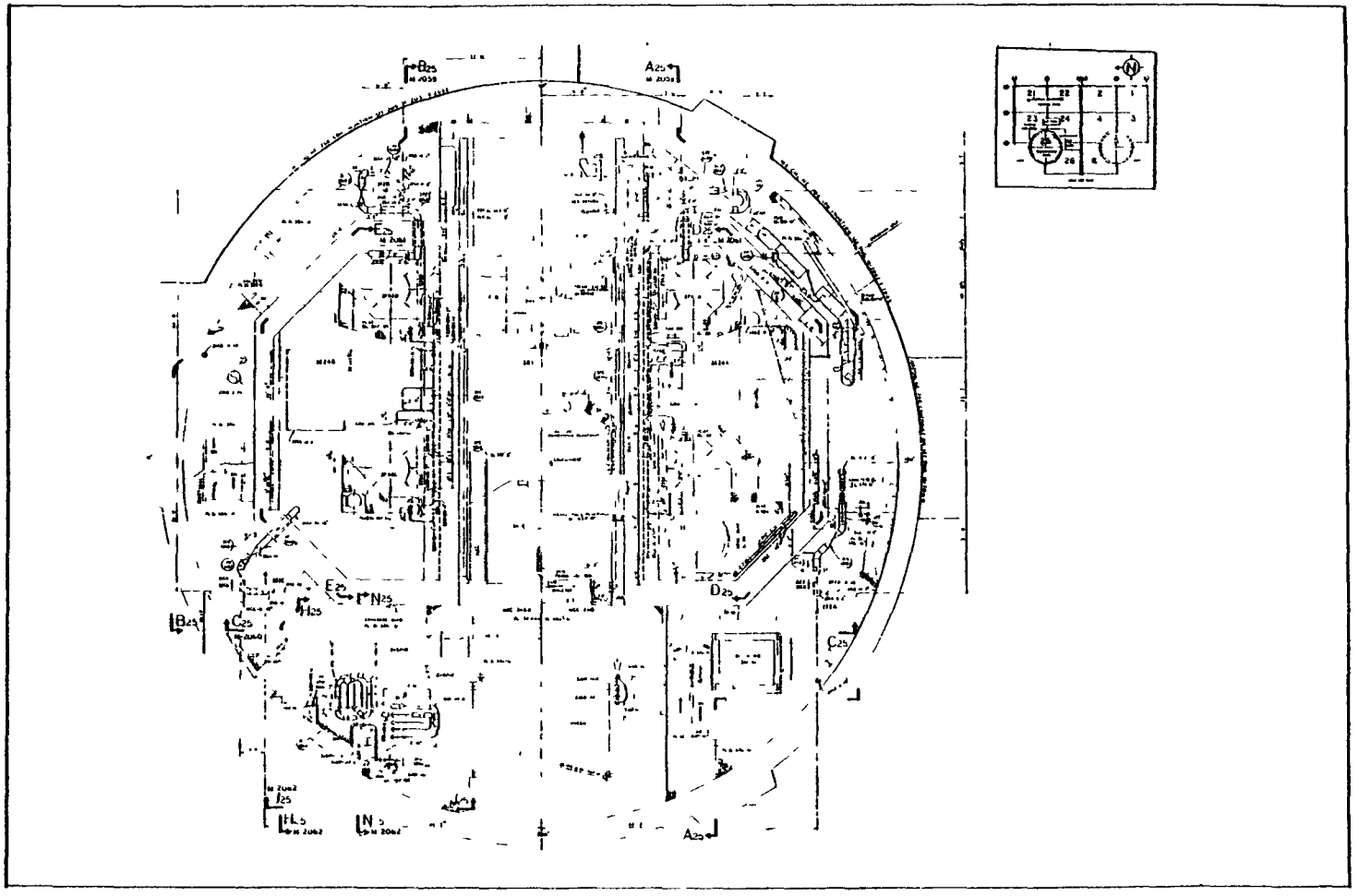

Figure B-15

Feedwater Failure Elev. 376

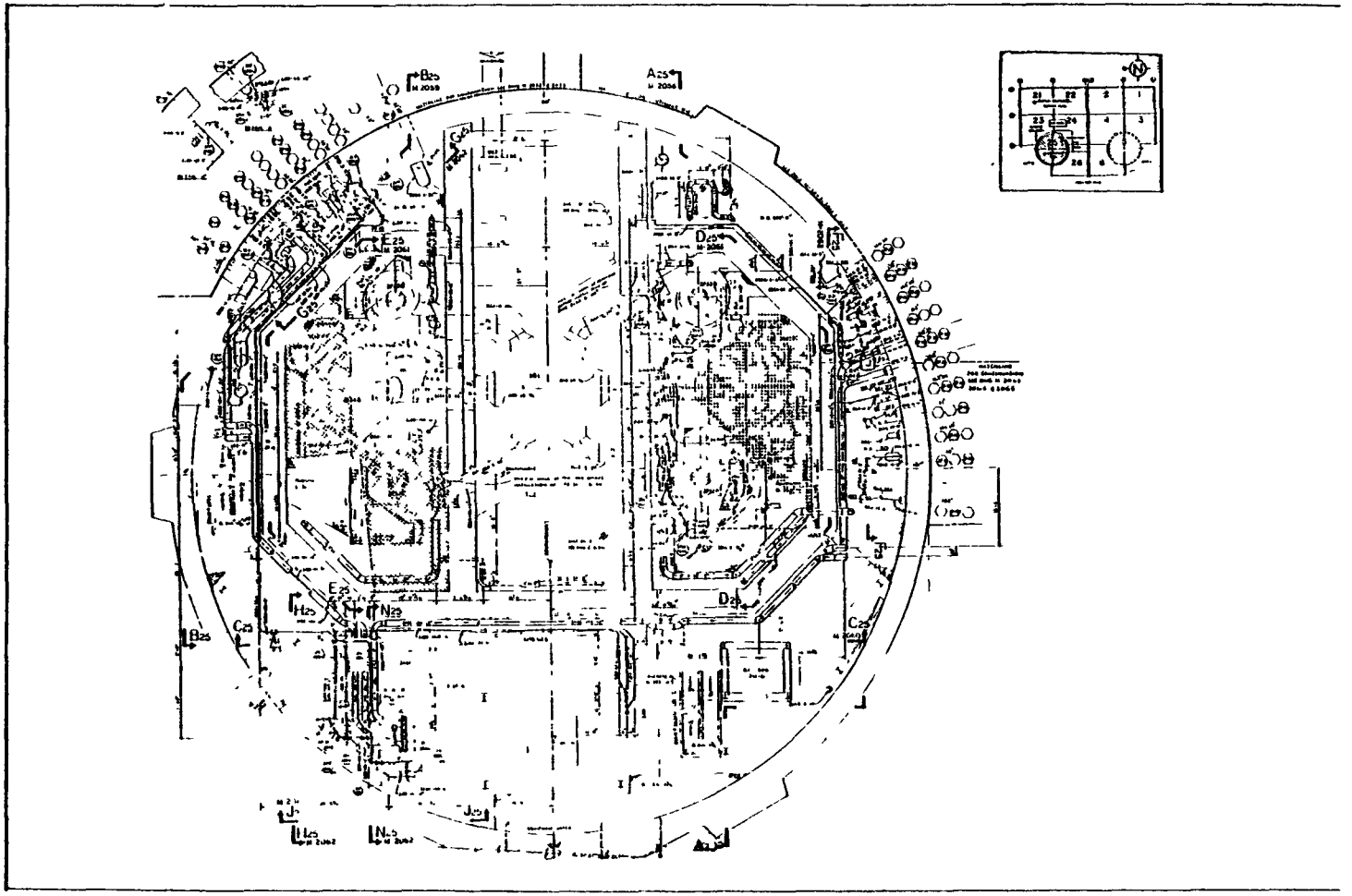

Figure B-16

Feedwater Failure Elev. 357

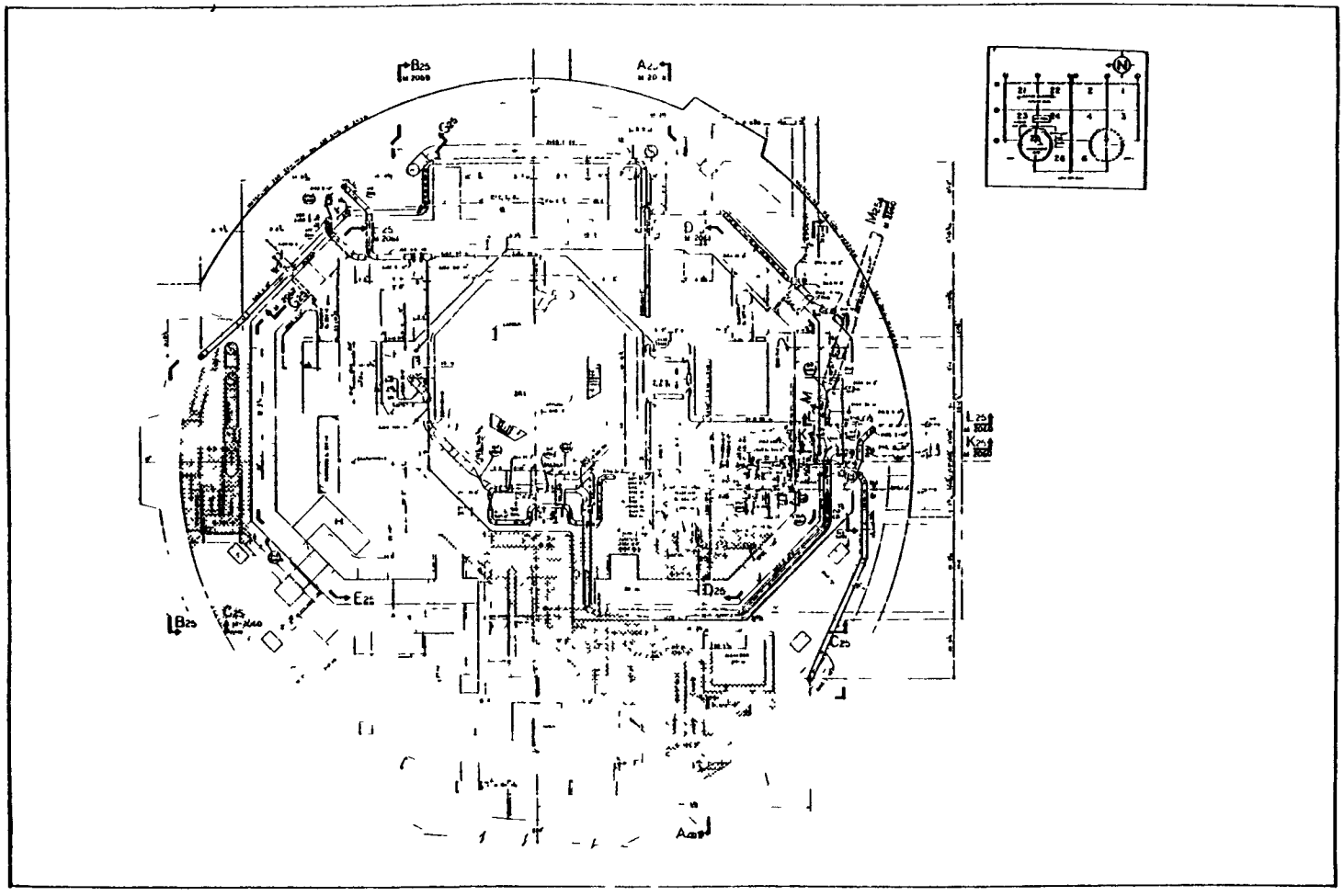

Figure B-17

Feedwater Failure Elevation View

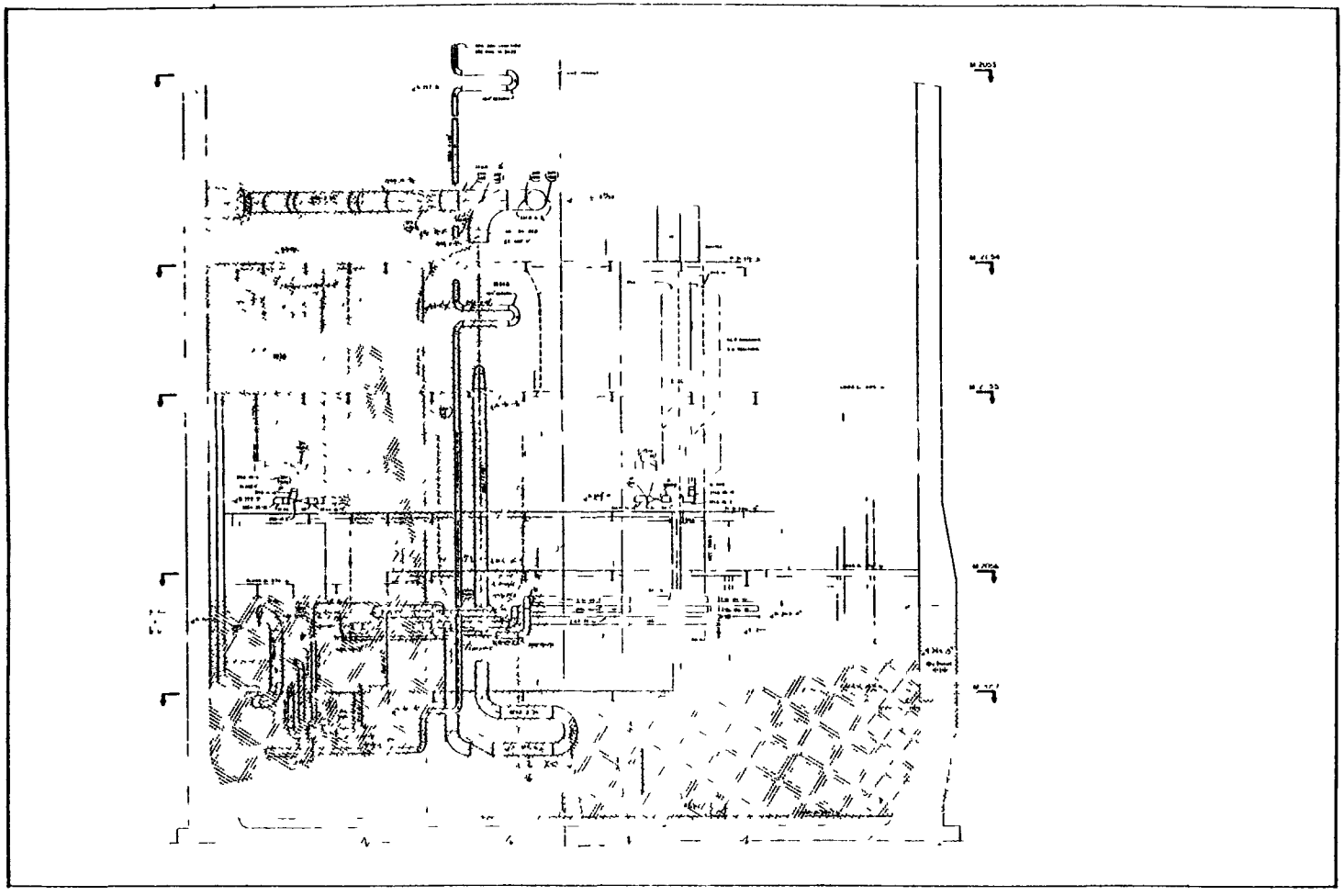

Figure B-18
Feedwater Failure Elevation View

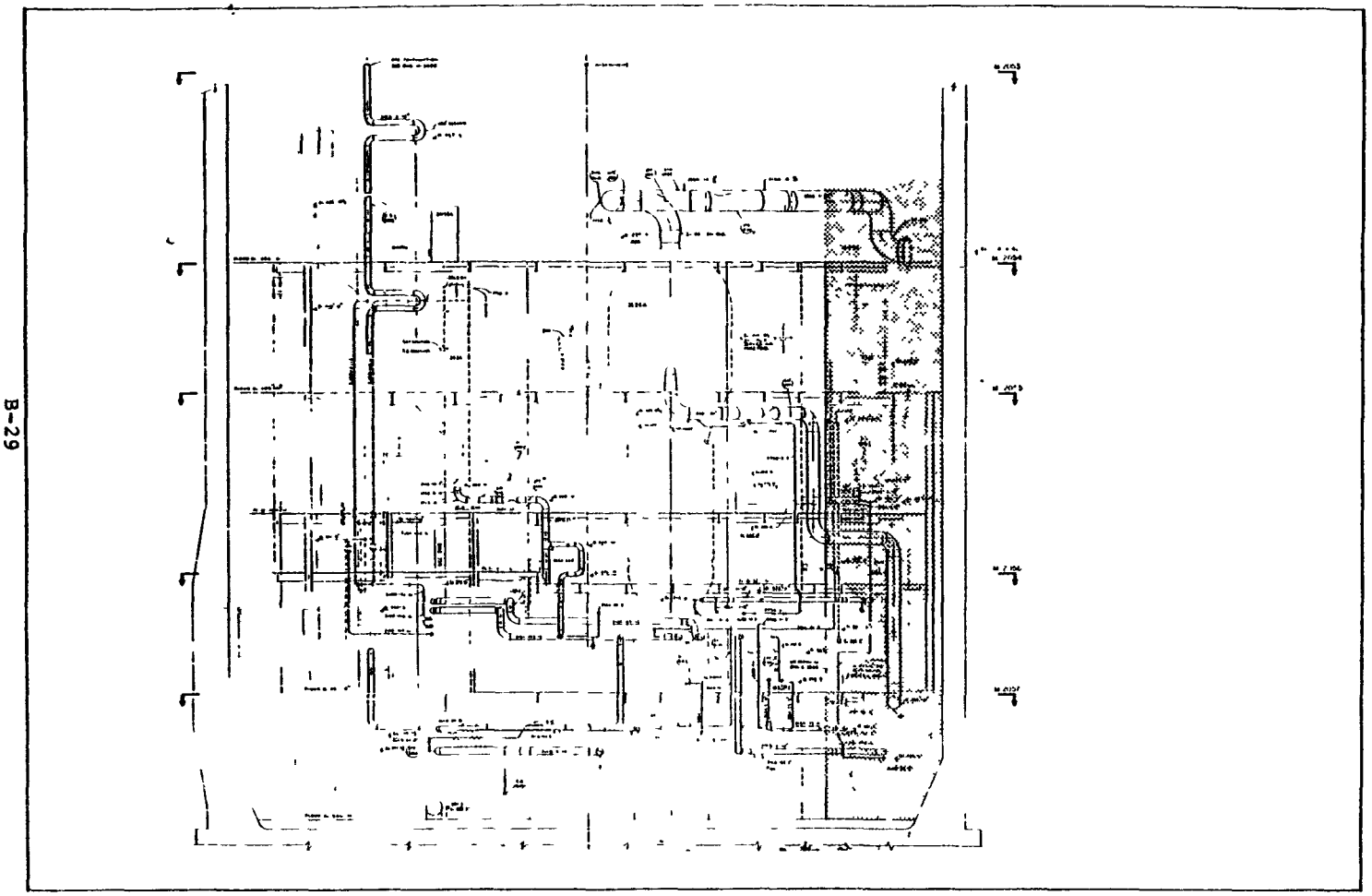

Figure B-19

Feedwater Failure Elevation View

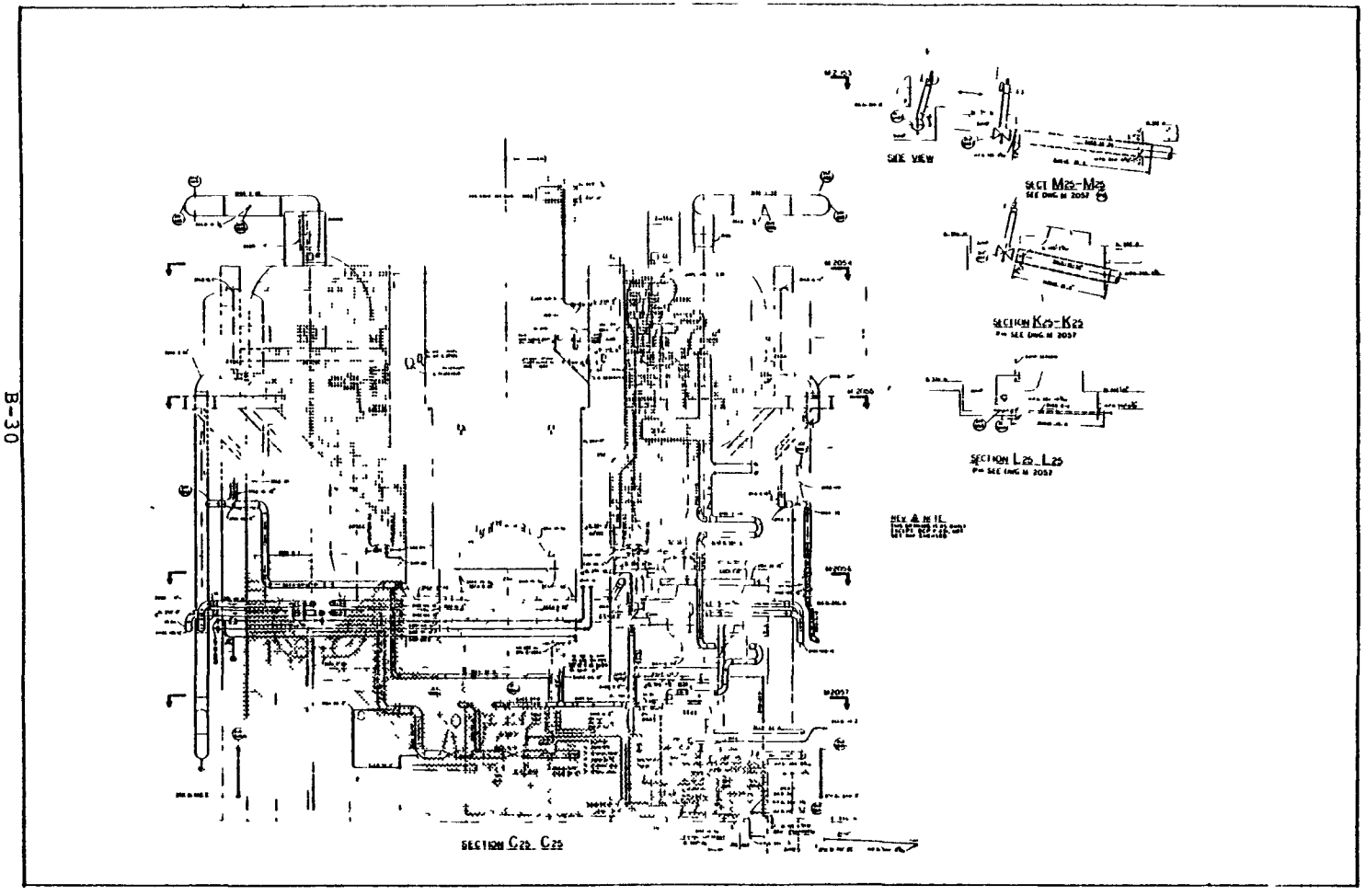

Tables B-8 and B-9 indicate that break 2DBB-1 is limiting as it generates 278 ft^2 of insulation debris while 2DBB-2 generates 96 ft^2. The transport analysis is therefore formed for the 2DBB-1 break.

4.0 DEBRIS TRANSPORT

4.1 Short Term Transport - Pipe Whip

No debris is generated by this mechanism.

4.2 Short Term Transport - Pipe Impact

No debris is generated by this mechanism.

4.3 Short Term Transport - Jet Impingement

The direction of the blowdown jet from break 90 on line 2DBB-1 is illustrated on Figures B-13, -14, -15 and -18. The break is located at approximately elevation 360 ft (i.e., above the 357 ft grating). This double ended failure will produce two jets: one in a direction downward toward the sump, the other upward toward the containment dome. As Figures B-1 through B-5 illustrate, the upward jet can penetrate above elevation 426 ft 6 in. due to the presence of grating. However, any insulation dislodged above elevation 357 ft will not reach the sump due to the grating. Therefore, only the downward jet must be considered.

As the figures show, the downward jet travels in the vicinity of the sump. No insulation, however, impinges directly on the sump screens due to the shadowing effects of the steam generator cavity wall. At the end of the short term transport, the debris is distributed in the vicinity of the sump.

4.4 Long Term Transport - Recirculation Phase

Only totally encapsulated calcium silicate insulation is affected by the postulated failure of 2DBB-1 and 2DBB-2. Following the same reasoning as was used for the main steam line failure, the limiting velocity is determined for the annulus region.

Figure B-1 shows the locations of the limiting annulus flow areas. For containment water depth of 6.1 ft and passage widths of 7.5 and 11 ft, the flow areas are 45 and 68 ft^2. The resulting velocities are:

$$14.5\ ft^3/sec \times 1/45\ ft^2 = 0.322\ ft/sec$$

$$14.5\ ft^3/sec \times 1/68\ ft^2 = 0.213\ ft/sec$$

These velocities are high enough to move particles which will

not pass through the screens (refer to Table B-3). Accordingly, total blockage of the outboard screen is assumed.

5.0 SUMP EFFECTS

Table B-6 indicates that the unblocked screen pressure drop is 1.163×10^{-3} ft of fluid. Head loss increase due to total blockage of the outboard screens can be developed as follows according to Equation 25:

$$h = \left(\frac{n}{c^2}\right)\left(\frac{1-\alpha^2}{\alpha^2}\right)\left(\frac{\bar{V}^2}{2g_c}\right)$$

Total flow is 6475 gpm or 14.5 ft^3/sec

Total available screen area is 98 ft^2 (inboard screen)

Velocity is therefore 14.5 $ft^2/sec \times 1/98\ ft^2 = 0.148$ ft/sec

Head loss increase due to outboard screen blockage is presented in Table B-10.

Table B-10

Head Loss - Outboard Screen Blocked

Screen	N_{RE}	c	α	$\bar{V}$ (ft/sec)	h (ft of fluid)
No. 4	154	0.9	0.32	0.148	3.68×10^{-3}
No. 14	552	1.05	0.505	0.148	9.0×10^{-4}

Original head loss	1.63×10^{-3} ft
Blocked head loss	4.5×10^{-3} ft
Increase in head loss	2.87×10^{-3} ft

The failure of 2DBB-1 generates debris in the vicinity of the ECCS sump. The limiting cross sectional areas are such that debris entrainment is possible. Assuming blockage of the entire outboard screen by accumulated debris, the increased head loss is insignificant. The failure of 2DBB-1, the limiting failure in the annulus region, will not adversely affect the operation of the ECCS sump.

APPENDIX C

MAINE YANKEE

Appendix C

Maine Yankee

1.0 BACKGROUND

Maine Yankee was selected for analysis due to the presence of large quantities of encapsulated fibrous insulation.

2.0 DETERMINATION OF INITIATING EVENTS

The Maine Yankee FSAR was written prior to the issuance of the standard review format and does not address specific design basis break locations inside containment. The following break locations were examined so that the limiting case could be identified:

Feedwater at steam generator nozzle

Main steam at steam generator nozzle

Hot leg exiting reactor well

Hot leg entering steam generator at valve

Hot leg at steam generator nozzle

Crossover leg at steam generator nozzle

Crossover leg entering reactor coolant pump

Cold leg exiting reactor coolant pump

Cold leg at valve

Cold leg at reactor cavity wall

Emergency feedwater at containment penetration

All other pipes are of smaller diameter and will produce blowdown jets whose consequences are less severe than those produced by the breaks identified above.

Loop 2 (Figure C-1) is located within a cavity without a safety injection tank and the quantity of insulation within

FIGURE C-1
CONTAINMENT PLAN, ELEV. 2'-0"

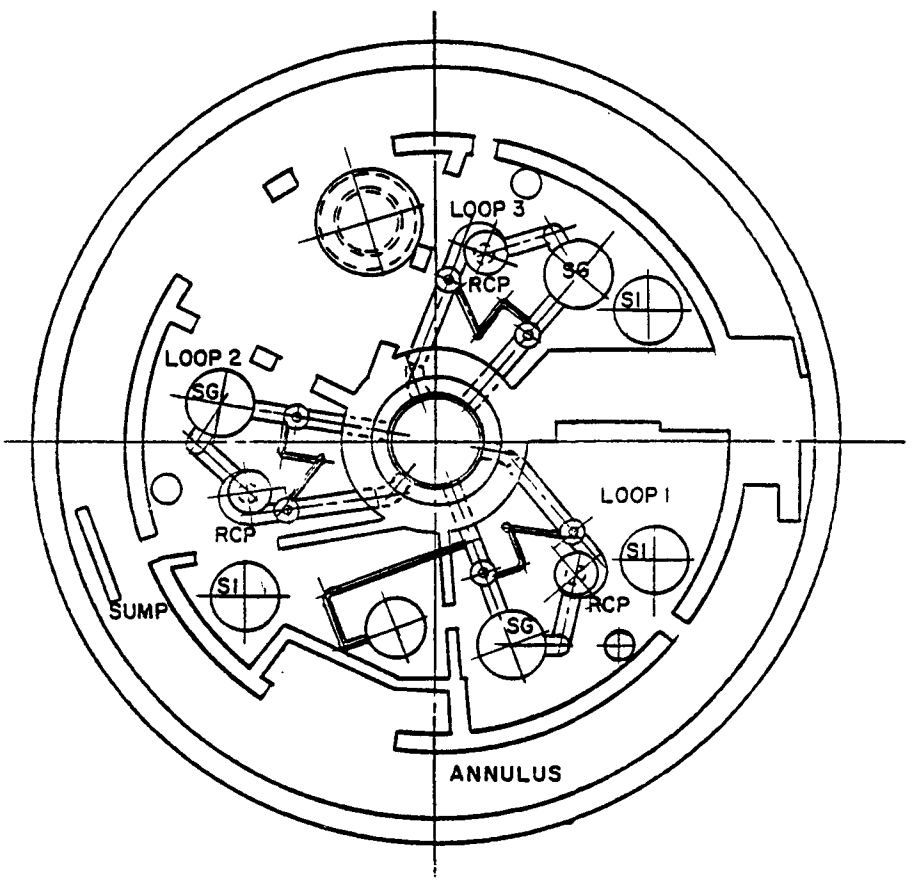

LEGEND:-
SG - STEAM GENERATOR
SI - SAFETY INJECTION TANK
RCP - REACTOR COOLANT PUMP

the cavity must be less than that in either loop 1 or loop 3. As loops 1 and 3 are somewhat symmetrical and loop 1 is nearer to the sump, loop 1 is the subject of this analysis. (See Figures C-1 through C-7.)

3.0 INSULATION DEBRIS GENERATION

As main steam line breaks produce more debris than feedwater (compare Figures C-8 and C-9), the feedwater break is not considered. As the hot leg breaks produce similar jet patterns, a single break is postulated at the valve center. As the cold leg breaks also produce similar jet patterns, a single break is postulated at the valve center. As a result of these similarities, the breaks analyzed for loop 1 are:

Table C-1

Break Locations

Break	Descriptions	Figure
1	Main steam at steam generator nozzle	C-9
2	Hot leg at valve center	C-10
3	Hot leg at steam generator nozzle	C-11
4	Crossover at steam generator nozzle	C-12
5	Crossover at reactor coolant pump	C-13
6	Cold leg at valve center	C-14
7	Emergency feedwater at penetration	C-15

FIGURE C-2
CONTAINMENT PLAN ELEV. 20'-0"

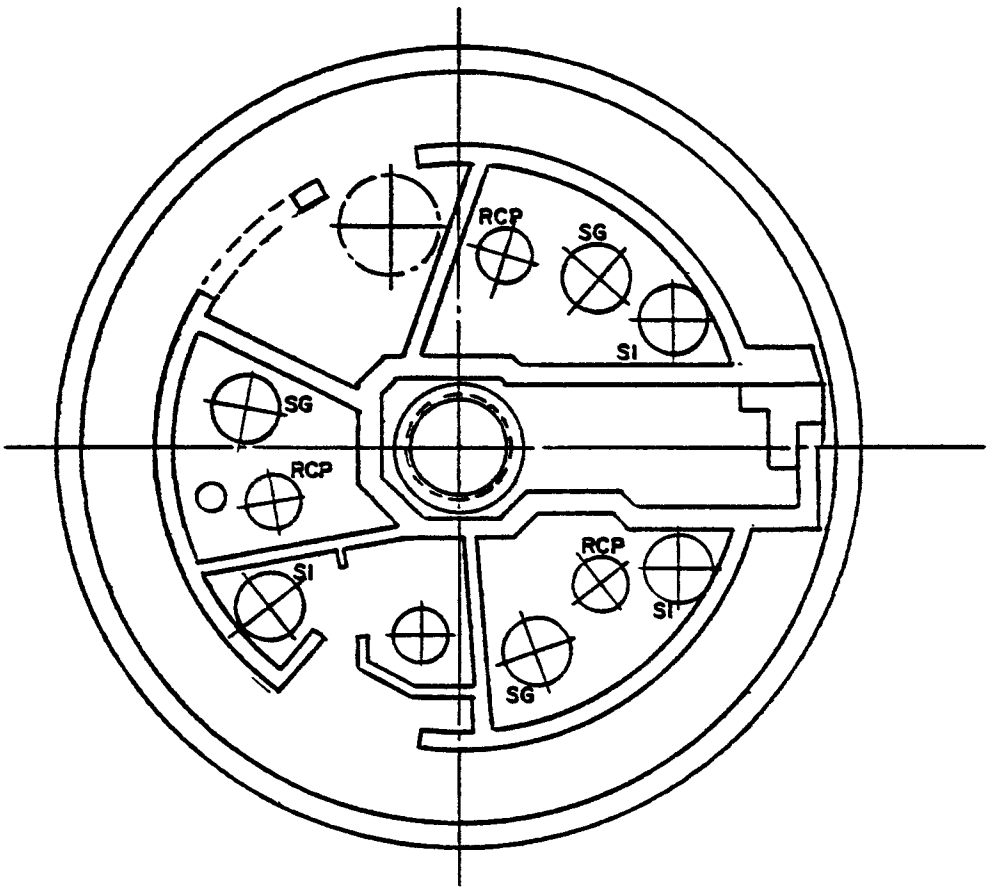

LEGEND:-
SG - STEAM GENERATOR
SI - SAFETY INJECTION TANK
RCP - REACTOR COOLANT PUMP

FIGURE C-3
CONTAINMENT PLAN ELEV. 46'-0"

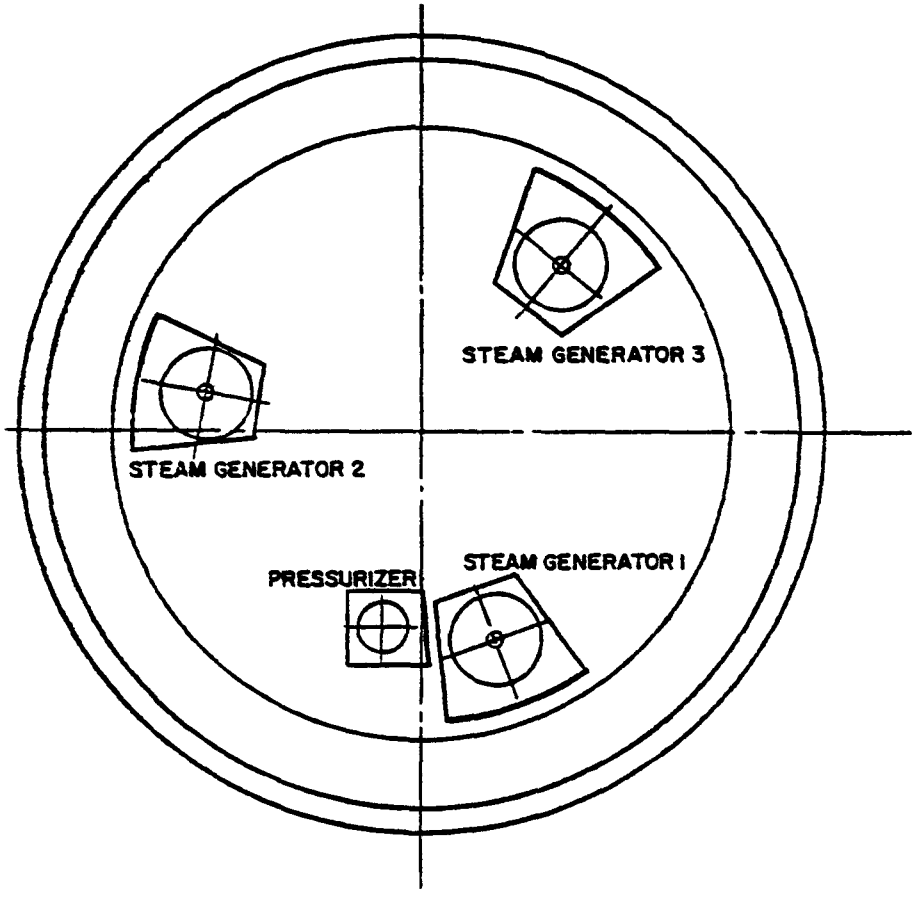

FIGURE C-4

ELEVATION VIEW LOOP 2 STEAM GENERATOR

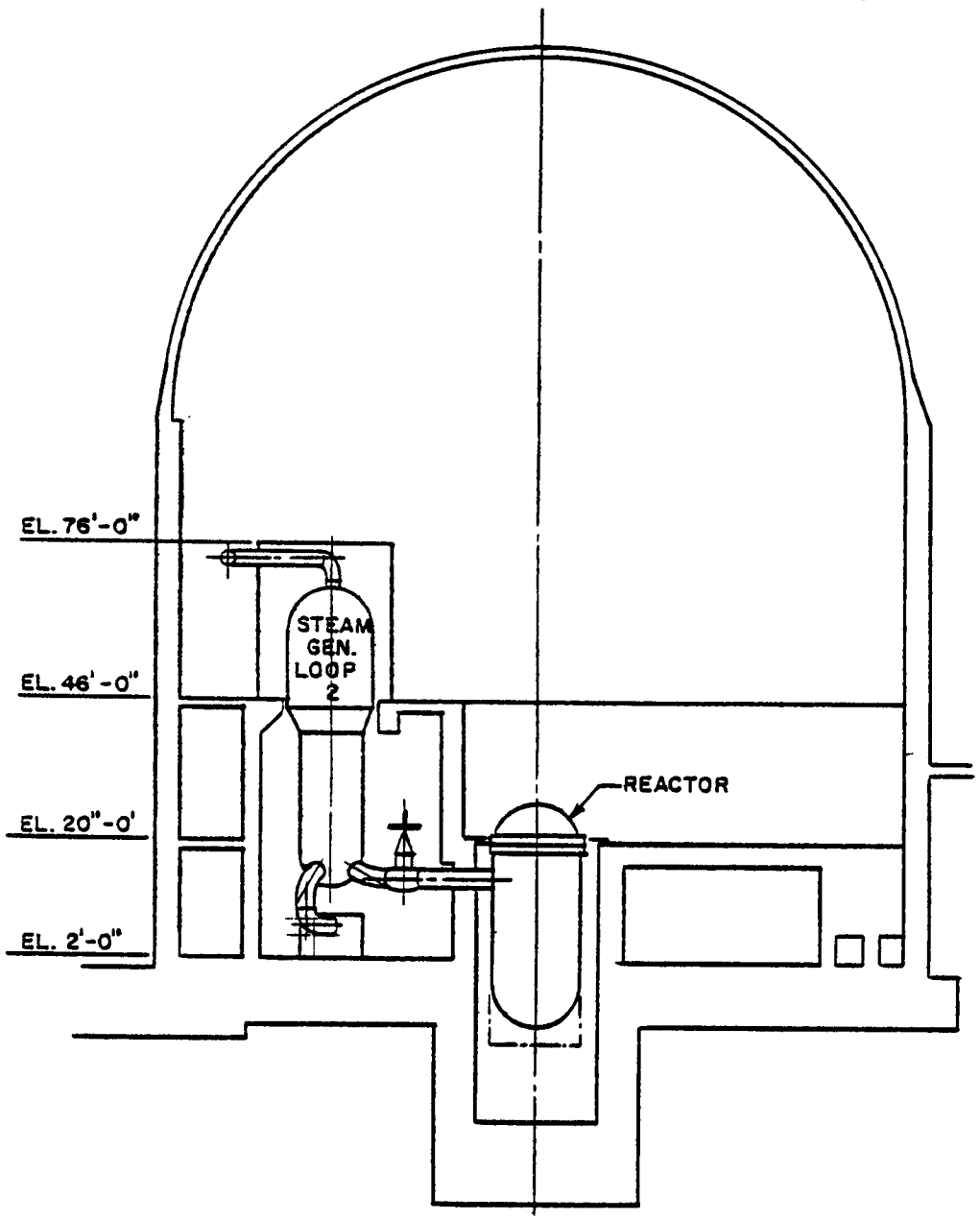

FIGURE C-5
ELEVATION VIEW LOOPS 1 & 3 STEAM GENERATOR

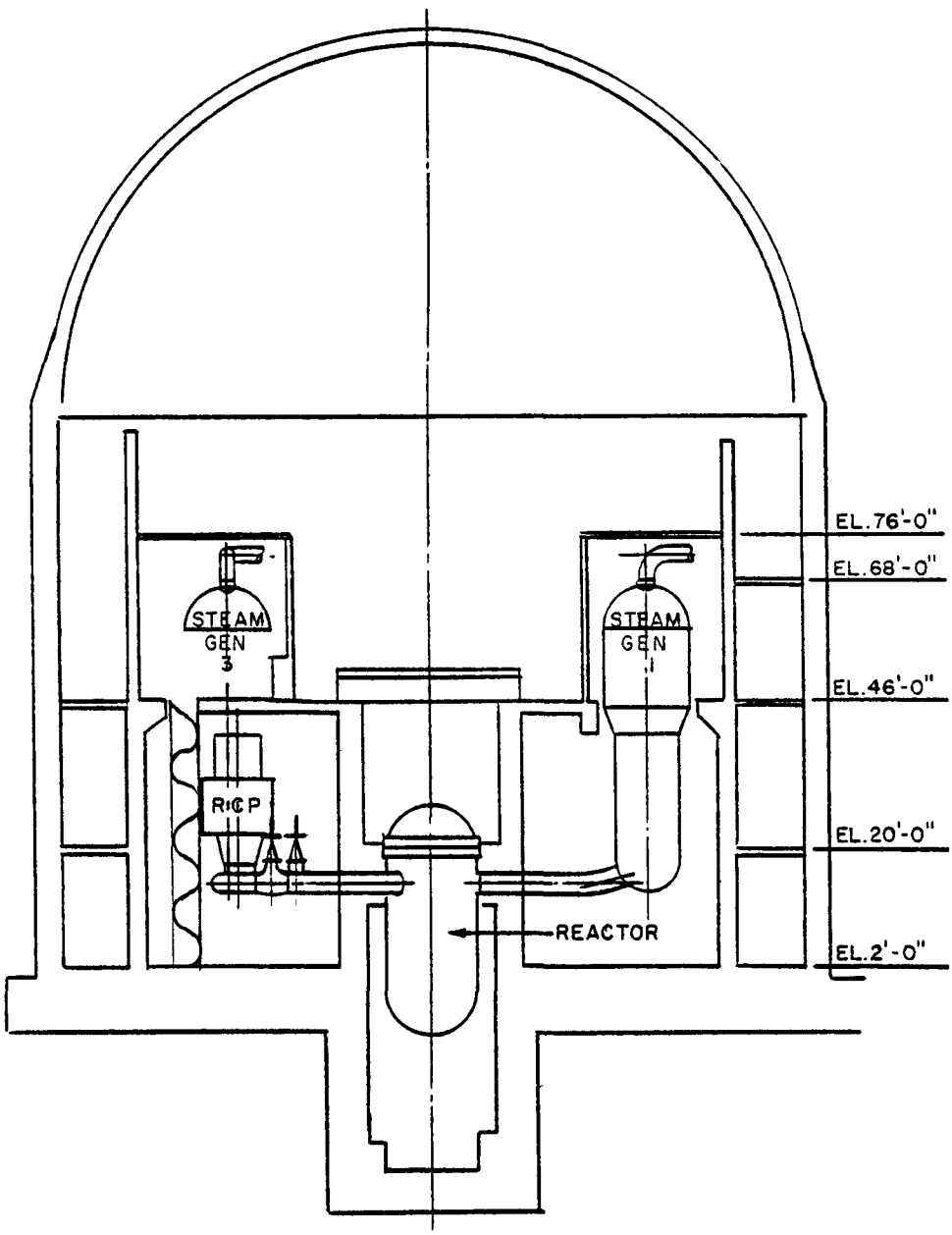

FIGURE C-6
PRESSURIZER COMPARTMENT

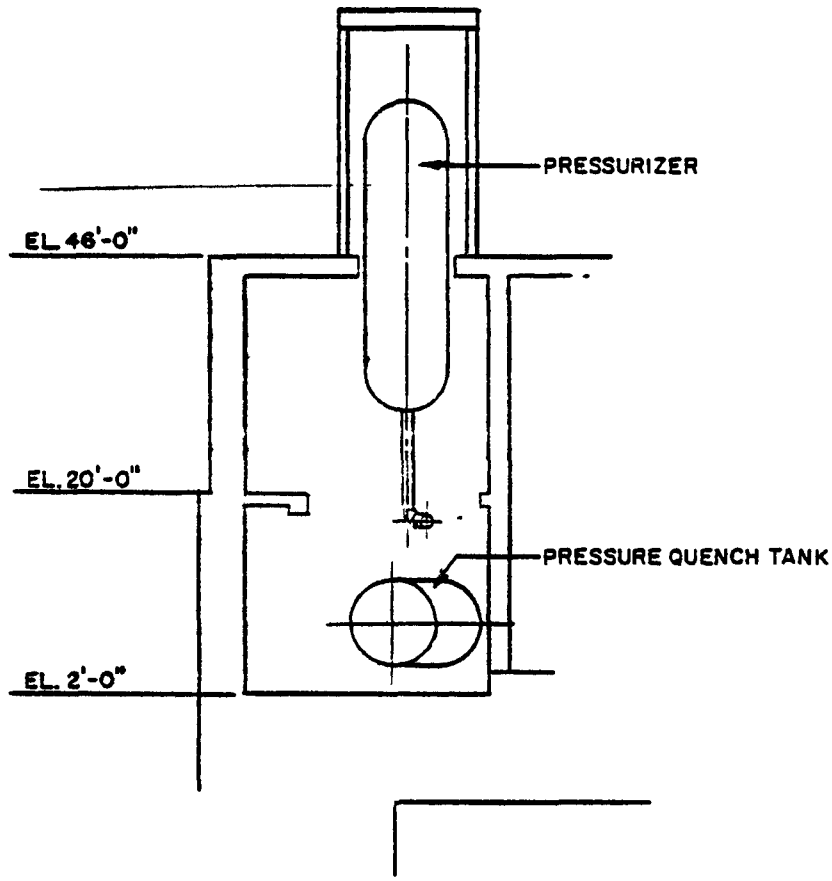

FIGURE C-7
CONTAINMENT SUMP.

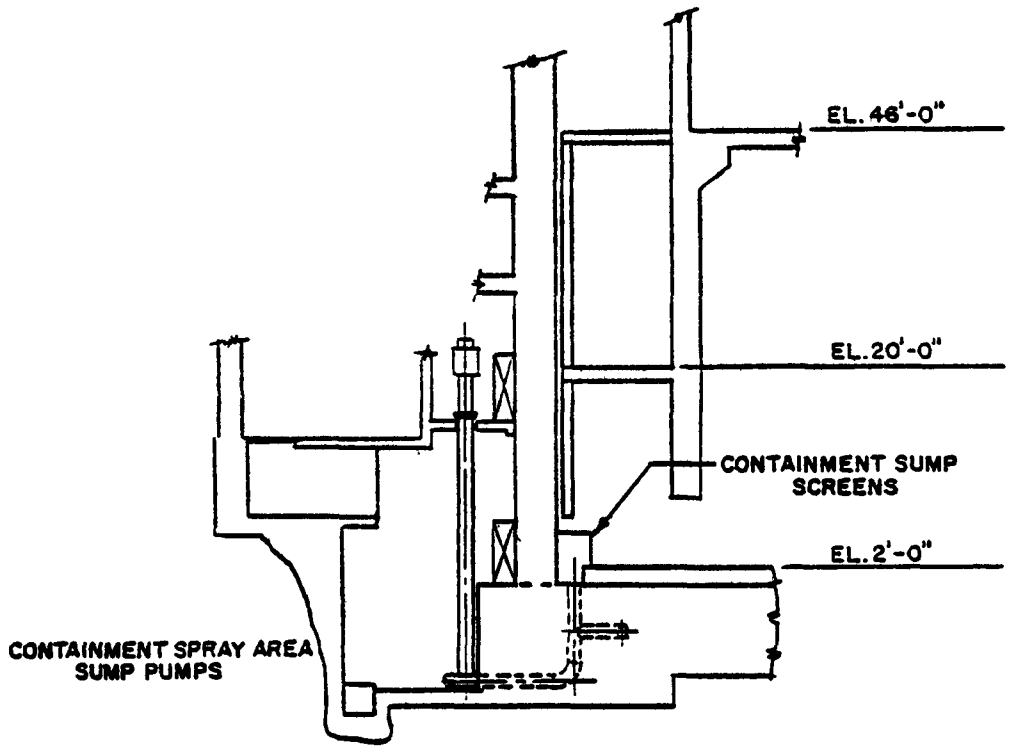

FIGURE C-8
FEEDWATER FAILURE

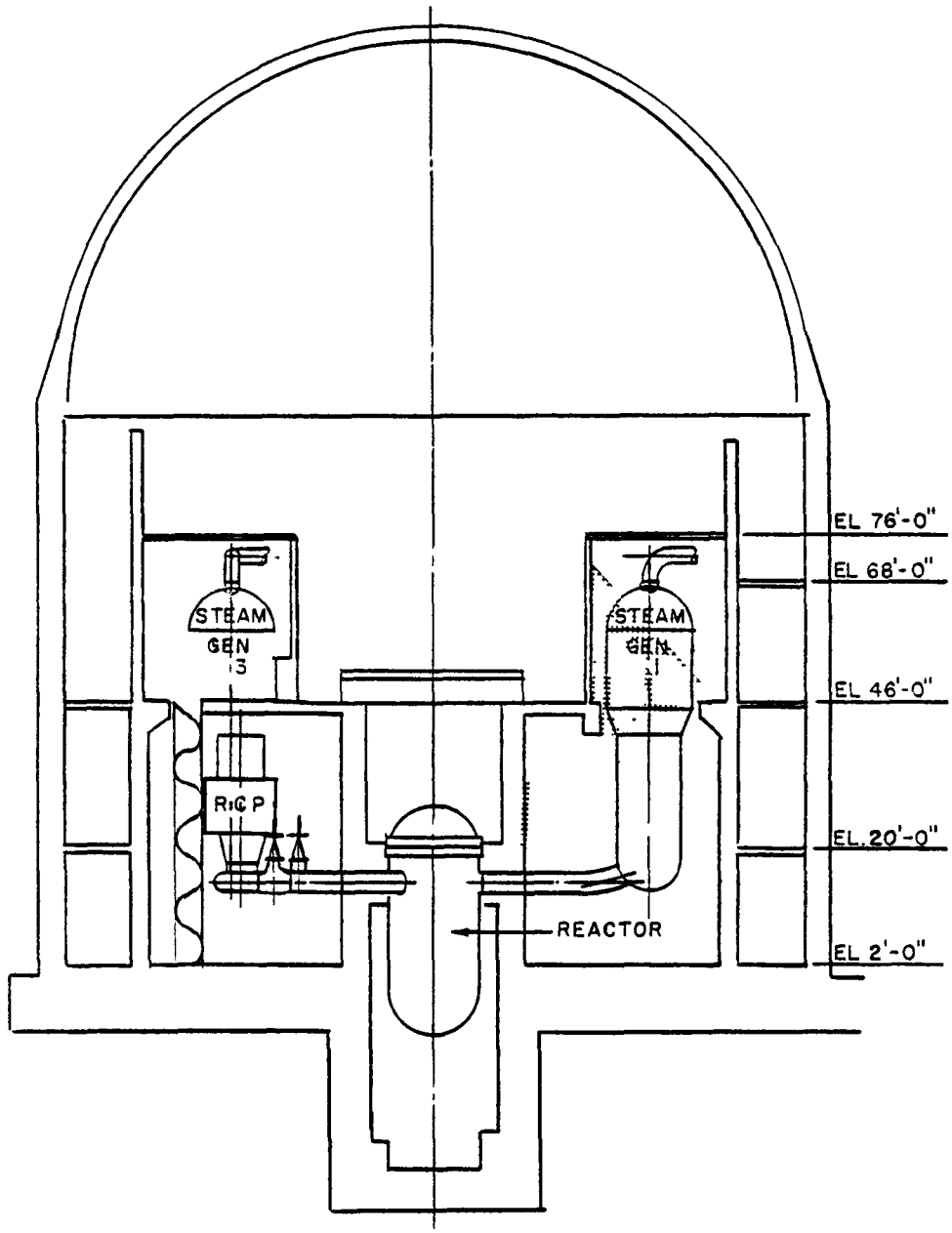

FIGURE C-9
BREAK I: MAIN STEAM AT STEAM GENERATOR NOZZLE

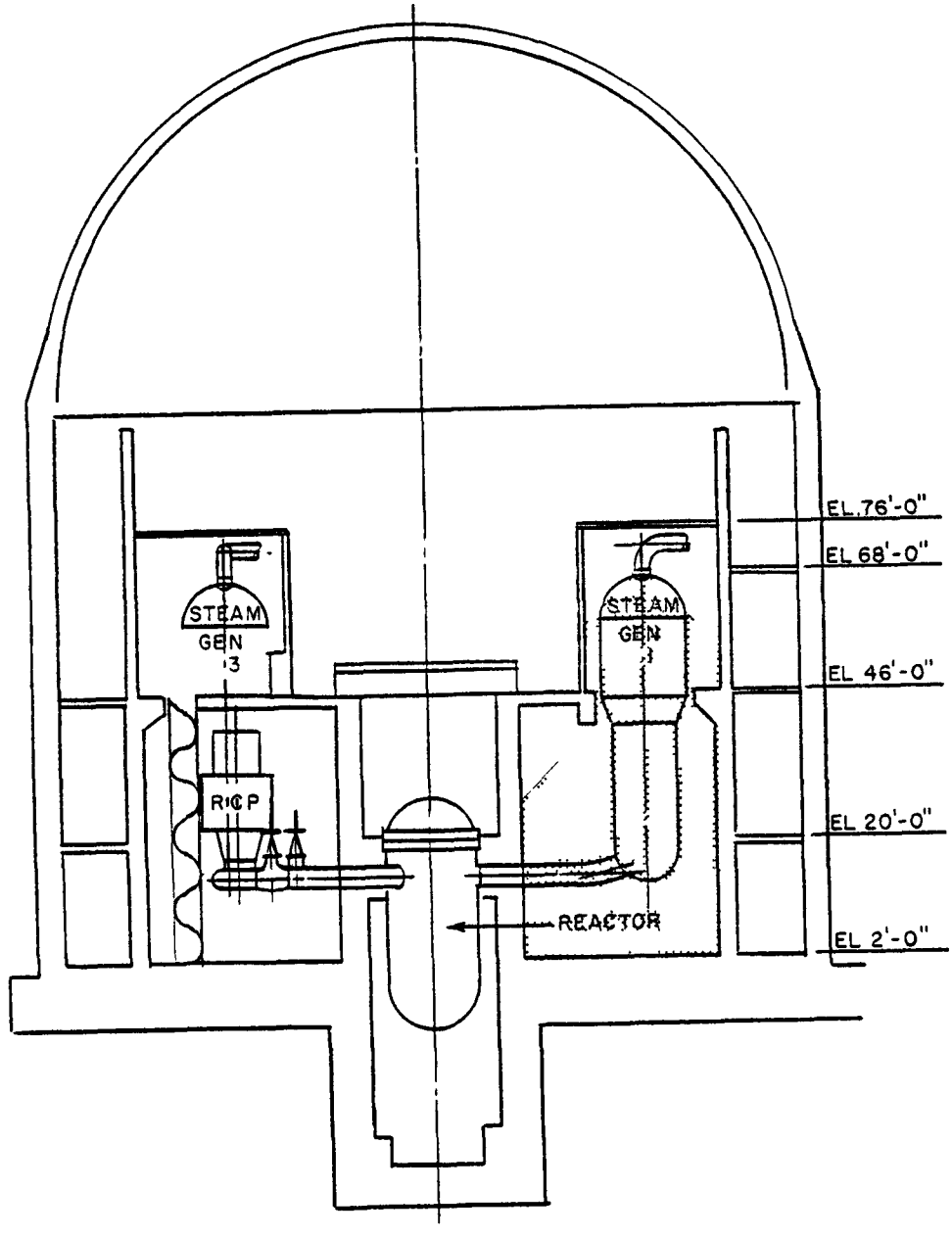

Break 1: Main Steam at Steam Generator Nozzle

3.1 Pipe Whip

The reaction load produced on the main steam line by the release of high temperature/pressure fluid causes the main steam line to move in a vertically upward direction until impact with the steam generator cavity ceiling occurs. (Refer to Figure C-9.) The insulation on the moving line segment will be ejected tangent to the main steam line's arc of rotation at the point of impact. The ejected insulation in this instance will strike the steam generator cavity ceiling and then fall vertically downward. Refer to Table C-2 for the quantities of debris generated by this mechanism.

3.2 Pipe Impact

As Figures C-4, -5 and -9 illustrate, no piping runs are located in the path of the moving main steam line segment. Therefore, no insulation debris generation is attributed to this mechanism.

3.3 Jet Impingement

Figure C-9 illustrates the path of the expanding jet issuing from the main steam failure. Table C-2 summarizes the quantities and types of debris generated by this mechanism. Jet expansion angle is calculated using the Attachment 2 procedure.

Break 2: Hot Leg at Valve Center

3.1 Pipe Whip

The reaction load produced on the hot leg by the release of high temperature/pressure fluid causes the hot leg to move in a horizontal direction without impact on any structure. (Refer to Figures C-9 and C-10.) The insulation on the hot leg segment is assumed to fall to the containment floor. Refer to Table C-3 for the quantities of insulation generated by this mechanism.

Table C-2

Debris Summary, Break 1: Main Steam at Steam Generator Nozzle

Insulation Type	Item	Length (ft)	Diam (ft)	Area (ft^2)
Calcium-Silicate	Steam Generator, Upper	28	15	1319
	Steam Generator, Lower	30	12	1130
	Allowance, 20%			564
Blanket	Primary Pipe	3.33	16	168
	Allowance, 20%			33
Fiberglass	Allowance, 50% of blanket insulation total			100
Total				3314

Note: Allowances as percentages of component insulation are given for small bore pipe.

Table C-3

Debris Summary, Break 2: Hot Leg at Valve Center

Insulation Type	Item	Diam (ft)	Length (ft)	Area (ft^2)
Calcium-Silicate	Steam Generator	12	20	845
Blanket	Primary Pipe	3.33	12	126
	Allowance, 20%			25
Fiberglass	Allowance, 50% of blanket insulation total			75
Total				1071

Note: Allowances as percentages of component insulation are given for small bore pipe. No allowance is required for steam generator.

FIGURE C-10
BREAK 2: HOT LEG AT VALVE CENTER

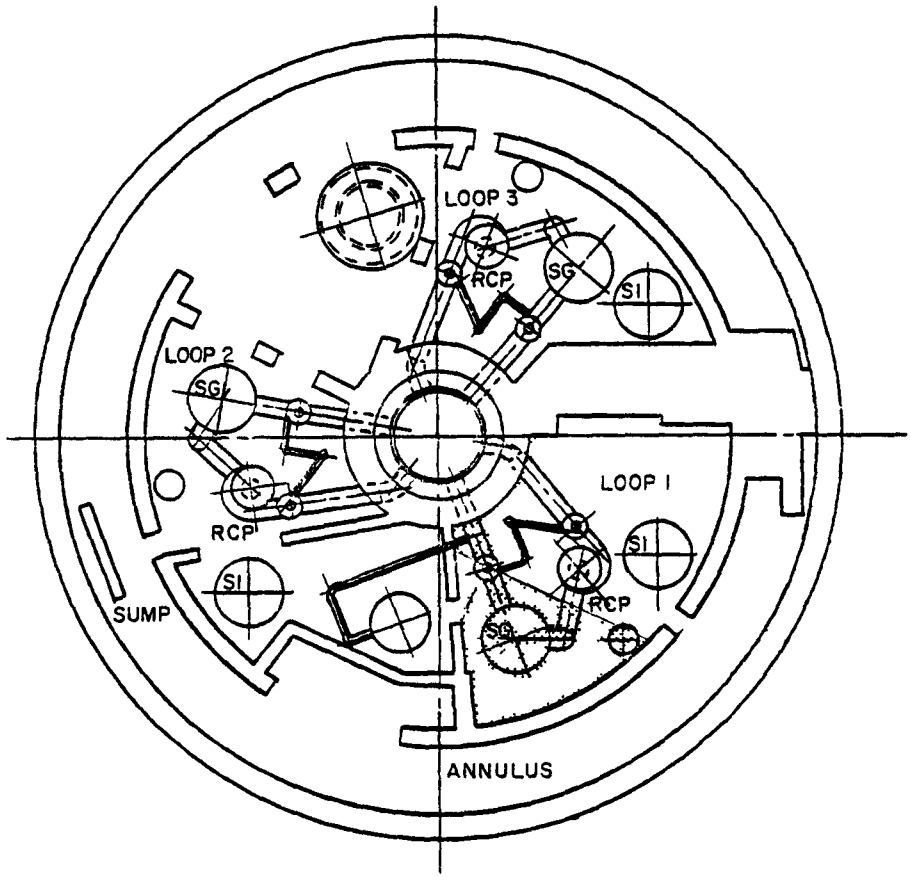

LEGEND:-
SG - STEAM GENERATOR
SI - SAFETY INJECTION TANK
RCP - REACTOR COOLANT PUMP

3.2 Pipe Impact

As Figures C-9 and C-10 illustrate, no piping runs are affected by the hot leg failure as no pipe whip occurs. Consequently, no insulation debris generation is attributed to this mechanism.

3.3 Jet Impingement

Figure C-10 illustrates the path of the expanding jet issuing from the hot leg failure. Table C-3 summarizes the quantities and types of debris generated by this mechanism. Attachment 2 was used to determine the jet characteristics.

Break 3: Hot Leg at Steam Generator Nozzle

3.1 Pipe Whip

The reaction load produced on the hot leg by the release of high temperature/pressure fluid causes the hot leg to move in a vertically downward direction until impact with the containment floor occurs. (Refer to Figures C-9 and C-11.) The insulation on the moving line segment will be ejected tangent to the hot leg line's arc of rotation at the point of impact. The ejected insulation will strike the containment floor near the reactor cavity wall. Refer to Table C-4 for the quantities of insulation generated by this mechanism.

3.2 Pipe Impact

As Figures C-9 and C-11 illustrate, the bypass piping and pressurizer surge line are located in the path of the moving hot leg segment. Consequently, debris generation for these lines is recorded in Table C-4.

3.3 Jet Impingement

Figure C-11 illustrates the path of the expanding jet issuing from the hot leg failure. Table C-4 summarizes the quantities and type of debris generated by this mechanism. Attachment 2 was used to determine the jet characteristics.

FIGURE C-11
BREAK 3: HOT LEG AT STEAM GENERATOR NOZZLE

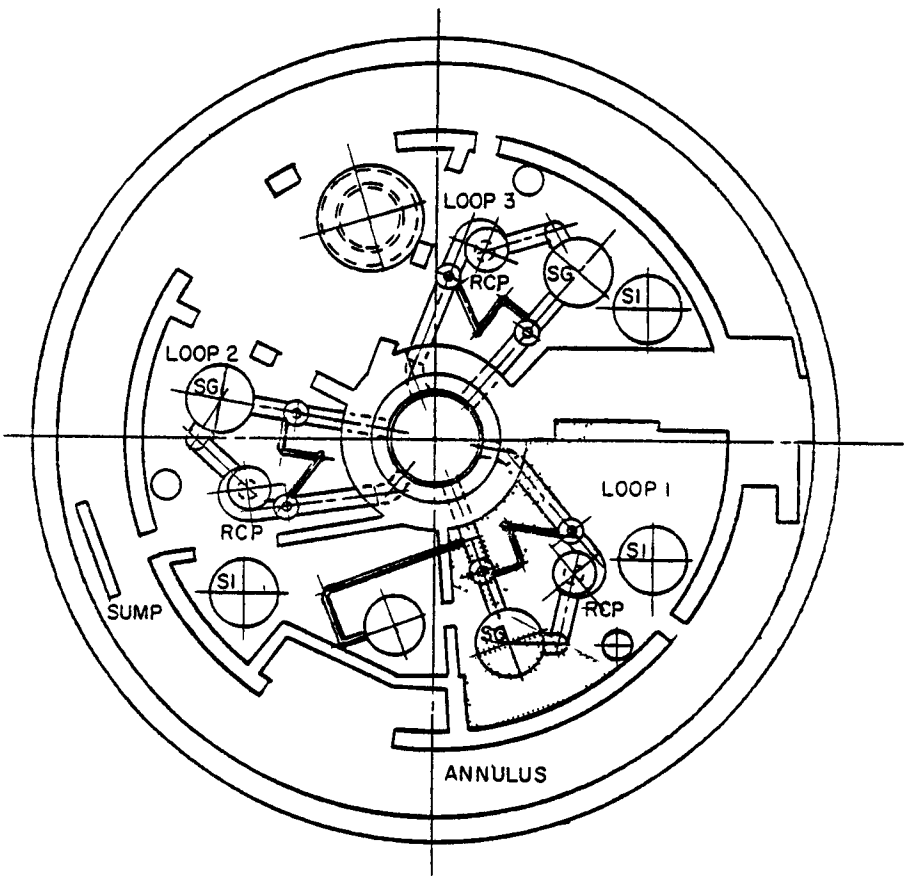

LEGEND:-
SG - STEAM GENERATOR
SI - SAFETY INJECTION TANK
RCP - REACTOR COOLANT PUMP

Table C-4

Debris Summary, Break 3: Hot Leg at Steam Generator Nozzle
or
Break 4: Crossover at Steam Generator Nozzle

Insulation Type	Item	Diam (ft)	Length (ft)	Area (ft^2)
Calcium-Silicate	Steam Generator	12	30	1213
	Allowance, 20%			240
Blanket	Primary Pipe	3.33	10	105
	Allowance, 20%			21
Fiberglass	Allowance, 50% of blanket insulation total			63
Total				1642

Note: Allowances as percentages of component insulation are given for small bore pipe.

Break 4: Crossover at Steam Generator Nozzle

3.1 Pipe Whip

The reaction load produced on the crossover line by the release of high temperature/pressure fluid causes the crossover line to rotate in a clockwise direction (when viewed from the steam generator) until impact with the containment floor occurs. (Refer to Figure C-12.) The insulation on the moving line segment will be ejected tangent to the crossover line's arc of rotation at the point of impact. The ejected insulation will strike the containment floor near the steam generator outer wall. Refer to Table C-4 for the quantities of insulation generated by this mechanism.

3.2 Pipe Impact

As Figure C-12 illustrates, no piping runs are located in the path of the moving crossover piping line segment. Therefore, no insulation debris generation is attributed to this mechanism.

3.3 Jet Impingement

Figure C-12 illustrates the path of the expanding jet issuing from the crossover failure. Table C-4 summarizes the quantities and types of debris generated by this mechanism. Attachment 2 was used to determine the jet characteristics.

Break 5: Crossover at Reactor Coolant Pump

3.1 Pipe Whip

The reaction load produced on the crossover line by the release of high temperature/pressure fluid causes the crossover line to rotate in a downward direction until impact with the containment floor occurs. (Refer to Figure C-9 and C-13.) The insulation on the moving line segment will be ejected tangent to the crossover line's arc of rotation at the point of impact. The ejected insulation will strike the containment floor near the reactor coolant pump supports. Refer to Table C-5 for the quantities of insulation generated by this mechanism.

FIGURE C-12

BREAK 4: CROSSOVER AT STEAM GENERATOR NOZZLE

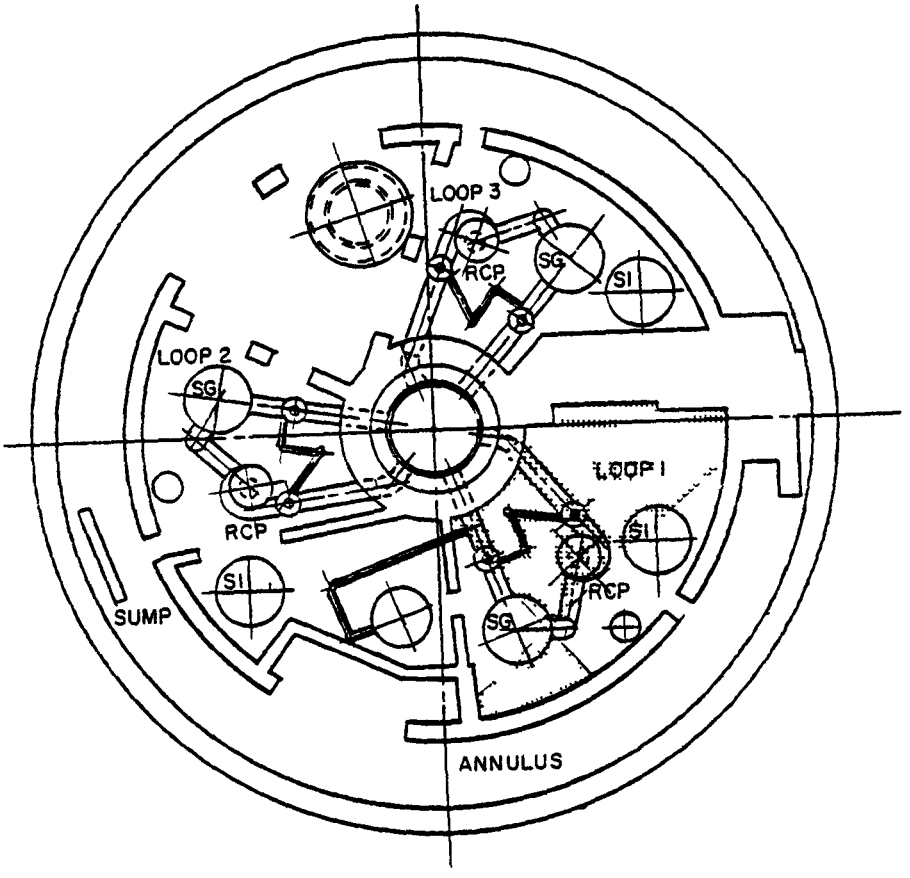

LEGEND:-

SG - STEAM GENERATOR

SI - SAFETY INJECTION TANK

RCP - REACTOR COOLANT PUMP

Table C-5

Debris Summary, Break 5: Crossover at Reactor Coolant Pump (RCP)

Insulation Type	Item	Diam (ft)	Length (ft)	Area (ft^2)
Calcium-Silicate	Steam Generator	12	20	845
	RCP	5	10	157
	Allowance, 20%			200
Blanket	Primary Pipe	3.33	21	219
	Allowance, 20%			42
Fiberglass	Allowance, 50% of blanket insulation total			132
Total				1595

Note: Allowances as percentages of component insulation are given for small bore pipe.

Table C-6

Debris Summary, Break 6: Cold Leg at Valve Center

Insulation Type	Item	Diam (ft)	Length (ft)	Area (ft^2)
Calcium-Silicate	RCP	5	10	157
	Allowance, 20%			31
Blanket	Primary Pipe	3.33	13	136
	Allowance, 20%			27
Fiberglass	Allowance, 50% of blanket insulation total			80
Total				431

Note: Allowances as percentages of component insulation are given for small bore pipe.

FIGURE C-13

BREAK 5: CROSSOVER AT REACTOR COOLANT PUMP

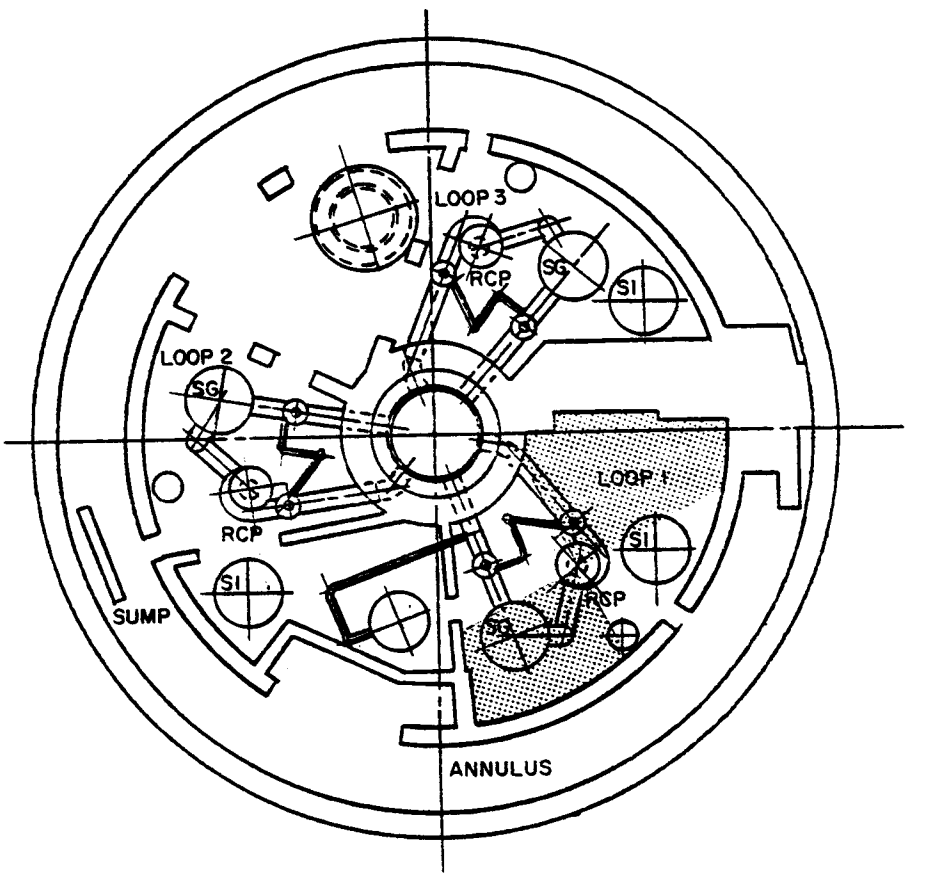

LEGEND:-

SG - STEAM GENERATOR

SI - SAFETY INJECTION TANK

RCP - REACTOR COOLANT PUMP

3.2 Pipe Impact

As Figures C-9 and C-13 illustrate, no piping runs are located in the path of the moving crossover pipe line segment. Therefore no insulation debris generation is attributed to this mechanism.

3.3 Jet Impingement

Figures C-13 illustrates the path of the expanding jet issuing from the crossover failure. Table C-5 summarizes the quantities and types of debris generated by this mechanism.

Break 6: Cold Leg at Valve Center

3.1 Pipe Whip

The reaction load produced on the cold leg by the release of high temperature/pressure fluid causes the cold leg to rotate in a horizontal plane until impact with the steam generator compartment wall occurs. (Refer to Figure C-14.) The insulation on the moving line segment will be ejected tangent to the cold leg line's arc of rotation at the point of impact. The ejected insulation will strike the steam generator compartment wall and settle to the floor near the wall. Refer to Table C-6 for the quantities of insulation generated by this mechanism.

3.2 Pipe Impact

As Figures C-5, -9 and -14 illustrate, no piping runs are located in the path of the cold leg moving line segment. Therefore, no insulation debris generation is attributed to this mechanism.

3.3 Jet Impingement

Figure C-14 illustrates the path of the expanding jet issuing from the cold leg failure. Table C-6 summarizes the quantities and types of debris generated by this mechanism. Attachment 2 is used to determine the jet characteristics.

FIGURE C-14

BREAK 6: COLD LEG AT VALVE CENTER

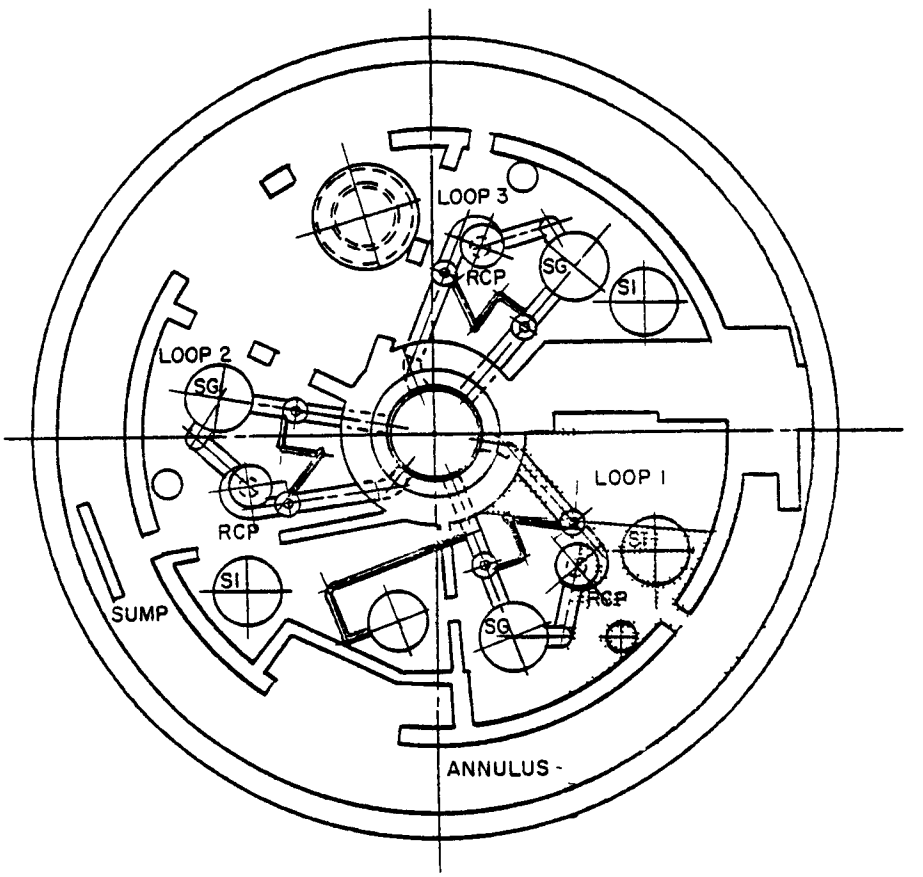

LEGEND:-

SG - STEAM GENERATOR

SI - SAFETY INJECTION TANK

RCP - REACTOR COOLANT PUMP

Break 7: Emergency Feedwater at Containment Penetration

3.1 Pipe Whip

The reaction load produced on the emergency feedwater line by the release of high temperature/pressure fluid causes the emergency feedwater line to move in a vertically upward direction until impact with the elevation 20 ft slab occurs. (Refer to Figures C-9 and C-15.) The insulation on the moving line segment will be ejected tangent to the emergency feedwater line's arc of rotation at the point of impact. The ejected insulation in this instance will strike the underside of the elevation 20 ft slab and fall down into the piping annulus. Refer to Table C-7 for the quantities of insulation generated by this mechanism.

3.2 Pipe Impact

As Figures C-3, -4 and -15 illustrate, several piping runs are located in the path of the moving emergency feedwater line segment. All relevant insulation debris generation is recorded in Table C-7 for this mechanism.

3.3 Jet Impingement

Figure C-15 illustrates the path of the expanding jet issuing from the emergency feedwater failure. Table C-7 summarizes the quantities and types of debris generated by this mechanism. Attachment 2 is used to determine the jet characteristics.

4.0 DEBRIS TRANSPORT

The pipe whip, pipe impact and jet impingement mechanisms of debris generation cannot transport any debris to the sump due to geometrical placement of the sump relative to steam generator cavity wall openings.

Following termination of short term transport, the debris for breaks 1 through 6 will be confined to the steam generator cavity, and the debris for break 7 will be confined to the piping annulus. Sump impact does not occur in any case.

FIGURE C-15

BREAK 7: EMERGENCY FEEDWATER AT CONTAINMENT PENETRATION

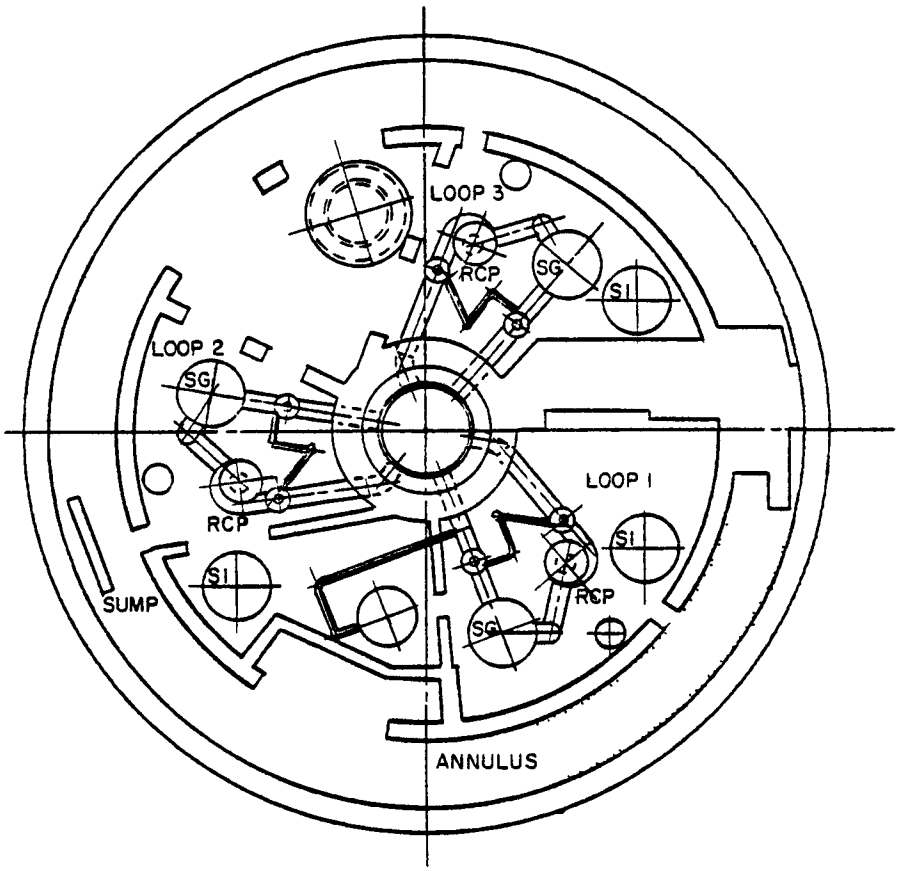

LEGEND:-

SG - STEAM GENERATOR

SI - SAFETY INJECTION TANK

RCP - REACTOR COOLANT PUMP

Table C-7

Debris Summary, Break 7: Emergency Feedwater at Penetration

Calcium-Silicate

Line	Diam (in.)	Length (ft)	Area (ft^2)
WGCB- 6-601	3	8	6
WGCB-18-601	3	8	6
WAPD	6	8	13

Allow 25 ft^2 for small bore pipe.

Fiberglass

Line	Diam (in.)	Length (ft)	Area (ft^2)
PCC-237	6	8	13
PCC-234	4	8	8
PCC-169	4	8	8
PCC-168	4	8	8
PCC-289	6	8	13
PCC-290	6	8	13
PCC-236	6	8	13
PCC-287	6	8	13
PCC-288	6	8	13
PCC-194	6	8	13
PCC-195	6	8	13
PCC-196	6	8	13

Allow 25 ft^2 for small bore pipe.

4.4 Long Term Transport - Recirculation Phase

The introduction of the contents of the refueling water storage tank into containment results in a post LOCA water level of approximately 2.5 ft. This is based on 26,700 ft^3 from the RWST plus 2,000 ft^3 from the spray chemical addition tank plus 1,500 ft^3 from the safety injection tanks. This yields a total injected volume of 30,200 ft^3. The containment floor area is 11,500 ft^2, yielding the 2.5 ft water depth. This amount of water is sufficient to cause insulation with densities less than that of water to float and migrate to the sump.

Insulations more dense than water will be transported to the sump if local recirculation induced velocities are sufficiently high that the fluid drag force exceeds the frictional resistance to motion developed between the debris and the containment floor when the effects of lift and buoyancy are included.

4.4.1.1 Containment Floor - Recirculation Mode

Maximum recirculation flow is 8700 gpm and water depth is approximately 2.5 ft (Maine Yankee FSAR). Referring to Figure C-1, a number of openings in the shield wall exist to allow the injection flow to return to the containment sump. Figure C-16 illustrates the flow paths. As flow resistance is directly proportional to distance and inversely proportional to flow area, the following network is developed to determine the recirculation flow through each opening.

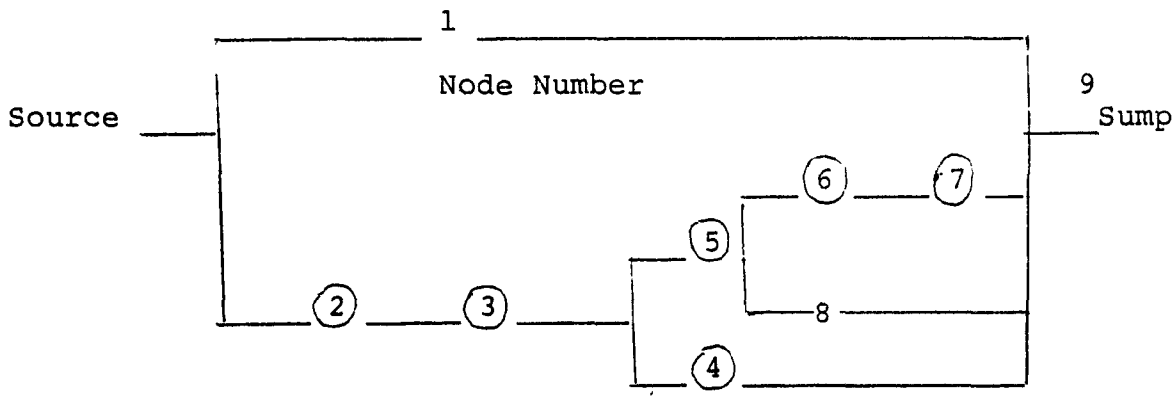

FIGURE C-16
CONTAINMENT CIRCULATION

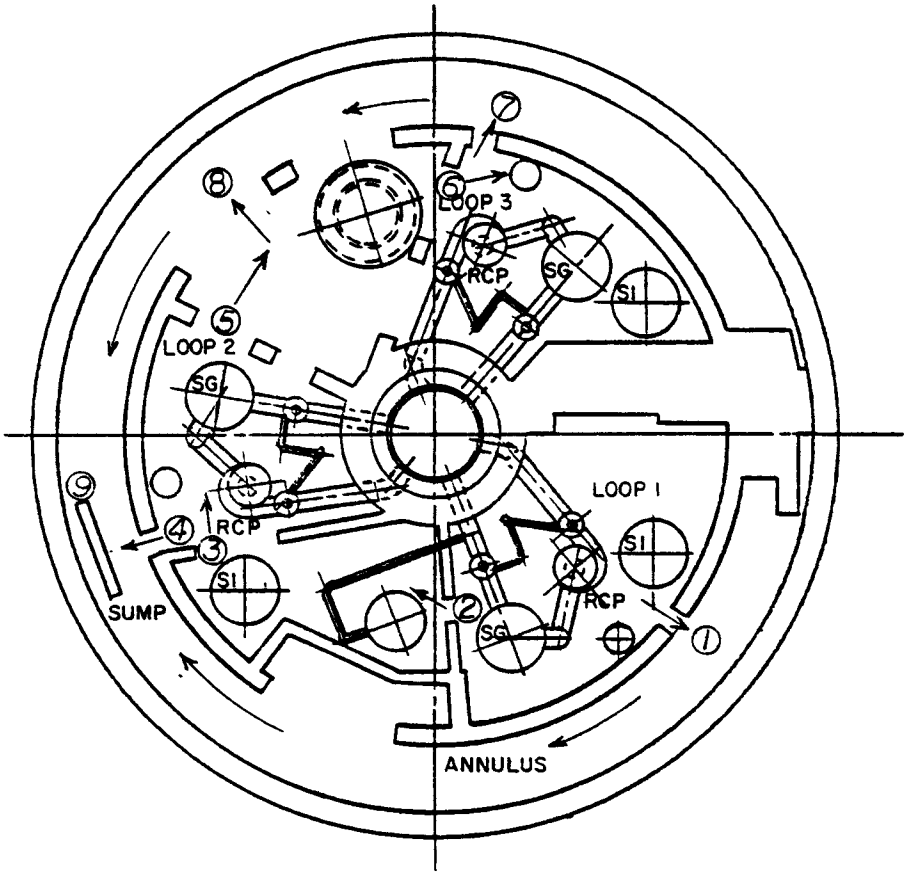

LEGEND:-
SG - STEAM GENERATOR
SI - SAFETY INJECTION TANK
RCP - REACTOR COOLANT PUMP

For each node in the network there is a resistance corresponding to the opening. For each branch in the network there is a resistance corresponding to the distance between openings. Table C-8 summaries the area, distances and resistances.

Table C-8

Resistance of Containment Flow Paths

Branch Resistances

From	To	Distance L, (ft)	Area A, (ft^2)	Distance/Area (L/A) (1/ft)
Source	1	14	140	.1
Source	2	25	88	.28
1	9	120	25	4.5
2	3	35	57	.61
3	4	10	25	.4
3	5	37	73	.506
4	9	8	25	.32
5	6	29	73	.39
5	8	29	19	1.52
6	7	17	15	1.13
8	9	70	25	2.8
7	9	126	25	5.04

Opening Resistances

Node	L	A	L/A
1	3	10	.3
2	2	14	.14
3	3	55	.054
4	3	14	.21
5	3	71	.04
6	3	92	.03
7	3	14	.21
8	3	150	.02

Substituting these values into the network and simplifying yields:

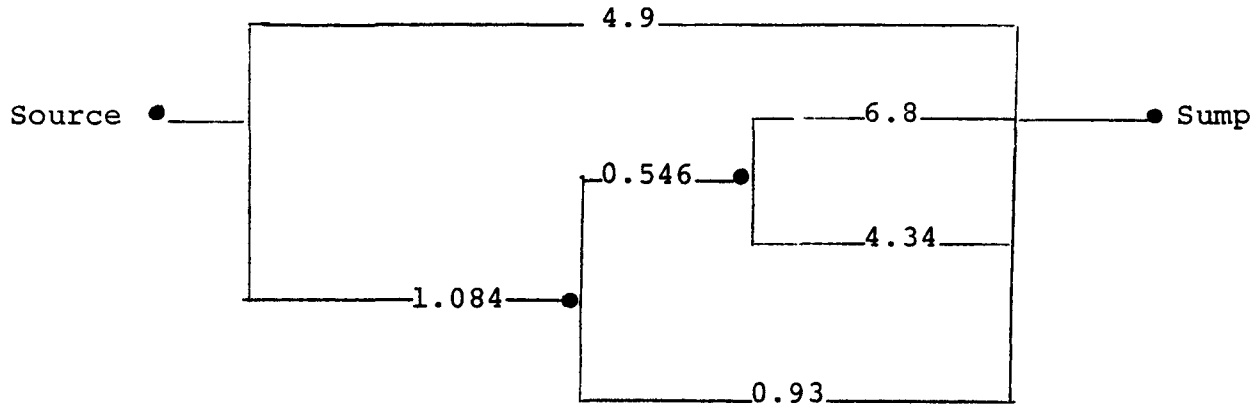

Reduction of this network yields an equivalent resistance of 0.6. Section 4.4.1.1 indicates

$$\Delta P = R_{equiv.} \dot{m}^2$$

Assuming $\dot{m} = 1$, the fractional flow through each branch can be determined. For $\dot{m} = 1$, $\Delta P = 0.6$, and the branch flows are as shown in Table C-9. In like manner, the velocities through the openings are given in Table C-10.

Table C-11 summarizes the debris generated by each postulated break. As fibrous insulation is the item of concern in this analysis, break 5 is selected for further analysis.

5.0 SUMP EFFECTS

Following termination of the blowdown event, the debris within steam generator compartment 1 will be subjected to the velocity fields given in Tables C-9 and C-10.

The object of the sump analysis is twofold: first, to determine the possibility of transport for the debris contained in compartment 1 and second, for the debris which can be transported, to evaluate the increased pressure drop across the sump screens.

Table C-9

Branch Flows and Velocities

From	To	Fraction of Total Flow	Total Flow (ft^3/sec)	Branch Flow (ft^3/sec)	Area of Path (ft^2)	Branch Velocity (ft/sec)
Source	1	.348	19.4	6.75	140	.05
Source	2	.652	19.4	12.65	88	.14
1	9	.348	19.4	6.75	25	.27
2	3	.652	19.4	12.65	57	.22
3	5	.274	19.4	5.31	73	.07
3	4	.378	19.4	7.3	25	.29
5	6	.151	19.4	2.93	73	.04
6	7	.151	19.4	2.93	15	.19
7	9	.151	19.4	2.93	25	.12
5	8	.123	19.4	2.4	19	.13
8	9	.123	19.4	2.4	25	.10
4	9	.378	19.4	7.3	25	.29

Table C-10

Velocities Through Shield Wall Openings

Node	Flow (ft^3/sec)	Area (ft^2)	Velocity (ft/sec)
1	6.75	10	.68
2	12.65	14	.90
3	12.65	55	.23
4	7.3	14	.53
5	5.31	71	.07
6	2.93	92	.03
7	2.93	10	.21
8	2.4	150	.02

Table C-11

Summary of Debris Generation (ft^2)

Break	Calcium-Silicate	Blanket	Fiberglass	Total
1	3384	201	100	3685
2	845	151	75	1071
3	1453	126	63	1642
4	1453	126	63	1642
5	1202	262	132	1596
6	188	163	80	431
7	50	0	166	215

Table C-11 gives for break 5:

Calcium Silicate Insulation	1202 ft^2
Blanket	262 ft^2
Fiberglass	132 ft^2
Total	1596 ft^2

DETERMINATION OF TRANSPORT POTENTIAL

Fibrous Debris

As a first approximation, the technique of Section 4.7.1 will be used, and all fibrous insulation is assumed to migrate to the sump. The calcium silicate transport is treated as follows:

Calcium Silicate

Maine Yankee employs calcium silicate molded block insulation. The material has a fabricated density of approximately 12 lbm/ft^3 and a theoretical density of 160 lbm/ft^3. As fabricated, it has a void fraction of .925. The weight in water per cubic foot of bulk material is therefore:

$$\text{Weight in water} = (\rho_{\text{insulation}} - \rho_{\text{water}})\ (1 - \text{void fraction})$$

$$= (160-62)0.075 = 7.35\ lbm/ft^3$$

As the actual particle size distribution for the resulting debris is unknown, a series of sizes is selected to envelop the range of transport velocities required to move the debris from compartment 1 to the sump. This is illustrated in Table C-12, which shows that only very small debris particles can be transported by the velocities existing in containment. Consequently, calcium silicate debris transport is not expected to occur, and sump blockage due to such debris impingement is not included in the sump screen pressure drop evaluation.

Pressure Drop at Screens Due to Fibrous Debris Accumulation

From the plant drawings and the height of water in containment after the RWST inventory has been injected, the area of sump screens submerged is 108 ft^2 (sump screen perimeter multiplied by water depth).

Table C-12

Transport Velocities

Shape	Length or Radius (ft)	Width (ft)	Depth (ft)	Volume (ft^3)	Weight in Water (lbm)	Required Velocity to Cause Motion (ft/sec)
Sphere	.0052	-	-	7.4×10^{-8}	5.44×10^{-7}	.10
Sphere	.0208	-	-	4.7×10^{-6}	3.45×10^{-5}	.21
Sphere	.0416	-	-	3.77×10^{-5}	2.77×10^{-4}	.34
Sphere	.0833	-	-	3.03×10^{-4}	2.22×10^{-3}	.48
Sphere	.1666	-	-	2.42×10^{-3}	1.79×10^{-2}	.68
Block 1:1:1	.0833	.0833	.0833	5.78×10^{-4}	4.25×10^{-3}	.42
Block 1:3:1	.0833	.2499	.0833	1.73×10^{-3}	1.27×10^{-2}	.42
Block 1:7:1	.0833	.5881	.0833	4.05×10^{-3}	3.24×10^{-2}	.42
Block 3:9:1	3.0	1.0	.333	1.0	7.35	.84
Block 1:1:0.5	.0833	.0833	.0416	2.88×10^{-4}	2.12×10^{-3}	.29
Block 1:1:0.25	.0833	.0833	.0208	1.44×10^{-4}	1.06×10^{-3}	.21

Assuming uniform debris deposition, 394 ft^2 of debris is deposited on 108 ft^2 of screen, giving a bed depth of 11 in.

Using Equation 27, the pressure loss is:

$$\Delta P = \frac{3.5\ \mu\ q\ S_v^2}{A_b} (1-\varepsilon)^{1.5} [1+57(1-\varepsilon)^3]\ \ell$$

For this case:

ℓ = 11 in. or 28 cm

μ = 0.0068 poise

S_v = 2420 cm^2/cm^3

q = 8700 gpm or 5.488 x 10^5 cm^3/sec

A_b = 108 ft^2 or 1.003 x 10^5 cm^2

ε = 1-νC'

ν = 0.384 cm^3/g

C' = 12 lbm/ft^3 or 0.192 g/cm^3

ε = 1 - (0.384 x 0.192)

ε = 0.926

and

$$\frac{\Delta P}{\ell} = \frac{3.5(0.0068)(5.488 \times 10^5)(2420)^2}{1.003 \times 10^5}(1-0.926)^{1.5}[1+57(1-0.926)^3]$$

ΔP = 1.56 x 10^6 dynes/cm^2/cm

ΔP = 6.35 psi, which may exceed design NPSH margin.

In Section 4.7.2, there are data which indicate less than 100% migration of fibrous debris. Accordingly,

Debris generated	394 ft^2
Immediately sinking debris	158 ft^2
Debris remaining	236 ft^2

Of the 236 ft^2 of debris, half forms fine suspended fibers, and half forms floating flocs which sink in 2 to 5 days.

The pressure drop of the preceding calculation could be reduced by a factor of 158/394, or 40%, yielding a pressure drop of 3.8 psi which is still excessive. Had this reduction produced screen losses nearer to the design NPSH margin, the procedure of Section 5.4 would have to be followed as bed pressure loss due to individual fiber accumulation is not a linear function of bed thickness as Section 5.3 assumes. The rough calculation above indicated that continuation with Section 5.4 was unwarranted as the pressure drop is unacceptable.

Conclusion

On the basis of the assumptions in this analysis, the quantity of debris generated by break 5 is sufficiently high to interfere with sump operation. It must be noted, however, that no credit is taken for trapping of floating debris as it migrates toward the sump. This possibility must be addressed before a final determination on the acceptability of the degree of blockage can be made.

APPENDIX D

SEQUOYAH NUCLEAR UNIT 2

Appendix D

Sequoyah Nuclear Unit 2

1.0 INTRODUCTION

Sequoyah Nuclear Unit 2 (SNU-2) was selected as it is typical of PWR installations employing reflective metallic insulation inside containment. Although Appendix A indicates that relatively high velocities are required to transport reflective metallic insulation, the presence of the recirculation sump within one of the steam generator cavities introduces other considerations in addition to local velocities.

2.0 IDENTIFICATION OF INITIATING EVENTS

The SNU-2 FSAR identifies the design basis break locations in Section 3.6.2. As SNU-2 employs reflective metallic insulation exclusively within containment, only those breaks which direct insulation debris toward the sump need be considered due to the relatively high transport velocity required to move submerged reflective metallic insulation. This requirement eliminates loops 2 and 3 from analysis. (Refer to Figure D-1 for relative locations of loops 1-4 and the recirculation sump.)

As a result of these considerations, the following initiating events are used in this analysis.

Break	Description
1	Feedwater Line at Containment Penetration
2	Hot Leg Failure (Steam Generator 4 Nozzle)
3	Hot Leg Failure (50° Elbow 4)
4	Reactor Coolant Pump 4 Outlet Nozzle
5	Steam Generator 4 Outlet Nozzle
6	Steam Generator 1 Outlet Nozzle
7	Loop Closure Weld, Loop 1

FIGURE D-1
CONTAINMENT PLAN VIEW

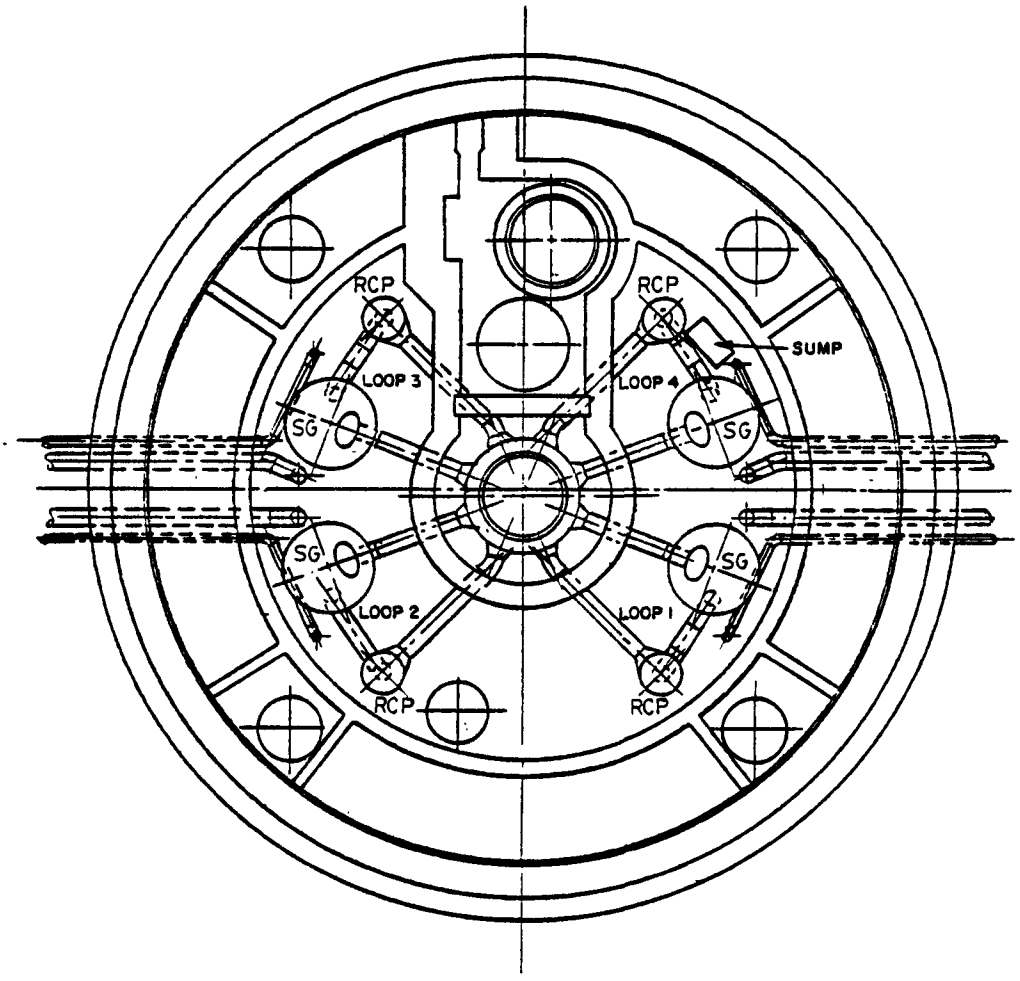

LEGEND
SG - STEAM GENERATOR
RCP - REACTOR COOLANT PUMP

Additional high energy pipe is present within the shield wall area but, due to its smaller diameter, the jet produced and its consequences cannot be as severe as those breaks listed above. Breaks 1 through 7 therefore bound the debris generation problem.

Main steam and feedwater line breaks above elevation 733.63 ft are not considered potential debris generators as a continuous concrete floor is interposed between these lines and the sump. Refer to Figures D-2 and D-3 for relative locations of main steam, feedwater piping, the 733.63 ft elevation slab and the recirculation sump area.

Feedwater piping below elevation 733.63 ft is included as break 1. Main steam breaks are not considered as the jet magnitude, size and direction are bounded by breaks 1, 5, 6 and 7.

3.0 DEBRIS GENERATION

Break 1: Feedwater Line at Containment Penetration

3.1 Pipe Whip

Figure D-4 illustrates the path of the expanding feedwater jet. Due to the short length of the free end segment which is not within the jet, no pipe whip debris generation is assumed for this break. The debris contribution of the free end segment within the jet is added to the jet impingement generated debris.

3.2 Pipe Impact

The free end segment within the jet is capable of motion. However, since no major insulated pipes or components are present within the segment's trajectory, no debris generation by pipe impact is considered.

3.3 Jet Impingement

The Attachment 2 procedure gives an expansion angle for primary system breaks of 90° and indicates that jet pressure reduction to the 0.5 psig cutoff does not occur.

Figure D-2

Containment Elevation View Looking West

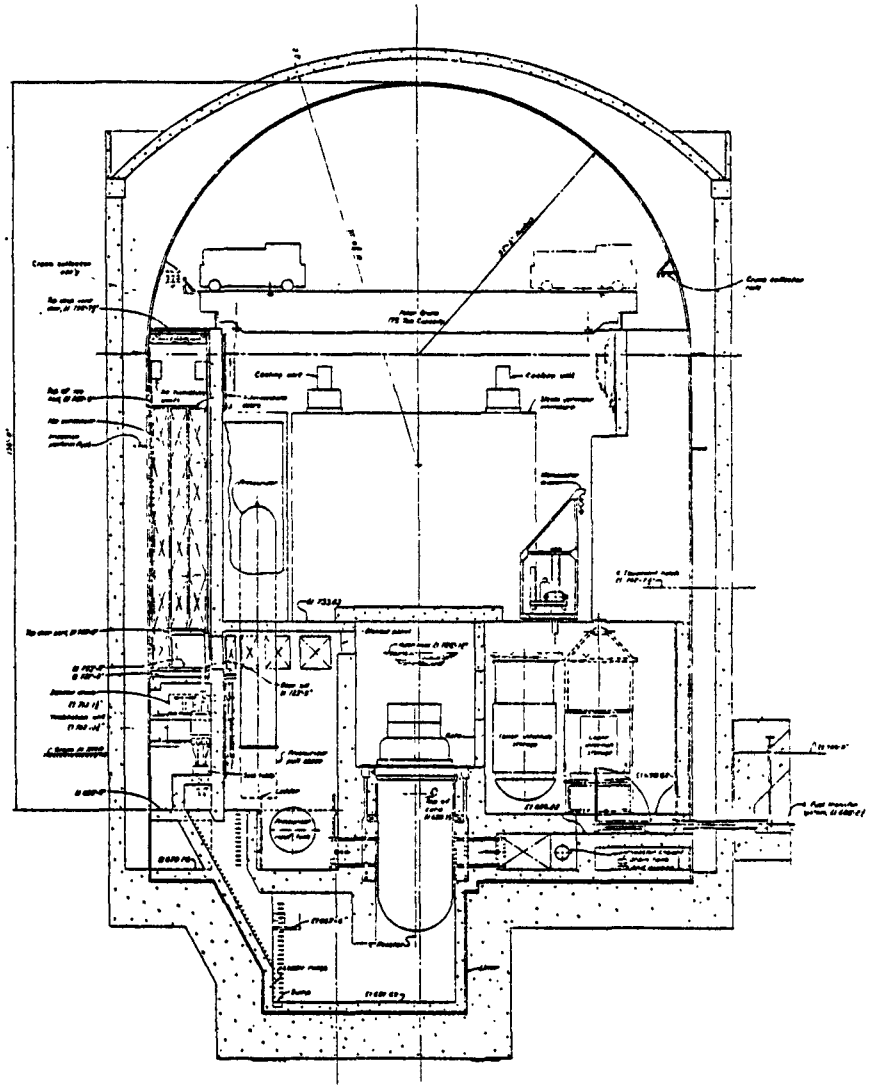

Figure D-3

Containment Elevation Looking South West

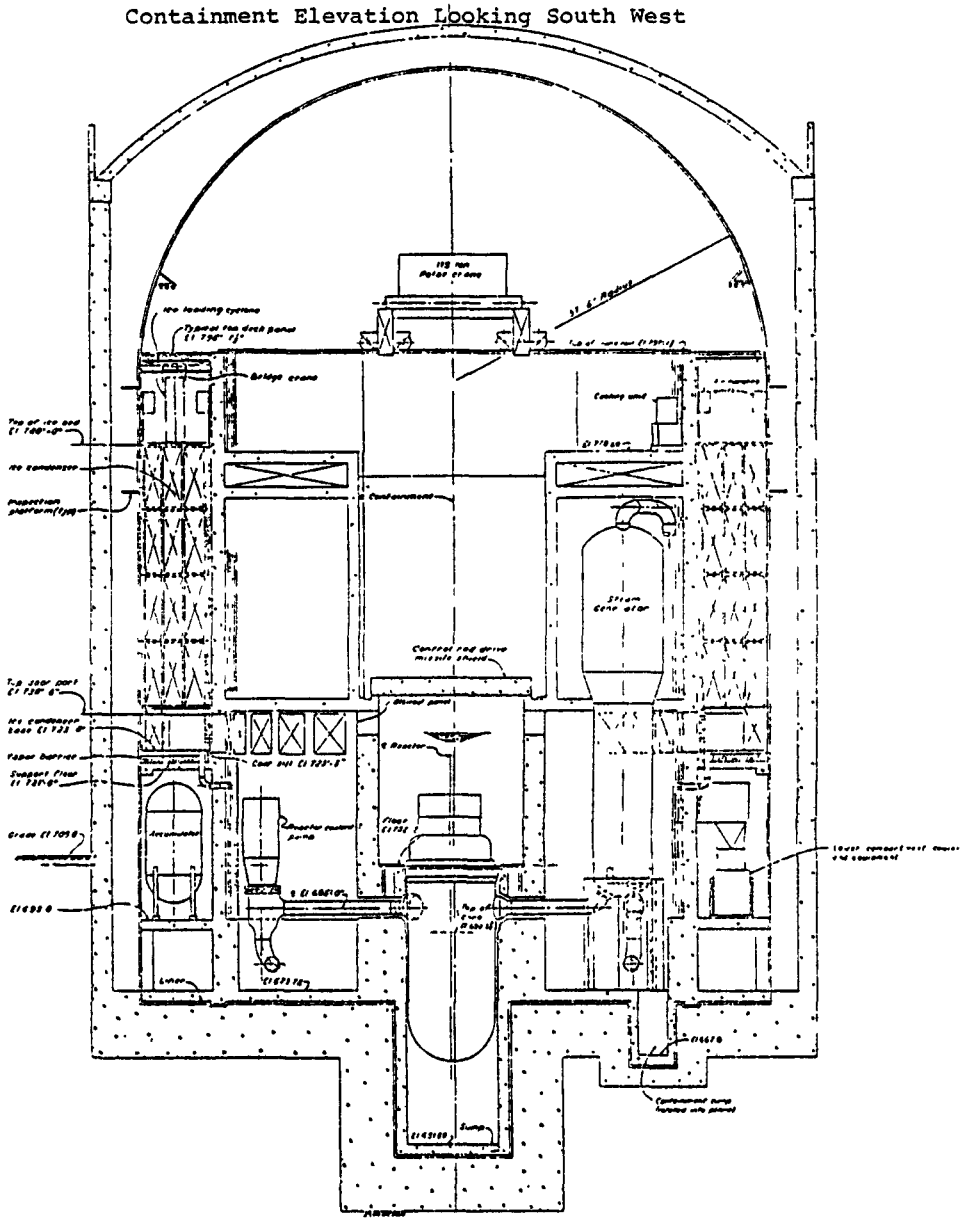

FIGURE D-4
BREAK I: FEEDWATER LINE AT CONTAINMENT PENETRATION

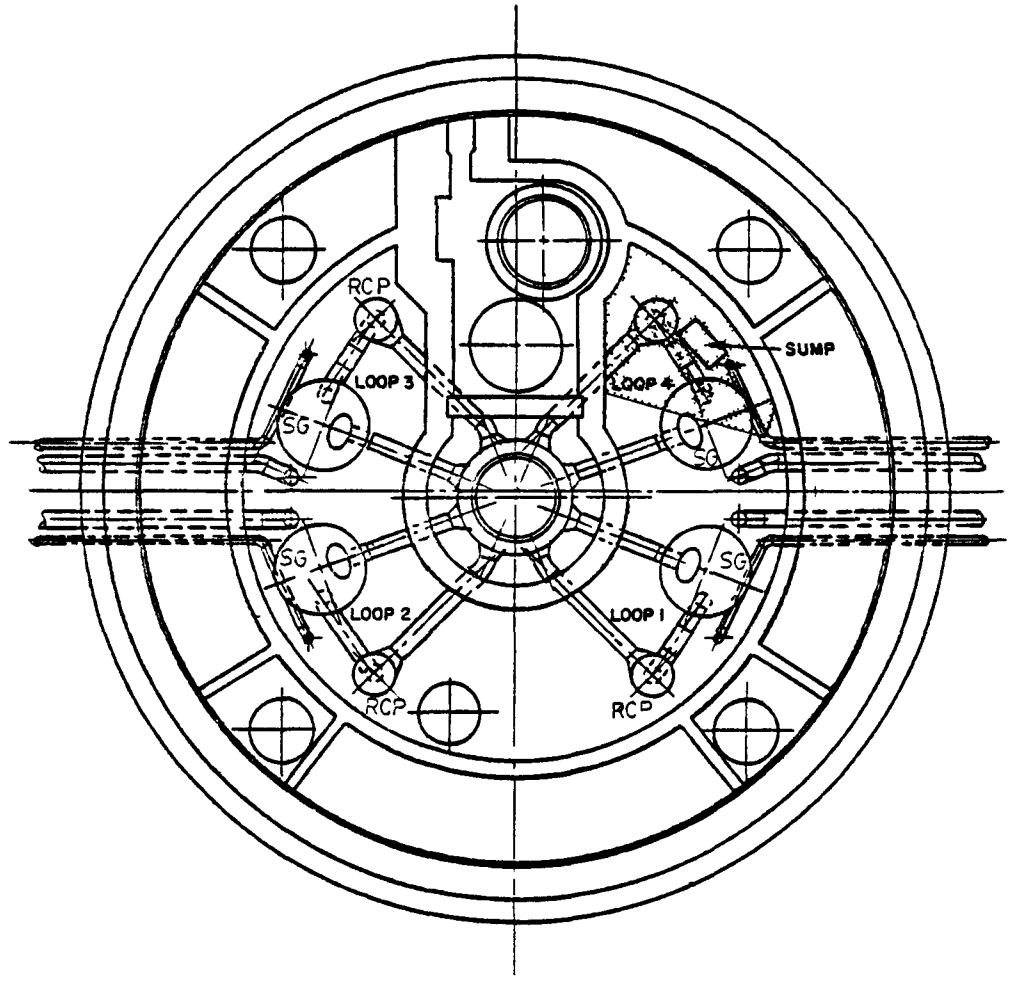

LEGEND
SG - STEAM GENERATOR
RCP - REACTOR COOLANT PUMP

The jet path for break 1, illustrated on Figure D-4, intercepts the targets listed in Table D-1 which lists the total insulation debris generated.

Breaks 2 and 3: Hot Leg Failure

As the jet cone, arc of rotation and pipe impact phenomena are very similar for breaks 2 and 3, only one debris generation analysis is performed.

3.1 Pipe Whip

Figure D-5 illustrates the jet path and Figure D-6 illustrates the motion of the ruptured pipe segment. The free end segment rotates through a 90° arc coming to rest on the reactor cavity wall. The debris generated by this mechanism is limited to the insulation covering the free end segment and is tabulated on Table D-2.

3.2 Pipe Impact

As Figures D-5 and D-6 illustrate, no other pipes or insulated components are struck by the moving free end segment. Therefore, no debris generation occurs by this mechanism.

3.3 Jet Impingement

Table D-2 lists the targets intercepted by the jet exiting both ends of the hot leg failure. It includes the effect of rotation of the free end segment.

Break 4: Reactor Coolant Pump 4 Outlet Nozzle

3.1 Pipe Whip

The break location is illustrated on Figure D-7. As the motion of the free end segment will not strike other insulated pipes or components, the debris generation by this mechanism is limited to the insulation on the cold leg.

Table D-1

Debris Summary, Break 1: Feedwater Line at Containment Penetration

Item Number	Component Name	Diameter (ft)	Length (ft)	Area (ft^2)
1	Feedwater Line	1.25	25	100
2	1-S1-4	1	6	20
3	1-S1-2	0.75	8	20
4	1-FCP-2	0.5	16	25
5a	1-ERCW-112	0.417	22	30
5b	1-ERCW-113	0.417	22	30
			Subtotal	225
6	Small pipe and other equipment		10% of subtotal	23
			Total	248

FIGURE D-5
BREAKS 2&3: HOT LEG FAILURE

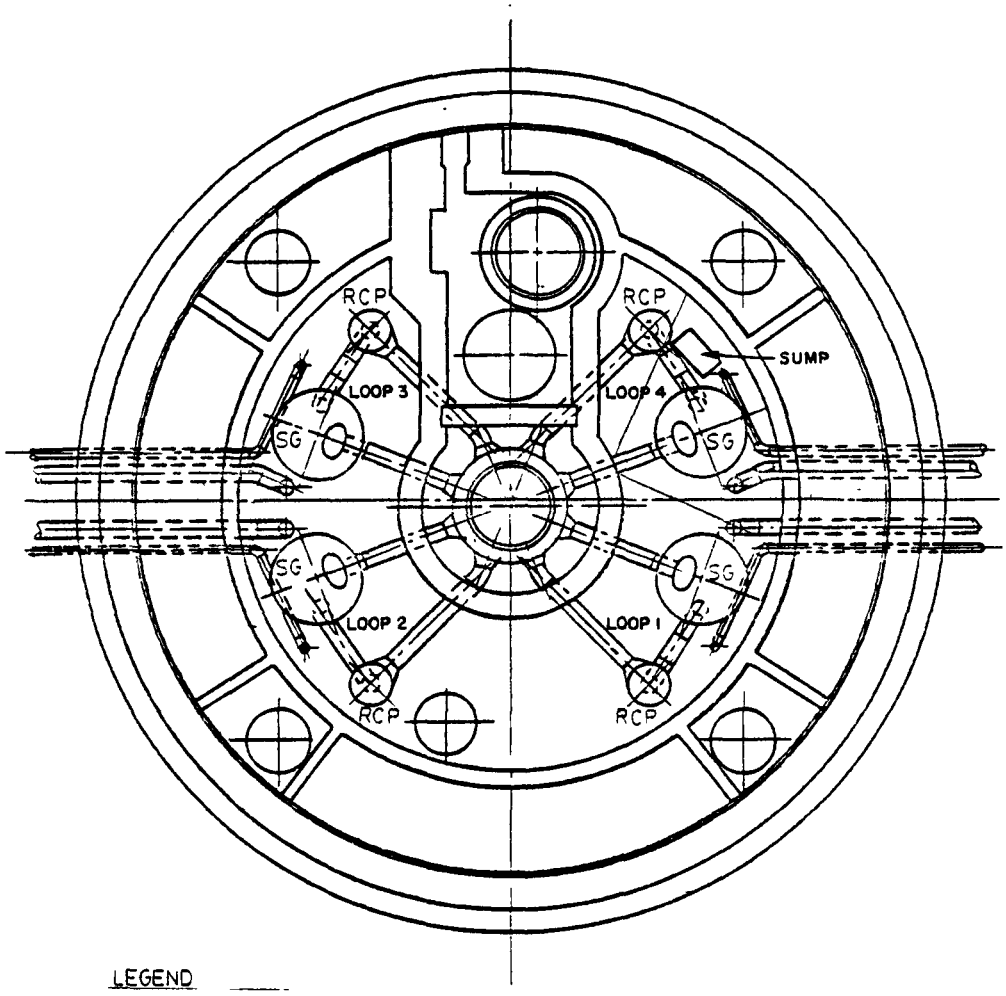

LEGEND

SG - STEAM GENERATOR

RCP - REACTOR COOLANT PUMP

FIGURE D-6
MOTION OF HOT LEG FREE END SEGMENT.

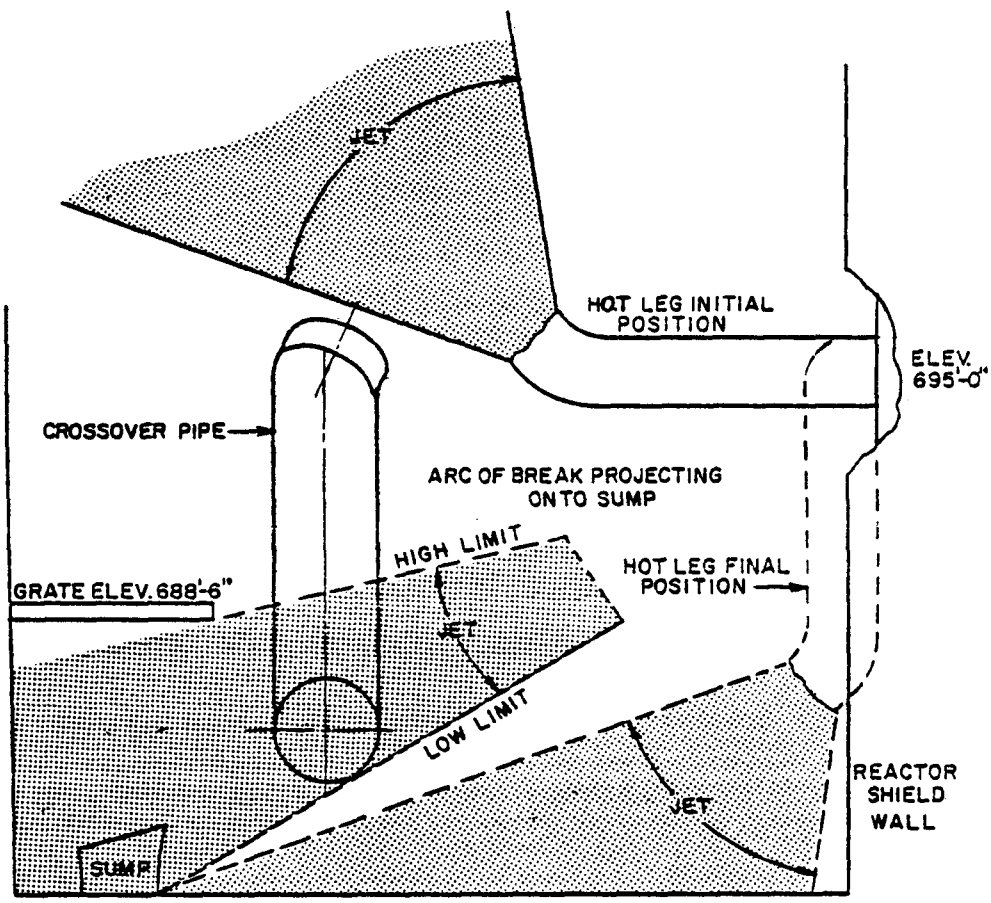

Table D-2

Debris Summary, Breaks 2 & 3: Hot Leg Failure

Item Number	Component Name	Diameter (ft)	Length (ft)	Area (ft^2)
1	Hot Leg	2.583	10	80
2	Lower Part Steam Generator 4	11.375	36	1300
3	Bottom Steam Generator 4	11.375	-	100
4	Crossover Leg	2.833	20	200
5	RHR Pipe	1.333	35	150
6	1-RC-15	0.5	33	50
7	1-PW-100	0.417	33	45
8	1-WD-100	0.5	24	40
9a	1-ERCW-115	0.417	39.5	25
9b	1-ERCW-114	0.417	39.5	25
10	1-SI-4	1.0	14	45
11	1-CVC-4	0.417	40	50
12a	1-ERCW-112	0.417	29	50
12b	1-ERCW-113	0.417	29	50
13	Feedwater Line 4	1.55	39	200
14	1-FPC-100	0.5	32.5	50
15	Main Steam Line 4	2.666	24.5	200
			Subtotal	2660
16	Smaller pipe and other equipment		10% of subtotal	266
			Total	2926

FIGURE D-7
BREAK 4: REACTOR COOLANT PUMP 4 OUTLET NOZZLE

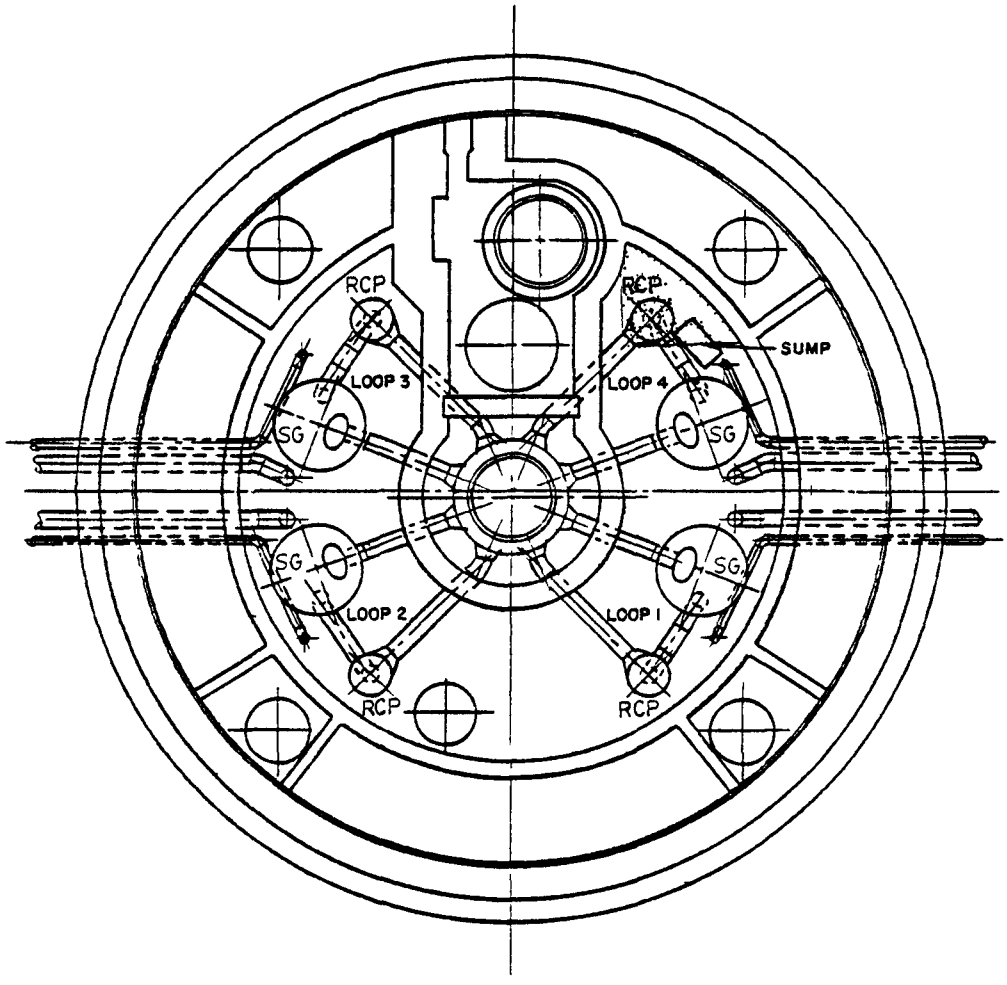

LEGEND

SG - STEAM GENERATOR

RCP - REACTOR COOLANT PUMP

3.2 Pipe Impact

No debris generation by this mechanism occurs for this break.

3.3 Jet Impingement

Figure D-7 illustrates the jet path, and Table D-3 lists the targets intercepted by the jet.

Break 5: Steam Generator 4 Outlet Nozzle

3.1 Pipe Whip

Rupture of the loop 4 crossover pipe at the steam generator outlet nozzle would cause crossover pipe rotation about the reactor coolant pump intake nozzle. Consequently, the pipe whip debris generated by this failure is limited to the insulation on the crossover pipe.

3.2 Pipe Impact

As the crossover pipe free end segment strikes no piping or equipment, debris generation by pipe impact does not occur.

3.3 Jet Impingement

Figure D-8 illustrates the path of the jet exiting the steam generator nozzle. Table D-4 summarizes the debris formed by jet impingement as well as pipe whip.

Break 6: Steam Generator 1 Outlet Nozzle

3.1 Pipe Whip

The crossover leg between the loop 1 steam generator and reactor coolant pump will rotate downward about the reactor coolant pump inlet nozzle until the crossover strikes the containment floor. Consequently, only the crossover pipe insulation is considered to be pipe whip generated debris.

Table D-3

Debris Summary, Break 4: Reactor Coolant Pump 4 Outlet Nozzle

Item Number	Component Name	Diameter (ft)	Length (ft)	Area (ft^2)
1	Cold Leg	2.458	8	60
2	Crossover Leg	2.833	13	115
3	1-RHR-6	1.333	15	60
4	1-CC-5 1-CC-4	0.5	35	55
5	1-CC-10	0.5	35	55
6	1-S1-4	1	37	120
7	1-WD-100	0.5	8	15
8	1-WD-102	0.417	19	25
9	Reactor Coolant Pump 4	6	6	115
10	1-FCP-2 1-FCP-100	0.5	30	50
11a	1-ERCW-112	0.417	11	15
11b	1-ERCW-113	0.417	11	15
12	1-CVC-4	0.417	30	40
13	1-S1-2	0.75	5	12
14	1-FW-4	1.5	35	165
			Subtotal	917
15	Small bore pipe		10% of subtotal	92
			Total	1009

FIGURE D-8
BREAK 5: STEAM GENERATOR 4 OUTLET NOZZLE

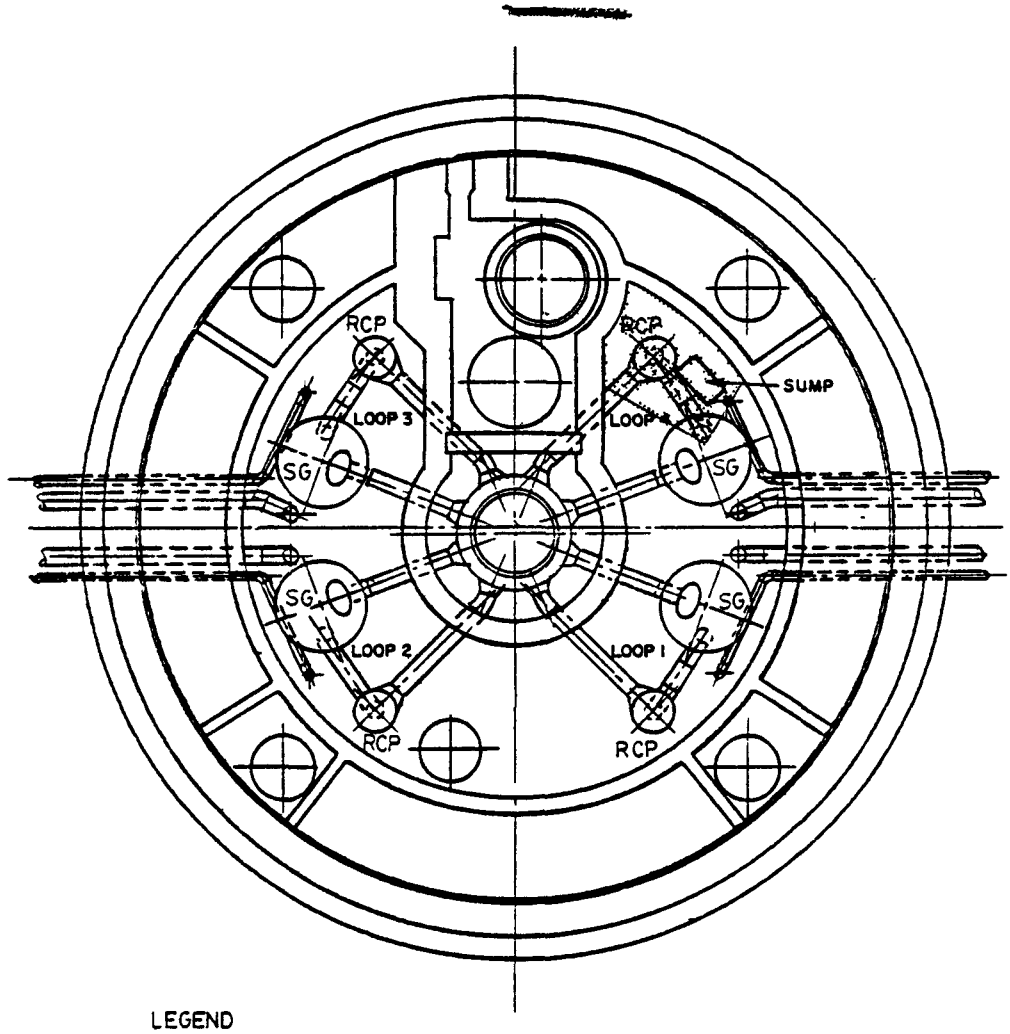

LEGEND

SG STEAM GENERATOR

RCP REACTOR COOLANT PUMP

Table D-4

Debris Summary, Break 5: Steam Generator 4 Outlet Nozzle

Item Number	Component Name	Diameter (ft)	Length (ft)	Area (ft^2)
1	Crossover Leg	2.75	22	200
2	1-RHR-6	1.333	22	95
3	1-CC-10	0.5	13	20
4	1-CC-5	0.5	12	20
5	Reactor Coolant Pump 4	6	6	115
6	Cold Leg	2.458	4	30
			Subtotal	480
7	Small pipe and other equipment		10% of subtotal	48
			Total	528

3.2 Pipe Impact

As the crossover pipe strikes no insulated target in its arc of rotation, no insulation debris is generated by the pipe impact mechanism.

3.3 Jet Impingement

Figure D-9 illustrates the path of the break 6 jet, and Table D-5 summarizes the debris generated by the jet impingement and pipe whip mechanisms.

Break 7: Loop Closure Weld, Loop 1

3.1 Pipe Whip

The consequences of pipe whip are the same as for break 6.

3.2 Pipe Impact

As no insulated structures, pipes or components are struck, debris generation by this mechanism does not occur.

3.3 Jet Impingement

Figure D-10 illustrates the path of the break 7 jet, and Table D-6 summarizes the targets intercepted by the jet as well as the debris generated by pipe whip.

FIGURE D-9
BREAK 6: STEAM GENERATOR I OUTLET NOZZLE

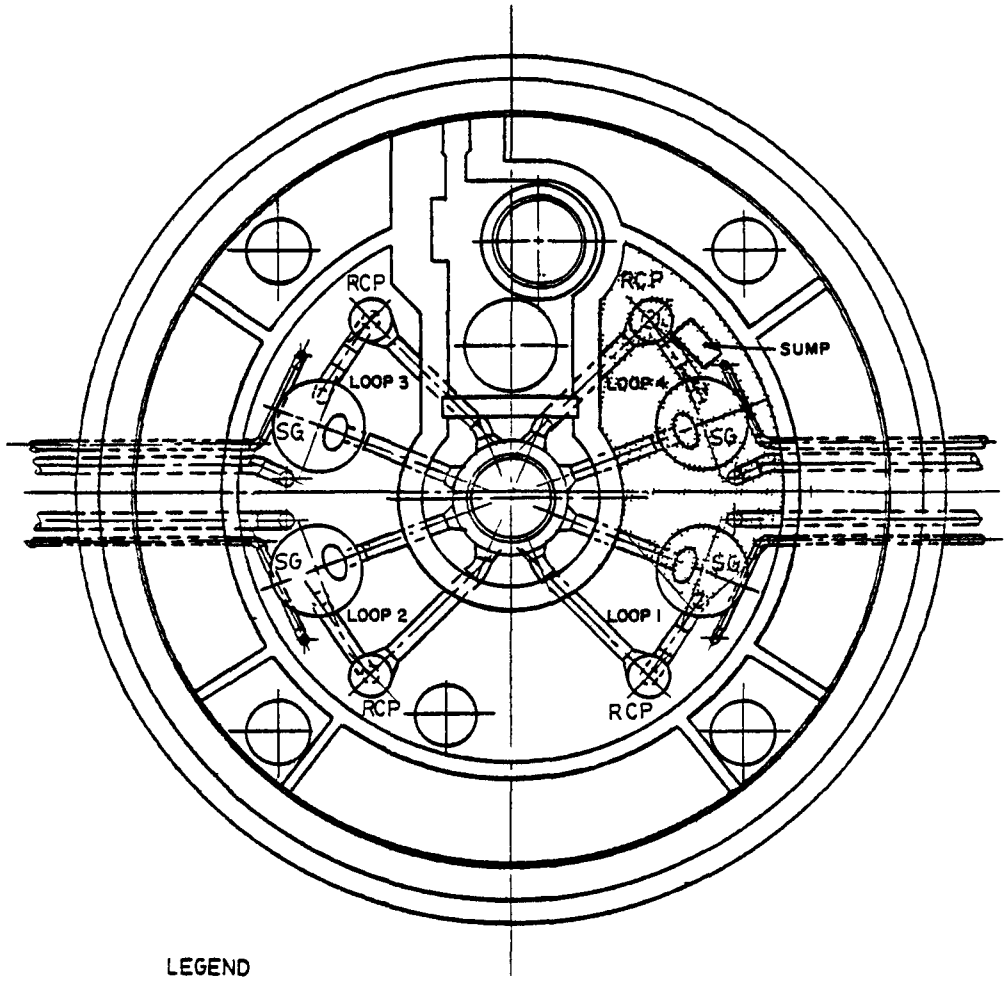

LEGEND

SG - STEAM GENERATOR

RCP REACTOR COOLANT PUMP

Table D-5

Debris Summary, Break 6: Steam Generator 1 Outlet Nozzle

Item Number	Component Name	Diameter (ft)	Length (ft)	Area (ft^2)
1	Lower Part Steam Generator 4	11.375	36	1290
2	Bottom Steam Generator 4	11.375	-	100
3	Lower Part Steam Generator 1	11.375	12	425
4	Bottom Steam Generator 1	11.375	-	100
5	1-RHR-6	1.33	34	150
6	Crossover Leg 4	2.75	16	140
7a	1-ERCW-115	0.417	33	45
7b	1-ERCW-114	0.417	33	45
8	1-FW-4	1.5	48	230
9	1-S1-4	1	5	15
10	1-MS-4	2.92	17	160
11a	1-ERCW-102	0.417	30	40
11b	1-ERCW-103	0.417	30	40
12	1-RC-13	0.5	48	75
13	1-FW-1	1.5	8	40
14	1-CVC-4	0.417	32	40
15	1-ERCW-100	0.417	8	11
	1-ERCW-101	0.417	8	11
			Subtotal	2957
16	Small pipe and other equipment		10% of subtotal	300
			Total	3257

FIGURE D-10
BREAK 7: LOOP CLOSURE WELD, LOOP 1

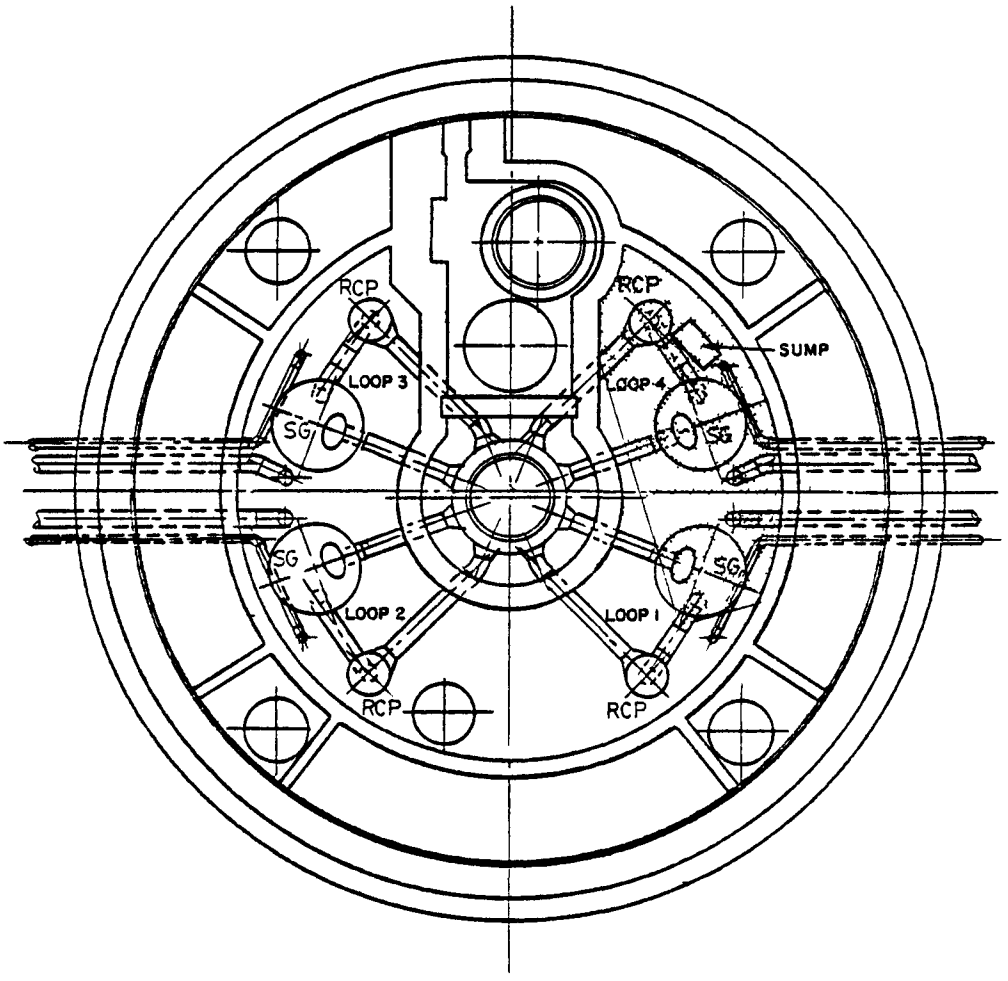

LEGEND
SG - STEAM GENERATOR
RCP - REACTOR COOLANT PUMP

Table D-6

Debris Summary, Break 7: Loop Closure Weld, Loop 1

Item Number	Component Name	Diameter (ft)	Length (ft)	Area (ft^2)
1	Lower Part Steam Generator 4	11.375	36	1290
2	Bottom Steam Generator 4	11.375	-	100
3	Lower Part Steam Generator 1	11.375	36	1290
4	Bottom Steam Generator 1	11.375	-	100
5	Cold Leg 4	2.458	8	65
6	Hot Leg 4	2.583	10	80
7	Reactor Coolant Pump 4	6	6	110
8	1-RHR-6	1.333	59	250
9	1-S1-4	1	36	110
10	1-CC-10	0.5	52	80
11	1-CC-5	0.5	52	80
12a	1-ERCW-115	0.417	51	70
12b	1-ERCW-114	0.417	51	70
13	1-WD-100	0.5	42	65
14	1-WD-102	0.417	18	10
15	1-PW-100	0.417	50.5	65
16	1-RC-13	0.5	50.5	80
17	1-ERCW-103	0.417	49	65
	1-ERCW-102	0.417	49	65
18	Hot Leg 1	2.583	5	40
19	1-CVC-4	0.417	32	40
20	1-SI-2	0.666	5	10
21	1-FCP-2	0.500	30	50
	1-FCP-100			
22	1-ERCW-112	0.417	11	15
	1-ERCW-113	0.417	11	15
23	1-SI-5	1	14.5	45

Table D-6 (Cont'd.)

Item Number	Component Name	Diameter (ft)	Length (ft)	Area (ft^2)
24	1-RHR-3	0.833	13	35
25	1-FW-4	1.25	39	150
26	1-FW-1	1.25	39	150
27	1-S1-3	0.666	4	10
28	1-FPC-100 1-FPC-2	0.5	65.5	105
29	Main Steam Line 4	2.666	24.5	205
30	Main Steam Line 1	2.666	24.5	205
			Subtotal	5120
31	Small pipe and other equipment		10% of subtotal	512
			Total	5632

4.0 DEBRIS TRANSPORT

Three short term transport phenomena exist: pipe whip, pipe impact and jet impingement. The Section 3.0 analysis indicates that neither the pipe impact nor pipe whip transport phenomena need be considered. Therefore, only jet impingement is analyzed.

4.3 Short Term Transport - Jet Impingement

Break 1: Feedwater Line at Containment Penetration

The debris generated by this failure will be transported to the crane wall behind the sump. The debris will fall to the containment floor at termination of blowdown, potentially blocking the back screens of the sump intake (refer to Figure D-4).

Breaks 2 and 3: Hot Leg Failure

Due to the vertical displacement of the hot leg during rotation (refer to Figure D-6), the debris dislodged from the crossover pipe can be directly deposited on the front sump screens. The angle between the high and low limits shown on Figure D-7 is approximately 18° while the angle subtending the sump is approximately 5°. Therefore, 5/18 of the rotation impacts the sump, and 45 ft^2 of insulation are intercepted by the jet. Consequently, 12 ft^2 impact the screen, with the remainder resting against the crane wall.

Since the other items targeted are above the grating over the sump, the debris is transported to the crane wall.

Break 4: Reactor Coolant Pump 4 Outlet Nozzle

The jet (Figure D-7) transports all insulation to the crane wall without intercepting the sump.

Break 5: Steam Generator 4 Outlet Nozzle

The jet from this nozzle intercepts the entire sump. However, as the break location is above the sump grate, only the portion which bypasses the grate and intercepts the sump deposits debris directly on the sump screens. The high limit/low limit angle is 24°. The sump subtending angle is 2°, and debris trapped on the sump screen is 2/24 of 55 ft^2 (crossover pipe insulation), or 5 ft^2.

The balance of the insulation intercepted by the break 5 jet is transported to the crane wall.

Break 6: Steam Generator 1 Outlet Nozzle

The presence of main steam and feedwater piping as well as the loop 4 steam generator makes debris impact on the sump screens nearly impossible. However, the debris will be transported to the crane wall and could conceivably fall behind the sump grating.

Break 7: Loop Closure Weld, Loop 1

As this jet follows the path of the break 6 jet, the effects on debris transport are essentially the same.

4.4 Long Term Transport - Recirculation Phase

Following the blowdown/safety injection phase, the recirculation system is activated and the long term transport problem begins. As demonstrated in Appendix A, a relatively high local velocity is required to transport submerged reflective metallic insulation. The unblocked sump is not capable of inducing flows of the required velocity, as shown below.

Sump Velocity - Unblocked

Required Recirculation Flow = 9875 gpm

Sump Screen Area - Flow can approach unimpeded from either side on the front of the sump screen (Figure D-1). The area is therefore equal to the sum of the front and both side surface areas:

$$(7.5 \times 2) + 2(2.75 \times 2) = 26\ ft^2$$

Then:

$$\text{Velocity} = Q \frac{\text{gal}}{\text{min}} \times \frac{\text{min}}{60 \text{ sec}} \times \frac{1 \text{ ft}^3}{7.48 \text{ gal}} \times \frac{1}{A \text{ ft}^2}$$

$$= \frac{Q}{448.8A} = \frac{9875}{448.8(26)} = 0.84 \text{ ft/sec}$$

For unblocked cases, no long term transport will occur as the sump velocity at the screens is below that required to transport reflective metallic insulation.

Sump Velocity - Blocked

Breaks 1, 4, 6 and 7 block the rear of the sump intake. This is the same as the unblocked case as no flow through the back screen is assumed. Accordingly, the intake velocity of 0.84 ft/sec is insufficient to entrain submerged reflective metallic insulation.

Breaks 2, 3 and 5 have additional blockage. In addition to the 15 ft^2 of back screens, the following frontal and side areas are blocked:

Break	Blockage (ft^2) Front/Side	Velocity (ft/sec)
2	12	1.56
3	12	1.56
5	5	1.04

The velocities are computed assuming that blocked areas pass no flow resulting in increased pressure loss. The tabulation indicates that no long term recirculation occurs for break 5, but breaks 2 and 3 require further investigation.

5.0 SUMP EFFECTS

As breaks 2 and 3 block approximately 73% of the intake screen area, an analysis of the head loss is required to assure continued recirculation pump operation.

Knowing

$$H = \frac{K\bar{V}^2}{2g_c}$$

where

h = head loss

K = loss coefficient (0.52, Ref. 16)

$\bar{V}$ = flow velocity

g_c = Newton's constant

$$h = \frac{0.52\ (1.56)^2}{2\ (32.2)} = 0.02 \text{ ft of water}$$

The 0.02 ft of water head loss is negligible.

Conclusion

The breaks analyzed for Sequoyah Nuclear Unit 2 bound the range of possible conditions. As break 2 generates maximum flow velocity and produces acceptable pressure drop increases, all other breaks which generate lower velocities must also produce less severe pressure drop increases. No break deposits sufficient debris on or near the sump to prevent operation of the recirculation pumps.

APPENDIX E

PRAIRIE ISLAND NUCLEAR GENERATING PLANT UNIT 2

Appendix E

Prairie Island Nuclear Generating Plant Unit 2

1.0 INTRODUCTION

Prairie Island Nuclear Generating Plant Unit 2 (PI-2) employs reflective metallic insulation within containment for all pipes, process vessels, etc. Fiberglass insulation is used for pipe hangers only.

Figure E-1 shows the layout of the PI-2 containment with the locations of major equipment.

2.0 DETERMINATION OF INITIATING EVENTS

Appendix I of Amendment 24 to the Prairie Island Nuclear Generating Plant (PI-2) FSAR identifies design basis break locations in the following systems:

Number	System
1	Main Steam
2	Feedwater
3	Letdown Line
4	Steam Generator (SG) Blowdown
5	Steam Feed - Auxiliary Feedwater Turbine
6	Chemical and Volume Control System
7	*Hot Leg
8	*Cold Leg
9	*Crossover Piping

*Design basis accident inside containment (FSAR Section 14.3.1)

As the consequences of breaks 3, 4, 5 and 6 cannot be as severe as breaks 1, 2, 7, 8 and 9 due to smaller line sizes, they are ignored in the analysis which follows.

FIGURE E-1
CONTAINMENT PLAN VIEW

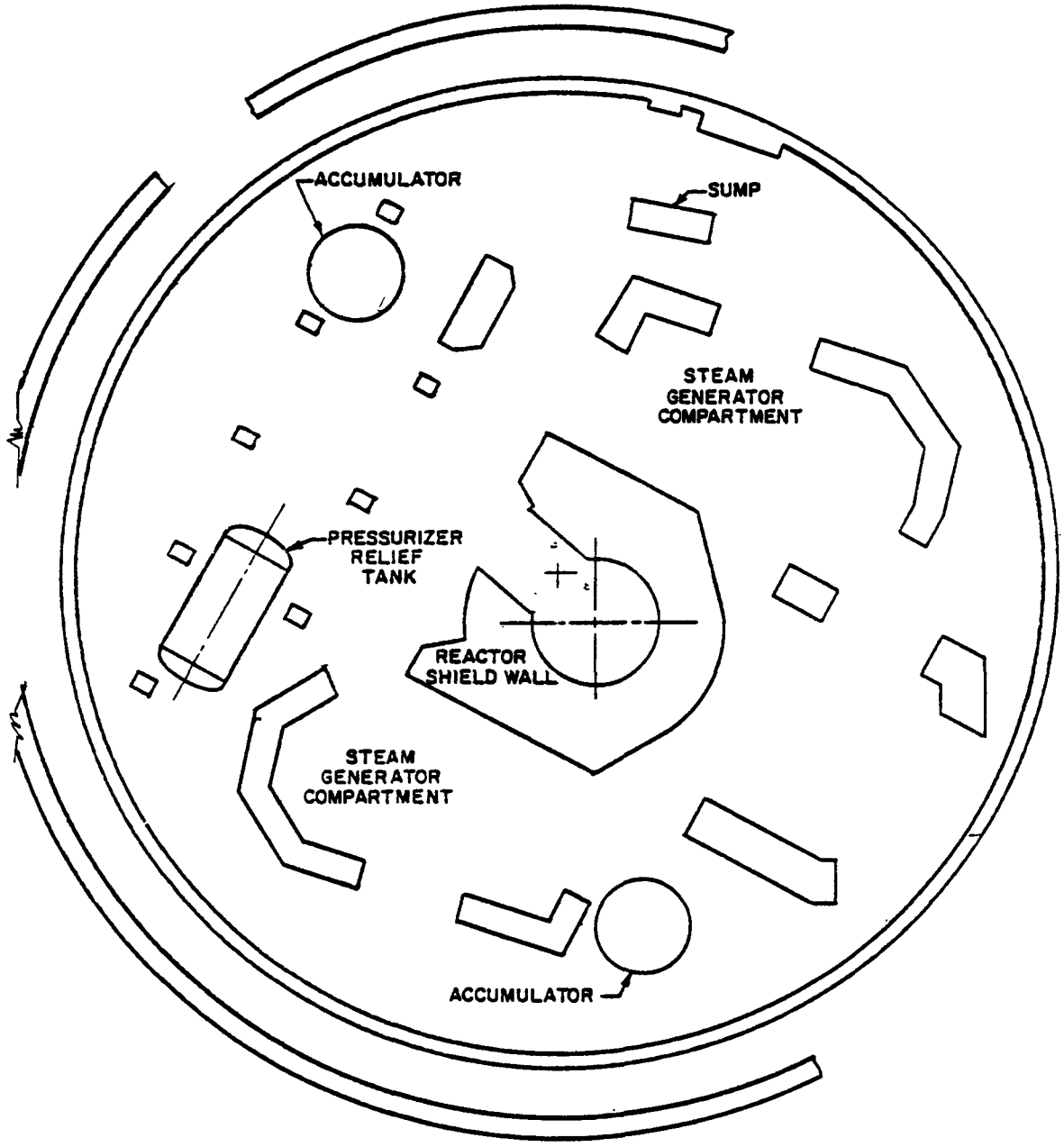

3.0 INSULATION DEBRIS GENERATION

General

Sections 14.2.5 and 14.3.1 of the PI-2 FSAR state that high energy piping inside containment is restrained or anchored such that a whipping pipe segment cannot impact adjacent pipes, components or structures. Accordingly, no discussion of the pipe impact debris generation mechanism is included in this analysis. Jet expansion is again taken as 90°, and all target components are assumed sources of debris, if insulated. Accordingly, no individual jet expansion calculations are provided.

Break 1: Main Steam

3.1 Pipe Whip

As Figure E-2 illustrates, the main steam break is assumed at the steam generator nozzle. The resulting blowdown load imposes a reaction load on the main steam piping. Pipe whip restraints prevent unacceptable pipe motions (i.e., collision with other pipes or the containment structure). It is therefore assumed that the pipe segment remains in the jet cone. Insulation debris is therefore considered as jet impingement generated debris.

3.3 Jet Impingement

Figure E-2 shows that the main steam jet targets the reactor coolant pump, the hot and cold legs, the crossover line, the pressurizer, the pressurizer surge line, portions of the main steam lines and portions of the feedwater system. Attachment E-1 lists the quantities and types of insulation used within the PI-2 containment. Table E-1 lists the quantities involved in break 1. The insulation used on the main steam and feedwater pipe hangers is a fiberglass type, 3 in. thick with a bulk density of 11.25 lbm/ft^3.

FIGURE E-2
BREAK I: MAIN STEAM

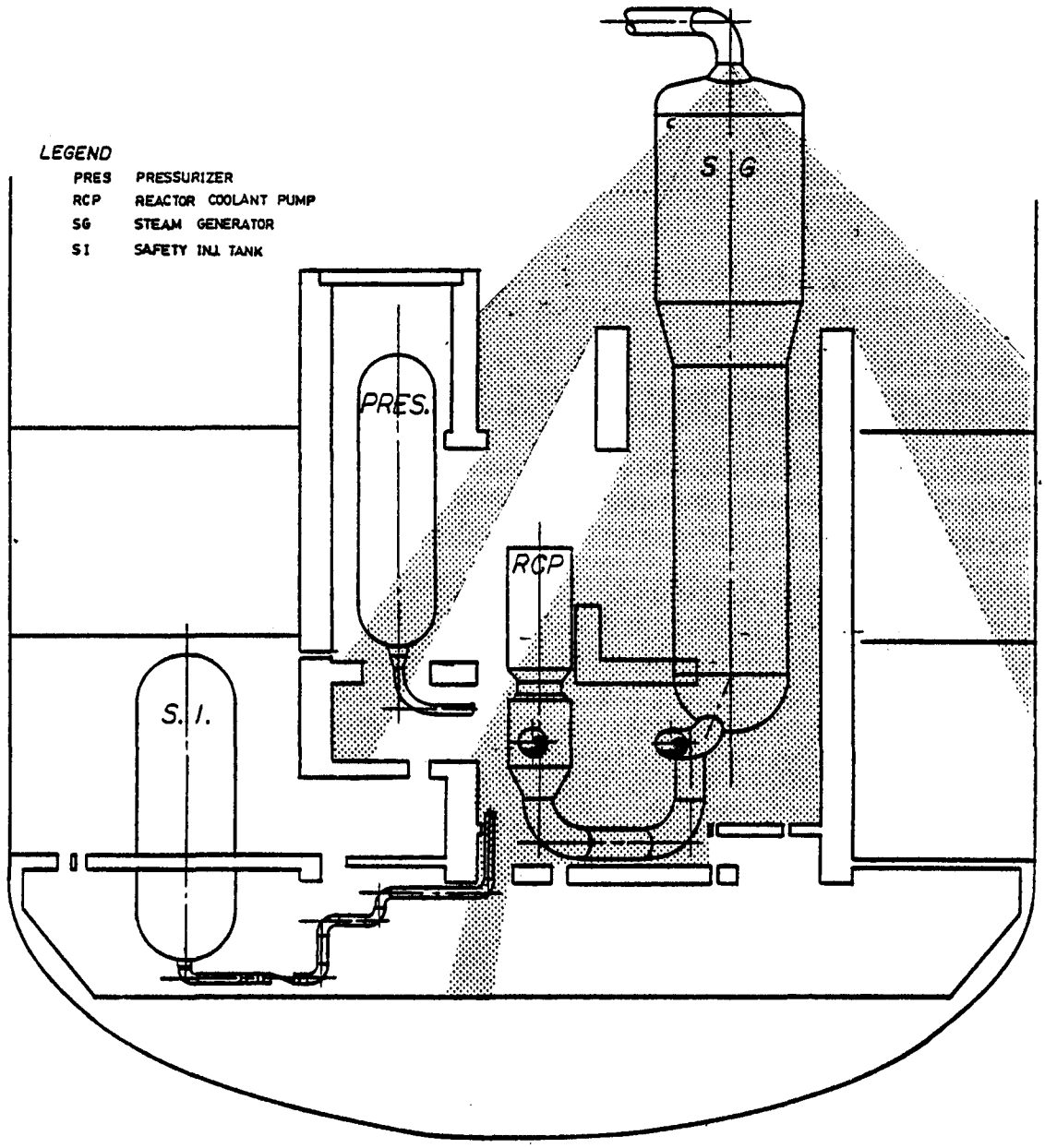

Table E-1

Debris Summary, Break 1: Main Steam

Target	Quantity Present (ft^2)		Quantity Involved* (ft^2)	Type
Steam Generator	3012		3012	RM
Reactor Coolant Pump	255		125	RM
Hot Leg/Cold Leg	330		330	RM
Pressurizer	760		150	RM
Pressurizer Surge	250		50	RM
Main Steam	1170		70	RM
Feedwater Line	490		40	RM
		Subtotal	3777	
Small Bore Pipe (allowance 10%)			380	
		Total	4157	
Feedwater Hanger	101		101	FG
Main Steam Hanger	58		58	FG
		Total	159	

*Based on portion of item intercepted by jet with inclusion of out-of-plane segments.

Note: RM - Reflective Metallic
FG - Fiberglass

Break 2: Feedwater

3.1 Pipe Whip

The design basis break in the feedwater system is chosen at the steam generator nozzle. The nozzle attaches to the steam generator below the trunnions shown on Figure E-2. The reaction load displaces the pipe horizontally until contact with the restraints occurs.

3.3 Jet Impingement

The jets exiting either side of the double ended feedwater failure have their axes oriented parallel to the containment floor. The jet exiting the steam generator will move as shown on Figure E-3. No equipment, pipes or structures are targeted by this end of the break. The jet exiting the feedwater line will impact the steam generator. Table E-2 summarizes the quantity of insulation ejected by break 2.

Break 7: Hot Leg

3.1 Pipe Whip

The hot leg is restrained in such a fashion as to prevent impact with adjacent piping. This is required to guarantee the operability of the safety injection system. Consequently, insulation debris by pipe whip is limited to the hot leg piping. As the hot leg is fully enclosed by the jets exiting the piping and steam generator, the insulation quantity generated by pipe whip is tallied under the jet impingement mechanism.

3.3 Jet Impingement

Figure E-4 illustrates the path of the hot leg jet. As the figure shows, the steam generator, hot leg, cold leg, crossover pipe, feedwater pipe, steam generator supports and portions of the RHR system are located within the jet cones. Table E-3 summarizes the debris generated by break 7.

FIGURE E-3
BREAK 2: FEEDWATER.

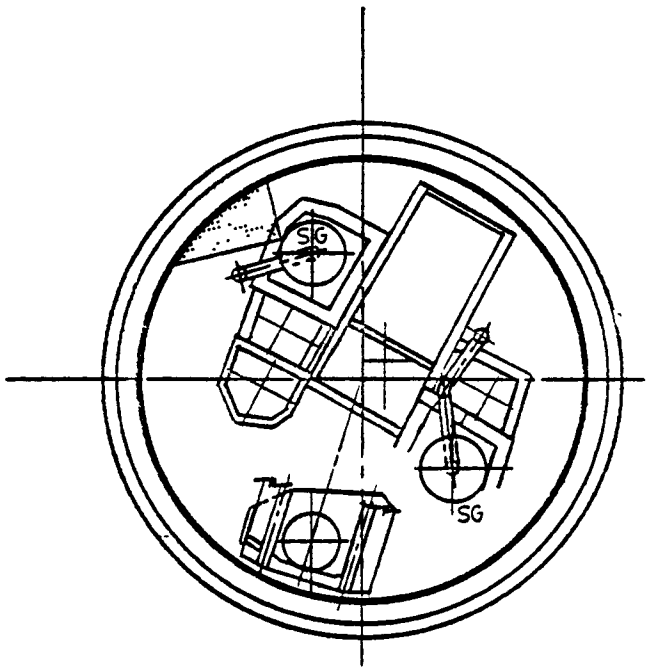

LEGEND

SG — STEAM GENERATOR

Table E-2

Debris Summary, Break 2: Feedwater

Target	Quantity Present (ft^2)		Quantity Involved* (ft^2)	Type
Feedwater Line	490		40	RM
Steam Generator	3012		1000	RM
		Subtotal	1040	
Small Bore Pipe (allowance 10%)			100	
		Total	1140	
Feedwater Hanger	101		101	FG
Main Steam Hanger	58		58	FG
		Total	159	

*Based on portion of item intercepted by jet with inclusion of out-of-plane segments.

RM - Reflective Metallic
FG - Fiberglass

FIGURE E-4
BREAK 7: HOT LEG

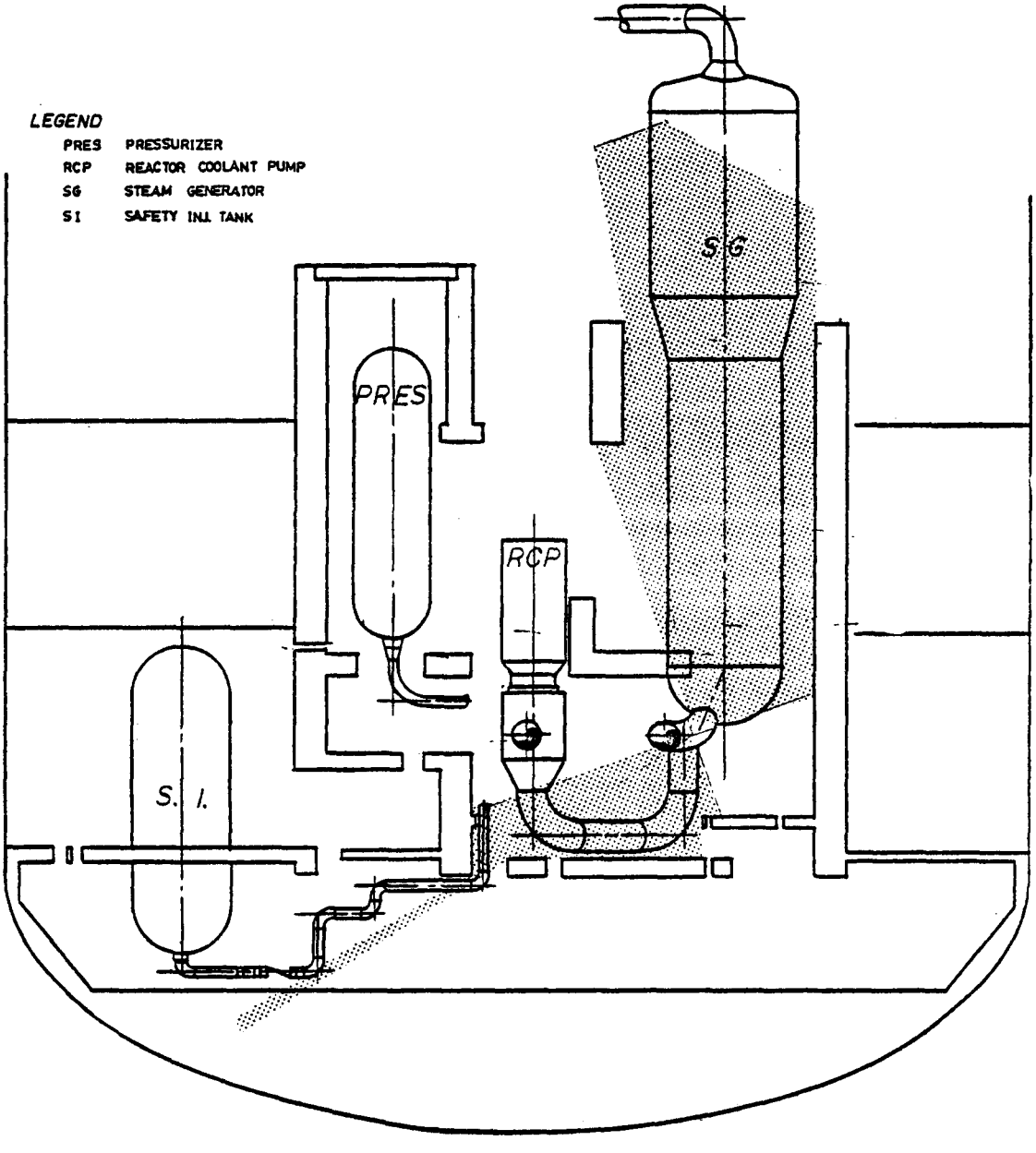

Table E-3

Debris Summary, Break 7: Hot Leg

Item	Quantity Present (ft^2)	Quantity* Involved (ft^2)	Type
Steam Generator	3012	3012	RM
Feedwater Line	490	40	RM
Hot Leg/Cold Leg	330	330	RM
Steam Gen. Supports	285	140	RM
RHR Piping	442	90	RM
	Subtotal	3612	
Small Bore Pipe (allowance 10%)		360	
	Total	3972	
Main Steam Hanger	101	101	FG
Feedwater Hanger	58	58	FG
	Total	159	

*Based on portion of item intercepted by jet with inclusion of out-of-plane segments.

RM - Reflective Metallic
FG - Fiberglass

Break 8: Cold Leg

3.1 Pipe Whip

The cold leg from the reactor cavity wall (RC) to the reactor coolant pump (RCP) is restrained to minimize the consequences of a cold leg rupture. This restraint places both ends of the postulated rupture within the jet cones. Consequently the debris generated by pipe break is recorded under the jet impingement mechanism.

3.3 Jet Impingement

Figure E-5 illustrates the jet diameter as viewed from the reactor cavity wall and Figure E-6 shows the jet divergence. The crossover leg, cold leg, pressurizer surge line and the reactor coolant pump are targeted by the break 8 jet. The return jet from the RCP towards the reactor cavity is not shown. It targets the cold leg whose insulation debris contribution is already tallied.

Table E-4 summarizes the quantity of debris formed by this failure.

Break 9: Crossover Piping

3.1 Pipe Whip

The failure of the crossover pipe at the RCP nozzle will cause the crossover pipe to rotate downward about its steam generator nozzle connection until the crossover pipe strikes the 710 ft elevation slab. The debris generated by this mechanism will travel tangent to the arc of motion of the crossover pipe at the point of impact which in this case is vertically downward. The insulation will be intercepted by the 710 ft slab.

3.3 Jet Impingement

Figure E-7 illustrates the path of the jet exiting both ends of the crossover pipe failure. The figure shows the steam generator, reactor coolant pump, feedwater, hot leg, cold let, pressurizer surge line and pressurizer are all targeted by these jets.

Table E-5 summarizes the insulation debris generated by break 9.

FIGURE E-5
BREAK 8: COLD LEG

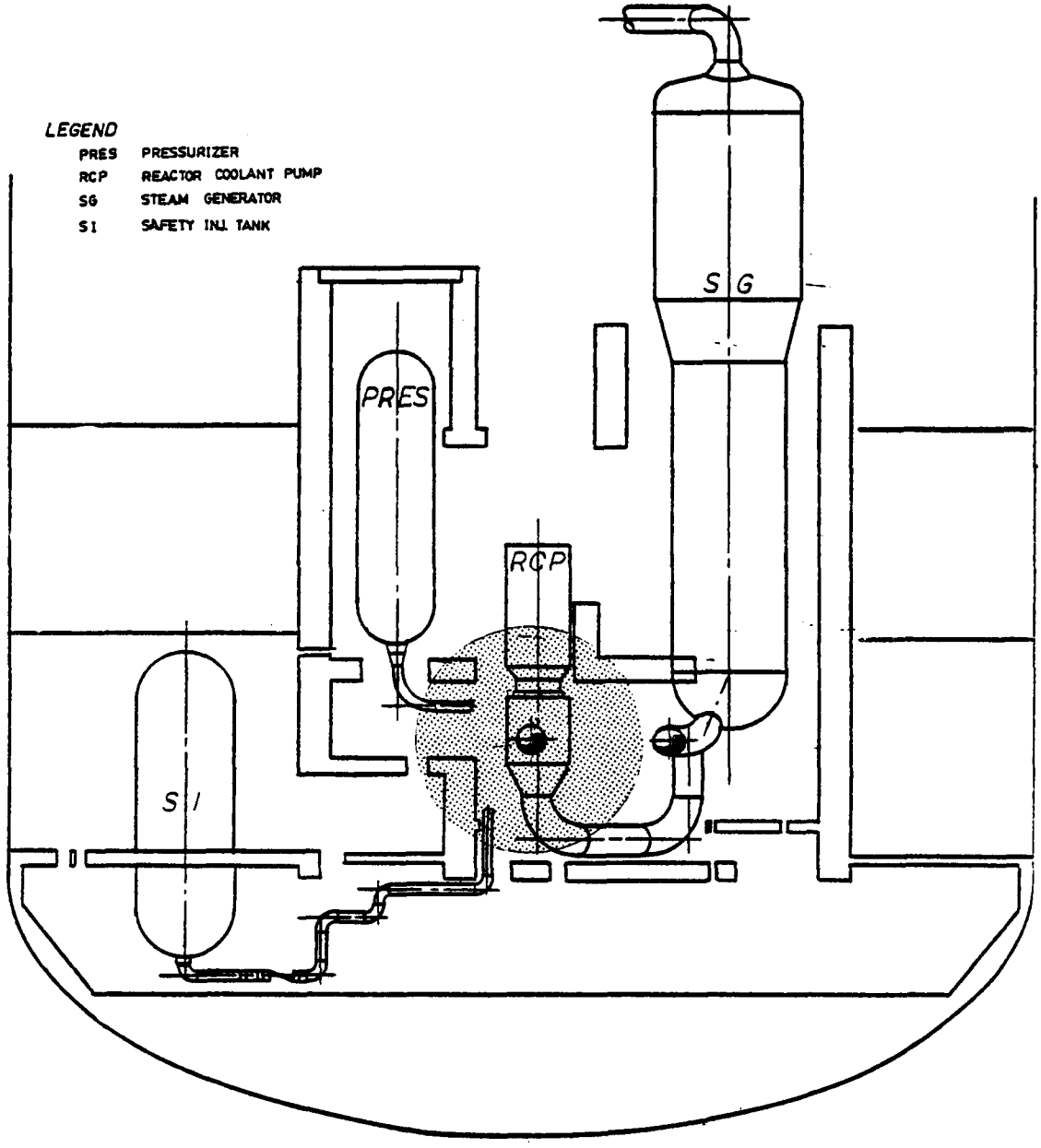

FIGURE E-6
BREAK 8: COLD LEG

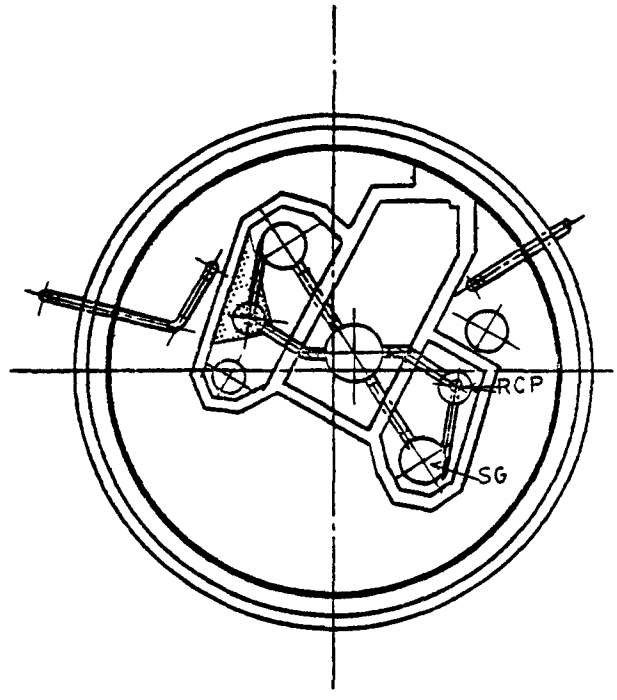

LEGEND

SG - STEAM GENERATOR

RCP - REACTOR COOLANT PUMP

Table E-4

Debris Summary, Break 8: Cold Leg

Item	Quantity Present (ft^2)	Quantity Involved (ft^2)	Type
Crossover Pipe	425	425	RM
Cold Leg/Hot Leg	330	330	RM
Pressurizer Surge	247	100	RM
RC Pump	255	255	RM
		Subtotal 1110	
Small Bore Pipe (allowance 10%)		111	RM
		Total 1221	

RM - Reflective Metallic

FIGURE E-7
BREAK 9: CROSSOVER PIPING

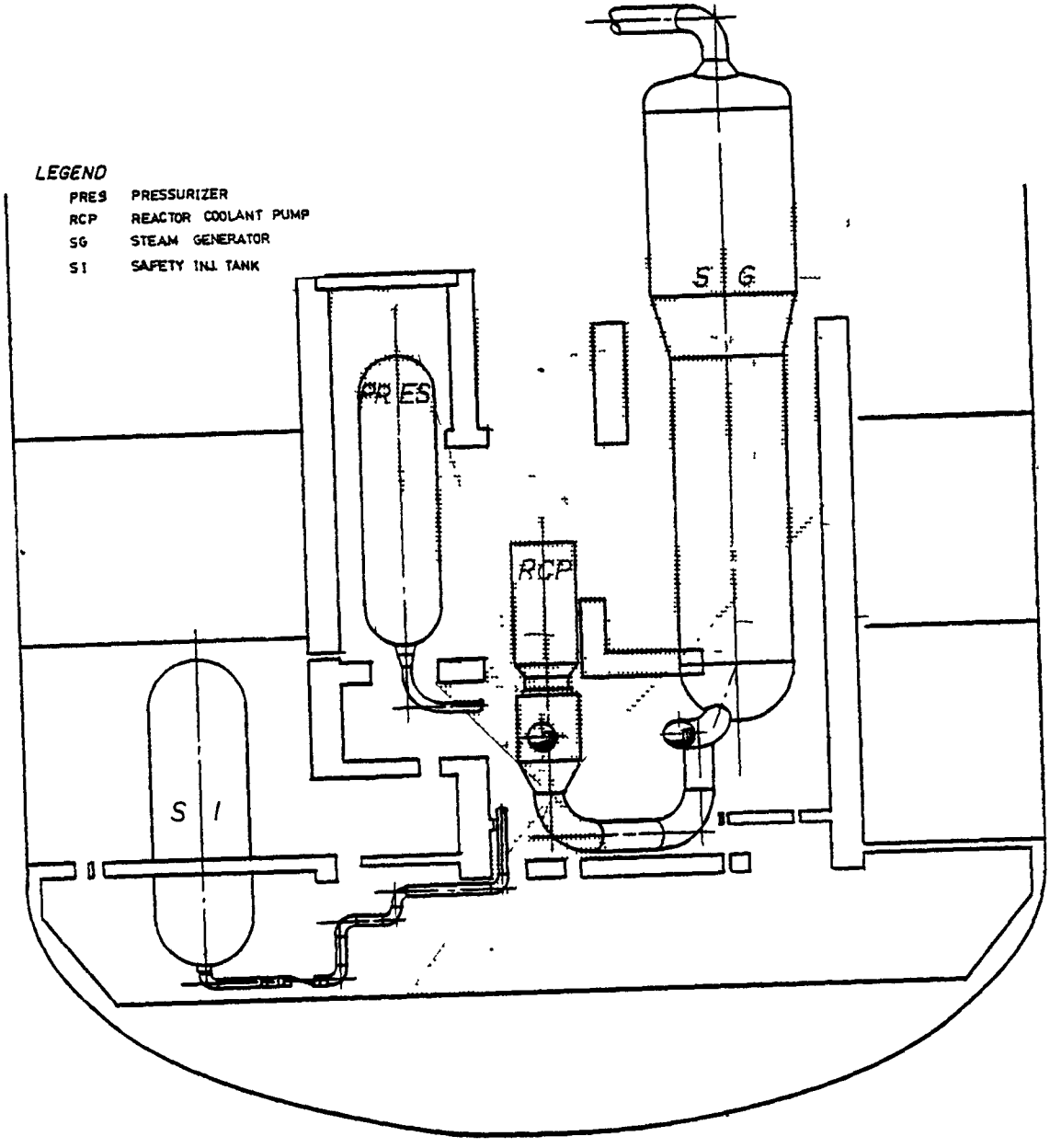

Table E-5

Debris Summary, Break 9: Crossover Piping

Item	Quantity Present (ft^2)	Quantity Involved (ft^2)	Type
Steam Generator	3012	2500	RM
RC Pump	255	255	RM
Hot Leg/Cold Leg	330	330	RM
Surge Line	247	100	RM
Feedwater Line	490	40	RM
Pressurizer	760	760	RM
Crossover	425	425	RM
		Subtotal 4410	
Small Bore Pipe (allowance 10%)		440	RM
		Total 4850	
Main Steam Hanger	101	101	FG
Feedwater Hanger	58	58	FG
		Total 159	FG

RM - Reflective Metallic
FG - Fiberglass

4.0 DEBRIS TRANSPORT

4.3 Short Term Transport - Jet Impingement

The main steam, hot leg, cold leg, and crossover failures are all capable of transporting insulation to the sump region. However, due to the presence of numerous obstacles, direct impingement on the sump screen is not possible. In all cases, the quantity of insulation reaching the sump area (elevation 687 ft 6 in.) is determined by accounting for the partial slab at elevation 715 ft and the area of the communicating passages between the 711 ft slab and the sump region at 687 ft 6 in.

As all jets expand at 90^{o}, they fully encompass the compartment at elevation 715 ft, yielding:

Area of jet at el. 715 ft - 500 ft^2
Area of el. 715 ft slab - 160 ft^2
Area of unblocked flow path - 340 ft^2

The ratio of unblocked flow path to jet area at elevation 715 ft indicates that 68% of the debris reaches the 711 ft slab. (Refer to Figure E-7.)

At the 711 ft slab the flow is stagnated with resultant radial outflow. The quantity of debris ejected from the slab equals the product of debris reaching the slab and the ratio of vented perimeter to total perimeter as follows:

$$\text{Ejected to sump region} = \text{Debris at 711 ft} \times \frac{\text{vented perimeter}}{\text{total perimeter}}$$

Vented perimeter 31 ft

Total perimeter 85 ft

Ratio 0.36

Therefore for a given quantity of debris in the jet above elevation 715 ft, the quantity reaching the sump region is: 0.68 x 0.36 or 24.5% of the total.

Table E-6 summarizes the debris transport.

Table E-6

Break	Total Debris (ft^2)	Debris Retained On 715 ft_2Slab (ft^2)	Debris Retained On 711 ft_2Slab (ft^2)	Debris In Sump Region (ft^2)
1	4157 RM	1330	1809	1018
	159 FG	51	69	39
2	1140 RM	0	0	0
	159 FG	0	0	0
7	3972 RM	1271	1728	973
	159 FG	51	69	39
8	1221 RM	390	531	300
	0 FG	0	0	0
9	4850 RM	1552	2110	1188
	159 FG	51	69	39

RM - Reflective Metallic
FG - Fiberglass

4.4 Long Term Transport - Recirculation Phase

Activation of the recirculation mode will cause motion of submerged reflective metallic insulation if the local velocity exceeds that required to move the panels. The fiberglass insulation is assumed to float and reach the sump.

5.0 SUMP EFFECTS

The net containment floor area of 8660 ft^2 will flood to a depth of 4.4 feet when the 36,100 ft^3 in the RWST plus the two 1100 ft^3 safety injection tanks empty into the reactor. Consequently, the 2 ft 9 in. sump will be completely covered.

The maximum pump rate of 2600 gpm gives a sump screen velocity of about 0.1 ft/sec which is insufficient to cause motion of submerged reflective metallic insulation and is also incapable of drawing down floating debris. However, if the fiberglass should sink, it would plug the screen reducing the flow rate as follows:

Given: Maximum fiberglass in the sump region - 39 ft^2

Unblocked sump screen area - 60 ft^2

Unblocked sump screen flow velocity - 0.1 ft/sec

From Attachment E-1 the fiberglass has a thickness of 3 in., giving (assuming uniform distribution) a layer 1.95 in. deep on the 60 ft^2 screens. Using the procedure of Section 5.3, the pressure drop is 0.133 psi. This increase in head loss must be evaluated by comparison with available NPSH margin before a conclusion can be reached regarding the acceptability of this degree of blockage.

ATTACHMENT E-1

Summary of Insulation

Type & Quantities

Extracted from Regulatory Information Distribution System

Accession Number: 8101120076 Document Date: 81/01/07
Docket Number: 05000306

Prairie Island Nuclear Station Unit 2

Table 2

Unit No. 2 (Page 1 of 4)

Location	Type Material	Manufacturer	Brand Name	Attachment	Quantity Square Feet
Reactor Vessel Insulation	Stainless Steel	Universal Fabricated Prod	Transco Inc	Stainless Steel Screws	3044
#21 Steam Generator	Stainless Steel	Diamond Power Specialty Corp	Mirror Insulation	Stainless Screws & Buckles	3012
#22 Steam Generator					3012
#21 RC Pump					255
#22 RC Pump					255
Pressurizer Unit #2					760
Excess Letdown Heat Exchanger					61
6" Regenerative Heat Exchanger					150
Surge Line					247
High Head Safety Inject Loop A & B					36
RTD Loop A					93
RTD Loop B					91
Loop A Coolant Leg Hot & Cold					330
Loop B Coolant Leg Hot & Cold					330
Interm Coolant Leg Loop A					425
Interm Coolant Leg Loop B					425
2" Steam Generator Blowdown Loop A					272

Table 2

Unit No. 2 (Page 2 of 4)

Location	Type Material	Manufacturer	Brand Name	Attachment	Quantity Square Feet
2" Steam Generator Blowdown Loop B	Stainless Steel	Diamond Power Specialty Corp	Mirror Insulation	Stainless Steel Screws & Buckles	108
3" Spray Line	↓	↓	↓	↓	367
3" Spray Line Loop B					42
2" Aux Spray Line Loop B					52
#21 Steam Generator Lateral Support					285
#22 Steam Generator Lateral Support					285
1" Excess Letdown Heat Exchange					87
3" Aux Feedwater Loop A & B					16
#21 Main Steam					1280
#22 Main Steam					1170
#21 Feedwater					394
#22 Feedwater					490
RHR A Loop					520
RHR B Loop					442
CVS Charging Line Loop B					216
3/8" Leakoff RV Flange	↓	↓	↓	↓	272

Table 2

Unit No. 2 (Page 3 of 4)

Location	Type Material	Manufacturer	Brand Name	Attachment	Quantity Square Feet
2" Letdown to RHR	Stainless Steel	Diamond Power Specialty Corp	Mirror Insulation	Stainless Steel Screws Buckles	386
2" Letdown Interm drain Loop B Reg Heat Exchanger	↓	↓	↓	↓	156
1" Volume Control Excess Heat Exchanger	↓	↓	↓	↓	17
Low Head Safety Injection Loop A & B	↓	↓	↓	↓	98
Pressurizer Safety Valve	↓	↓	↓	↓	18
Accumulator Injection Loop B	↓	↓	↓	↓	54
Accumulator Injection Loop A	↓	↓	↓	↓	43
Interm Leg Drain Leg Loop A & B	↓	↓	↓	↓	72.8
Main Steam and Feedwater A and B Loops	Fibrous Glass Insul 1000° Glass Cloth Cover	Pittsburgh Corning Clark Schwedel Insul	Temp Mat CS9383 Style 1925	18 gauge SS Wire Fastened to 1" dia SS Discs	
MSH 47	↓	↓	↓	↓	58
MSH 51	↓	↓	↓	↓	42
MSH 43	↓	↓	↓	↓	16
MSH 39	↓	↓	↓	↓	38
MSH 42	↓	↓	↓	↓	24
MSH 38	↓	↓	↓	↓	16
FWH 66	↓	↓	↓	↓	21
FWH 682A	↓	↓	↓	↓	14
FWH 613A	↓	↓	↓	↓	18

Table 2

Unit No. 2 (Page 4 of 4)

Location (Hanger No.)	Type Material	Manufacturer	Brand Name	Attachment	Quantity Square Feet
Main Steam and Feedwater A and B Loops	Fibrous Glass Insul 1000° Glass Cloth Cover	Pittsubrgh Corning Clark Schwedel Insul	Temp Mat CS9383 Style 1925	18 gauge SS Wire Fastened To 1" dia SS Discs	
FWH 72					101
FWH 735A					14
FWH 53					35
MSH 48					58
MSH 52					42
MSH 46					16
MSH 45					20
MSH 55					20
MSH 83					40
MSH 41					-0
MSH 37					35
FWH 67					12
FWH 65					9
FWH 64					9
FWH 69					16
FWH 62					14
FWH 54					28

Table 3 - Density and Thickness for Thermal Insulation Used in Prairie Island Containment Buildings

Insulation Type	Density (lb/cf)	Thickness (inches)
Reactor Vessel Transco	15.75	3.5
RCS Mirror	15.75	3.5
Temp Mat/Glass	11.25	3

*U.S. GOVERNMENT PRINTING OFFICE: 1982 361-297/2429 1-3